CTR 2/3-18-88/1-1175-5

Effect of Depth to Bedrock on the Accuracy of Backcalculated Moduli Obtained with Dynaflect and FWD Tests

Chia-Ray Seng, Kenneth H. Stokoe, II,
and José M. Roesset

RESEARCH REPORT 1175-5

Project 2/3-18-88/1-1175

CENTER FOR TRANSPORTATION RESEARCH
BUREAU OF ENGINEERING RESEARCH
THE UNIVERSITY OF TEXAS AT AUSTIN

JANUARY 1993

1. Report No.	2. Government Accession No.	3.
FHWA/TX-93+1175-5		

4. Title and Subtitle
EFFECT OF DEPTH TO BEDROCK ON THE ACCURACY OF BACKCALCULATED MODULI OBTAINED WITH DYNAFLECT AND FWD TESTS

5. Report Date
January 1993

6. Performing Organization Code

7. Author(s)
Chia-Ray Seng, Kenneth H. Stokoe II, and José M. Roesset

8. Performing Organization Report No.
Research Report 1175-5

9. Performing Organization Name and Address
Center for Transportation Research
The University of Texas at Austin
Austin, Texas 78712-1075

10. Work Unit No. (TRAIS)

11. Contract or Grant No.
Research Study 2/3-18-88/1-1175

12. Sponsoring Agency Name and Address
Texas Department of Transportation
Transportation Planning Division
P. O. Box 5051
Austin, Texas 78763-5051

13. Type of Report and Period Covered
Interim

14. Sponsoring Agency Code

15. Supplementary Notes
Study conducted in cooperation with the U.S. Department of Transportation, Federal Highway Administration. Research Study Title: "Development of Dynamic Analysis Techniques for Falling Weight Deflectometer Data"

16. Abstract

The main objective of this study is to investigate the importance of depth to bedrock in surface loading tests. Two surface loading tests, the Dynaflect and Falling Weight Deflectometer (FWD), were investigated analytically using four typical in-service Texas highway pavement profiles.

The dynamic effect of these surface loading tests was in terms of deflection ratios, "dynamic" deflections divided by static deflections. "Dynamic" deflections represent those deflections which are actually measured when these tests are performed on real pavements. The amplitude of the deflection ratio is an important index of the potential error generated in any static interpretation procedure. The results show that the stiffness of the subgrade has the most significant effect on the maximum amplitude of the deflection ratio (deflection ratio at resonant conditions). The softer the subgrade is, the higher is the amplitude of the maximum deflection ratio. This behavior agrees with the trend in backcalculated layer moduli using static interpretation programs.

Equations for estimating the resonant depth to bedrock (depth to bedrock corresponding to the maximum deflection ratio) based on the subgrade stiffness are suggested for both the Dynaflect and FWD tests.

For the FWD test, equations are developed for estimating the actual depth to bedrock based on the damped natural period on the free vibrations of the pavement system immediately after the FWD load application. In these equations, the stiffness of the subgrade has a major effect while the degree of saturation of the subgrade is only marginally important.

An approach for estimating the stiffness of the subgrade based on the offset time of the first pulses in the deflection-time recordings in the FWD test is suggested. The most important advantage of this approach is that the stiffness of the subgrade can be determined simultaneously with performance of the FWD test. Therefore, the actual depth to bedrock and resonant depth to bedrock can be determined and the dynamic effect can be taken into account.

17. Key Words	18. Distribution Statement
Field Testing, Analytical Study, Falling Weight Deflectometer, Bedrock Depth, Backcalculated Moduli, Pavements, Subgrades	No restrictions. This document is available to the public through the National Technical Information Service, Springfield, Virginia 22161.

19. Security Classif. (of this report)	20. Security Classif. (of this page)	21. No. of Pages	22. Price
Unclassified	Unclassified	124	

EFFECT OF DEPTH TO BEDROCK ON THE ACCURACY OF BACKCALCULATED MODULI OBTAINED WITH DYNAFLECT AND FWD TESTS

by

Chia-Ray Seng
Kenneth H. Stokoe, II
José M. Roesset

Research Report 1175-5

Development of Dynamic Analysis Techniques for Falling Weight Deflectometer Data
Research Project 2/3-18-88/1-1175

conducted for the

Texas Department of Transportation

in cooperation with the

U.S. Department of Transportation
Federal Highway Administration

by the

CENTER FOR TRANSPORTATION RESEARCH
Bureau of Engineering Research
THE UNIVERSITY OF TEXAS AT AUSTIN

January 1993

IMPLEMENTATION STATEMENT

In this study, the depth to bedrock is shown to have potentially a significant adverse effect on backcalculated layer moduli in the FWD test. This adverse effect occurs around the resonant bedrock depth, the depth at which reflections from the bedrock create the largest surface motions. Backcalculated subgrade moduli obtained with FWD deflection basins at the resonant depth to bedrock underestimate the actual subgrade moduli by 20 to 50 percent. This results in the backcalculated base moduli being too high (generally 2 times the actual base moduli).

A new procedure for performing the FWD test is suggested. In this new procedure, the stiffness of the subgrade is found in a new way, the actual bedrock depth is found from free vibrations in the test, and the impact of bedrock depth is evaluated in the field. This procedure needs field verification and will require modification of the data acquisition system in the FWD device.

Prepared in cooperation with the Texas Department of Transportation and the
U.S. Department of Transportation

DISCLAIMERS

The contents of this report reflect the views of the authors, who are responsible for the facts and the accuracy of the data presented herein. The contents do not necessarily reflect the official views or policies of the Federal Highway Administration or the Texas Department of Transportation. This report does not constitute a standard, specification, or regulation.

NOT INTENDED FOR CONSTRUCTION,
BIDDING, OR PERMIT PURPOSES

Kenneth H. Stokoe, II (Texas No. 49095)
Research Supervisor

METRIC (SI*) CONVERSION FACTORS

APPROXIMATE CONVERSIONS TO SI UNITS

Symbol	When You Know	Multiply by	To Find	Symbol
	LENGTH			
in	inches	2.54	centimeters	cm
ft	feet	0.3048	meters	m
yd	yards	0.914	meters	m
mi	miles	1.61	kilometers	km
	AREA			
in^2	square inches	645.2	millimeters squared	mm^2
ft^2	square feet	0.0929	meters squared	m^2
yd^2	square yards	0.836	meters squared	m^2
mi^2	square miles	2.59	kilometers squared	km^2
ac	acres	0.395	hectares	ha
	MASS (weight)			
oz	ounces	28.35	grams	g
lb	pounds	0.454	kilograms	kg
T	short tons (2,000 lb)	0.907	megagrams	Mg
	VOLUME			
fl oz	fluid ounces	29.57	milliliters	mL
gal	gallons	3.785	liters	L
ft^3	cubic feet	0.0328	meters cubed	m^3
yd^3	cubic yards	0.0765	meters cubed	m^3

NOTE: Volumes greater than 1,000 L shall be shown in m^3.

	TEMPERATURE (exact)			
°F	Fahrenheit temperature	5/9 (after subtracting 32)	Celsius temperature	°C

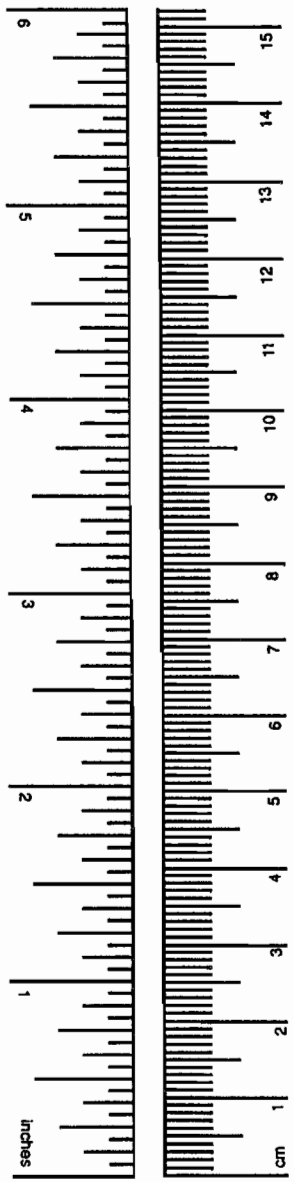

APPROXIMATE CONVERSIONS FROM SI UNITS

Symbol	When You Know	Multiply by	To Find	Symbol
	LENGTH			
mm	millimeters	0.039	inches	in
m	meters	3.28	feet	ft
m	meters	1.09	yards	yd
km	kilometers	0.621	miles	mi
	AREA			
mm^2	millimeters squared	0.0016	square inches	in^2
m^2	meters squared	10.764	square feet	ft^2
m^2	meters squared	1.20	square yards	yd^2
km^2	kilometers squared	0.39	square miles	mi^2
ha	hectares (10,000 m^2)	2.53	acres	ac
	MASS (weight)			
g	grams	0.0353	ounces	oz
kg	kilograms	2.205	pounds	lb
Mg	megagrams (1,000 kg)	1.103	short tons	T
	VOLUME			
mL	milliliters	0.034	fluid ounces	fl oz
L	liters	0.264	gallons	gal
m^3	meters cubed	35.315	cubic feet	ft^3
m^3	meters cubed	1.308	cubic yards	yd^3
	TEMPERATURE (exact)			
°C	Celsius temperature	9/5 (then add 32)	Fahrenheit temperature	°F

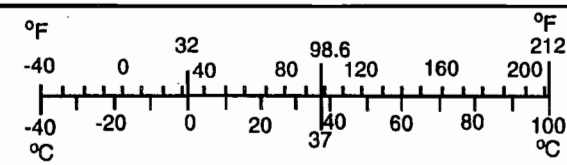

These factors conform to the requirement of FHWA Order 5190.1A.

* SI is the symbol for the International System of Measurements

TABLE OF CONTENTS

SUMMARY

Analytical simulations of the Dynaflect and Falling Weight Deflectometer (FWD) tests were performed on four typical in-service pavement profiles (three flexible pavements and one rigid pavement). Stiffnesses of the pavement surface layer, base, subbase, and subgrade were varied over ranges typical of in-service pavements. Depths to bedrock below the pavement surface varied from a few feet to over 100 feet (30 m).

The effect of depth to bedrock (also referred to as the "dynamic" effect) was expressed in terms of deflection ratios ("dynamic" deflections divided by static deflections). "Dynamic" deflections represent those deflections which are actually measured when these tests are performed on pavements. The amplitude of the deflection ratio is an important index of the potential error generated in any static interpretation procedure. The results show that the stiffness of the subgrade has the most significant effect on the maximum amplitude of the deflection ratio (deflection ratio at resonant conditions). The softer the subgrade, the higher the amplitude of the maximum deflection ratio. This behavior agrees with the trend in backcalculated layer moduli using static interpretation programs.

In the Dynaflect test, the resonant depth to bedrock (the depth to bedrock corresponding to the maximum deflection ratio) is determined predominately by the stiffness of the subgrade layer. Two sets of equations (one for the flexible pavements and one for the rigid pavement) were developed for estimating the resonant depth to bedrock based on the subgrade stiffness. For these pavements, Young's modulus of the subgrade varied from 16 to 142 ksi (0.11 to 0.98 MN/m^2), and the resonant depth to bedrock ranged from 25 to 85 feet (7.8 to 26.3 m).

As in the case of the Dynaflect test, the maximum deflection ratio at a given depth to bedrock also occurs at the farthest measurement station (station 7) in the FWD test. However, the resonant peak exhibited in the FWD deflection ratios is much wider than that in the Dynaflect test, and decreases more slowly to 1 when compared with the sharp decrease in the deflection ratio in the FWD test. The reason for these differences is that the FWD test contains a wide range in frequencies, while the Dynaflect test contains one frequency (8 Hz).

The resonant depth to bedrock obtained with the FWD test varied from 5.5 to 20 feet (1.7 to 6.2 m) when Young's modulus of the subgrade varied from 16 to 142 ksi (0.11 to 0.98 MN/m^2). These resonant depths to bedrock are much shallower than those obtained with the Dynaflect test (varied from 25 to 85 feet [7.8 to 26.3 m]). This trend occurs because the predominate frequency in the FWD test is about 30 Hz, while the frequency used in the Dynaflect test is 8 Hz. Therefore, the resonant depths to bedrock obtained with the FWD test are approximately one fourth of those obtained with the Dynaflect test. Equations for estimating the resonant depth to bedrock for the FWD test were developed for both the flexible and rigid pavements.

CHAPTER 1. INTRODUCTION

1.1 BACKGROUND

In the last two decades, nondestructive testing has become widely used for the structural evaluation of pavement systems and the backcalculation of layer moduli. Nondestructive tests for this purpose can be divided into two main categories: surface loading tests and stress wave tests. Surface loading tests are by far the most widely used. In these tests, pavement structure and layer moduli are interpreted from the load-deformation response of the pavement system. Dynamic loading devices (e.g., Road Rater, Dynaflect, and Falling Weight Deflectometer) have become popular devices for performing surface loading tests. In particular, the Falling Weight Deflectometer (FWD) has gained wide acceptance in the past decade. Some of the primary reasons for its popularity are that:

1. field operation is relatively simple, fast, and economical;
2. relatively large loads can be applied to the pavement surface; and
3. simplified procedures have been developed for depth analysis.

The other general category of nondestructive pavement tests for structural evaluation and layer moduli is stress wave tests. These tests are based on generating stress waves at one point in the pavement structure and measuring the times required for the waves to propagate to other points in the pavement structure. Some examples of stress wave tests are:

1. the impact-echo test for measuring the thicknesses of concrete slabs which are similar to the surface layer of rigid pavements (Sansalone and Carino, 1989);
2. the crosshole seismic method for evaluating the moduli of the pavement layers (Heisey, 1981); and
3. the Spectral-Analysis-of-Surface-Waves Method (SASW) for evaluating layer moduli of pavements (Nazarian and Stokoe, 1984).

Even though these methods have a strong theoretical basis, they have been used sparingly in pavement studies because they can be time consuming to use in the field, they presently require significant expertise to interpret, and they only load the pavement materials at very small strains.

In the case of surface loading tests, the main problem in pavement evaluations arises in interpretation of the field data that has been performed in the simplified analyses. The field data are motions of the pavement surface at various distances from the dynamically loaded area. Interpretation of these motions has been based on static analyses. However, the Road Rater, Dynaflect, and Falling Weight Deflectometer all load the pavement dynamically, and static analyses cannot take the dynamic response of the pavement system into account (Roesset and Shao, 1985; Uzan et al, 1989). Previous work has shown that the static and dynamic responses of a pavement may be significantly different (Davies and Mamlouk, 1985; and Roesset and Shao, 1985).

Besides dynamic effects, nonlinear behavior of the pavement, base, and subgrade may also occur in the surface loading tests. Early work performed by Nazarian and Stokoe (1987) using an approximate nonlinear characterization shows that nonlinear behavior in the base and subgrade can be significant at large amplitude loadings, such as the 20-kip (89 kN) load applied in the FWD test. Chang et al (1992), using refined nonlinear models combined with a finite element analysis, conducted a series of studies on the effects of nonlinear behavior on the dynamic response of pavements. They showed that nonlinear behavior can be significant and localized around a heavily loaded area if testing is performed on a flexible pavement with a rather thin surface layer and a soft subgrade. However, they also showed that only the dynamic response of the pavement system needs to be considered at small to intermediate loads for many pavement systems, and that very little nonlinearity can be generated in heavy, rigid pavements.

1.2 OBJECTIVES

The main objective of this study is to investigate the importance of dynamic loading in surface loading tests. Two surface loading tests, the Dynaflect and Falling Weight Deflectometer, have been investigated using computer programs developed by J. M. Roesset and his graduate students at The University of Texas at Austin (Chang, 1991; Chang et al, 1992). Testing was simulated at pavement profiles modeled after four pavement systems in Texas. The dynamic character of the surface loading tests was properly taken into account in these analytical studies. Therefore, surface motions measured under the dynamic loads could be compared with movements which would be determined by a static analysis of the surface test, as presently done in the profession.

For both Dynaflect and FWD tests, the deflection basins obtained from the dynamic surface loading were compared with deflection basins which would be obtained if a static loading had occurred. The differences between the basins were studied because they imply the magnitude of errors which result from backcalculation of moduli by static interpretations. As it turns out, the depth to bedrock (distance from the pavement surface to the top of bedrock) is an important factor in dynamic surface loading tests. Depth to bedrock was, therefore, also studied by using the four model pavement systems and varying the thickness of the subgrade in each pavement system.

1.3 ORGANIZATION

The test methods, model profiles, and computer analyses are presented in Chapter 2.

Parametric studies on the effect of depth to bedrock on the pavement motions measured in the Dynaflect and FWD tests are presented in Chapter 3 and Chapter 4, respectively. The differences of dynamic motions and static motions are expressed in terms of deflection ratios; that is, the dynamic deflections measured during testing divided by the deflections under an equivalent static load (called the static deflections). For each test, variations in the amplitude of deflection ratios with various depths to bedrock and different stiffness combinations of the pavement layers are presented.

To aid in identifying problems in applying the Dynaflect and FWD tests at sites with shallow bedrock conditions, equations to predict the depth to bedrock where the maximum dynamic effect will occur is suggested for the Dynaflect test in Chapter 3 and for the FWD test in Chapter 4. An approach to determining if bedrock conditions are adversely affecting the FWD measurements in the field and an approach to estimating the depth to bedrock from the free vibration of the pavement system in extended deflection-time records in the FWD test are also developed in Chapter 4. Finally, a new way of estimating the stiffness of the subgrade from the time lag between deflections measured at station 5 and station 7 in the FWD test is presented in Chapter 4.

Potential errors in layer moduli from backcalculations based on static analyses can be related to the magnitude of the deflection ratios. These errors were investigated in the FWD test with the aid of the static analysis program, MODULUS (Uzan et al, 1989). These results are presented in Chapter 5.

Conclusions and recommendations for use in field testing with the Dynaflect and FWD tests are presented in Chapter 6.

CHAPTER 2. TEST METHODS, MODEL PROFILES AND COMPUTER ANALYSES

2.1 INTRODUCTION

The two surface loading tests which were studied analytically herein are the Dynaflect and FWD tests. The characteristics of each loading system which were modeled are discussed in this chapter. The pavement profiles that were used in the studies are then presented. Finally, the assumptions and limitations of the computer programs used in these studies are discussed.

2.2 TEST METHODS

The Dynaflect was the first nondestructive test studied. The loading system of the Dynaflect consists of two counter-rotating eccentric masses, each of which generates a 500-pound (2.24-kN) harmonic (steady-state) load at a frequency of 8 Hz. The deflection basin is measured with five vertical velocity transducers spaced at 12-inch (30 cm) intervals along a center line. The position of the geophones (vertical velocity transducers) with respect to the loading wheels is shown schematically in Figure 2.1a.

The FWD was the second nondestructive test studied. The analyses that were conducted used the FWD test more often than the Dynaflect test because the FWD test is more widely used. The FWD test has a hydraulically lifted drop weight that generates an impulsive force on the pavement surface. The resulting deflections are measured by a set of seven vertical velocity transducers. The configuration of the FWD test is shown schematically in Figure 2.1b. The simplified loading history of the FWD test and its corresponding load spectrum are shown in Figure 2.2. It should be noted that the peak magnitude of the load is taken as one unit, where the unit can be 1 pound (0.44 N). Since a linear system is assumed (see Section 2.4), one only has to multiply the calculated deflections by the magnitude of the actual load to obtain the actual deflections that would be measured under that load, assuming no nonlinear behavior.

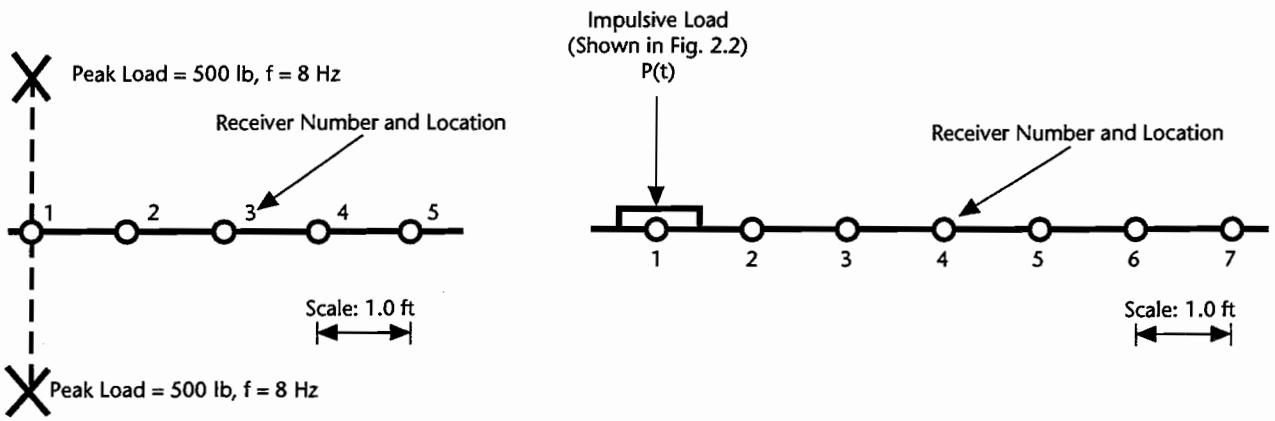

(a) Plan view of Dynaflect test

(b) Cross-sectional view of FWD test

Figure 2.1 Schematic configurations of Dynaflect and FWD tests

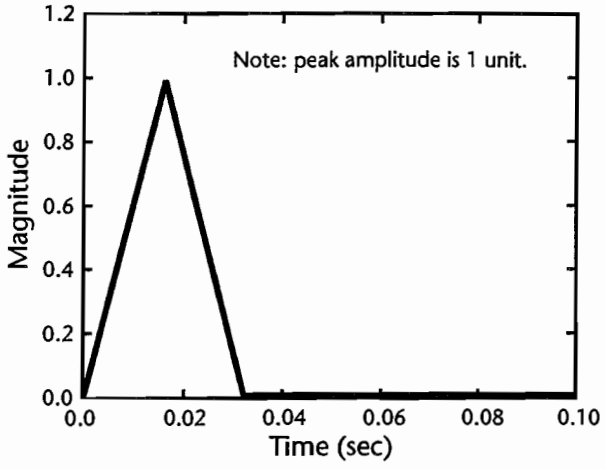

(a) Loading history of FWD test

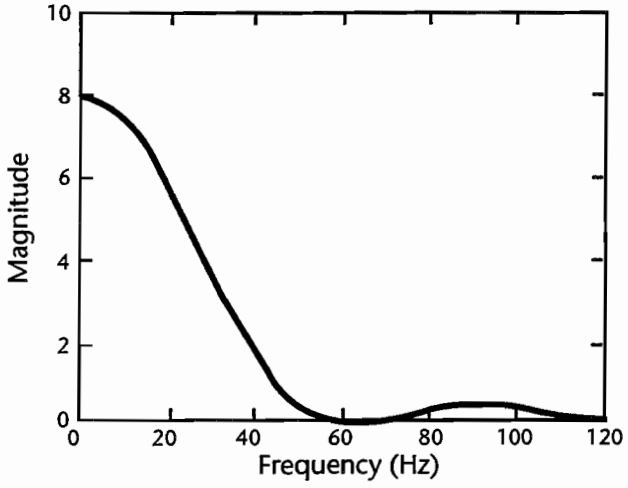

(b) Load spectrum of FWD test

Figure 2.2 ***Simplified loading history of FWD test and its corresponding load spectrum (from Chang, 1991)***

2.3 MODEL PROFILES

Four typical in-service Texas highways were selected for use as models in these analyses. They are: FM137 (Profile 1) near Paris, FM195 (Profile 2) near Paris, Route 1 (Profile 3) near Austin, and Interstate Highway 10 (Profile 4) near El Paso. Each profile is modeled as a horizontally layered stratum which is infinitely wide. The infinite width has essentially no effect on the results from surface loading tests, as long as the test is performed at least 4 feet (1.2 m) from the pavement edge (Kang, 1990; Kang et al, 1991). Therefore, all tests on these model profiles are assumed to meet the above requirement.

The idealized cross-sections of the four test profiles are illustrated in Figure 2.3. Three of the profiles (Profiles 1, 2, and 3) are flexible pavement systems composed of an asphalt concrete (AC) layer, a granular base, and a soil subgrade. Profile 4 is a rigid pavement system which is composed of a continuously reinforced concrete (CRC) layer, an AC base, a granular subbase, and a soil subgrade. The material properties of the four pavement profiles are given in Table 2.1. As can be seen in the table, the thicknesses of all layers except the subgrade layer were fixed. The thickness of the subgrade layer was varied from 5 to 120 feet (1.5 to 36 m) for the study of the Dynaflect test, and varied from 5.5 to 90 feet (1.7 to 27.4 m) for the study of the FWD test. A smaller range of depth to bedrock was used in the study of the FWD test because the resonant conditions of the FWD test occur at shallow depths.

The stiffnesses of the pavement layers were varied in these studies. The stiffnesses used in the Dynaflect and FWD studies are presented in Chapter 3 and Chapter 4, respectively.

2.4 COMPUTER ANALYSES

Computer programs UTDYNF and UTFWD were used in the Dynaflect and FWD studies, respectively. These programs were developed by J. M. Roesset and Der-Wen Chang at The University of Texas at Austin (Chang, 1991; Chang et al, 1992). Both UTDYNF and UTFWD use a Green's flexibility influence function to simulate the dynamic response corresponding to a vertical disk load applied on a simplified pavement system. In the computer programs, the pavement profiles are modeled as an axisymetric and horizontally layered stratum. The effect of finite width cannot be taken into account. As mentioned in Section 2.3, Kang et al (1991) suggested that, as long as the test is conducted 4 feet (1.2 m) from the edge of pavement, the effect of finite width is insignificant. Hence, it will be assumed that all testing modeled herein is performed at least 4 feet (1.2 m) from the edge of the pavement (or any significant joint or crack).

To backcalculate layer moduli from the static and dynamic motions predicted with UTFWD, a microcomputer-based program developed for the Texas Department of Transportation was used. This program, named MODULUS (Uzan et al, 1989), is capable of backcalculating pavement layer moduli from the deflection basins obtained with the FWD test. As with UTFWD, it uses a linear elastic approach. However, one of the key aspects of MODULUS is that it involves a static interpretation method to backcalculate layer moduli. The dynamic characteristic of the FWD is thus ignored.

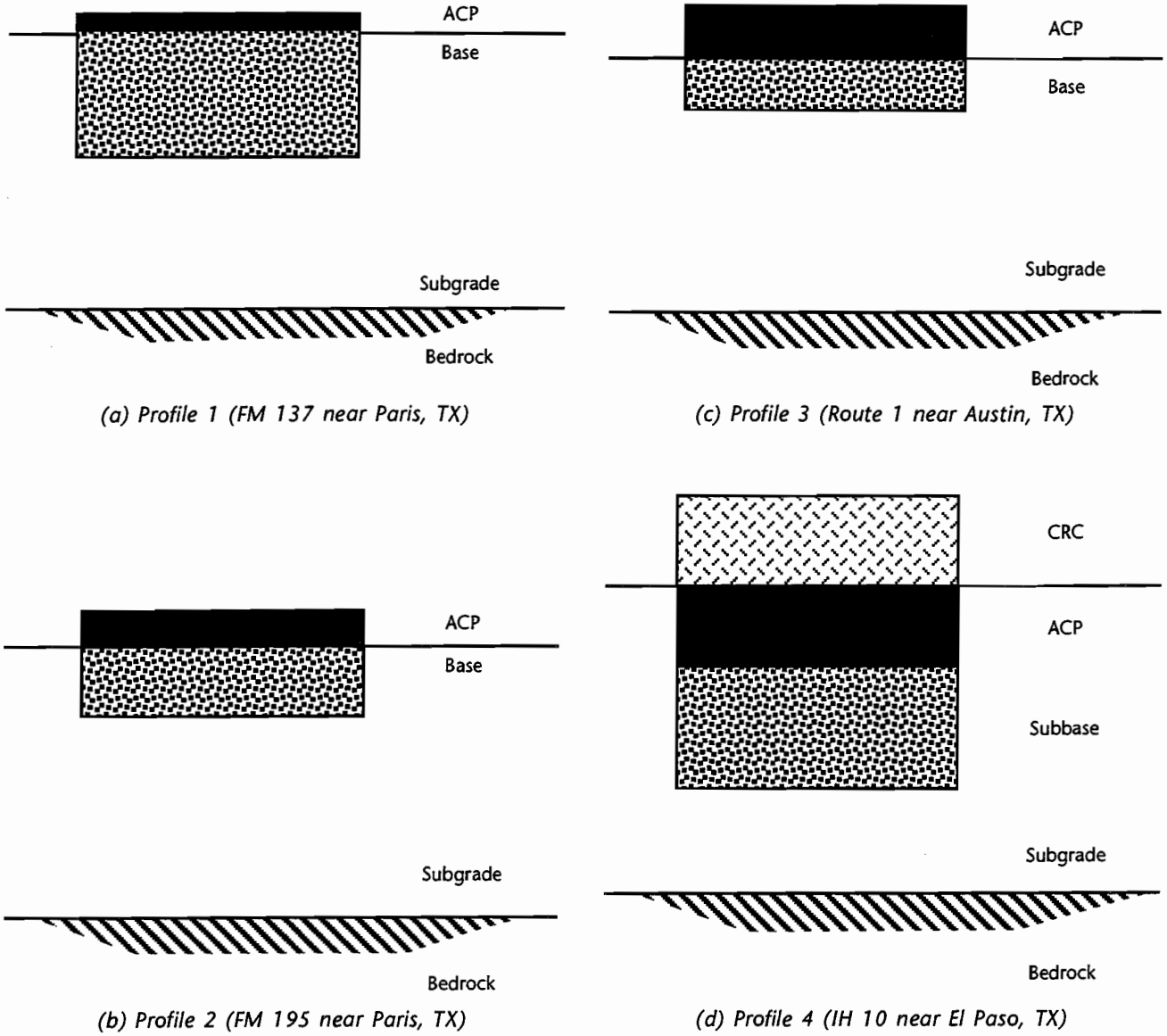

Figure 2.3 Idealized cross-sections of the four pavement profiles

Table 2.1 Material properties of the four pavement profiles

Profile No.	Modelled After	Material Type	Thickness (in.)	Poisson's Ratio	Unit Weight (pcf)	Damping Ratio
1	FM137 (near Paris, Tx)	ACP	1	0.27	140	0.02
		Base	12	0.25	125	0.02
		Subgrade	*	0.33	125	0.02
2	FM195 (near Paris, Tx)	ACP	4	0.27	140	0.02
		Base	6	0.25	125	0.02
		Subgrade	*	0.33	110	0.02
3	Route 1 (near Austin, Tx)	ACP	7	0.27	145	0.02
		Base	6	0.25	130	0.02
		Subgrade	*	0.33	130	0.02
4	IH10 (near El Paso, Tx)	CRC	10	0.2	145	0.02
		AC Base	6	0.27	145	0.02
		Subbase	12	0.25	125	0.02
		Subgrade	*	0.33	125	0.02

* Subgrade thickness was varied from 5 to 120 ft for the Dynaflect test and was varied from 5.5 to 90 ft for the FWD test.

CHAPTER 3. PARAMETRIC STUDY OF THE DYNAFLECT TEST

3.1 INTRODUCTION

Analytical simulations of the Dynaflect test were conducted using computer program UTDYNF (Chang, 1991; Chang et al, 1992). The four pavement profiles shown in Figure 2.2 were studied. The main purposes of these studies were:

1. to determine the resonant depth to bedrock with various stiffness combinations of pavement layers,
2. to develop an equation for estimating the resonant depth to bedrock, the depth where use of a static interpretation method involves the largest errors, and
3. to study the variations of the deflection ratios (pavement surface motions under dynamic loading divided by surface motions under an equivalent static load) as a function of various stiffness combinations of pavement layers.

3.2 MODEL PARAMETERS

The material properties of the four pavement profiles are given in Table 2.1. The stiffness of each pavement layer is represented by its shear wave velocity (V_s) and Young's modulus (E). The relationship between V_s and E can be expressed by:

$$E = 2 * (1 + \nu) * \rho * V_s^2 \qquad (3.1)$$

where ν = Poisson's ratio, and
ρ = mass density of the material (total unit weight divided by gravitational acceleration).

Young's modulus of the subgrade layer was varied from 16 to 142 ksi (0.11 to 0.98 MN/m^2) (V_s = 500 to 1500 fps (125.5 to 457.5 m/s)) to simulate variations in subgrade material, density, and moisture content. Young's modulus of the granular base or granular subbase was varied from 70 to 300 ksi (0.48 to 2.07 MN/m^2) (V_s = 1000 to 2000 fps (305 to 610 m/s)) to consider the effects of moisture and density changes. Young's modulus of the asphalt concrete layer was varied from 312 to 1920 ksi (2.15 to 13.2 MN/m^2) (V_s = 2000 to 5000 fps (610 to 1525 m/s)) to consider the effects of temperature and density changes on the asphalt. The stiffness of the CRC was the only pavement layer not varied. Young's modulus of the CRC was set to a constant value of 5425 ksi (37.4 MN/m^2) (V_s = 8500 fps (2592.5 m/s)).

The ranges of stiffnesses used for the pavement layers are listed in Table 3.1. The depth to bedrock at each profile was varied from 5 to 120 feet (1.5 to 36.6 m) in increments of 2.5 feet (0.76 m). This depth is the distance from the top of the pavement surface to the top of bedrock.

Table 3.1 ***Ranges in stiffnesses used for the pavement layers in the four pavement profiles***

Material Type	Shear Wave Velocity (fps)	Assumed Poisson's Ratio	Approx. Young's Modulus* (ksi)
CRC	8,500	0.20	5,425
Asphalt Concrete	2,000	0.27	312
	3,000	0.27	690
	4,000	0.27	1,225
	5,000	0.27	1,920
Granular Base or Subbase	1,000	0.25	67
	1,500	0.25	152
	2,000	0.25	270
Subgrade	500	0.33	16
	750	0.33	36
	1,000	0.33	63
	1,500	0.33	142

3.3 DEFLECTION BASINS

Deflection basins were obtained with computer program UTDYNF for both static and dynamic loadings. For static loading, a very small

frequency (0.75 Hz) was used. For dynamic loading, a frequency of 8 Hz was used. A typical plot of the dynamic deflections at the Dynaflect measurement stations as a function of depth to bedrock is shown in Figure 3.1a. A similar plot of static deflections as a function of depth to bedrock is shown in Figure 3.1b. The ratios of dynamic deflections to static deflections are called the deflection ratios and are shown in Figure 3.1c. The depth to bedrock corresponding to the maximum deflection ratio is called the resonant depth to bedrock.

First consider the variation in static deflections with depth to bedrock as shown for Profile 1 in Figure 3.1b. Initially, static deflections at all measurement stations increase as subgrade thickness increases, simply because a thicker section of subgrade material is being strained. This effect is very pronounced for depths to bedrock ranging from 5 to about 15 feet (1.5 to 4.6 m). As the thickness of the subgrade increases above 15 feet (4.6 m), the effect decreases significantly because of the stress distribution associated with a small loaded area. Any backcalculation method based on a static interpretation of the Dynaflect assumes exactly this response (Figure 3.1b).

On the other hand, the dynamic loading from the Dynaflect results in the surface measurement stations changing with depth to bedrock as shown in Figure 3.1a. For shallow depths to bedrock, say 5 to 15 feet (1.5 to 4.6 m) in Profile 1, surface dynamic motions increase more rapidly than the static motions as the subgrade thickness increases. More importantly, this increase is followed by a predominate peak which, in turn, is followed by a decrease in dynamic motions. This significant peak in the dynamic motions occurs in the bedrock depth range of 15 to 35 feet (4.6 to 10.7 m). This is the dynamic amplification effect. At depths greater than about 40 feet (12.2 m), the dynamic deflections are quite similar to the static deflections. This dynamic behavior is easily seen in the deflection ratio as a function of depth to bedrock in Figure 3.1c.

The significant amplifications in the dynamic motions compared with the static motions are easily seen in bedrock depth ranges of about 10 to 30 feet (3.1 to 9.2 m) for Profile 1 with a soft subgrade layer (E = 16 ksi (0.11 MN/m^2)). Moreover, the maximum deflection ratio always occurs at the farthest measurement station (station 5), which indicates that the further away from the source the measurement station is in the Dynaflect test, the larger the relative dynamic effect is.

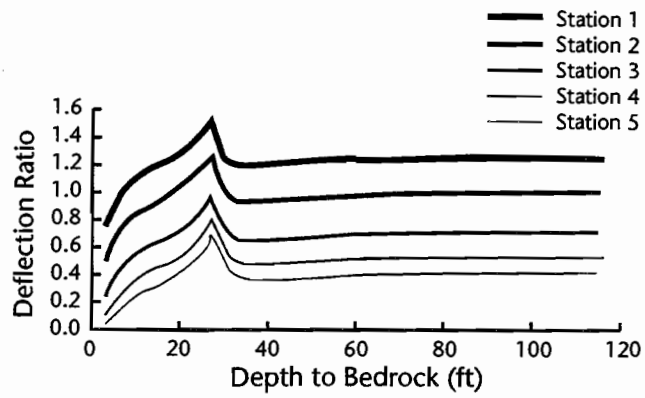

(a) Dynamic deflections

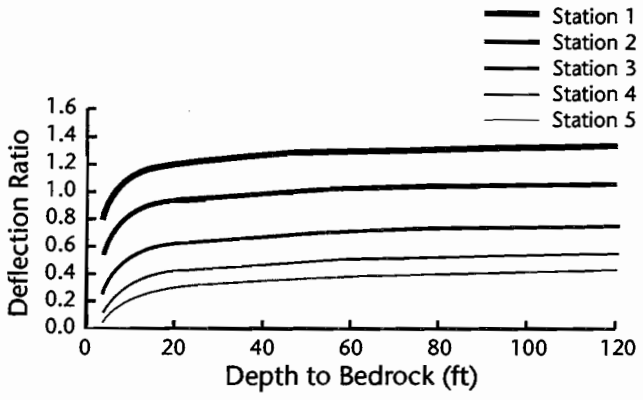

(b) Static deflections

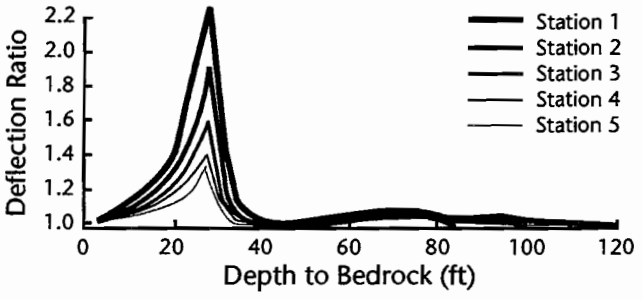

(c) Deflection ratios

Figure 3.1 ***Delfection basins and deflection ratios as a function of depth to bedrock obtained for Dynaflect testing at Profile 1 (E of AC = 312 ksi, E of base = 67 ksi, and E of subgrade - 16 ksi)***

Dynamic and static deflection basins as a function of distance from the source obtained at the peak deflection ratio (termed the resonant depth to bedrock) are shown in Figures 3.2 and 3.3 for Profile 1 (flexible pavement) and Profile 4 (rigid pavement), respectively. As can be seen, the dynamic deflections at all measurement stations are approximately 0.35 mils (0.0089 mm) larger than the static deflections for the soft

subgrade condition in Profile 1, as shown in Figure 3.2a. This difference represents more than a 100 percent difference (error) in the static measurement at station 5 and about a 30 percent difference at station 1. These differences are clearly shown by the deflection ratios in Figure 3.1c.

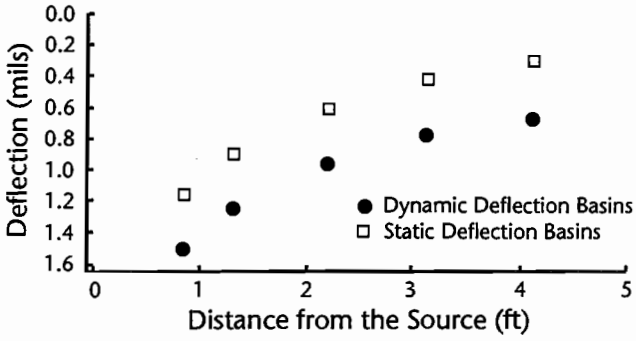

(a) S-wave velocity of subgrade = 500 fps (E = 16 ksi)

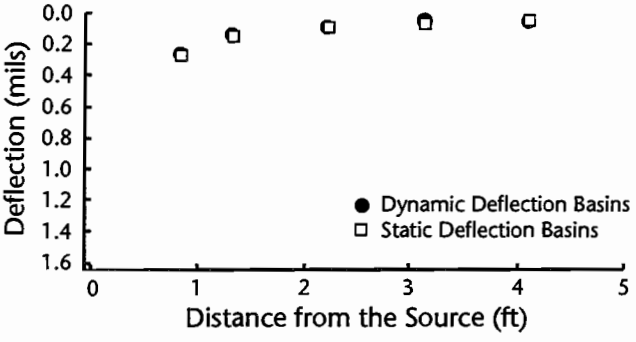

(b) S-wave velocity of subgrade = 1,500 fps (E = 142 ksi)

Figure 3.2 Dynamic and static deflection basins obtained at the resonant depth to bedrock for Dynaflect testing at profile 1 (V_s of AC = 3,000 fps (E = 690 ksi), V_s of base = 1,000 fps (E = 647 ksi))

When the stiffest subgrade condition is used at Profile 1, the dynamic deflections are only about 0.018 mils (0.000046 mm) larger than the static deflections, as shown in Figure 3.2b. In this case, the difference between dynamic and static deflections ranges from about 17 percent at station 5 to about 7 percent at station 1. These differences are shown by the deflection ratios in Figure A.1d.

For Profile 4, there is less variation in the deflection basins with distance from the source than in Profile 1. This response can be seen by comparing Figures 3.2a and 3.3a. This occurs because Profile 4 represents a rigid pavement while Profile 1 represents a very flexible pavement. However, there is still a significant difference between the static and dynamic deflection basins for Profile 4 with the softest subgrade condition. This difference is about 0.4 mils (0.0102 mm) at the resonant bedrock depth (Figure 3.3a) and represents about a 175 percent difference at station 5 and 120 percent difference at station 1. There is little difference (less than 16 percent) between the dynamic and static deflections for the stiffest subgrade condition at Profile 4, as shown in Figure 3.3b.

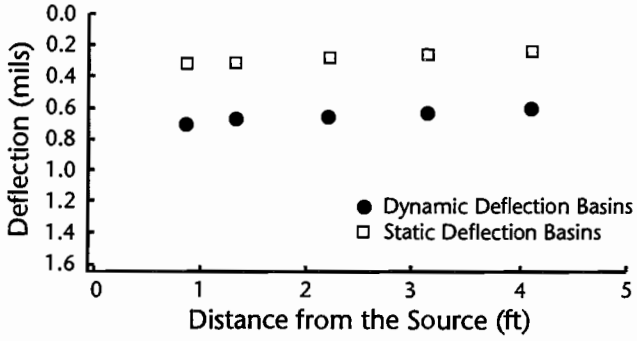

(a) S-wave velocity of subgrade = 500 fps (E = 16 ksi)

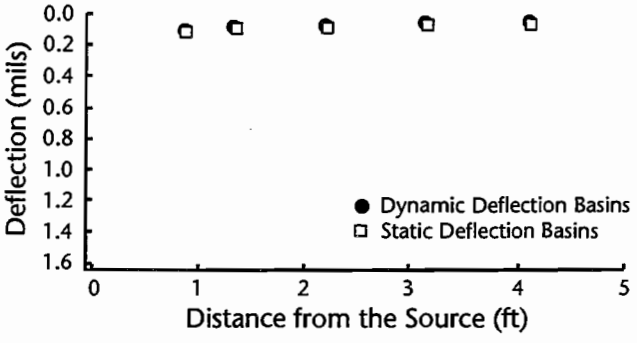

(b) S-wave velocity of subgrade = 1,500 fps (E = 142 ksi)

Figure 3.3 Dynamic and static deflection basins obtained at the resonant depth to bedrock for Dynaflect testing at Profile 4 (V_s of CRC = 8,500 fps (E = 5425 ksi), V_s of AC = 3,000 fps (E = 690 ksi) and V_s of subbase = 1,000 fps (E = 67 ksi))

The complete results of all simulations of the Dynaflect test with various stiffness combinations for the four pavement profiles are presented in Appendix A, Figures A.1 through A.48. These results are discussed in more detail in the next two sections.

3.4 RESONANT DEPTH TO BEDROCK

As shown in Section 3.3, use of a static interpretation method with the deflection basins obtained from Dynaflect tests with bedrock depths near the resonant depth can lead to significant errors in the deflections and, hence, to significant

errors in the backcalculations of layer moduli. (The magnitude of the errors in the backcalculations is studied in Chapter 5 with regard to the FWD test and are not studied with regard to the Dynaflect test.) Therefore, it is important to know the resonant depth to bedrock and how it varies with various stiffness combinations of the pavement layers.

The resonant bedrock depths as a function of the various stiffness combinations for Profile 1 are shown in Figure 3.4. It is interesting to find that the resonant depths to bedrock are predominately determined by the stiffness of the subgrade layer. The variations of the stiffnesses of the AC and granular base layers have little effect on the resonant depths to bedrock. For instance, in Figure 3.4c, for a subgrade with shear wave velocity of 1000 fps (305 m/s) (corresponding to E = 63 ksi (0.43 MN/m^2)), the resonant depths ranged from 55 to 57.5 feet (16.8 to 17.5 m), while the stiffnesses of the base varied by four and the stiffnesses of the asphalt varied by about six. On the other hand, when the stiffness of the subgrade was increased by 2.25 times (going from E = 63 ksi to E = 142 ksi (0.43 to 0.98 MN/m^2)), the average resonant depth increased from 56 feet (17.1 m) (Figure 3.4c) to 85 feet (26.0 m) (Figure 3.4d). This comparison clearly illustrates the importance of the stiffness of the subgrade in Profile 1.

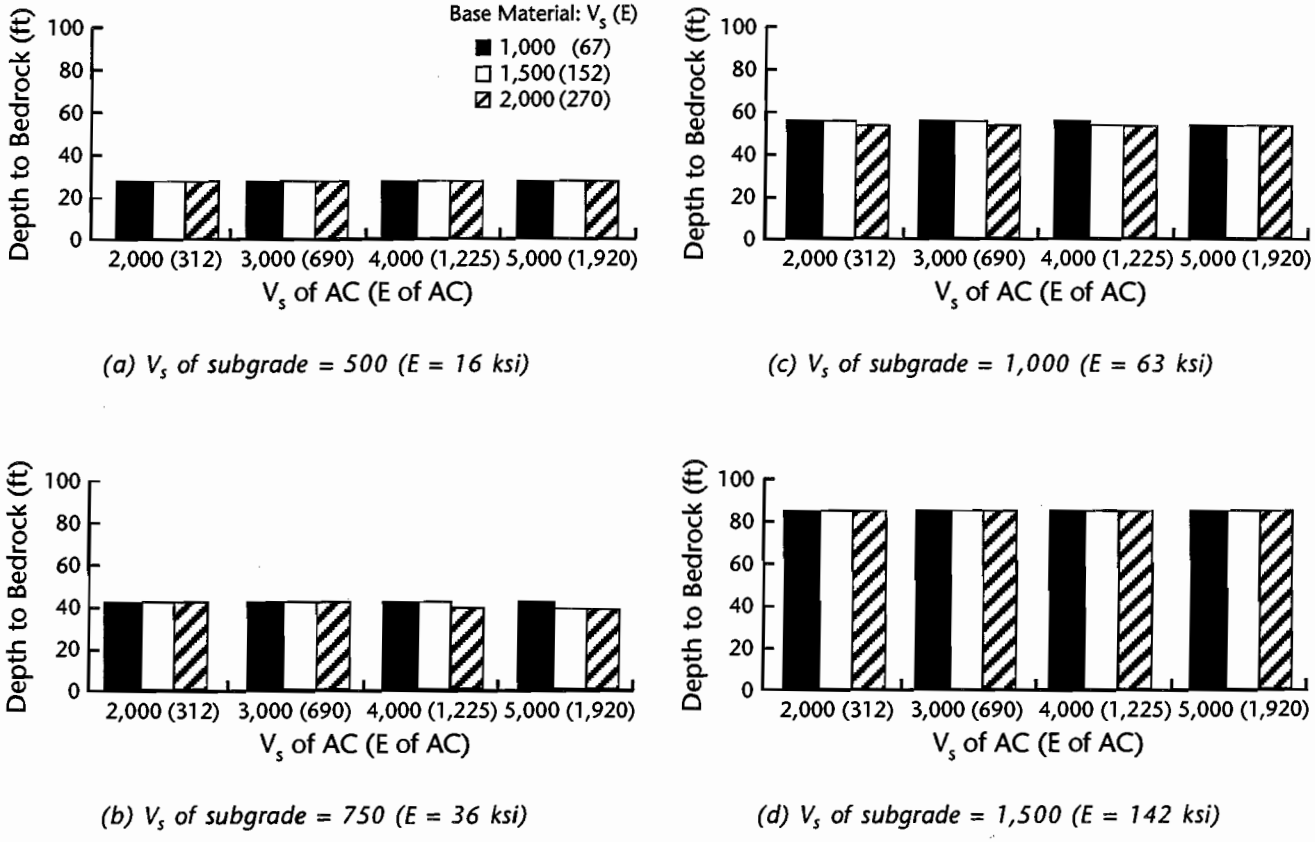

(a) V_s of subgrade = 500 (E = 16 ksi)

(c) V_s of subgrade = 1,000 (E = 63 ksi)

(b) V_s of subgrade = 750 (E = 36 ksi)

(d) V_s of subgrade = 1,500 (E = 142 ksi)

***Figure 3.4** Resonant depths to bedrock for Dynaflect testing at Profile 1 with various stiffness combinations of the pavement layer (units: V_s = fps, E = ksi)*

A similar importance of the subgrade stiffness in the resonant depths to bedrock was found for the other three pavement profiles, as shown in Figures 3.5, 3.6, and 3.7. A list of the ranges in depths and average depths for all profiles is given in Table 3.2. As one can see in the table, Profile 4, which is a rigid pavement, exhibits slightly shallower resonant depths to bedrock compared with the other pavement profiles. The resonant depths are about 3 percent to 9 percent less than the other profiles and result from Profile 4 being composed of the stiffest and thickest surface layers.

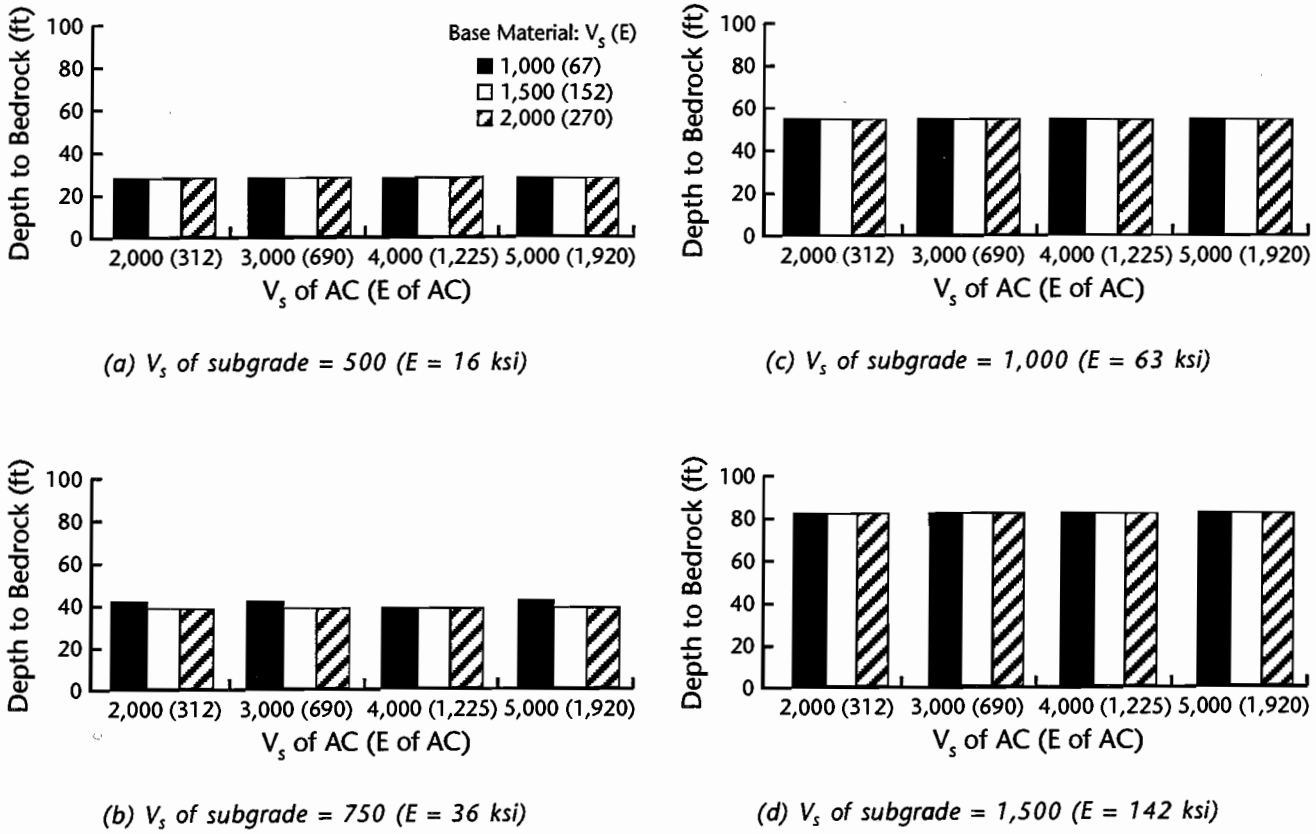

(a) V_s of subgrade = 500 (E = 16 ksi)

(c) V_s of subgrade = 1,000 (E = 63 ksi)

(b) V_s of subgrade = 750 (E = 36 ksi)

(d) V_s of subgrade = 1,500 (E = 142 ksi)

Figure 3.5 ***Resonant depths to bedrock for Dynaflect testing at Profile 2 with various stiffness combinations of the pavement layer (units: V_s = fps, E = ksi)***

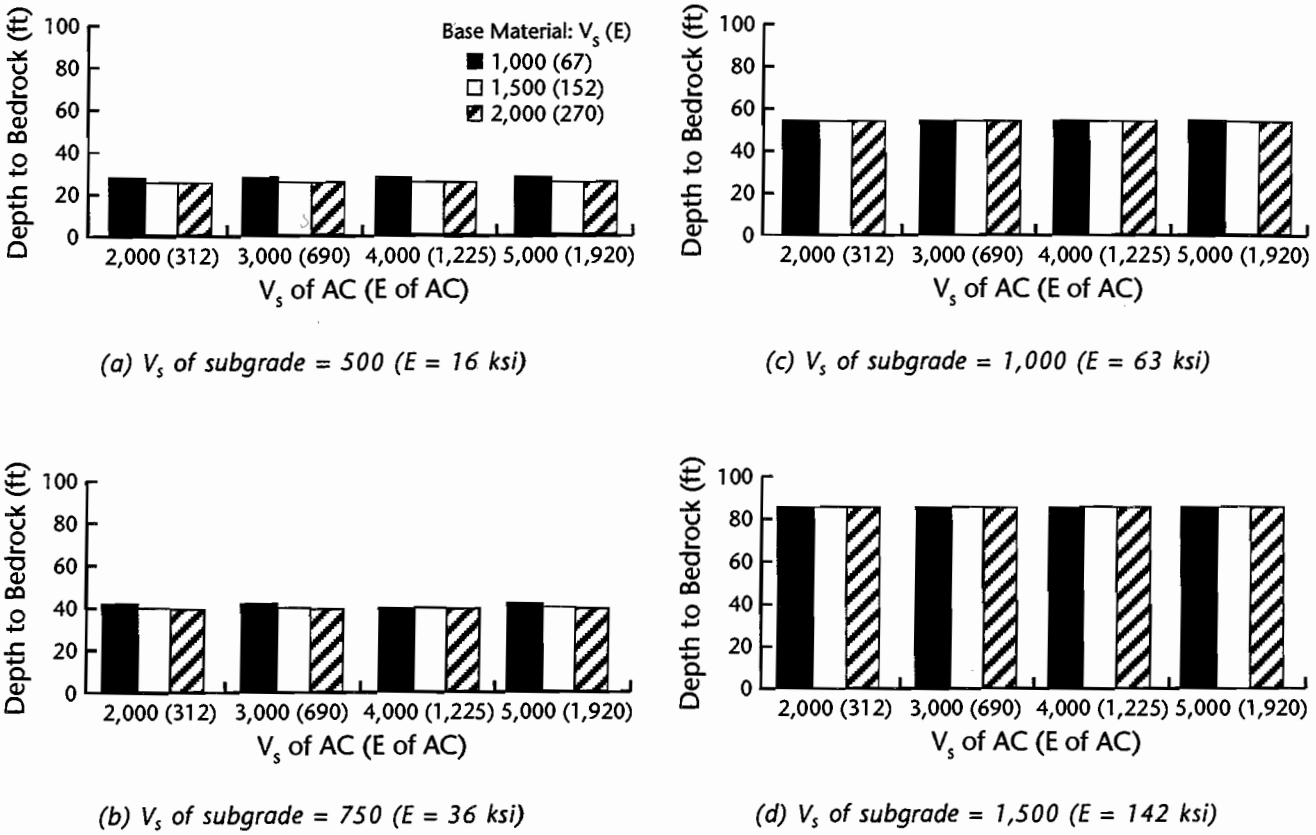

Figure 3.6 ***Resonant depths to bedrock for Dynaflect testing at Profile 3 with various stiffness combinations of the pavement layer (units: V_s = fps, E = ksi)***

To develop an equation for predicting the resonant depth to bedrock, the average resonant depth to bedrock (RDb) for each profile for each subgrade stiffness was plotted versus the subgrade shear wave velocity, as shown in Figure 3.8. This was done because the stiffnesses of the other layers had little effect on the results. As can be seen, the results appear to form two groups, one is for Profiles 1, 2, and 3 (all are flexible pavements) and the other is Profile 4 (the rigid pavement). Two straight lines were fitted through the two data groups, which resulted in:

$$RDb = 0.056V_s \tag{3.2}$$

for the flexible pavements with the resonant depth to bedrock, RDb, in feet and V_s in feet per second (fps). For the rigid pavement, the equation becomes:

$$RDb = 0.052V_s \tag{3.3}$$

with RDb in feet and V_s in fps. Equation 3.1 and 3.2 can be expressed in term of Young's modulus as:

$$RDb = 0.019\sqrt{E} \tag{3.4}$$

for the flexible pavement with the unit weight of the subgrade material assumed to be 110 pounds per cubic foot (pcf), Poisson's ratio assumed to be 0.33, RDb in feet and E in pounds per square foot (psf), and

$$RDb = 0.017\sqrt{E} \tag{3.5}$$

for the rigid pavements with RDb in feet and E in psf.

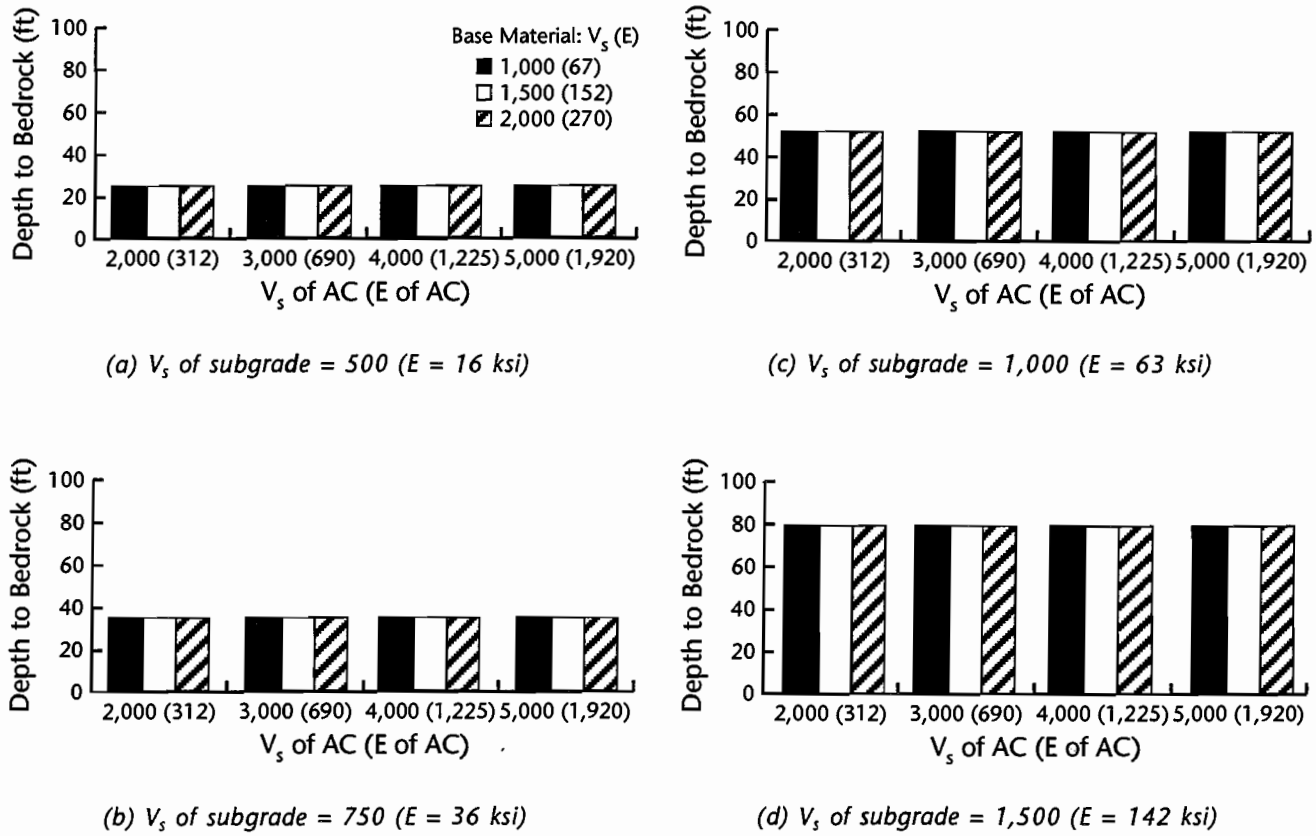

Figure 3.7 ***Resonant depths to bedrock for Dynaflect testing at profile 4 with various stiffness combinations of the pavement layer (units: V_s = fps, E = ksi)***

Table 3.2 ***Variations in the average resonant depths to bedrock obtained with dynaflect testing at the four pavement profiles***

Shear Wave Velocity of Subgrade (fps)	Approximate Young's Modulus (ksi)	Range in Depths (ft)	Resonant Depth to Bedrock* (ft)			
			Profile 1 FM137	Profile 2 FM195	Profile 3 Route 1	Profile 4 IH 10
500	16	Maximum	27.50	27.50	27.50	25.00
		Minimum	27.50	27.50	25.00	25.00
		Average	27.50	27.50	25.83	25.00
750	36	Maximum	42.50	42.50	42.50	37.50
		Minimum	40.00	40.00	40.00	37.50
		Average	40.79	41.25	40.83	37.50
1,000	63	Maximum	57.50	57.50	55.00	52.50
		Minimum	55.00	55.00	55.00	52.50
		Average	56.04	56.04	55.00	52.50
1,500	142	Maximum	85.00	85.00	85.00	80.00
		Minimum	85.00	85.00	85.00	80.00
		Average	85.00	85.00	85.00	80.00

* The depth represents the thickness from the pavement surface to the top of the bedrock.

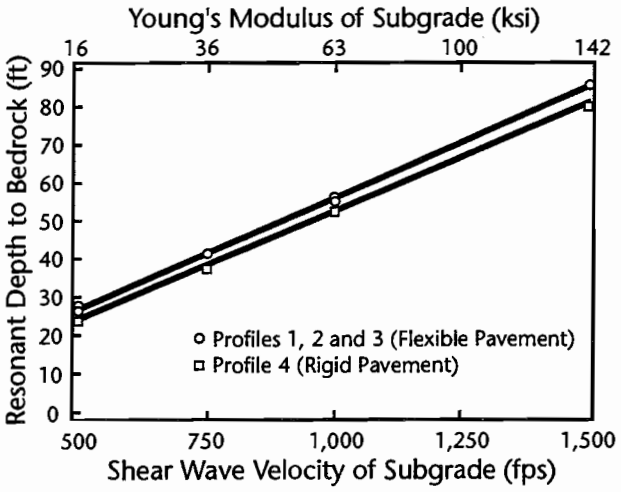

Figure 3.8 ***Average resonant depth to bedrock versus the stiffness of the subgrade obtained with Dynaflect testing at the four pavement profiles***

Davies and Mamlouk (1985) conducted an analytical investigation for the Road Rater test, which is also a steady-state surface loading test, on a rigid pavement profile. They developed the following equation for predicting the resonant thickness of subgrade (H):

$$H = 0.4 * \frac{V_s}{f} \qquad (3.6)$$

with H in feet, V_s in fps, and f in Hz.

In order to compare with the equation suggested by Davies and Mamlouk (1985), the resonant depth to bedrock (RDb) was expressed in terms of the resonant thickness of the subgrade (H) as a function of the shear wave velocity of subgrade, as shown in Figure 3.9. Again, the results form clearly two groups: one for the flexible pavements (Profiles 1, 2, and 3) and the other for the rigid pavement (Profile 4) (Fig. 3.9a). Two straight lines were fitted through the two data groups, which resulted in:

$$H = 0.055V_s \qquad (3.7)$$

for the flexible pavement with H in feet , and V_s in fps, and

$$H = 0.05V_s \qquad (3.8)$$

for the rigid pavement, with H in feet and V_s in fps. Following the approach used by Davies and Mamlouk (1985), Equation 3.8 can be expressed in terms of frequency (f) as:

$$H = 0.4 * \frac{V_s}{f} \qquad (3.9)$$

which is identical to the equation proposed by Davies and Mamlouk (1985).

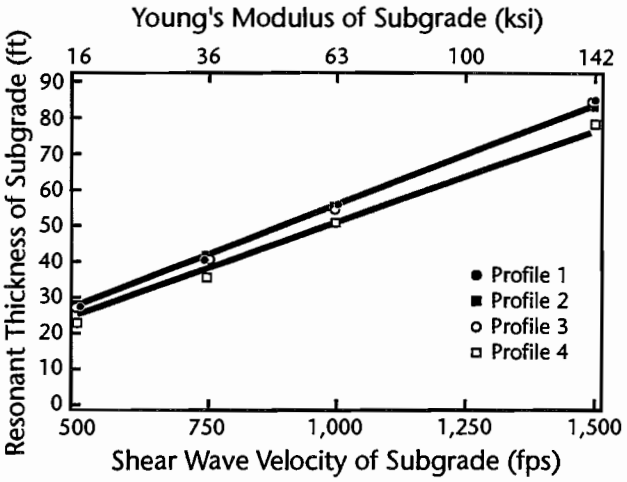

Figure 3.9 ***Average resonant thickness of subgrade versus the subgrade stiffness obtained with Dynaflect testing at the four pavement profiles***

3.5 AMPLITUDE OF THE MAXIMUM DEFLECTION RATIO

As discussed earlier, the amplitude of the deflection ratio (dynamic deflection divided by static deflection) at each Dynaflect measurement station is an important index of the potential error generated in any static interpretation procedure (as discussed in Chapter 5 for the FWD test). Figure 3.10 shows the maximum deflection ratios as a function of various stiffnesses combinations of Profile 1. It should be noted that the maximum ratios are for measurements at station 5. Variations of the stiffnesses of the AC and base layers have little effect on the values of the maximum deflection ratio, as shown in Table 3.3. For example, if V_s of the AC varies from 2000 to 5000 fps (610 to 1525 m/s) (E = 312 to 1920 ksi (2.15 to 13.2 MN/m^2)), the deflection ratio only varies from 2.24 to 2.04 (approximately a 10 percent decrease) when V_s of the base is 1000 fps (305 m/s) (E = 70 ksi (0.48 MN/m^2)) and V_s of the subgrade is 500 fps (152.5 m/s) (E = 16 ksi (0.11 MN/m^2)),

as shown in Figure 3.10a. Moreover, if V_s of the base varies from 1000 to 2000 fps (305 to 610 m/s) (E = 67 to 270 ksi (0.46 to 1.86 MN/m^2)), the deflection ratio varies from 2.24 to 1.98 (approximately a 13 percent decrease) when V_s of the AC is 2000 fps (610 m/s) (E = 270 ksi (1.86 MN/m^2)) and V_s of the subgrade is 500 fps (152.5 m/s) (E = 16 ksi (0.11 MN/m^2)), as shown in Figure 3.10a.

Variations in the stiffness of the subgrade layer have the most significant effect on the amplitudes of the maximum deflection ratios. If V_s of the subgrade varies from 500 to 750 fps (152.5 to 228.8 m/s) (E = 16 to 36 ksi (0.11 to 0.25 MN/m^2)), there is an approximately 17 percent decrease in the deflection ratios. If V_s of the subgrade varies from 500 to 1500 fps (125.5 to 457.5 m/s) (E =16 to 142 ksi (0.11 to 0.98 MN/m^2)), there is a 50 percent reduction in the deflection ratios. Again, it is important to keep in mind that the deflection ratio at station 5 is being discussed above and changes in the deflection ratio are considerably less for station 1 (and other stations), as shown in Appendix A. However, station 5 is critical in backcalculating layer moduli and, hence, was chosen for discussion.

Profile 2 and Profile 3 exhibit trends similar to those of Profile 1 (Figures 3.11 and 3.12). For Profile 4, the amplitudes of the deflection ratios obtained at the softest subgrade condition are about 50 percent higher than those obtained at Profiles 1, 2, and 3. This relationship is only true for the softest subgrade at Profile 4, as shown in Table 3.3. For the three other subgrade stiffnesses, the deflection ratios are about equal to or slightly less than those at Profiles 1, 2, and 3 (see Table 3.3 and Figure 3.3). It is interesting to see that the deflection ratios of Profile 4 are larger than the other three pavements for the softest subgrade because Profile 4 has the thickest and the stiffest upper layers (Figure 3.13). However, as can be seen in Figures 3.2a and 3.3a in Section 3.3, the differences in dynamic and static deflections obtained at Profile 4 are larger than the differences of dynamic and static deflections obtained at Profile 1. This explains why the deflection ratios (dynamic deflections divided by static deflections) obtained at Profile 4 with the softest subgrade condition are larger than the deflection ratios obtained at a flexible pavement (Profile 1).

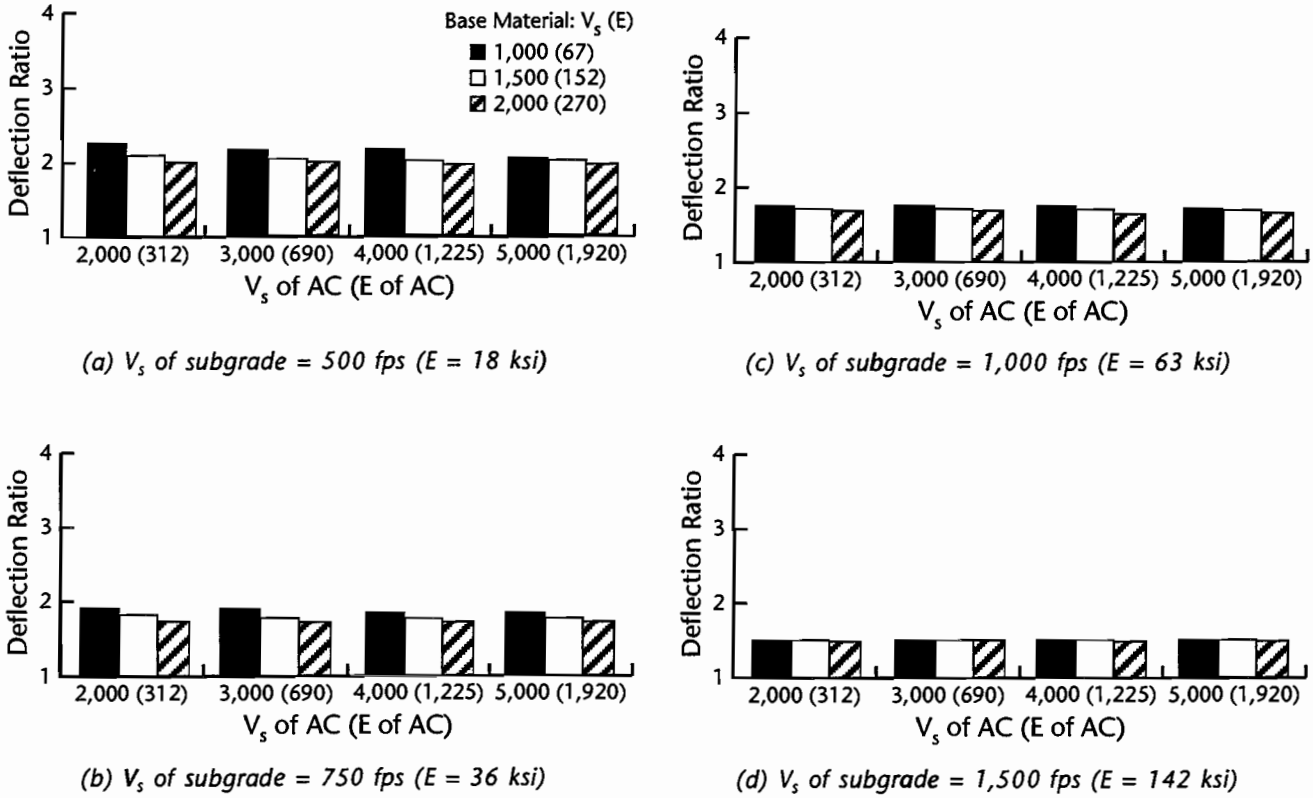

(a) V_s of subgrade = 500 fps (E = 18 ksi)

(c) V_s of subgrade = 1,000 fps (E = 63 ksi)

(b) V_s of subgrade = 750 fps (E = 36 ksi)

(d) V_s of subgrade = 1,500 fps (E = 142 ksi)

Figure 3.10 Maximum deflection ratios for Dynaflect testing at Profile 1 with various stiffness combinations of the pavement layer (units: V_s = fps, E = ksi)

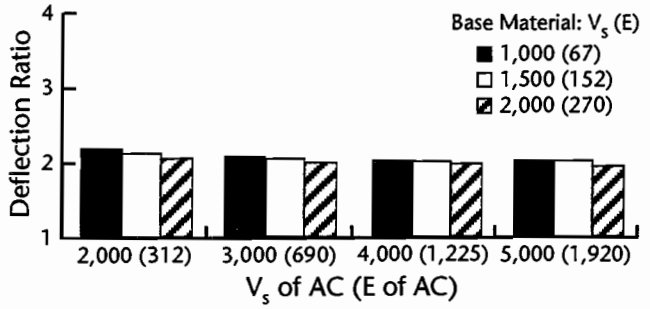

(a) V_s of subgrade = 500 fps (E = 18 ksi)

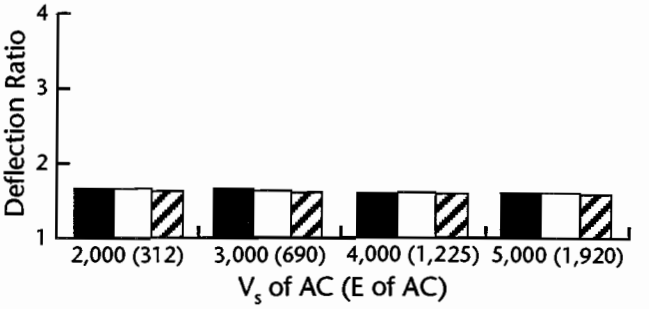

(c) V_s of subgrade = 1,000 fps (E = 63 ksi)

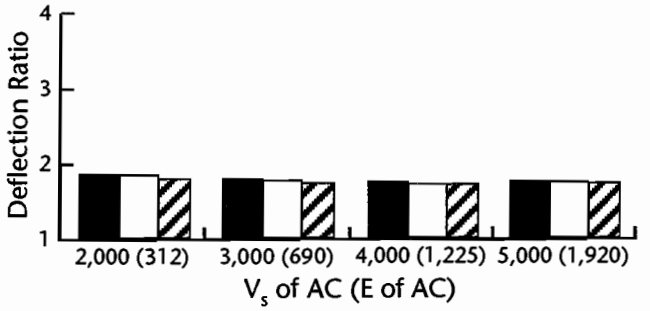

(b) V_s of subgrade = 750 fps (E = 36 ksi)

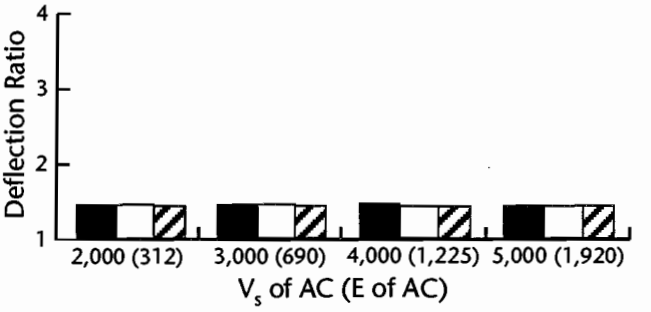

(d) V_s of subgrade = 1,500 fps (E = 142 ksi)

Figure 3.11 Maximum deflection ratios for Dynaflect testing at Profile 2 with various stiffness combinations of the pavement layer (units: V_s = fps, E = ksi)

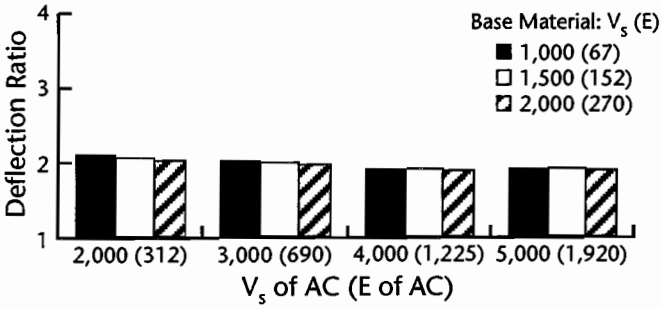

(a) V_s of subgrade = 500 fps (E = 18 ksi)

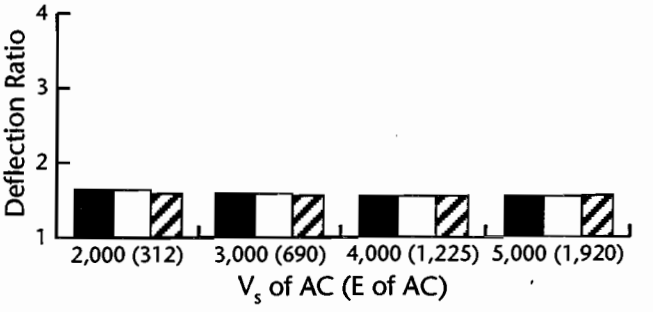

(c) V_s of subgrade = 1,000 fps (E = 63 ksi)

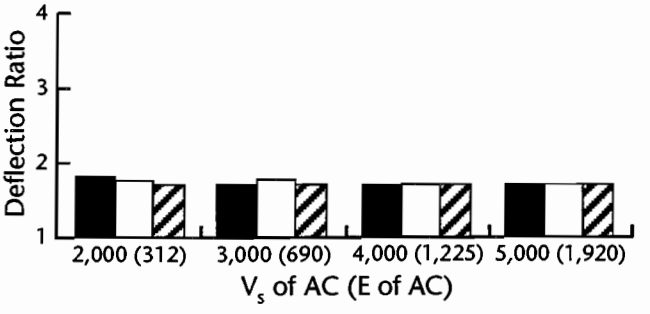

(b) V_s of subgrade = 750 fps (E = 36 ksi)

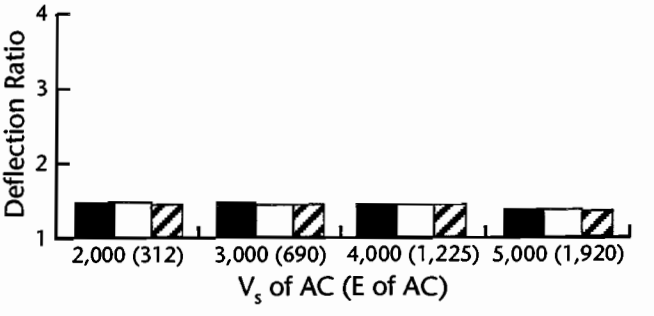

(d) V_s of subgrade = 1,500 fps (E = 142 ksi)

Figure 3.12 Maximum deflection ratios for Dynaflect testing at Profile 3 with various stiffness combinations of the pavement layer (units: V_s = fps, E = ksi)

Table 3.3 Variations in the deflection ratios obtained at station 5 for Dynaflect testing at the resonant depth to bedrock at the four pavement profiles

Shear Wave Velocity of Subgrade (fps)	Approximate Young's Modulus (ksi)	Range in Ratio	Maximum Deflection Ratio			
			Profile 1 FM137	Profile 2 FM195	Profile 3 Route 1	Profile 4 IH 10
500	16	Maximum	2.24	2.20	2.10	2.92
		Minimum	1.92	1.92	1.86	2.72
		Average	2.03	2.03	1.93	2.83
750	36	Maximum	1.92	1.88	1.82	1.82
		Minimum	1.68	1.69	1.68	1.72
		Average	1.77	1.75	1.71	1.78
1,000	63	Maximum	1.70	1.68	1.66	1.60
		Minimum	1.57	1.55	1.52	1.50
		Average	1.63	1.60	1.57	1.56
1,500	142	Maximum	1.47	1.45	1.46	1.34
		Minimum	1.43	1.41	1.39	1.28
		Average	1.46	1.44	1.43	1.31

3.6 SUMMARY

The Dynaflect test was studied analytically using computer program UTDYNF (Chang, 1991; Chang et al, 1992). Four typical in-service pavement profiles (three flexible pavements and one rigid pavement) were studied (Figure 2.2). The stiffness of each pavement layer was varied to simulate expected variations in the pavement materials.

The dynamic effect of the Dynaflect test was expressed in terms of the deflection ratios (dynamic deflections divided by static deflections). The resonant depth to bedrock (the depth to bedrock corresponding to the maximum deflection ratio) is determined predominately by the stiffness of the subgrade layer. Variations in the stiffnesses of the other pavement layers have little effect on the resonant bedrock depth. The maximum variations in resonant bedrock depths were 25 feet (7.8 m) to 85 feet (26.4 m) for the Dynaflect test at 8 Hz.

Two equations (one for flexible pavements and one for rigid pavements) were developed for estimating the resonant depth to bedrock. The equation for rigid pavements is in good agreement with the equation proposed by Davies and Mamlouk (1985). They did similar studies for the Road Rater test (also a steady-state test) on a rigid pavement.

The amplitude of the deflection ratio is an important index of the potential error generated in any static interpretation procedure of the Dynaflect test. The stiffness of the subgrade layer has the most significant effect on the amplitudes of the maximum deflection ratios. The softer the subgrade, the higher the amplitude of the maximum of deflection ratio. This indicates that the error generated in a static interpretation procedure of the Dynaflect test will decrease as the subgrade stiffness increases.

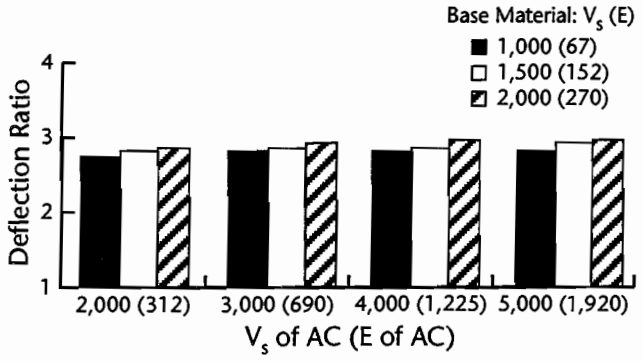

(a) V_s of subgrade = 500 fps (E = 18 ksi)

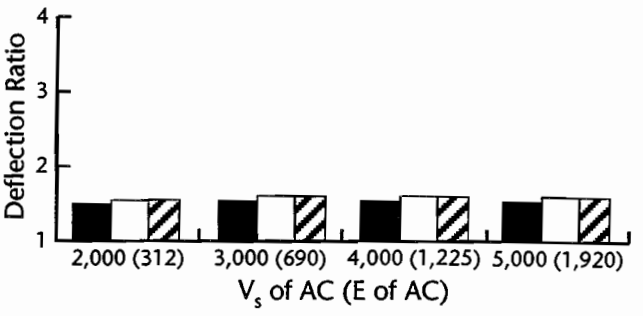

(c) V_s of subgrade = 1,000 fps (E = 63 ksi)

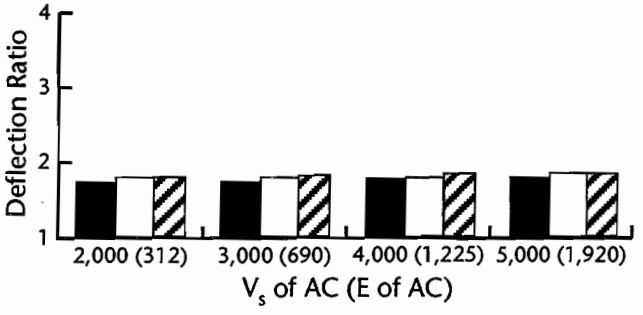

(b) V_s of subgrade = 750 fps (E = 36 ksi)

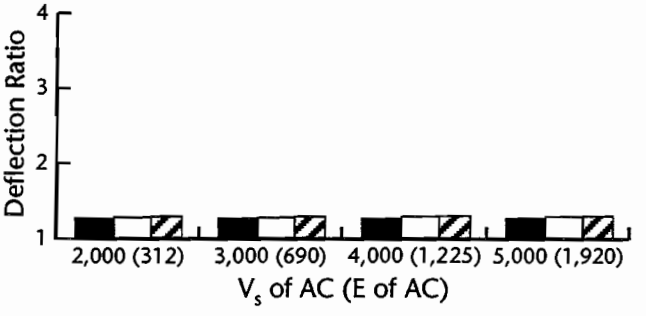

(d) V_s of subgrade = 1,500 fps (E = 142 ksi)

Figure 3.13 Maximum deflection ratios for Dynaflect testing at Profile 4 with various stiffness combinations of the pavement layer (units: V_s = fps, E = ksi)

CHAPTER 4. PARAMETRIC STUDY OF THE FALLING WEIGHT DEFLECTOMETER TEST

4.1 INTRODUCTION

Analytical simulations of the FWD test were conducted using the UTFWD program (Chang, 1991; Chang et al, 1992). The four pavement profiles shown in Figure 2.3 were studied. These profiles are the same ones used in the Dynaflect study presented in Chapter 3. The main purposes of these studies were:

1. to determine the resonant depth to bedrock with various stiffnesses of the subgrade, including unsaturated and saturated conditions;
2. to develop equations for estimating the resonant depth to bedrock;
3. to develop a method for estimating the depth to bedrock based on the free vibrations of the pavement system created by the FWD test; and
4. to develop an approach for estimating the stiffness of the subgrade layer based on the phase shift between the first pulses at two measurement stations in the deflection-time records of the FWD test.

The loading in the FWD test is described in Section 2.2 of this report. The deflection basins presented herein are normalized with respect to the load. Therefore, actual deflections under any load are simply calculated by multiplying the normalized deflection by the desired load.

4.2 MODEL PARAMETERS

Based on the earlier studies with the Dynaflect test, variations in the stiffnesses of the surface and base layers had little effect on the deflection basins. Therefore, only the subgrade stiffness was varied in this study of the FWD test. The stiffnesses of the other pavement layers were kept constant, such that the shear wave velocity of the CRC equaled 8500 fps (2593 m/s) (E = 5425 ksi (37.4 MN/m^2)), the shear wave velocity of the AC equaled 3000 fps (915 m/s) (E = 690 ksi (4.8 MN/m^2)), and the shear wave velocity of the base equaled 1000 fps (305 m/s) (E = 67 ksi (0.46 MN/m^2)). The shear wave velocity of the subgrade layer was varied from 500 to 1500 fps (150 to 450 m/s) and the corresponding Young's modulus was varied from 16 to 142 ksi (0.11 to 0.98 MN/m^2). In addition, the depths to bedrock of the four pavement profiles were varied from 5.5 to 90 feet (1.65 to 27 m).

To simulate an unsaturated subgrade, a Poisson's ratio of 0.33 was used. The material properties of the four pavement profiles with unsaturated subgrade conditions are given in Table 4.1. To simulate a saturated subgrade, the P-wave velocity of the subgrade was set equal to 5000 fps (1525 m/s). This velocity represents typical field conditions for uncemented saturated soils (Richart et al, 1970). The shear wave velocities of the saturated subgrades were varied from 500 to 1500 fps (150 to 450 m/s), as in the unsaturated subgrade condition. As a result, Poisson's ratio varied from 0.495 to 0.451, as S-wave velocity of the subgrade varied from 500 to 1500 fps (150 to 450 M/s). Hence, Young's modulus for the saturated subgrade varied from 18 to 155 ksi (0.12 to 1.07 MN/m^2). The material properties of the four pavement profiles with saturated subgrades are given in Table 4.2.

Table 4.1 Material properties of the four pavement profiles with unsaturated subgrade conditions

a) FM137 (Profile 1)

Material Type	Thickness (in.)	Poisson's Ratio	Unit Weight (pcf)	Damping Ratio	S-wave Velocity (fps)	P-wave Velocity (fps)	Young's Modulus (ksi)
ACP	1	0.27	140	0.02	3,000	5,345	690.4
Base	12	0.25	125	0.02	1,000	1,732	67.4
Subgrade*	h**	0.33	110	0.02	500	993	15.8
		0.33	110	0.02	750	1,488	35.5
		0.33	110	0.02	1,000	1,985	63.1
		0.33	110	0.02	1,500	2,978	142.0

b) FM195 (Profile 2)

Material Type	Thickness (in.)	Poisson's Ratio	Unit Weight (pcf)	Damping Ratio	S-wave Velocity (fps)	P-wave Velocity (fps)	Young's Modulus (ksi)
ACP	4	0.27	140	0.02	3,000	5,345	690.4
Base	6	0.25	125	0.02	1,000	1,732	67.4
Subgrade	h	0.33	110	0.02	500	993	15.8
		0.33	110	0.02	750	1,488	35.5
		0.33	110	0.02	1,000	1,985	63.1
		0.33	110	0.02	1,500	2,978	142.0

c) Route 1 (Profile 3)

Material Type	Thickness (in.)	Poisson's Ratio	Unit Weight (pcf)	Damping Ratio	S-wave Velocity (fps)	P-wave Velocity (fps)	Young's Modulus (ksi)
ACP	7	0.27	145	0.02	3,000	5,345	715.1
Base	6	0.25	130	0.02	1,000	1,732	70.1
Subgrade	h	0.33	130	0.02	500	993	18.7
		0.33	130	0.02	750	1,489	42.0
		0.33	130	0.02	1,000	1,985	74.6
		0.33	130	0.02	1,500	2,979	167.9

d) IH 10 (Profile 4)

Material Type	Thickness (in.)	Poisson's Ratio	Unit Weight (pcf)	Damping Ratio	S-wave Velocity (fps)	P-wave Velocity (fps)	Young's Modulus (ksi)
CRC	10	0.2	145	0.02	8,500	13,880	5424.2
ACP	6	0.27	145	0.02	3,000	5,345	715.1
Base	12	0.25	125	0.02	1,000	1,732	67.4
Subgrade	h	0.33	110	0.02	500	993	15.8
		0.33	110	0.02	750	1,488	35.5
		0.33	110	0.02	1,000	1,985	63.1
		0.33	110	0.02	1,500	2,978	142.0

* There are four different S-wave velocities for each subgrade.
** Thickness of subgrade (h) was varied from 5.5 to 90 ft.

Table 4.2 Material properties of the four pavement profiles with saturated subgrade conditions

a) FM 137 (Profile 1)

Material Type	Thickness (in.)	Poisson's Ratio	Unit Weight (pcf)	Damping Ratio	S-wave Velocity (fps)	P-wave Velocity (fps)	Young's Modulus (ksi)
ACP	1	0.270	140	0.02	3,000	5,345	690.4
Base	12	0.250	125	0.02	1,000	1,732	67.4
Subgrade*	h**	0.495	110	0.05	500	5,000	17.4
		0.489	110	0.05	750	5,000	39.5
		0.479	110	0.05	1,000	5,000	69.8
		0.451	110	0.05	1,500	5,000	154.8

b) FM 195 (Profile 2)

Material Type	Thickness (in.)	Poisson's Ratio	Unit Weight (pcf)	Damping Ratio	S-wave Velocity (fps)	P-wave Velocity (fps)	Young's Modulus (ksi)
ACP	4	0.270	140	0.02	3,000	5,345	690.4
Base	6	0.250	125	0.02	1,000	1,732	67.4
Subgrade	h	0.495	110	0.05	500	5,000	17.7
		0.489	110	0.05	750	5,000	39.5
		0.479	110	0.05	1,000	5,000	69.8
		0.451	110	0.05	1,500	5,000	154.8

c) Route 1 (Profile 3)

Material Type	Thickness (in.)	Poisson's Ratio	Unit Weight (pcf)	Damping Ratio	S-wave Velocity (fps)	P-wave Velocity (fps)	Young's Modulus (ksi)
ACP	7	0.270	145	0.02	3,000	5,345	715.1
Base	6	0.250	130	0.02	1,000	1,732	70.1
Subgrade	h	0.495	130	0.05	500	5,000	21.0
		0.489	130	0.05	750	5,000	46.7
		0.479	130	0.05	1,000	5,000	82.5
		0.451	130	0.05	1,500	5,000	183.0

d) IH 10 (Profile 4)

Material Type	Thickness (in.)	Poisson's Ratio	Unit Weight (pcf)	Damping Ratio	S-wave Velocity (fps)	P-wave Velocity (fps)	Young's Modulus (ksi)
CRC	10	0.200	145	0.02	8,500	13,880	5424.2
ACP	6	0.270	145	0.02	3,000	5,345	715.1
Base	12	0.250	125	0.02	1,000	1,732	67.4
Subgrade	h	0.495	110	0.05	500	5,000	17.7
		0.489	110	0.05	750	5,000	39.5
		0.479	110	0.05	1,000	5,000	69.8
		0.451	110	0.05	1,500	5,000	154.8

* There are four different S-wave velocities for each subgrade.
**Thickness of subgrade (h) was varied from 5.5 to 90 ft.

The results of the analytical simulation of the FWD test were expressed in terms of deflection ratios (ratios of dynamic deflections to static deflections) as a function of depth to bedrock. These results are presented in Appendix B and are discussed below.

4.3 DEFLECTION BASINS

A typical example of the deflection basins created by the FWD test as a function of depth to bedrock is shown in Figure 4.1. The dynamic deflections at all measurement stations (receivers) vary only at shallow bedrock depths, depths ranging from 5.5 to about 10 feet (1.7 to 3.1 m), as shown in Figure 4.1a. This is quite different from the Dynaflect test, in which large variations in bedrock depth, ranging from 25 to 85 feet (7.8 to 26.3 m), influenced the measured dynamic deflections.

As in the case of the Dynaflect test, the maximum deflection ratio also occurs at the farthest receiver station in the FWD test. However, the resonance peak exhibited in the FWD deflection ratios is much wider than that in the Dynaflect test and decreases more slowly to 1 when compared with the sharp decrease in the deflection ratio in the Dynaflect test. This difference is easily seen by comparing Figures 3.1c and 4.1c. The reason for this difference is that the FWD test contains a wide range in frequencies, while the Dynaflect test contains mainly one frequency (8 Hz).

A second observation about the deflection ratio in the FWD test is that the deflection ratio at the first measurement station (under the load) remains nearly equal to 1 throughout the entire range of bedrock depths. This indicates that there is little dynamic effect on the measured surface motions at the FWD source.

Dynamic and static deflection basins as a function of distance from the source obtained at the peak deflection ratio (termed the resonant depth to bedrock) are shown in Figure 4.2 and 4.3 for Profile 1 (flexible pavement) with unsaturated and saturated subgrade conditions, respectively. As can be seen, there is little difference at the source between dynamic deflections and static deflections for Profile 1 with the softest subgrade (Figure 4.2a). The differences between dynamic deflections and static deflections become larger as the distance from the source increases. This behavior explains why the deflection ratio at the nearest station is the smallest and the deflection ratio at the farthest station is the largest, as illustrated in Figure 4.1c.

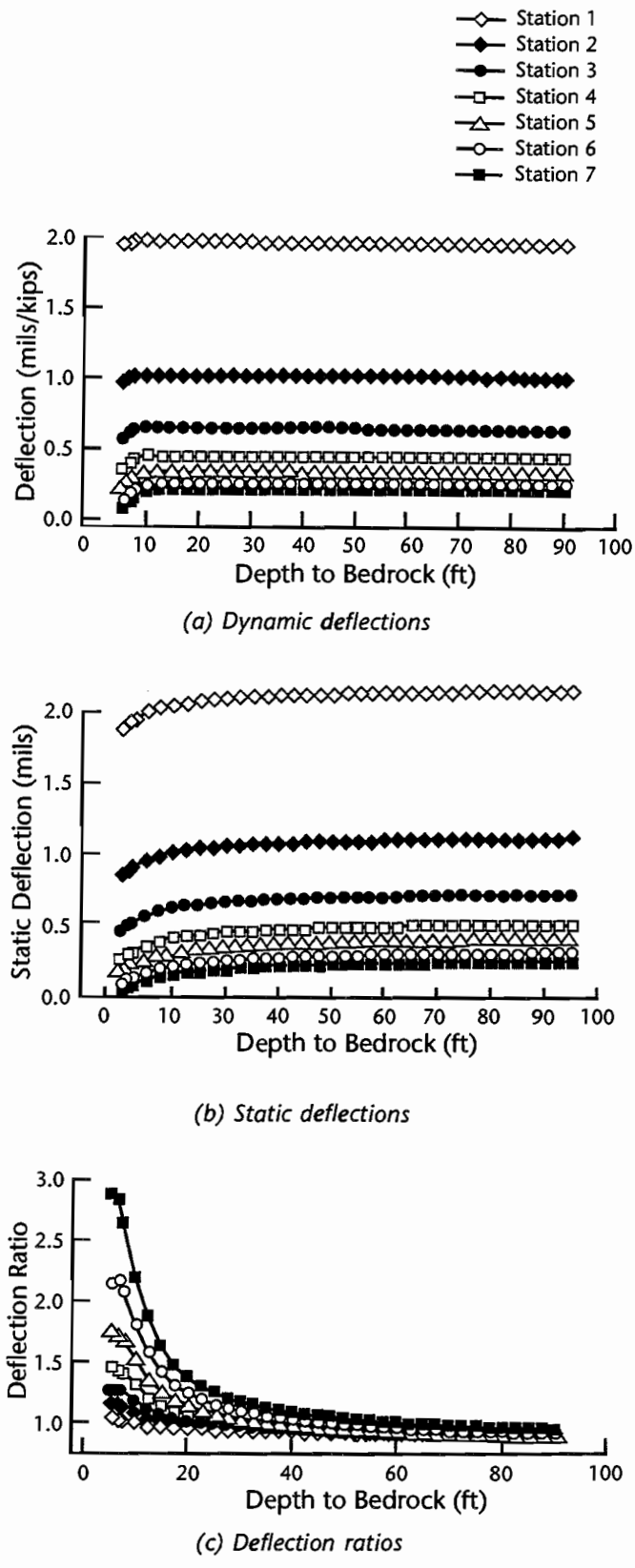

Figure 4.1 ***Deflection basins obtained with FWD testing for Profile 1 with unsaturated subgrade conditions (V_s of subgrade = 500 fps (155 m/s) and E = 16 ksi (0.11 MN/m²))***

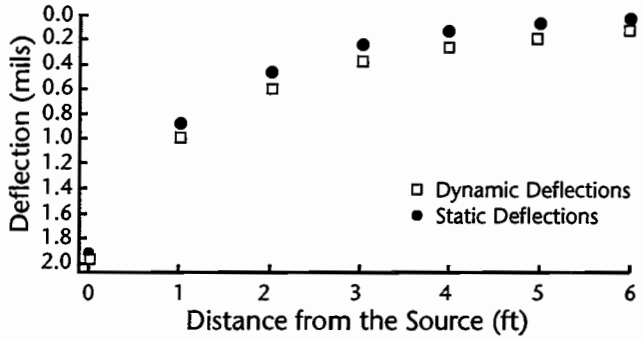

(a) S-wave velocity of subgrade = 500 fps (E = 16 ksi)

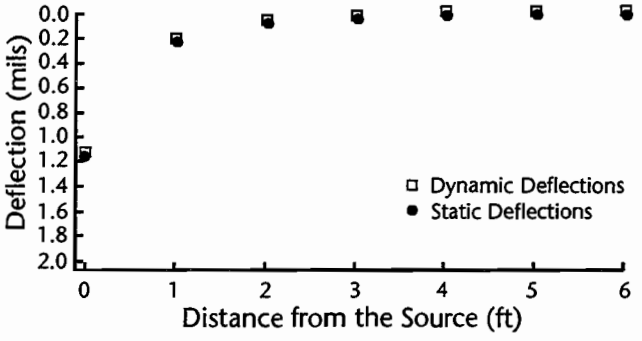

(b) S-wave velocity of subgrade = 1,500 fps (E = 142 ksi)

Figure 4.2 ***Deflection basins as a function of distance from the FWD source for Profile 1 with unsaturated subgrade conditions***

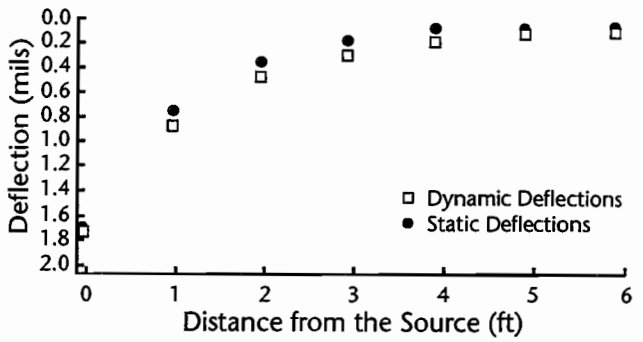

(a) S-wave velocity of subgrade = 500 fps (E = 16 ksi)

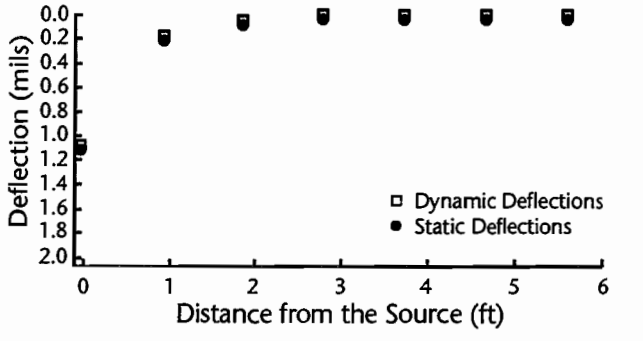

(b) S-wave velocity of subgrade = 1,500 fps (E = 142 ksi)

Figure 4.3 ***Deflection basins as a function of distance from the FWD source for Profile 1 with saturated subgrade conditions***

For the stiffest subgrade condition, there is little difference between the dynamic deflections and the static deflections, as shown in Figure 4.2b. This indicates that deflection ratios obtained from stiff subgrade conditions are smaller than those obtained from soft subgrade conditions. For the saturated subgrade conditions at Profile 1, the trends are similar to those first described for the unsaturated subgrade conditions, as shown in Figure 4.3.

Similar plots of deflection basins as a function of distance from the source for Profile 4 (rigid pavement) are shown in Figures 4.4 and 4.5 for unsaturated and saturated subgrade conditions, respectively. The amplitudes of the deflection basins are much smaller than those obtained with Profile 1, because the surface layer of Profile 4 is much thicker and stiffer than that of Profile 1. There is also less variation in the deflection basins with the distance from the source than in Profile 1. This response can be seen by comparing Figures 4.2a and 4.4a. This occurs because Profile 4 represents a rigid pavement, while Profile 1 represents a very flexible pavement. For saturated subgrade conditions (Figure 4.5), the trends are similar to those just described for the unsaturated subgrade conditions (Figure 4.4).

4.4 RESONANT DEPTH TO BEDROCK

The analytical simulations of the FWD tests for the four pavement profiles were expressed in terms of deflection ratios (ratios of dynamic deflections to static deflection) as a function of depth to bedrock. The resonant depth to bedrock for each pavement profile with each subgrade stiffness was determined as the depth to bedrock corresponding to the maximum deflection ratio. These results are presented in Appendix B.

The resonant depths to bedrock as a function of various subgrade stiffnesses for the four pavement profiles are summarized in Figure 4.6. The resonant depths to bedrock obtained with the FWD test varied from 5.5 to 20 feet (1.7 to 6.2 m), which are much shallower depths when compared with the resonant depths to bedrock obtained with the Dynaflect test (varied from 25 to 85 feet (7.8 to 26.3 m)). This is because the predominate frequency in the FWD test is about 30 Hz, so the resonant depths to bedrock obtained with the FWD test are approximately one fourth of those obtained with the Dynaflect test (f = 8 Hz).

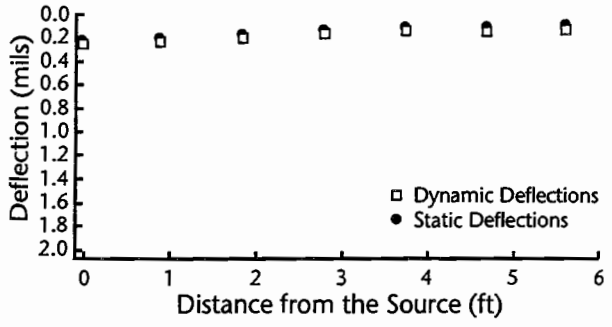

(a) S-wave velocity of subgrade = 500 fps (E = 16 ksi)

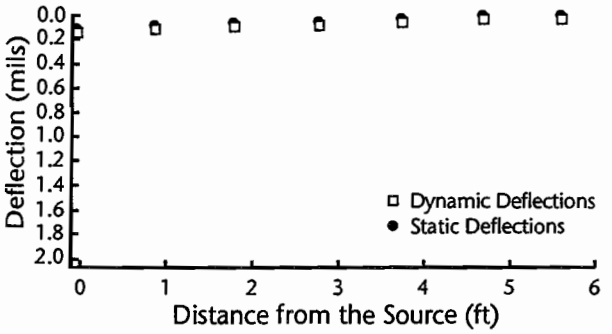

(b) S-wave velocity of subgrade = 1,500 fps (E = 142 ksi)

Figure 4.4 ***Deflection basins as a function of distance from the FWD source for Profile 4 with unsaturated subgrade conditions***

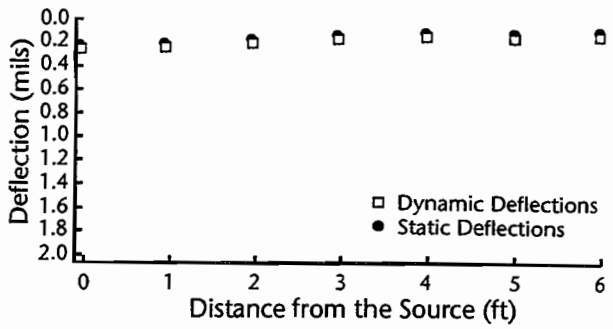

(a) S-wave velocity of subgrade = 500 fps (E = 16 ksi)

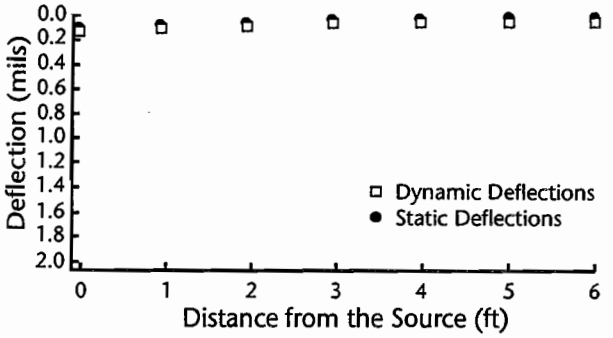

(b) S-wave velocity of subgrade = 1,500 fps (E = 142 ksi)

Figure 4.5 ***Deflection basins as a function of distance from the FWD source for Profile 4 with saturated subgrade conditions***

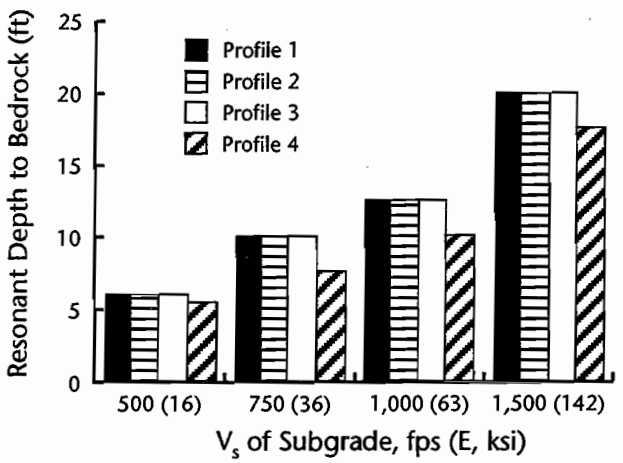

(a) Unsaturated subgrade conditions

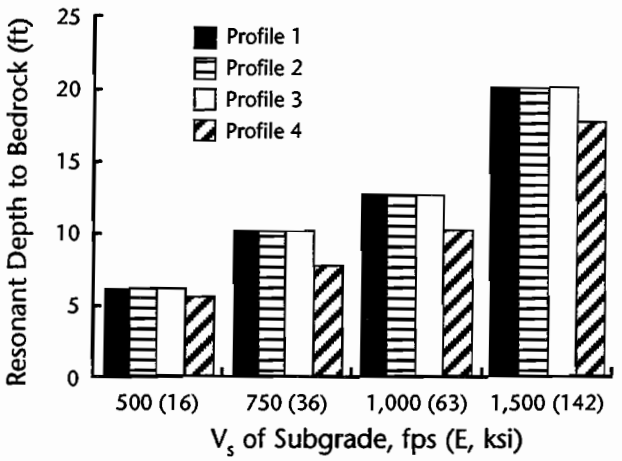

(b) Saturated subgrade conditions

Figure 4.6 ***Resonant depths to bedrock for FWD testing at the four pavement profiles with various subgrade stiffnesses***

As can be seen in Figure 4.7, the resonant depths to bedrock (RDb) form two groups: one for the flexible pavements (Profiles 1, 2, and 3) and the other for the rigid pavement (Profile 4). For flexible pavements, a straight line was fitted, which resulted in:

$$RDb = 0.013V_s \quad (4.1)$$

with H in feet and Vs in feet per seconds (fps). For the rigid pavement, a second-order polynomial curve was fitted, which resulted in:

$$RDb = 0.011V_s \quad (4.2)$$

with RDb in feet and V_s in fps. Equations 4.1 and 4.2 can also be expressed in terms of Young's Modulus (E) as:

$$RDb = 0.0043\sqrt{E} \quad (4.3)$$

for flexible pavements with the unit weight of the subgrade material assumed to be 110 pounds per cubic foot (pcf), Poisson's ratio assumed to be 0.33, RDb in feet and E in pounds per square foot (psf), and

$$RDb = 0.0036\sqrt{E} \quad (4.4)$$

for the rigid pavement with RDb in feet and E in psf.

4.5 AMPLITUDE OF THE MAXIMUM DEFLECTION RATIO

The amplitude of the deflection ratio (dynamic deflection divided by static deflection) at each measurement station is an important index of the potential error generated in any static interpretation procedure. Figure 4.8 shows the maximum deflection ratios as a function of various subgrade stiffnesses for the four pavement profiles. It should be noted that, as in the Dynaflect test, the maximum deflection ratio of the FWD test always occurs at the farthest measurement station (station 7).

As can be seen in Figure 4.8, the amplitudes of the maximum deflection ratios of the four pavement profiles decrease as the stiffness of the subgrade increases (for both unsaturated and saturated subgrade conditions). This means that the accuracy of backcalculated layer moduli based on the static interpretation method should improve as the subgrade stiffness increases. The results of backcalculated layer moduli using the MODULUS program (presented in Chapter 5) show this trend.

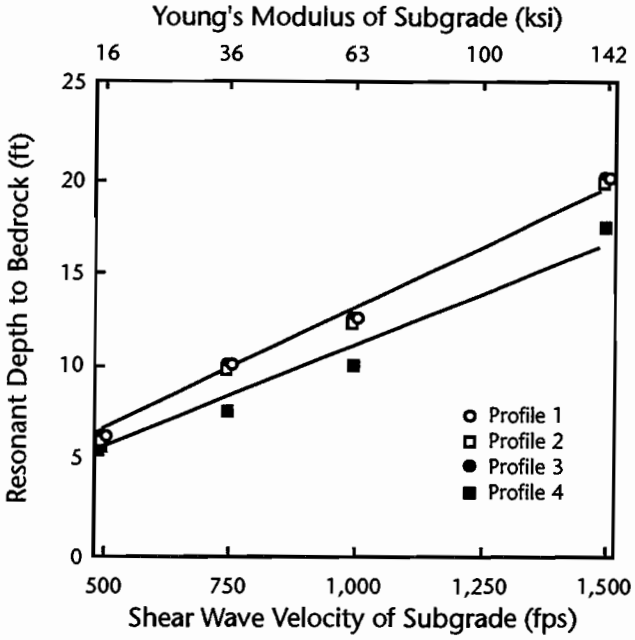

Figure 4.7 ***Curve fitting of the resonant depth to bedrock for FWD testing at the four pavement profiles with various subgrade stiffnesses***

There are some numerical problems with saturated subgrade conditions at shallow depths to bedrock (see Appendix B). The amplitudes of the maximum deflection ratio of station 7 were estimated according to the trend of the first three measurement stations (which were not affected by the numerical problems).

The estimated amplitudes of the maximum deflection ratios of the four pavement profiles obtained with saturated subgrade conditions are generally larger than those obtained with unsaturated subgrade conditions. This indicates that the backcalculated layer moduli obtained at pavement sites with unsaturated subgrade conditions based on a static interpretation method should be more accurate than those obtained at sites with saturated subgrade conditions.

Complete discussions on the accuracy of backcalculated layer moduli using a static interpretation computer program (MODULUS) are presented in Chapter 5.

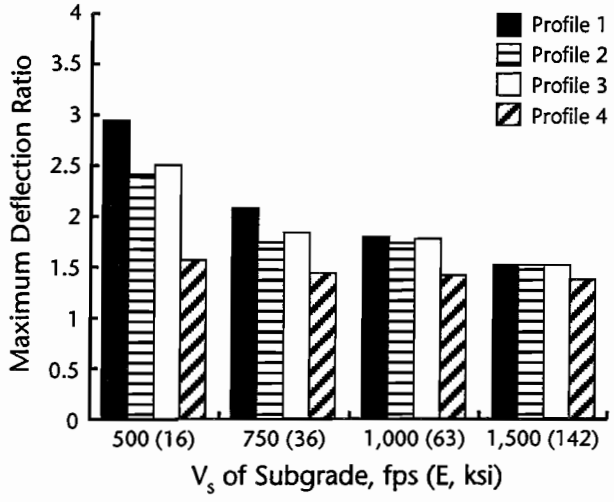

(a) Unsaturated subgrade conditions

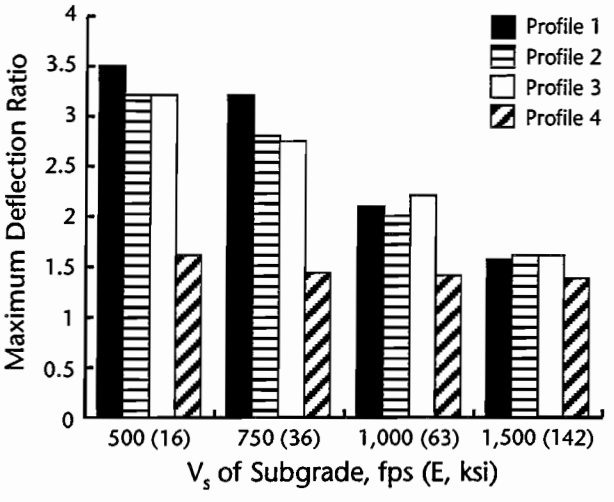

(b) Saturated subgrade conditions

Figure 4.8 ***Maximum deflection ratios for FWD testing at the four pavement profiles with various subgrade stiffnesses***

4.6 ESTIMATION OF DEPTH TO BEDROCK FROM THE FWD TEST

Chang et al (1992) developed a procedure for predicting the depth to bedrock based on the damped natural period of the free vibrations of the pavement system immediately after the FWD load application. Figure 4.9 illustrates the damped natural periods in the time-deflection records obtained from FWD tests with four shallow depths to bedrock. It should be noted that a much longer time interval (say 0.15 to 0.20 seconds) than normally recorded (0.06 seconds) must be measured to record the free vibrations.

Additional studies have been conducted herein. In these studies, various stiffnesses of the subgrade layer and different subgrade saturation conditions have been examined. This work was performed to provide a more complete evaluation of the estimation of bedrock depth. Three different degrees of saturation for unsaturated subgrade conditions were simulated by using Poisson's ratio of 0.20, 0.33, and 0.40 while keeping the shear wave velocity constant. The rest of the material properties are the same as those in Table 4.1 (except for the P-wave velocity). The material properties for the case of saturated subgrade conditions are shown in Table 4.2.

Four different shallow depths to bedrock—5, 7.5, 10, and 20 feet (1.5, 2.3, 3.1, and 6.1 m)—were studied. These depths were selected because the resonant depth to bedrock for the FWD test was always within 20 feet (6 m) of the pavement surface, as shown in Figure 4.2, unless a very stiff subgrade (V_s > 1,500 fps (458 m/s)) was encountered. The damped natural periods obtained with various Poisson's ratios, stiffnesses of subgrade, and depths to bedrock are presented in Appendix C.

4.6.1 Unsaturated Subgrade Conditions

The depth to bedrock versus damped natural period of the free vibration for each pavement profile with an unsaturated subgrade with Poisson's ratio of 0.20 is shown in Figure 4.10. It is obvious that there is a linear (or nearly linear) relationship between depth to bedrock and damped natural period for each stiffness of the subgrade. It should be noted, as was noted in Chapter 3, that depth to bedrock is defined as the total depth from the top of the pavement to the top of the bedrock.

Figure 4.11 is a combined plot of the results from:

(a) the flexible pavement profiles (Profiles 1, 2, and 3), and
(b) the rigid pavement profile (Profile 4).

The relationships between depth to bedrock and damped natural period for the flexible pavements can be expressed as:

$$Db = \frac{Td^{1.08} V_s^{1.13}}{5.325} \qquad (4.5)$$

with the shear wave velocity of the subgrade (V_s) in feet per second, the damped natural period (T_d) in seconds, and the depth to bedrock (Db) in feet. For the rigid pavement, the expression becomes:

$$Db = \frac{Td^{1.11} V_s^{1.14}}{5.433} \qquad (4.6)$$

with Db in feet, V_s in feet per second, and T_d in seconds.

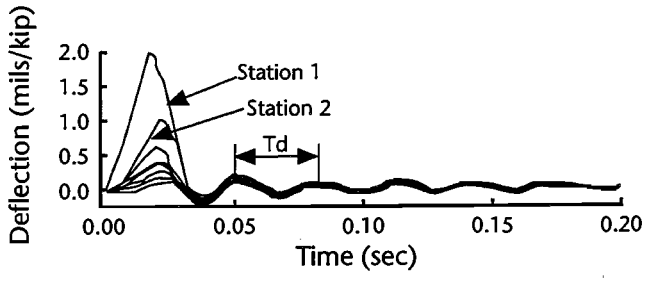

(a) Depth to bedrock = 5 feet

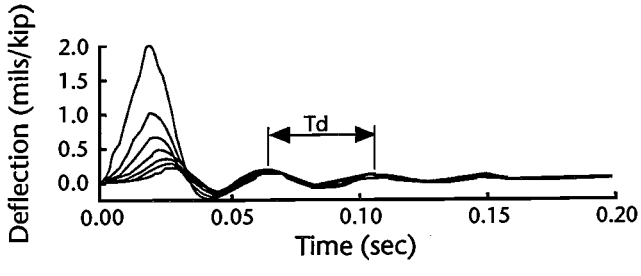

(b) Depth to bedrock = 7.5 feet

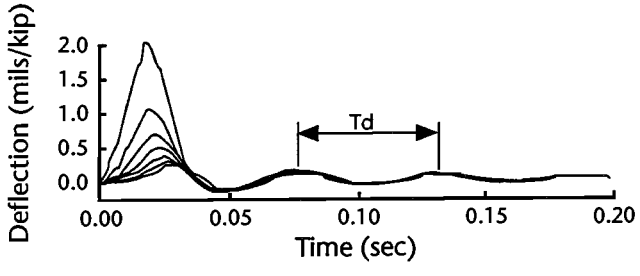

(c) Depth to bedrock = 10 feet

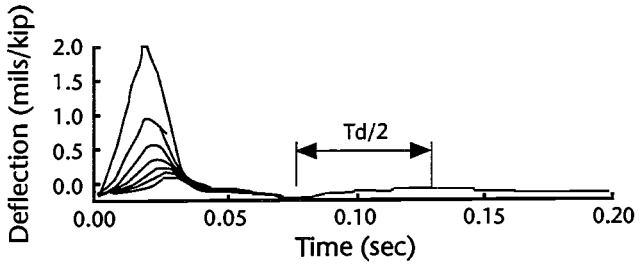

(d) Depth to bedrock = 20 feet

Figure 4.9 ***Deflection-time histories in FWD testing and damped natural periods (Td) for Profile 1 with various depths to bedrock (V_s of Subgrade = 500 fps (155 m/s) and E = 16 ksi (0.11 MN/m²))***

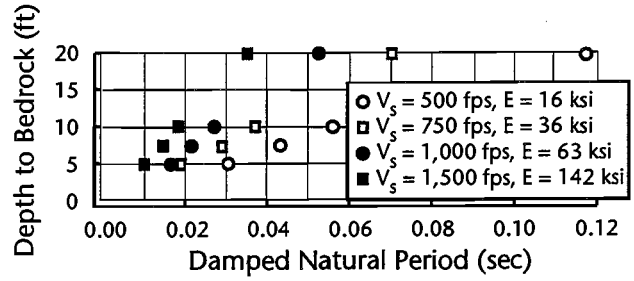

(a) Profile 1

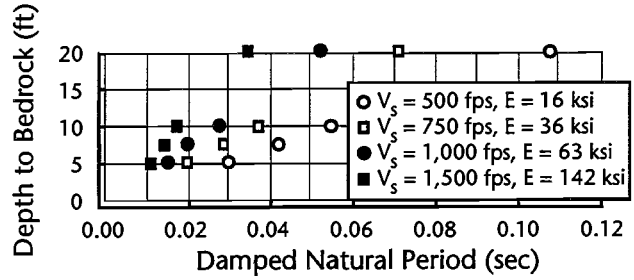

(b) Profile 2

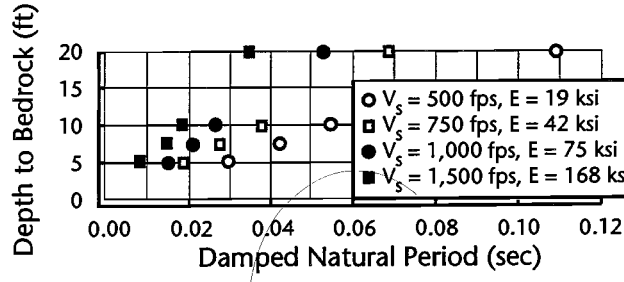

(c) Profile 3

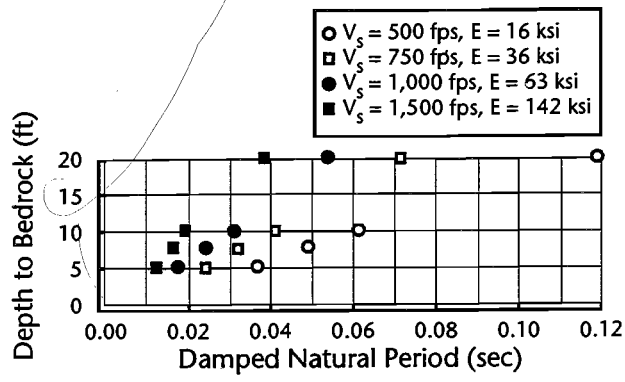

(d) Profile 4

Figure 4.10 ***Depth to bedrock versus damped natural period of the pavement system for FWD testing at the four pavement profiles with various stiffnesses of unsaturated subgrade (Poisson's ratio = 0.20)***

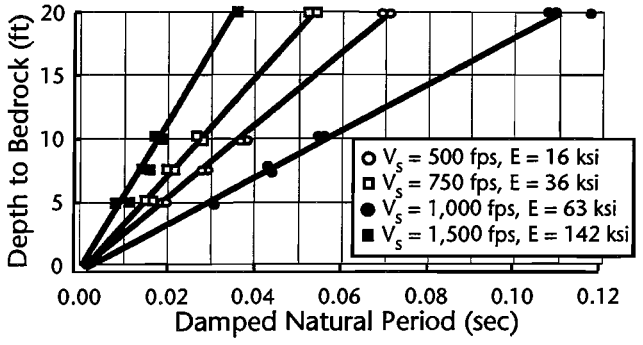

(a) Flexible pavements

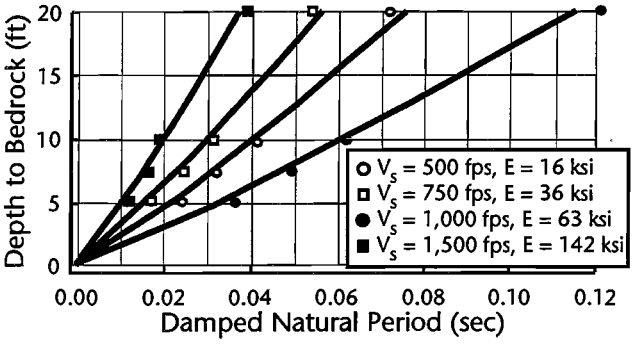

(b) Rigid pavements

Figure 4.11 ***Depth to bedrock versus damped natural period of the pavement system for FWD testing at: (a) flexible pavements and (b) rigid pavements (Poisson's ratio of the unsaturated subgrade = 0.20)***

The depth to bedrock versus damped natural period of each pavement profile with an unsaturated subgrade with Poisson's ratio of 0.33 is shown in Figure 4.12. The data from the three flexible profiles and one rigid pavement were plotted separately and linear curve fits were performed with the various subgrade stiffnesses, as shown in Figure 4.13. The fitted curves can be expressed by the following equations:

$$Db = \frac{Td^{1.08} V_s^{1.13}}{4.821} \qquad (4.7)$$

for the flexible pavements with Db in feet, V_s in feet per second, and T_d in seconds, and

$$Db = \frac{Td^{1.11} V_s^{1.14}}{5.045} \qquad (4.8)$$

for the rigid pavement, with Db in feet, V_s in feet per second, and T_d in seconds.

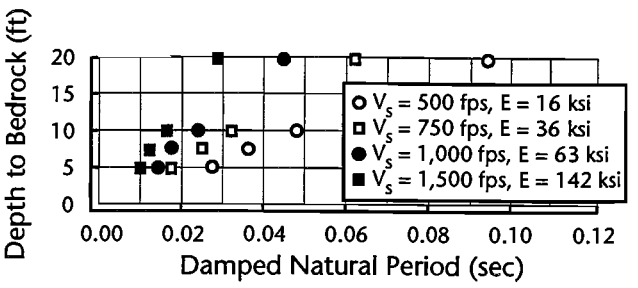

(a) Profile 1

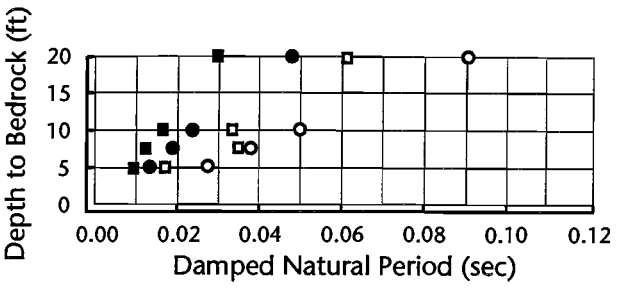

(b) Profile 2

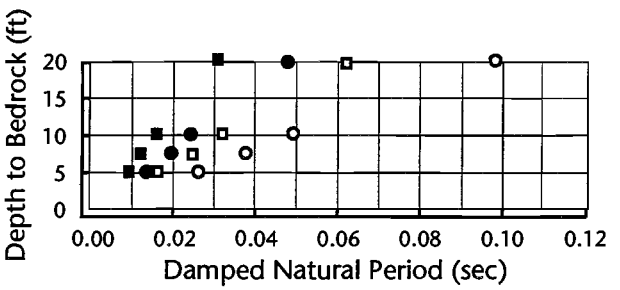

(c) Profile 3

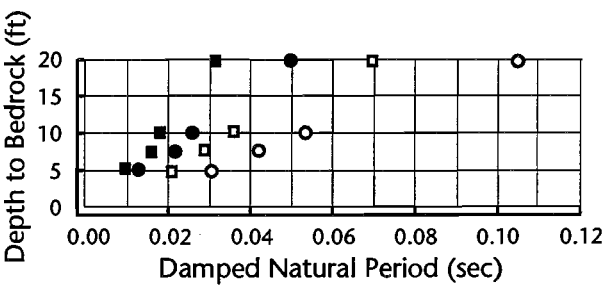

(d) Profile 4

Figure 4.12 ***Depth to bedrock versus natural period of the pavement system for FWD testing at the four pavement profiles with various stiffnesses of unsaturated subgrade (Poisson's ratio of subgrade = 0.33)***

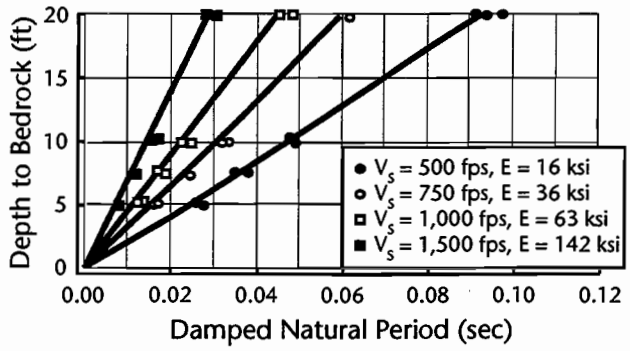

(a) Flexible pavements

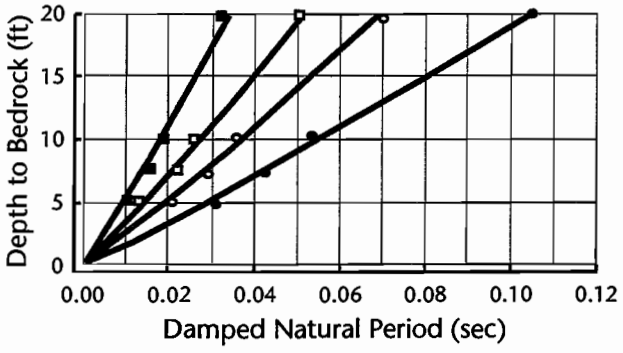

(b) Rigid pavements

Figure 4.13 ***Depth to bedrock versus damped natural period of the pavement system for FWD testing at: (a) flexible pavements and (b) rigid pavements (Poisson's ratio of subgrade = 0.33)***

For the case of the subgrade having Poisson's ratio equal to 0.40, the linear relationship between depth to bedrock and the damped natural period of each profile is shown in Figure 4.14. The combined plot of the flexible pavement and rigid pavement and curve fitting are shown in Figure 4.15. The equations are:

$$Db = \frac{Td^{1.08} V_s^{1.13}}{4.317} \qquad (4.9)$$

for the flexible pavement, with Db in feet, V_s in feet per second, and T_d in seconds, and

$$Db = \frac{Td^{1.11} V_s^{1.14}}{4.657} \qquad (4.10)$$

for the rigid pavement, with Db in feet, V_s in feet per second, and T_d in seconds.

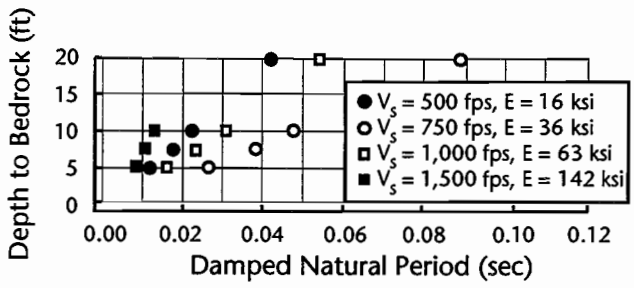

(a) Profile 1

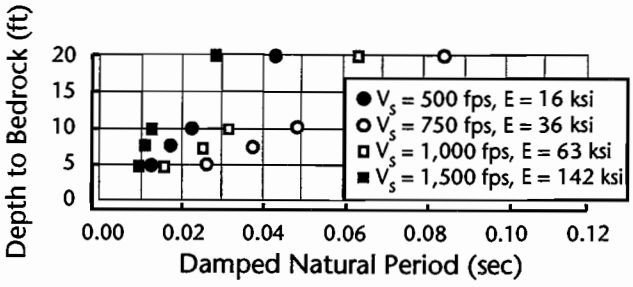

(b) Profile 2

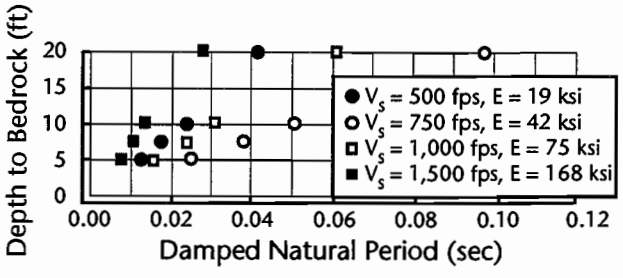

(c) Profile 3

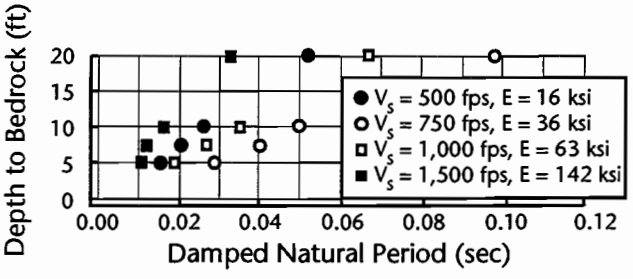

(d) Profile 4

Figure 4.14 ***Depth to bedrock versus natural period of the pavement system for FWD testing at the four pavement profiles with various stiffnesses of unsaturated subgrade (Poisson's ratio of subgrade = 0.40)***

Finally, the equations for the flexible pavements with different Poisson's ratios (υ) of subgrade can be combined into one equation. The equation thus becomes:

$$Db = \frac{Td^{1.08} V_s^{1.13}}{(6.33 - 5.04\upsilon)} \qquad (4.11)$$

with V_s in feet per second, Td in seconds, and Db in feet.

The equations for the rigid pavement with various Poisson's ratios (υ) can also be combined into one equation. The equation then becomes:

$$Db = \frac{Td^{1.11} V_s^{1.14}}{(6.21 - 3.88\upsilon)} \quad (4.12)$$

with V_s in feet per second, Td in seconds, and Db in feet.

Equations 4.11 and 4.12 can be simplified as the linear equations shown in Table 4.3. The coefficient of determination (r^2) for these simplified equations ranged from 0.97 to 0.98. It is more convenient and easier to use the simplified equations listed in Table 4.3 than the nonlinear equations described above.

4.6.2 Saturated Subgrade Conditions

For saturated subgrade conditions, there are four different values for Poisson's ratios (0.495, 0.489, 0.479, and 0.451) which correspond to the four stiffnesses of the subgrade that result in the P-wave velocity of the subgrade equaling 5000 fps (1525 m/s)(Table 4.2). Figure 4.16 shows the depth to bedrock versus damped natural period for each profile. The combined data of the three flexible pavements and one rigid pavement are shown in Figure 4.17. The fitted equation for the flexible pavement is:

$$Db = 0.456 V_s^{1.03} Td^{1.07} \quad (4.13)$$

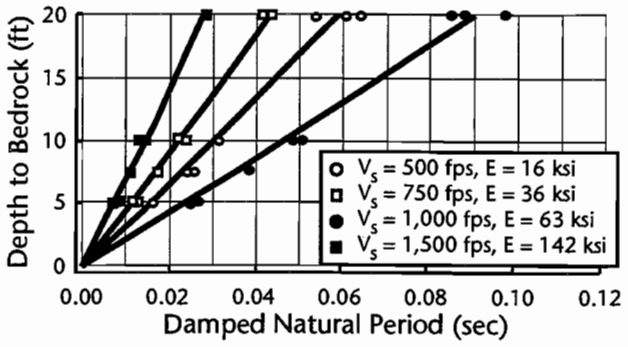

(a) Flexible pavements

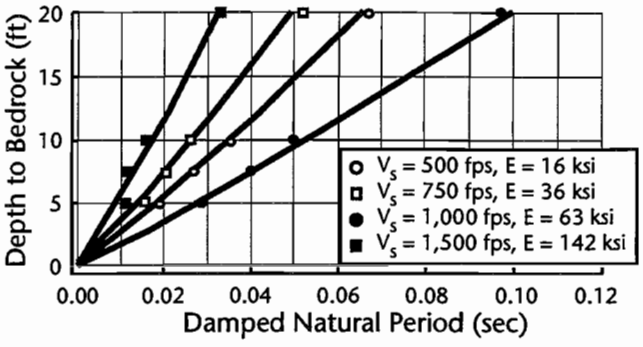

(b) Rigid pavements

Figure 4.15 ***Depth to bedrock versus damped natural period of the pavement system for FWD testing at: (a) flexible pavements and (b) rigid pavements (Poisson's ratio of subgrade = 0.40)***

Table 4.3 ***Simplified equations for estimating depth to bedrock with unsaturated subgrade conditions***

Correspond to Equations	Simplified Equations	r^2	Units	Equations
4.11	$Db = \frac{V_s}{(\pi - 2.24\,\upsilon)} Td$	0.97	Db: ft V_s: fps Td:sec	4.11a
4.11	$Db = \frac{Td}{(8.21\text{-}5.86\,\upsilon)} \sqrt{\frac{E}{(1+\upsilon)}}$	0.97	Db: ft E: psf Td: sec	4.11b
4.12	$Db = \frac{V_s}{(\pi - 1.44\,\upsilon)} Td$	0.98	Db: ft V_s: fps Td: sec	4.12a
4.12	$Db = \frac{Td}{(8.21\text{-}3.75\,\upsilon)} \sqrt{\frac{E}{(1+\upsilon)}}$	0.98	Db: ft E: psf Td: sec	4.12b

with V_s in feet per second, Td in seconds, and Db in feet. The fitted equation for the rigid pavement can be expressed as:

$$Db = 0.396 V_s^{1.05} Td^{1.08} \quad (4.14)$$

with V_s in feet per second, Td in seconds, and Db in feet.

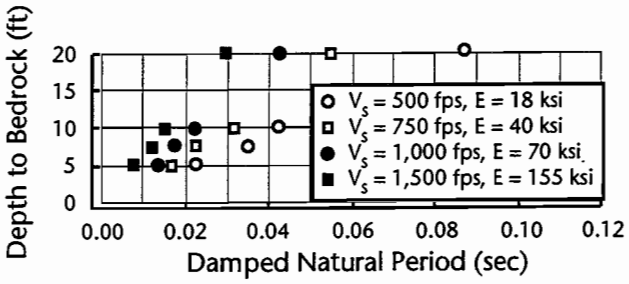

(a) Profile 1

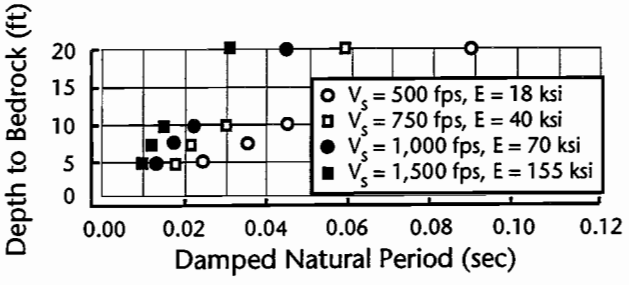

(b) Profile 2

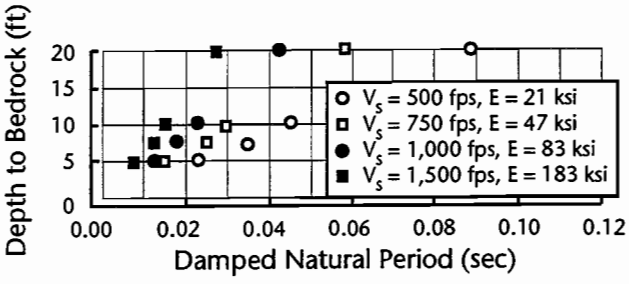

(c) Profile 3

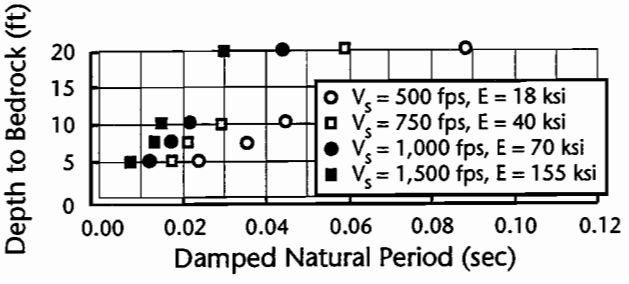

(d) Profile 4

Figure 4.16 ***Depth to bedrock versus natural period of the pavement system for FWD testing at the four pavement profiles with various stiffnesses of saturated subgrade***

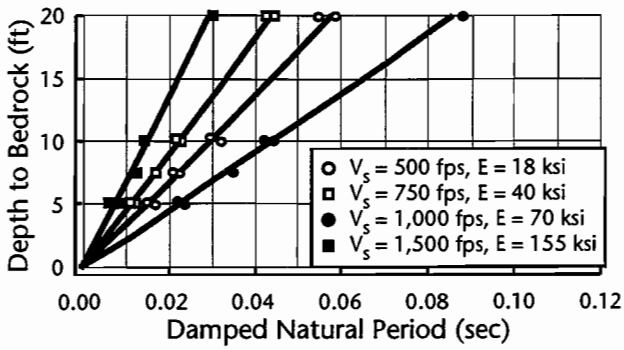

(a) Flexible pavements

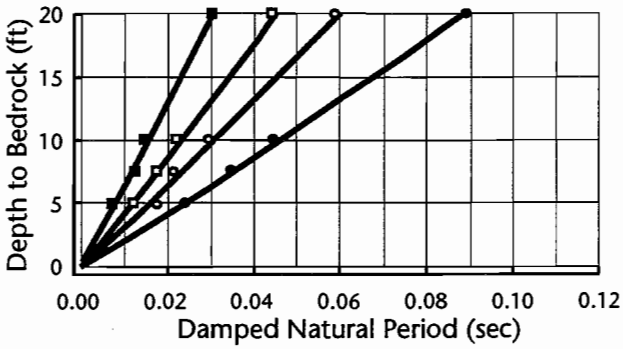

(b) A rigid pavement

Figure 4.17 ***Depth to bedrock versus damped natural period of the pavement system for FWD testing at: (a) flexible pavements and (b) a rigid pavement (saturated subgrade conditions)***

Equations 4.13 and 4.14 can be simplified as the linear equations listed in Table 4.4. The coefficient of determination for these simplified equations ranged from 0.98 to 0.99.

4.7 ESTIMATION OF THE SUBGRADE STIFFNESS FROM FWD TESTS

To use the equations in Section 4.6, a good estimate of the stiffness of the subgrade is required. The stiffness of the subgrade can be estimated by in situ seismic testing, by dynamic laboratory tests on undisturbed samples, or possibly by experience. However, a more convenient and accurate way to estimate subgrade stiffness was developed in this project. It was observed that one could measure the offset time (To) of the first pulse on the time-deflection records, as shown in Figure 4.18. The offset time is related to Rayleigh wave velocity of the subgrade. With the assumptions discussed below, and knowing the distance between two measurement stations, one can determine the shear wave velocity.

There are several assumptions which must be made to use the offset time method. First, the subgrade should be able to be approximated as a uniform material. Second, the wavelength should be long enough so that the surface, base, and subbase layers have little effect on the Rayleigh wave velocity. Generally, this means that the wavelength should be at least 10 times the total thickness of the surface, base, and subbase layers for untreated bases and subbases. Third, the bedrock needs to be deep enough so that it has little effect on the Rayleigh wave velocity. This condition is usually met if the bedrock depth is greater than 0.5 times the Rayleigh wavelength in the subgrade. Fourth, it is assumed that the near-field effects are so small that they can be ignored. Fifth, the first pulses of stations 5 and 7 were used to measure the offset time, because the deflections obtained at the stations away from the source should better represent the properties of the subgrade. Finally, the difference between the Rayleigh wave velocity and the shear wave velocity is less than 10 percent if Poisson's ratio of the material is greater than 0.2 (Richart, 1970), so it can be ignored. (Note: These assumptions frequently may not apply in normal test situations.)

Table 4.5 illustrates an example of comparisons between the estimated shear wave velocity of the subgrade and the actual shear wave velocity for Profile 1 with an unsaturated subgrade with Poisson's ratio equal to 0.20. Good estimations of the shear wave velocity of the subgrade are made in the case of the softest subgrade. However, as the stiffness of the subgrade increases, there are cases where estimations cannot be made. This happens because the first pulses in the deflection-time records were distorted and the peaks could not be determined, as shown in Figure 4.19. This effect may result from analytical approximations and deserves future investigation.

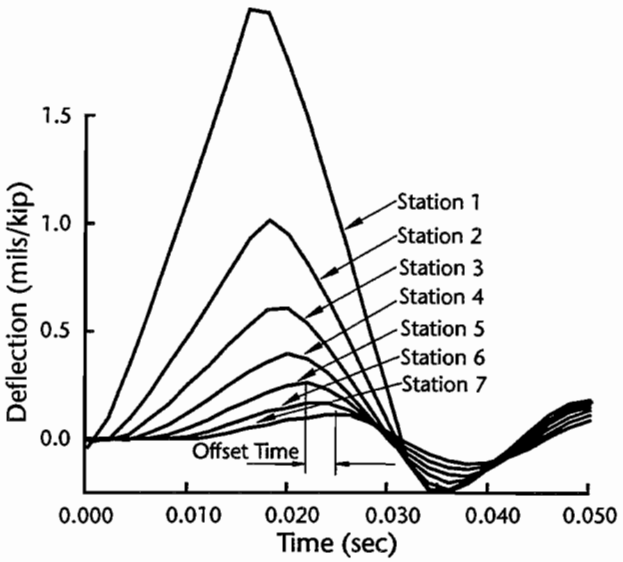

Figure 4.18 Offset time of the first pulses between station 5 and station 7 for FWD testing at Profile 1 (V_s of subgrade = 500 fps (155 m/s), E = 16 ksi (0.11 MN/m²), depth to bedrock = 5 feet (1.6 m))

4.8 SUMMARY

The FWD test was studied analytically using computer program UTFWD (Chang, 1991; Chang et al, 1992). Four pavement profiles, the same as those used in the study of the Dynaflect test, were studied. The stiffness of the subgrade layer was varied to simulate a typical range in pavement materials.

Table 4.4 Simplified equations for estimating depth to bedrock with saturated subgrade conditions

Correspond to Equations	Simplified Equations	r^2	Units	Equations
4.13	$Db = \frac{V_s}{2.22} Td$	0.99	Db: ft V_s: fps Td: sec	4.13a
4.13	$Db = \frac{\sqrt{E}}{7.0} Td$	0.99	Db: ft E: psf Td: sec	4.13b
4.14	$Db = \frac{V_s}{2.31} Td$	0.98	Db: ft V_s: fps Td: sec	4.14a
4.14	$Db = \frac{\sqrt{E}}{7.28} Td$	0.98	Db: ft E: psf Td: sec	4.14b

*Table 4.5 Estimated shear wave velocity of subgrade from offset time of the first pulses for FWD testing at Profile 1**

Units: V_s (fps), E (ksi)

Depth to Bedrock (ft)	Actual V_s of Subgrade (E of Subgrade)					
	500 (16)			750 (36)		
	To (sec)	Estimated V_s (fps)	Error** (%)	To (sec)	Estimated V_s (fps)	Error (%)
5	0.0035	571	14	na ***	na	na
7.5	0.0039	513	3	0.0028	714	-5
10	0.0040	500	0	0.0029	690	-8
20	0.0042	476	-5	0.0030	667	-11

Depth to Bedrock (ft)	Actual V_s of Subgrade (E of Subgrade)					
	1,000 (62)			1,500 (142)		
	To (sec)	Estimated V_s (fps)	Error (%)	To (sec)	Estimated V_s (fps)	Error (%)
5	na	na	na	na	na	na
7.5	na	na	na	na	na	na
10	0.0020	1,000	0	na	na	na
20	0.0021	952	-5	0.0013	1,538	3

* Poisson's ratio of Subgrade equals 0.20.
** Error = [(Estimated V_s /Actual V_s) - 1]* 100%
*** Offset time is not available because the first pulses in FWD tests are distorted.

Equations for estimating the resonant depth to bedrock were developed for both the flexible and rigid pavements. Saturated subgrade conditions did not change the trend of the resonant depth to bedrock with the stiffness of subgrade that was found under unsaturated subgrade conditions. The resonant depths to bedrock obtained with the FWD test with various subgrade stiffnesses are approximately one fourth of the resonant depths to bedrock obtained with the Dynaflect test. This is because the predominate frequency in the FWD test is about 30 Hz, which is about four times the frequency of the Dynaflect test (8 Hz).

Equations for estimating the depth to bedrock based on the damped natural period of the free vibrations of the pavement system immediately after the FWD load application have been presented. In these equations, effects of stiffness and degree of saturation of subgrade were taken into account.

A method for estimating the stiffness of the subgrade by the offset time of the first pulses at two measurement stations of the deflection-time records in FWD tests has been developed. The shear wave velocity of the subgrade can be estimated by dividing the offset time by the distance between these two stations. At present, it seems that this approach is more appropriate in those cases where the stiffness of the subgrade is soft to moderately stiff (V_s = 500 to 750 fps (155 to 233 m/s) or E = 16 to 36 ksi (0.11 to 0.25 MN/m^2) or where the bedrock depth is 10 feet (3.1 m) or more.

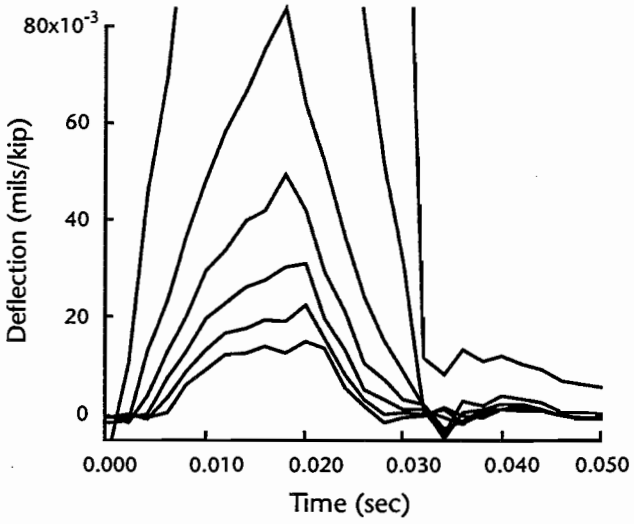

Figure 4.19 Distorted first pulses in FWD records obtained at Profile 1 with the stiffest subgrade and bedrock depth = 7.5 feet

CHAPTER 5. INFLUENCE OF DYNAMIC DEFLECTIONS ON BACKCALCULATED LAYER MODULI IN THE FWD TEST

5.1 INTRODUCTION

The computer program MODULUS (Uzan et al, 1989), which is based on static interpretation of the FWD test, was used to backcalculate layer moduli from the dynamic deflection basins obtained with the UTFWD program (Chang, 1991; Chang et al, 1992). The backcalculated moduli were then compared with the actual moduli used to generate the deflection basins.

The values of the moduli and the thicknesses of the pavement layers of the four pavement profiles were used to obtain the deflection basins using UTFWD. These deflection basins were then used as input parameters along with the actual thicknesses of the pavement layers. The backcalculated moduli from MODULUS were then determined using the "Run a Full Analysis" option in MODULUS.

The main purpose of these studies was to investigate the accuracy of backcalculating layer moduli from FWD measurements with a static interpretation method. The effects of the following conditions were studied:

1. depth to bedrock;
2. stiffness of the subgrade; and
3. saturated versus unsaturated subgrade conditions.

The stiffnesses of the base and surface layers were not studied. Based on the results of the study with the Dynaflect presented in Chapter 3, our research indicates that the stiffness of the subgrade and the depth to bedrock are the main factors influencing the dynamic deflections.

5.2 MODEL PARAMETERS

As in the parametric study of the FWD presented in Chapter 4, only the depth to bedrock and stiffness of the subgrade were varied. The stiffnesses of the other pavement layers were kept constant, such that the shear wave velocity of the CRC equaled 8500 fps (2593 m/s) (E = 5425 ksi (37.4 MN/m^2)), the shear wave velocity of the AC equaled 3000 fps (915 m/s) (E = 690 ksi (4.8 MN/m^2)), and the shear wave velocity of the base equaled 1000 fps (305 m/s) (E = 67 ksi (0.46 MN/m^2)). The shear wave velocity of the subgrade layer was varied from 500 to 1500 fps (150 to 450 m/s) and the corresponding Young's modulus varied from 16 to 142 ksi (0.11 to 0.98 MN/m^2).

To simulate an unsaturated subgrade, a Poisson's ratio of 0.33 was used. The material properties of the four pavement profiles with unsaturated subgrade conditions are given in Table 4.1. To simulate a saturated subgrade, the P-wave velocity of the subgrade was set equal to 5000 fps (1525 m/s). The shear wave velocities of the subgrades were varied from 500 to 1500 fps (150 to 450 m/s), as in the unsaturated subgrade condition. As a result, Poisson's ratio varied from 0.495 to 0.451, as S-wave velocity of subgrade varied from 500 to 1500 fps (150 to 450 m/s). Hence, Young's modulus for the saturated subgrade varied from 18 to 155 ksi (0.12 to 1.07 MN/m^2). The material properties of the four pavement profiles with saturated subgrades are given in Table 4.2.

5.3 DEFLECTION BASINS

Three kinds of deflection basins were used in the backcalculation study of layer moduli with MODULUS. A schematic illustration of the relative locations of the bedrock depths where these three deflection basins were taken is shown in Figure 5.1. The first basin was the dynamic deflection basin obtained at the resonant condition, as shown in Figure 5.1a. This deflection basin is denoted as the R-basin (resonant basin) and represents the case where static and dynamic deflections exhibit the largest differences, as shown in Figure 5.2. The second basin is for the static deflection basin obtained at the same depth to bedrock as the R-basin, but with a static loading applied to the pavement. This basin, denoted as the S-basin (Static basin), represents a case where one could presumably perform a backcalculation, based on a known depth

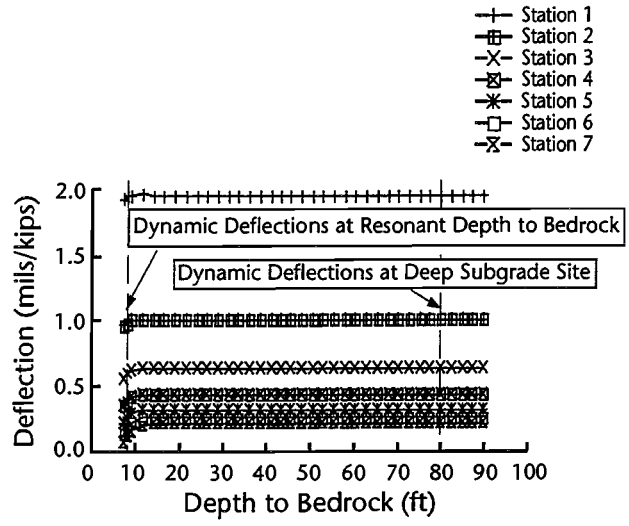

(a) Dynamic deflections

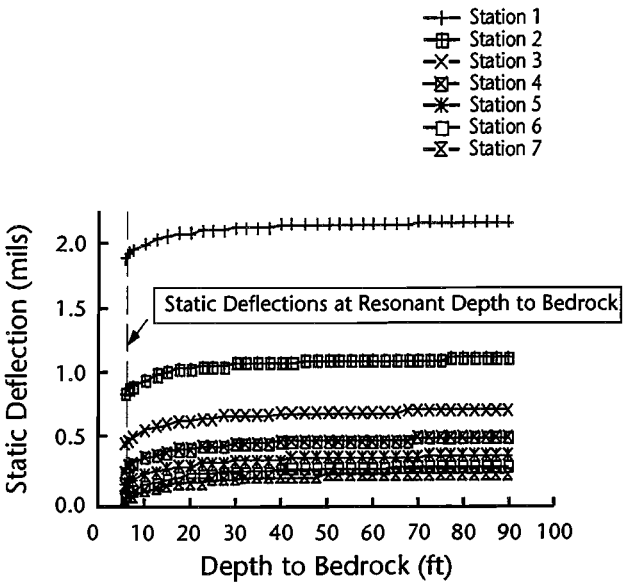

(b) Static deflections

Figure 5.1 ***Three kinds of deflection basins used to backcalculate layer moduli for FWD testing at Profile 1 (V_s of unsaturated subgrade = 500 fps (155 m/s) and E = 16 ksi (0.11 MN/m²))***

to bedrock. This is an erroneous assumption because the dynamics of the test still have not been taken into account. The third basin is the dynamic deflection basin obtained at each profile where the bedrock lies at a significant depth. A bedrock depth of 80 feet (24 m) was selected to represent this case. As seen in Figure 5.1a, this case represents the condition far away from the resonant condition where static and dynamic measurements are nearly the same. This case is denoted as the N-basin (non-resonant basin) and represents the case where a static backcalculation scheme should involve the fewest approximations.

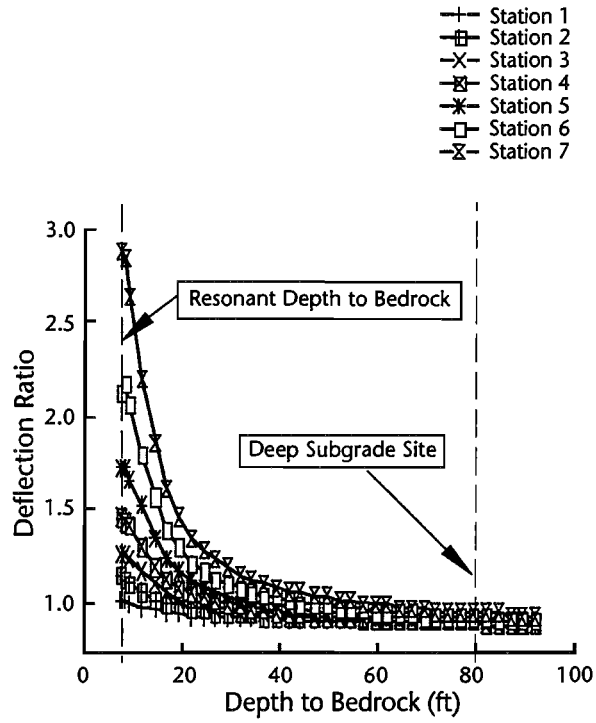

Figure 5.2 ***Deflection ratio versus depth to bedrock for FWD testing at Profile 1 (V_s of unsaturated subgrade = 500 fps (155 m/s) and E = 16 ksi (0.11 MN/m²))***

These three deflection basins at Profile 1 with unsaturated subgrade conditions are shown in Figure 5.3. For the case of the softest subgrade conditions, there is little difference at the source between dynamic deflections obtained at the resonant condition (R-basin) and the equivalent static deflections (S-basin) as shown in Figure 5.3a. The difference between the R-basin and S-basin becomes larger as the distance from the source increases. This behavior explains why the deflection ratio at the nearest measurement station is the smallest and the deflection ratio at the farthest measurement

station is the largest in the FWD test at resonance, as illustrated in Figure 5.2. The deflection basin obtained at the deep subgrade site (N-basin) exhibits the largest deflections because the thickest section of subgrade material is being strained. However, it is interesting to note that for the N-basin the dynamic deflections are slightly less than the static deflections—a result of inertia in the pavement system.

For the stiffest subgrade condition, there is little difference between the R-basin, S-basin, and N-basin, as shown in Figure 5.3b. This indicates that deflection ratios obtained from stiff subgrade conditions are smaller than those obtained from soft subgrade conditions. This relationship is clearly seen by comparing deflection ratios shown in Appendix B.

5.4 BACKCALCULATION OF LAYER MODULI OBTAINED FROM PROGRAM MODULUS

The results of the backcalculated layer moduli for the four pavement profiles are summarized in Tables 5.1, 5.2, 5.3, and 5.4 for Profiles 1, 2, 3 and 4, respectively. The backcalculated modulus is denoted as Ec and the actual (assumed) modulus used to generate the deflection basin is denoted as Eo in Tables 5.1 to 5.4. The difference between the backcalculated and the actual modulus is represented by the ratio of backcalculated modulus to actual modulus and is denoted as Ec/Eo.

5.4.1 Profile 1

Subgrade Moduli of Profile 1

For unsaturated subgrade conditions, the backcalculated subgrade moduli obtained from the R-basins are 20 percent to 50 percent less than the actual moduli, as shown by the solid symbols in Figure 5.4a. These differences generally decrease as the stiffness of subgrade increases. This trend occurs because deflections increase as the stiffness of the subgrade decreases.

The errors in backcalculated subgrade moduli obtained from N-basins and S-basins are less than 20 percent. This result indicates that backcalculated moduli obtained from dynamic deflection basins are quite accurate for FWD measurements performed well away from the resonant bedrock depth.

For saturated subgrade conditions, there are several cases where the MODULUS program does not converge to the backcalculated layer moduli (Table 5.1b). This is a natural case in which MODULUS, a statically based analysis, cannot converge with some dynamically generated deflection basins. However, with the available data in Figure 5.4b, one can see that, basically, the saturated subgrade condition exhibits trends similar to those exhibited in the case of the unsaturated subgrade conditions.

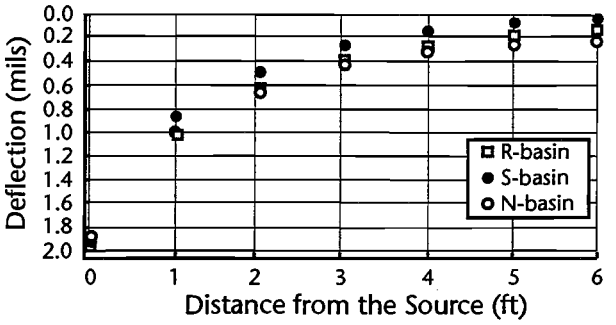

(a) S-wave velocity of subgrade = 500 fps, E = 16 ksi

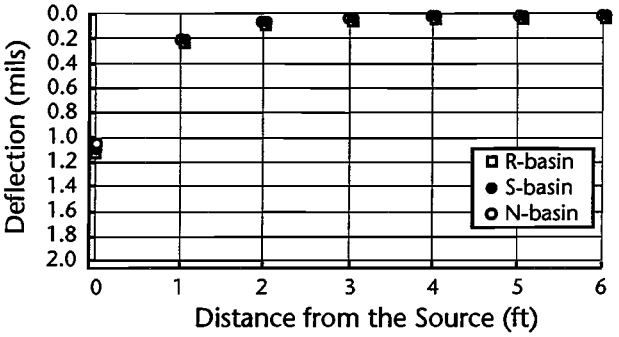

(b) S-wave velocity of subgrade = 1500 fps, E = 142 ksi

Figure 5.3 ***Three kinds of deflection basins for FWD testing at Profile 1 (V_s of unsaturated subgrade = 500 fps (155 m/s) and E = 16 ksi (0.11 MN/m²))***

Table 5.1 Comparison of backcalculated layer moduli with actual moduli for FWD tests at Profile 1

(a) Unsaturated subgrade conditions

		V_s of Subgrade (fps)											
		500			750			1,000			1,500		
Deflection Basin		N*	R**	S***	N	R	S	N	R	S	N	R	S
Thickness of Subgrade (in.)		947	59	59	947	117	117	947	137	137	947	227	227
AC (ksi)	True Eo	690	690	690	690	690	690	690	690	690	690	690	690
	Comp Ec	2,319	8,508	4,112	1,978	5,433	1,783	1,202	1,539	214	473	611	447
	Ec/Eo	3.36	12.33	5.96	2.87	7.87	2.58	1.74	2.23	0.31	0.68	0.89	0.65
Base (ksi)	True Eo	67	67	67	67	67	67	67	67	67	67	67	67
	Comp Ec	68	118	75	71	93	68	71	77	71	77	77	71
	Ec/Eo	1.01	1.76	1.12	1.06	1.39	1.02	1.06	1.14	1.07	1.15	1.14	1.05
Subgrade (ksi)	True Eo	16	16	16	36	36	36	63	63	63	142	142	142
	Comp Ec	17	9	14	35	23	34	60	52	71	119	115	149
	Ec/Eo	1.06	0.53	0.88	0.97	0.65	0.95	0.95	0.82	1.13	0.84	0.81	1.05

(b) Saturated subgrade conditions

		V_s of Subgrade (fps)											
		500			750			1,000			1,500		
Deflection Basin		N	R	S	N	R	S	N	R	S	N	R	S
Thickness of Subgrade (in.)		947	59	59	947	117	117	947	137	137	947	227	227
AC (ksi)	True Eo	690	690	690	690	690	690	690	690	690	690	690	690
	Comp Ec	-	-	-	2,379	7,409	1,722	1,910	-	187	606	1,387	512
	Ec/Eo	-	-	-	2.51	63.32	14.71	2.02	-	1.36	0.64	6.11	2.26
Base (ksi)	True Eo	67	67	67	67	67	67	67	67	67	67	67	67
	Comp Ec	-	-	-	74	150	69	70	-	76	76	77	72
	Ec/Eo	-	-	-	1.10	2.24	1.03	1.04	-	1.13	1.13	1.14	1.07
Subgrade (ksi)	True Eo	18	18	18	40	40	40	70	70	70	155	155	155
	Comp Ec	-	-	-	38	25	40	64	-	72	149	130	171
	Ec/Eo	-	-	-	0.96	0.63	1.02	0.91	-	1.03	0.96	0.84	1.10

* Dynamic deflection basins at deep subgrade site
** Dynamic deflection basins at resonant depth to bedrock
*** Static deflection basins at resonant depth to bedrock
Note: MODULUS program does not successfully converge at some cases so that some backcalculated moduli cannot be determined.

Table 5.2 Comparison of backcalculated layer moduli with actual moduli for FWD tests at Profile 2

(a) Unsaturated subgrade conditions

		V_s of Subgrade (fps)											
		500			750			1,000			1,500		
Deflection Basin		**N***	**R****	**S*****	**N**	**R**	**S**	**N**	**R**	**S**	**N**	**R**	**S**
Thickness of Subgrade (in.)		950	62	62	950	110	110	950	140	140	950	230	230
AC (ksi)	True Eo	690	690	690	690	690	690	690	690	690	690	690	690
	Comp Ec	1,329	5,157	1,374	1,083	2,604	1,032	1,515	1,358	1,469	1,701	1,213	2,675
	Ec/Eo	1.93	7.47	1.99	1.57	3.77	1.50	2.20	1.97	2.13	2.47	1.76	3.88
Base (ksi)	True Eo	67	67	67	67	67	67	67	67	67	67	67	67
	Comp Ec	281	270	359	267	445	263	181	285	173	116	173	68
	Ec/Eo	4.19	4.03	5.36	3.99	6.64	3.93	2.70	4.25	2.58	1.73	2.58	1.01
Subgrade (ksi)	True Eo	16	16	16	36	36	36	63	63	63	142	142	142
	Comp Ec	18	9	14	36	24	34	60	50	58	130	113	145
	Ec/Eo	1.11	0.58	0.88	1.00	0.68	0.95	0.96	0.79	0.91	0.92	0.80	1.02

(b) Saturated subgrade conditions

		V_s of Subgrade (fps)											
		500			750			1,000			1,500		
Deflection Basin		**N**	**R**	**S**	**N**	**R**	**S**	**N**	**R**	**S**	**N**	**R**	**S**
Thickness of Subgrade (in.)		950	62	62	950	110	110	950	140	140	950	230	230
AC (ksi)	True Eo	690	690	690	690	690	690	690	690	690	690	690	690
	Comp Ec	1,105	4,506	9,545	1,039	3,676	972	1,512	1,178	2,443	1,740	1,218	2,782
	Ec/Eo	1.60	6.53	13.83	1.51	5.33	1.41	2.19	1.71	3.54	2.52	1.77	4.03
Base (ksi)	True Eo	67	67	67	67	67	67	67	67	67	67	67	67
	Comp Ec	395	1,469	284	321	598	300	197	429	97	114	165	69
	Ec/Eo	9.22	21.93	4.24	4.79	8.93	4.48	2.94	6.40	1.44	1.70	2.46	1.03
Subgrade (ksi)	True Eo	18	18	18	40	40	40	70	70	70	155	155	155
	Comp Ec	19	9	13	38	25	37	64	51	70	139	124	163
	Ec/Eo	1.07	0.51	0.73	0.96	0.63	0.94	0.92	0.73	1.00	0.90	0.80	1.05

* Dynamic deflection basins at deep subgrade site

** Dynamic defection basins at resonant depth to bedrock

*** Static deflection basins at resonant depth to bedrock

Table 5.3 Comparison of backcalculated layer moduli with actual moduli for FWD tests at Profile 3

(a) Unsaturated subgrade conditions

		V_s of Subgrade (fps)											
		500			750			1,000			1,500		
Deflection Basin		**N***	**R****	**S*****	**N**	**R**	**S**	**N**	**R**	**S**	**N**	**R**	**S**
Thickness of Subgrade (in.)		947	59	59	947	117	117	947	137	137	947	227	227
AC (ksi)	True Eo	715	715	715	715	715	715	715	715	715	715	715	715
	Comp Ec	617	366	645	617	452	596	641	522	736	647	561	752
	Ec/Eo	0.86	0.51	0.90	0.86	0.63	0.83	0.90	0.73	1.03	0.91	0.79	1.05
Base (ksi)	True Eo	70	70	70	70	70	70	70	70	70	70	70	70
	Comp Ec	117	593	84	125	566	105	104	253	67	87	124	63
	Ec/Eo	1.68	8.47	1.20	1.78	8.09	1.50	1.49	3.62	0.95	1.25	1.76	0.89
Subgrade (ksi)	True Eo	19	19	19	42	42	42	75	75	75	168	168	168
	Comp Ec	21	10	21	42	29	40	72	55	75	157	135	174
	Ec/Eo	1.11	0.55	1.13	1.01	0.68	0.96	0.97	0.74	1.00	0.93	0.80	1.04

(b) Saturated subgrade conditions

		V_s of Subgrade (fps)											
		500			750			1,000			1,500		
Deflection Basin		**N**	**R**	**S**	**N**	**R**	**S**	**N**	**R**	**S**	**N**	**R**	**S**
Thickness of Subgrade (in.)		947	59	59	947	117	117	947	137	137	947	227	227
AC (ksi)	True Eo	715	715	715	715	715	715	715	715	715	715	715	715
	Comp Ec	466	894	1,600	516	543	611	585	509	789	608	564	759
	Ec/Eo	0.65	1.25	2.24	0.72	0.76	0.85	0.82	0.71	1.10	0.85	0.79	1.06
Base (ksi)	True Eo	70	70	70	70	70	70	70	70	70	70	70	70
	Comp Ec	250	895	480	193	857	99	143	308	62	102	127	67
	Ec/Eo	3.57	12.79	6.86	2.75	12.25	1.42	2.04	4.39	0.88	1.45	1.82	0.95
Subgrade (ksi)	True Eo	21	21	21	47	47	47	83	83	83	183	183	183
	Comp Ec	22	9	16	46	30	47	78	61	87	169	150	197
	Ec/Eo	1.06	0.43	0.76	0.97	0.65	1.00	0.94	0.74	1.06	0.92	0.82	1.08

* Dynamic deflection basins at deep subgrade site

** Dynamic defection basins at resonant depth to bedrock

*** Static deflection basins at resonant depth to bedrock

Table 5.4 Comparison of backcalculated layer moduli with actual moduli for FWD tests at Profile 4

(a) Unsaturated subgrade conditions

		V_s of Subgrade (fps)											
		500			750			1,000			1,500		
Deflection Basin		N*	R**	S***	N	R	S	N	R	S	N	R	S
Thickness of Subgrade (in.)		932	38	38	932	62	62	932	92	92	932	182	182
CRC (ksi)	True Eo	5,424	5,424	5,424	5,424	5,424	5,424	5,424	5,424	5,424	5,424	5,424	5,424
	Comp Ec	8,487	7,339	4,463	6,146	6,154	4,746	5,658	4,583	5,624	6,421	5,847	5,777
	Ec/Eo	1.56	1.35	0.82	1.13	1.13	0.88	1.04	0.84	1.04	1.18	1.08	1.07
AC (ksi)	True Eo	715	715	715	715	715	715	715	715	715	715	715	715
	Comp Ec	278	241	959	1,040	225	954	376	840	494	255	305	287
	Ec/Eo	0.39	0.34	1.34	1.45	0.31	1.33	0.53	1.17	0.69	0.36	0.43	0.40
Subbase (ksi)	True Eo	67	67	67	67	67	67	67	67	67	67	67	67
	Comp Ec	83	296	83	47	225	70	125	196	81	107	165	103
	Ec/Eo	1.24	4.42	1.23	0.70	3.36	1.04	1.87	2.93	1.21	1.60	2.46	1.53
Subgrade (ksi)	True Eo	16	16	16	36	36	36	63	63	63	142	142	142
	Comp Ec	27	7	13	50	23	33	75	46	68	155	122	153
	Ec/Eo	1.71	0.43	0.78	1.39	0.63	0.92	1.20	0.73	1.08	1.09	0.86	1.08

(b) Saturated subgrade conditions

		V_s of Subgrade (fps)											
		500			750			1,000			1,500		
Deflection Basin		N	R	S	N	R	S	N	R	S	N	R	S
Thickness of Subgrade (in.)		932	38	38	932	62	62	932	92	92	932	182	182
CRC (ksi)	True Eo	5,424	5,424	5,424	5,424	5,424	5,424	5,424	5,424	5,424	5,424	5,424	5,424
	Comp Ec	9,143	4,230	6,574	5,042	5,608	4,888	5,779	5,279	5,711	6,643	6,283	5,262
	Ec/Eo	1.69	0.78	1.21	0.93	1.03	0.90	1.07	0.97	1.05	1.22	1.16	0.97
AC (ksi)	True Eo	715	715	715	715	715	715	715	715	715	715	715	715
	Comp Ec	314	2,321	605	1,639	381	1,174	587	1,728	460	304	279	962
	Ec/Eo	0.44	3.25	0.85	2.29	0.53	1.64	0.82	2.42	0.64	0.42	0.39	1.35
Subbase (ksi)	True Eo	67	67	67	67	67	67	67	67	67	67	67	67
	Comp Ec	94	71	20	60	338	44	264	64	103	107	158	52
	Ec/Eo	1.40	1.06	0.30	0.90	5.04	0.66	2.30	0.96	1.53	1.59	2.35	0.77
Subgrade (ksi)	True Eo	18	18	18	40	40	40	70	70	70	155	155	155
	Comp Ec	30	6	14	54	24	45	83	55	86	170	140	189
	Ec/Eo	1.69	0.32	0.75	1.36	0.61	1.14	1.19	0.78	1.23	1.10	0.90	1.22

* Dynamic deflection basins at deep subgrade site

** Dynamic defection basins at resonant depth to bedrock

*** Static deflection basins at resonant depth to bedrock

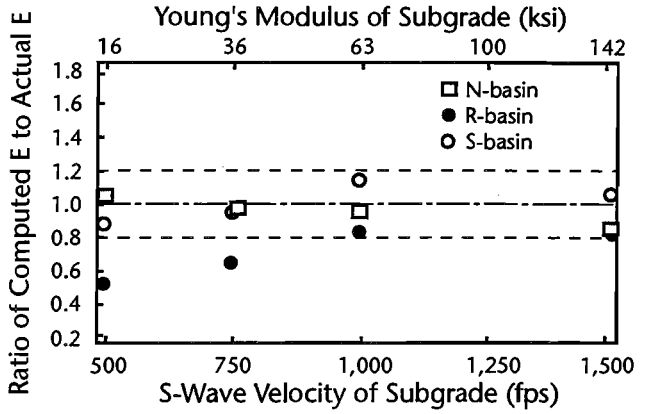

(a) Unsaturated subgrade conditions

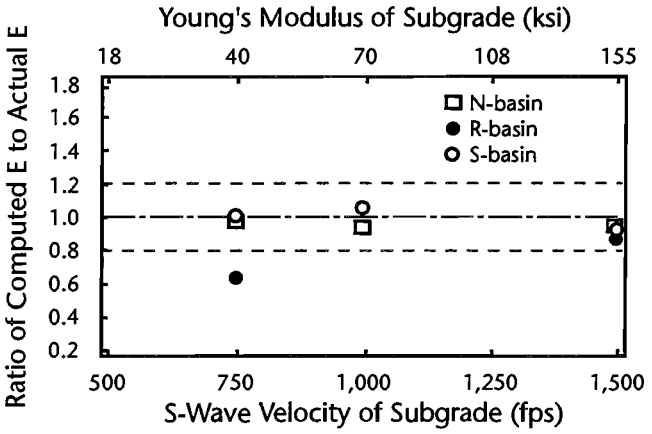

(b) Saturated subgrade conditions

Figure 5.4 ***Ratio of backcalculated subgrade moduli to actual subgrade moduli for FWD testing at Profile 1 with various subgrade stiffnesses***

Base Moduli of Profile 1

For unsaturated subgrade conditions, backcalculated base moduli obtained from both the S-basins and N-basins are very close to the actual moduli, as shown in Figure 5.5a. The differences are less than 15 percent, with the backcalculated moduli always larger. The backcalculated base moduli obtained from R-basins overestimate the actual moduli by 15 percent to 180 percent. This is because the backcalculated subgrade moduli obtained at R-basins are all too low. The poorest estimation was obtained with the softest subgrade because it involves the largest motions.

For the saturated subgrade condition, there are several cases where, for unknown reasons, the MODULUS program does not successfully backcalculate moduli, as shown in Table 5.1b. According to the available data, the trends are similar to those for the unsaturated subgrade, except that the errors obtained from the R-basins are even larger, as seen by comparing the solid points in Figures 5.5a and 5.5b.

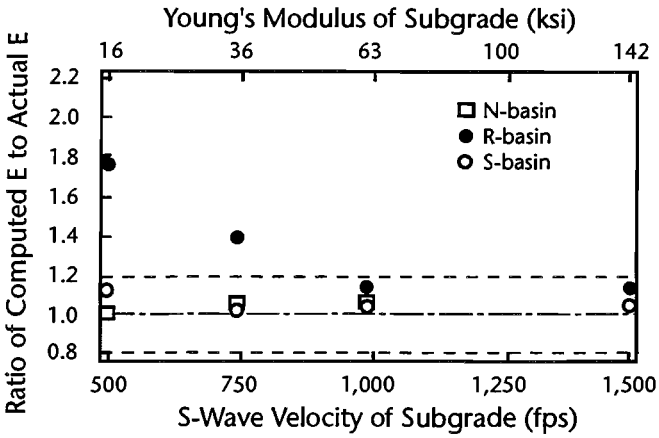

(a) Unsaturated subgrade conditions

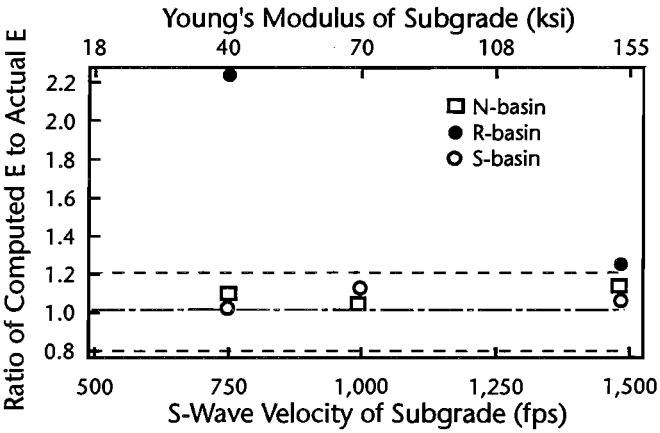

(b) Saturated subgrade conditions

Figure 5.5 ***Ratio of backcalculated base moduli to actual base moduli for FWD testing at Profile 1 with various subgrade stiffnesses***

AC Moduli of Profile 1

For the unsaturated and saturated subgrade conditions, the backcalculated AC moduli are at least two times larger than the actual AC moduli when the subgrade has a V_s of 1000 fps (310 m/s) (E = 63 ksi (0.43 MN/m^2)) or less, as shown in Table 5.1. However, the backcalculated moduli obtained with N-basins and S-basins with the stiffest subgrade exhibit good values (differences < 15 percent).

5.4.2 Profile 2

Subgrade Moduli of Profile 2

For Profile 2 with unsaturated subgrade conditions, the differences between backcalculated and actual subgrade moduli obtained from the N-basins (deep subgrade) and S-basins (static) are less than about 20 percent, as shown in Figure 5.6a. The backcalculated subgrade moduli obtained from the R-basins (resonant conditions) are 30 percent to 40 percent lower than the assumed actual moduli, as shown by the solid points in the figure.

Again, the saturated subgrade conditions exhibit a trend similar to that of the unsaturated subgrade conditions, as shown in Figure 5.6b. The errors in the backcalculated subgrade moduli obtained from the R-basins in the saturated subgrade conditions are about 5 percent higher than those in the unsaturated subgrade conditions.

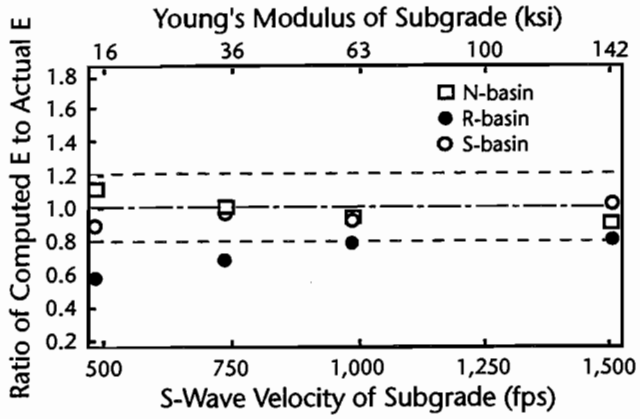

(a) Unsaturated subgrade conditions

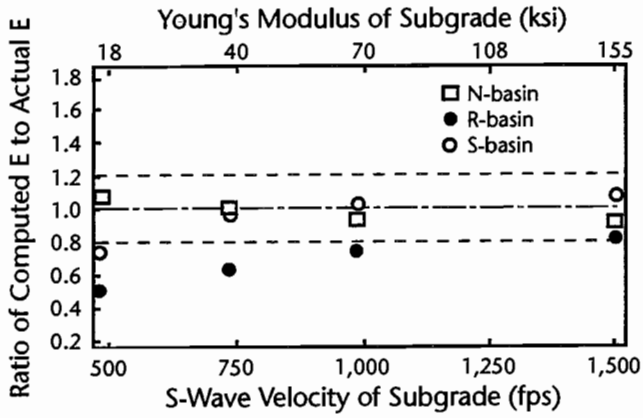

(b) Saturated subgrade conditions

Figure 5.6 ***Ratio of backcalculated subgrade moduli to actual subgrade moduli for FWD testing at Profile 2 with various subgrade stiffnesses***

Base Moduli of Profile 2

For Profile 2 with unsaturated subgrade conditions, the backcalculated base moduli obtained from all of the deflection basins are at least 2 times higher than the actual moduli, except for the stiffest subgrade case (see Figure 5.7a). For saturated subgrade conditions, the backcalculated base modulus from the R-basin with the softest subgrade condition is 25 times higher than the actual modulus. For the unsaturated subgrade conditions, there is good agreement in the backcalculated layer moduli for the stiffest subgrade condition.

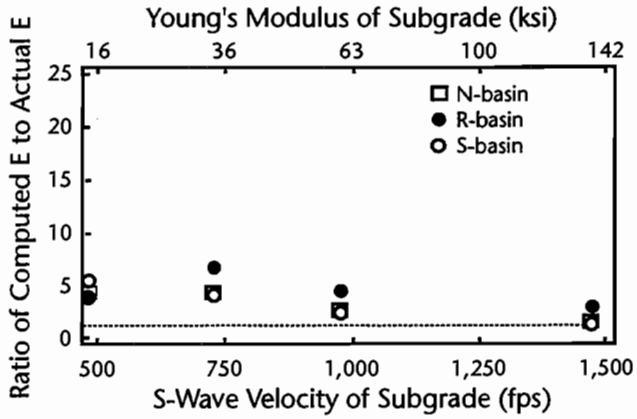

(a) Unsaturated subgrade conditions

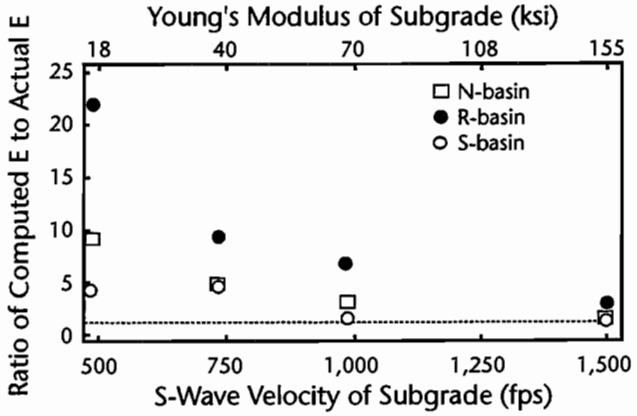

(b) Saturated subgrade conditions

Figure 5.7 ***Ratio of backcalculated base moduli to actual base moduli for FWD testing at Profile 2 with various subgrade stiffnesses***

AC Moduli of Profile 2

There is essentially no resolution in the backcalculated AC moduli for both the unsaturated and saturated subgrade conditions, as shown in Table

5.2. The backcalculated AC moduli are always greater than the actual moduli. The errors in the backcalculated AC moduli are always greater than 40 percent and are generally more than 100 percent.

5.4.3 Profile 3

Subgrade Moduli of Profile 3

For unsaturated subgrade conditions, the backcalculated subgrade moduli obtained from the N-basins and S-basins are very close to the actual moduli (differences are less than 10 percent), as shown in Figure 5.8a. The backcalculated subgrade moduli obtained from the R-basins are 20 percent to 40 percent lower than the actual moduli. Saturated subgrade conditions exhibit similar trends, as seen by comparing Figures 5.8a and 5.8b.

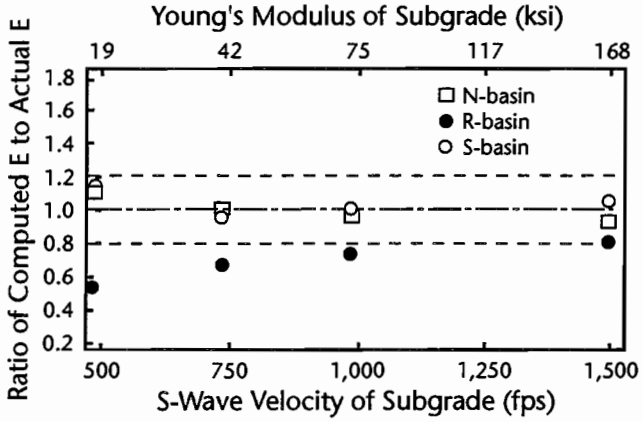

(a) Unsaturated subgrade conditions

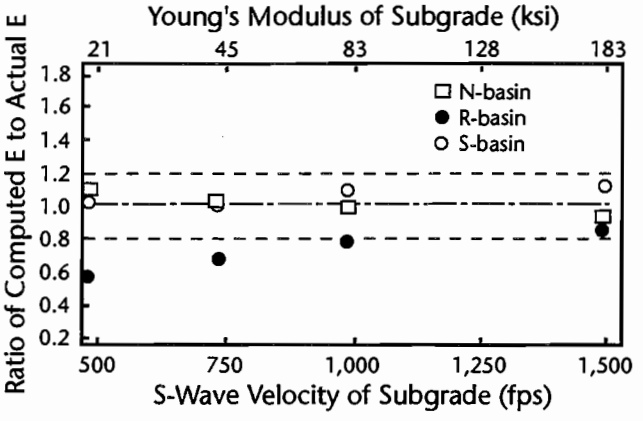

(b) Saturated subgrade conditions

Figure 5.8 ***Ratio of backcalculated subgrade moduli to actual subgrade moduli for FWD testing at Profile 3 with various subgrade stiffnesses***

Base Moduli of Profile 3

For Profile 3 with unsaturated subgrade conditions, the backcalculated base moduli obtained from the R-basins are unrealistically high, especially for the softest subgrade condition, as shown in Figure 5.9a. The differences in backcalculated base moduli obtained from the N-basins and S-basins (about 5 percent to 70 percent) are much less significant than those obtained from the R-basins (about 70 percent to 850 percent), but still quite different than the actual moduli, except for the stiffest subgrade condition. This trend results from the fact that the backcalculated subgrade moduli have been underestimated.

For saturated subgrade conditions, the backcalculated base moduli are even higher than those obtained for the unsaturated subgrade conditions, as seen by comparing Figures 5.9a and 5.9b.

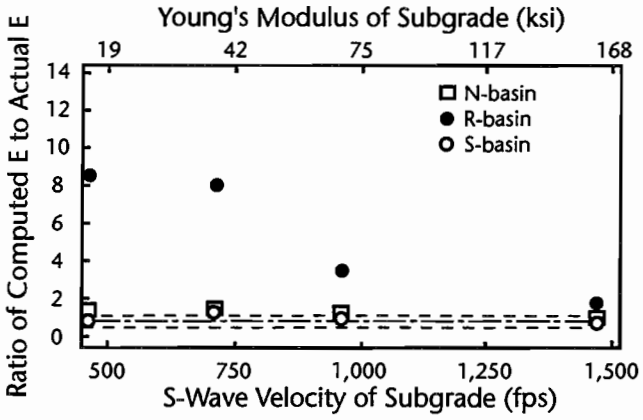

(a) Unsaturated subgrade conditions

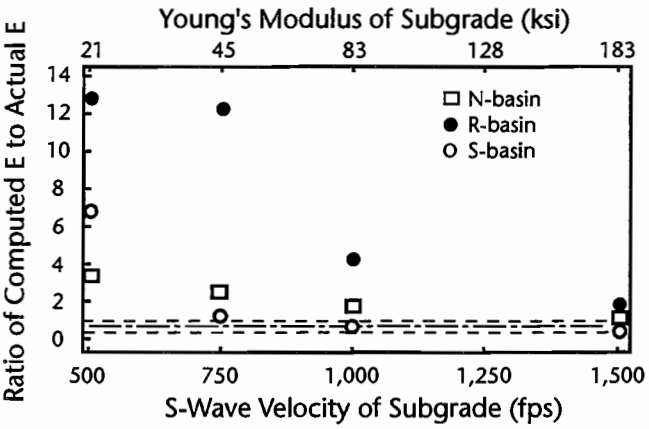

(b) Saturated subgrade conditions

Figure 5.9 ***Ratio of backcalculated base moduli to actual base moduli for FWD testing at Profile 3 with various subgrade stiffnesses***

AC Moduli of Profile 3

Profile 3 is the only flexible pavement profile which shows good resolution in backcalculated AC moduli, as shown in Table 5.3. For unsaturated subgrade conditions, the differences between backcalculated AC moduli obtained from the N-basin and S-basin and actual moduli are less than 15 percent. The difference in backcalculated AC moduli obtained from the R-basins vary from 50 percent to 30 percent as the subgrade stiffness increases.

For the saturated subgrade condition, the errors in backcalculated AC moduli are considerably larger than those of the unsaturated subgrade condition for the softer subgrade.

5.4.4 Profile 4

Subgrade Moduli of Profile 4

For unsaturated subgrade conditions, the backcalculated subgrade moduli obtained from the N-basins overestimate the actual moduli by 10 to 70 percent, as shown in Figure 5.10a. On the other hand, the backcalculated subgrade moduli obtained from the R-basins underestimate the actual moduli by 15 percent to 60 percent. As expected, the backcalculated subgrade moduli obtained from the S-basins have the least differences (within 20 percent).

The saturated subgrade condition exhibited a trend almost identical to that for unsaturated subgrade conditions, as seen by comparing Figure 5.10a with Figure 5.10b.

Subbase Moduli of Profile 4

For Profile 4 with unsaturated subgrade conditions, the backcalculated subbase moduli obtained from the R-basins overestimate the actual moduli by 240 percent to 440 percent, which are apparently incorrect, as shown in Figure 5.11a. The errors in the backcalculated subbase moduli obtained from the N-basins and S-basins are much smaller than those obtained from the R-basins, but still vary from 20 percent to 80 percent. For saturated subgrade conditions, as shown in Figure 5.11b, the differences of backcalculated subbase moduli obtained from R-basins varied significantly (5 percent to about 500 percent).

AC Base Moduli of Profile 4

Most of the backcalculated AC moduli do not show good comparisons with the actual moduli, as presented in Table 5.4. The differences between the backcalculated AC moduli and the actual moduli vary from 15 percent to 325 percent, with the poorest case occurring at the softest subgrade condition.

CRC Moduli of Profile 4

The differences of the backcalculated CRC moduli for all deflection basins (in the case of unsaturated subgrades) are less than 20 percent, except for those obtained from the softest subgrade conditions (Table 5.4). For saturated subgrade conditions, the trend is basically the same as can be seen by comparing Tables 5.4a and 5.4b.

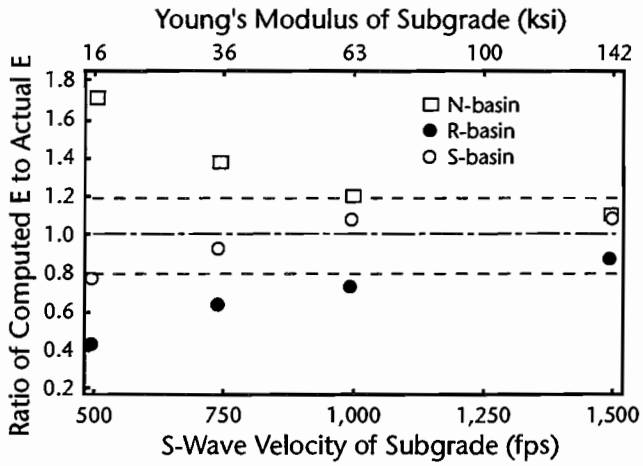

(a) Unsaturated subgrade conditions

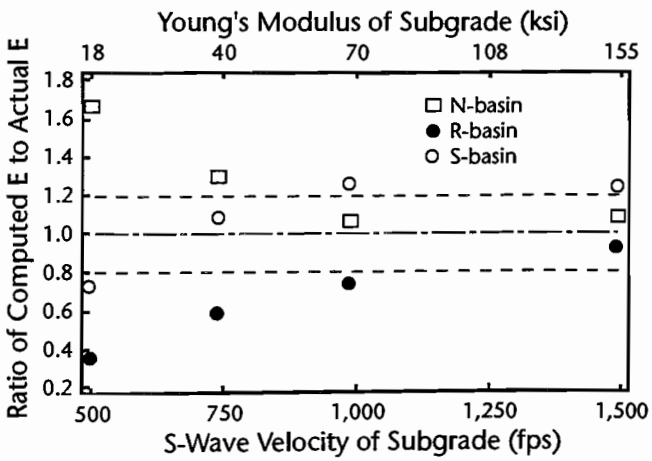

(b) Saturated subgrade conditions

Figure 5.10 Ratio of backcalculated subgrade moduli to actual subgrade moduli for FWD testing at Profile 4 with various subgrade stiffnesses

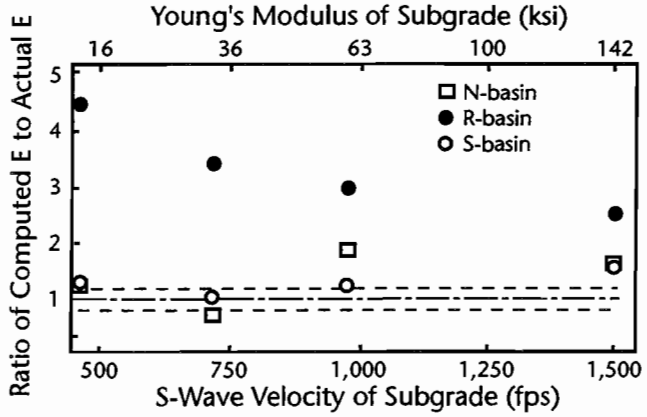

(a) Unsaturated subgrade conditions

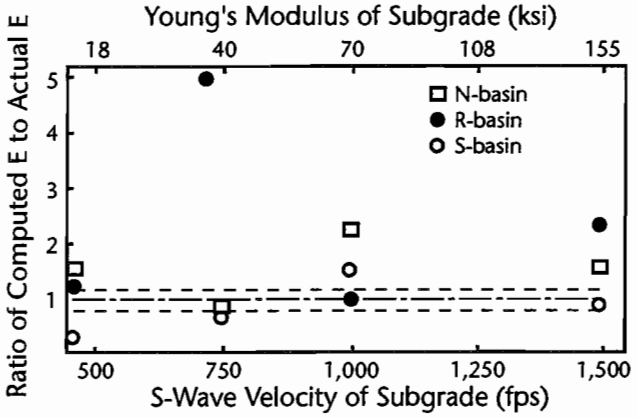

(b) Saturated subgrade conditions

Figure 5.11 ***Ratio of backcalculated base moduli to actual base moduli for FWD testing at Profile 4 with various subgrade stiffnesses***

5.5 SUMMARY

In some cases, the R-basins and S-basins obtained with saturated subgrade conditions at shallow depth to bedrock might be affected by the numerical problems in UTFWD. The results obtained with saturated subgrade conditions need further study.

Overall, the backcalculated subgrade moduli obtained from static deflection basins at resonant depth to bedrock (S-basins) and from dynamic deflection basins for deep subgrade profiles (N-basin), which represent nonresonant conditions, show better comparisons than those obtained with dynamic deflection basins at the resonant bedrock condition (R-basins).

The stiffness of the subgrade layer has a major effect on the accuracy of backcalculated layer moduli. The errors of the backcalculated layer moduli increase as the subgrade stiffness decreases. This behavior also agrees with the trend of variations of maximum deflection ratios presented in Section 4.5.

Profile 1, which has the thinnest surface layer, is the only profile which shows good comparisons in the backcalculated base moduli. For the other three profiles (Profiles 2, 3, and 4), the differences are generally greater than 100 percent, except for the stiffest subgrade conditions. For the results of the backcalculated AC moduli, Profile 3, which has the thickest surface layer in the three flexible pavements (Profiles 1, 2, and 3), shows the best comparisons. The differences are generally less than 15 percent for the backcalculated AC moduli obtained with the N-basins and S-basins. The relationship between the thickness of the surface layer and the accuracy of the backcalculated AC and Base moduli needs further study.

Generally, the amplitudes of deflection basins (generated with 10,000-pound loading) are less than one-thousandth of an inch (mil). However, the default input format in MODULUS can only read two digits after the point (unit in mils)—presumably because the FWD output provides data to only two digits after the decimal point. This might cause some reduction of resolution for backcalculated layer moduli obtained with the MODULUS program.

CHAPTER 6. CONCLUSIONS AND RECOMMENDATIONS

6.1 CONCLUSIONS REGARDING THE DYNAFLECT TEST

Analytical simulations of the Dynaflect test were conducted using the computer program UTDYNF (Chang, 1991; Chang et al, 1992). Four typical in-service pavement profiles (three flexible pavements and one rigid pavement) were studied. The dynamic effect of the Dynaflect test was expressed in terms of deflection ratios (dynamic deflections divided by static deflections).

At a given bedrock depth, the maximum value of deflection ratios is the largest for the furthest measurement station (station 5) and least for the nearest measurement station (station 1). At shallow depths to bedrock (approximately 5 to 10 feet (1.55 to 3.1 m)), deflection ratios of all measurement stations are very close to 1, so the dynamic and static deflection basins are basically the same. The deflection ratio increases to a peak value as the depth to bedrock increases. After the peak, the deflection ratio drops rapidly back to 1. The maximum value of the deflection ratio (at station 5) ranged from 1.3 to 2.9 in these studies.

The resonant depth to bedrock (the depth to bedrock corresponding to the maximum deflection ratio) is determined predominately by the stiffness of the subgrade layer. Two sets of equations (one for the flexible pavements and one for the rigid pavement) were developed for estimating the resonant depth to bedrock based on the subgrade stiffness. For these pavements, Young's modulus of the subgrade varied from 16 to 142 ksi (0.11 to 0.98 MN/m^2), and the resonant depth to bedrock ranged from 25 to 85 feet (7.8 to 26.3 m).

The amplitude of the deflection ratio is an important index of the potential error generated in any static interpretation procedure of the Dynaflect test. The stiffness of the subgrade layer has the most significant effect on the amplitude of the maximum deflection ratios. The softer the subgrade, the higher the amplitude of the maximum deflection ratio. This trend indicates that the error generated in a static interpretation procedure of the Dynaflect test would decrease as the subgrade stiffness increases.

6.2 CONCLUSIONS REGARDING THE FWD TEST

Analytical simulations of the FWD test were conducted using the computer program UTFWD (Chang, 1991; Chang et al, 1992). Four pavement profiles, the same as those used in the study of the Dynaflect test, were studied.

As in the case of the Dynaflect test, the maximum deflection ratio at a given depth to bedrock also occurs at the farthest measurement station (station 7) in the FWD test. However, the resonance peak exhibited in the FWD deflection ratios is much wider than that exhibited in the Dynaflect test and decreases more slowly to 1 when compared with the sharp decrease in the deflection ratio in the FWD test. The reason for these differences is that the FWD test contains a wide range in frequencies, while the Dynaflect test contains one frequency (8 Hz).

The resonant depth to bedrock obtained with the FWD test varied from 5.5 to 20 feet (1.7 to 6.2 m) when Young's modulus of the subgrade varied from 16 to 142 ksi (0.11 to 0.98 MN/m^2). These resonant depths to bedrock are much shallower than those obtained with the Dynaflect test (varied from 25 to 85 feet (7.8 to 26.3 m)). This trend occurs because the predominate frequency in the FWD test is about 30 Hz, while the frequency used in the Dynaflect test is 8 Hz. Therefore, the resonant depths to bedrock obtained with the FWD test are approximately one fourth of those obtained with the Dynaflect test. Equations for estimating the resonant depth to bedrock for the FWD test were developed for both the flexible and rigid pavements.

Equations are suggested for estimating the depth to bedrock based on the damped natural period of the free vibrations of the pavement system immediately after the FWD load application.

In these equations, the stiffness of the subgrade has a major effect, while the degree of saturation of the subgrade is only marginally important. To use these equations, site engineers have to measure the damped natural period in the deflection-time records of the FWD test and estimate the stiffness and Poisson's ratio of the subgrade.

A method for estimating the stiffness of the subgrade based on the offset time of the first pulses in the deflection-time recording in the FWD test has been developed. The method is best applied by using stations 5 and 7 in the FWD test. There are several assumptions that must be made when using this method. For example, the subgrade is approximated as a uniform material, the bedrock needs to be reasonably deep (this depends on the stiffness of the subgrade), and the difference between Rayleigh wave velocity and shear wave velocity is neglected. The most important advantage of this approach is that the stiffness of the subgrade can be estimated simultaneously with performance of the FWD test. The resonant depth to bedrock and the actual depth to bedrock can then be determined using the equations suggested in this study. Therefore, the error generated by the resonant bedrock condition can be either avoided in advance or corrected during the backcalculation process.

The computer program MODULUS (Uzan et al, 1989), which is based on static interpretation of the FWD test, was used to backcalculate layer moduli from the deflection basins obtained with the UTFWD program. Generally, the backcalculated layer moduli obtained from dynamic deflections measured at deep subgrade sites (N-basins) and from static deflection basins at the resonant bedrock depths (S-basins) exhibit much better comparisons with the actual moduli than backcalculated moduli obtained with dynamic deflections measured at the resonant bedrock condition (R-basins). Unfortunately, when FWD tests are performed at the resonant bedrock depth, dynamic deflections (not static) are measured.

At the resonant bedrock depth, the stiffness of the subgrade layer has a major effect on the accuracy of backcalculated layer moduli. The errors in the backcalculated layer moduli increase as the subgrade stiffness decreases. This behavior also agrees with the trend of variations in the maximum deflection ratios.

Usually, backcalculated subgrade moduli obtained with dynamic deflection basins at the resonant depth to bedrock (R-basins) underestimated the actual subgrade moduli by 20 to 50 percent. This results in the backcalculated base moduli being too high (generally 2 times the actual base moduli).

Profile 1, which has the thinnest surface layer, exhibits the best comparison for the backcalculated base moduli (less than 20 percent of difference) for the N-basins and S-basins. However, Profile 3, which has the thickest surface layer among these three flexible pavements, exhibits the best comparison on the backcalculated AC moduli (less than 20 percent of difference) for the N-basins and S-basins. Profile 4, which is a rigid pavement, exhibits good comparisons for the backcalculated CRC moduli. The differences are less than 20 percent for all these three deflection basins (N-, S- and R-basins).

The results obtained with saturated subgrade conditions need further study. Numerical problems with UTFWD seemed to occur at shallow bedrock depths for saturated subgrade conditions. Changes in the mesh size may be necessary to improve calculations of the deflection basins under these conditions.

6.3 RECOMMENDATIONS

Dynaflect testing should be conducted with special care, since its fixed frequency (8 Hz) cannot detect resonant bedrock conditions. The errors generated in backcalculated moduli using a static interpretation procedure can be significant if the test is performed at the resonant depth to bedrock.

A procedure for performing FWD testing is suggested below.

1. *Estimate the Stiffness of the Subgrade*
   The stiffness of the subgrade can be estimated by the offset time approach suggested in this study (simultaneously with the test), by in situ seismic testing (before the FWD test) or by dynamic laboratory tests on undisturbed samples (before the FWD test).

2. *Estimate the Resonant Depth to Bedrock*
   The resonant depth to bedrock can be determined with the estimated subgrade stiffness (Step 1) using equations suggested in this study (Section 4.4).

3. *Estimate the Actual Depth to Bedrock*
   The actual depth to bedrock can be determined based on the damped natural period of the free vibrations of the pavement system and the stiffness and Poisson's ratio of the subgrade. The stiffness of the subgrade can be determined by the offset time approach (Step 1). Site engineers have to

estimate the saturation condition of the subgrade and an appropriate value for Poisson's ratio of the subgrade.

4. *Compare the Actual Depth to Bedrock and the Estimated Resonant Depth to Bedrock*
   If the actual depth to bedrock is more than 20 feet (6.2 m) (deeper than the estimated resonant depth to bedrock), any errors generated in backcalculated moduli by a static interpretation procedure can be ignored. However, if the difference between the actual depth to bedrock and the resonant depth to bedrock is less than 20 feet (6.2 m), errors may be significant. In this case, the FWD test as presently performed needs to be analyzed dynamically.

The procedure just presented needs further field verifications. To measure the damped natural period of the free vibrations, the record of the motions of the pavement system immediately after the FWD load application should be extended to 200 milliseconds. The sampling rate in the data acquisition system of the FWD test should be less than 0.1 milliseconds, so the peak at each measurement station can be detected accurately.

BIBLIOGRAPHY

Chang, D. W. "Nonlinear Effects on Dynamic Response of Pavements Using the Non-Destructive Testing Techniques," doctoral dissertation, The University of Texas at Austin, 1991.

Chang, D. W., Kang, Y. V., Roesset, J. M., and Stokoe, II, K. H., "Effect of Depth to Bedrock on Deflection Basins Obtained with Dynaflect and FWD Tests," 1992 Annual Meeting of the Transportation Research Board, Washington, D.C., 1992.

Davies, T. G., and Mamlouk, M. S. "Theoretical Response of Mutilayer Pavement Systems to Dynamic Nondestructive Testing," Transportation Research Record 1022, pp 1-7, 1985.

Heisey, S. "Determination of In Situ Shear Wave Velocity from Spectral Analysis of Surface Waves," master's thesis, The University of Texas at Austin, 1981.

Hoar, R. J. "Field Measurement of Seismic Wave Velocity and Attenuation for Dynamic Analyses," doctoral dissertation, The University of Texas at Austin, 1982.

Kang, Y. V. "Finite Width on Dynamic Deflections on Pavements," doctoral dissertation, The University of Texas at Austin, 1990.

Kang, Y. V., Roesset J. M., and Stokoe, II, K. H. "Effect of Loading Position on Deflection Basins Obtained with Dynaflect and FWD Tests," 1991 Annual Meeting of the Transportation Research Board, Washington, D.C., 1991.

Nazarian, S. "In Situ Determination of Elastic Moduli of Soil Deposits and Pavement System by Spectral-Analysis-of-Surface-Waves Method," doctoral dissertation, The University of Texas at Austin, 1984.

Nazarian, S., and Stokoe, II, K. H. "Nondestructively Delineating Changes in Modulus Profiles of Secondary Roads," Transportation Research Record 1136, pp 96-107, 1987.

Richart, F. E., Woods, R. D., and Hall, J. R. *Vibrations of Soils and Foundations*. Prentice-Hall, Inc., 1970.

Roesset, J. M., and Mamlouk, M. S. "Dynamic Interpretation of Dynaflect and Falling Weight Deflectometer Tests," Transportation Research Record 1022, pp 7-16, 1985.

Sansalone, M., and Carino, N. J. "Detecting Delaminations in Concrete Slabs With and Without Overlays Using the Impact-Echo Method," *ACI Material Journal*, 86, pp 175-84, 1990.

Uzan, J., Lytton, R. L., and Germann, F. P. "General Procedure for Backcalculating Layer Moduli," ASTM STP 1026, American Society for Testing and Materials, pp 217-228, 1989.

APPENDIX A. RESULTS OF ANALYTICAL SIMULATION OF THE DYNAFLECT TEST

The analytical simulation of the Dynaflect test was obtained using computer program UTDYNF (Chang, 1991; Chang et al, 1992). The motions are expressed in terms of deflection ratios as a function of depth to bedrock in this appendix. Deflection ratio is defined as the dynamic deflection divided by the static deflection. Depth to bedrock is the total depth from the surface of the pavement to the top of the bedrock.

There are some numerical problems which caused small spikes on some of the deflection ratios. However, these numerical problems did not have any effect on the values of the maximum deflection ratios and the resonant depths to bedrock. These spikes were removed from the figures in this appendix.

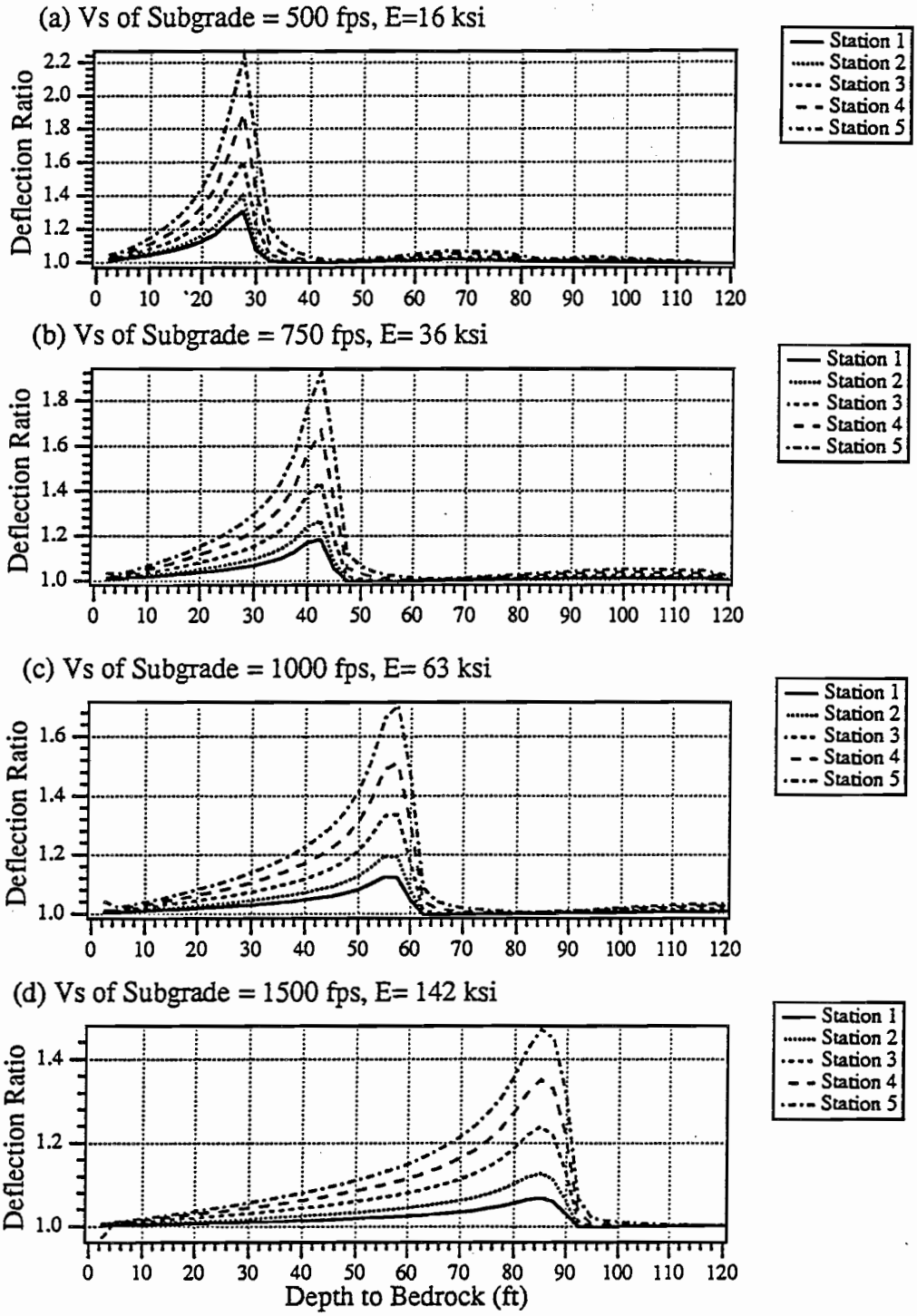

Figure A.1 Deflection ratio versus depth to bedrock for Dynaflect testing at Profile 1 (V_s of AC = 2000 fps (E = 312 ksi) and V_s of base = 1000 fps (E = 67 ksi))

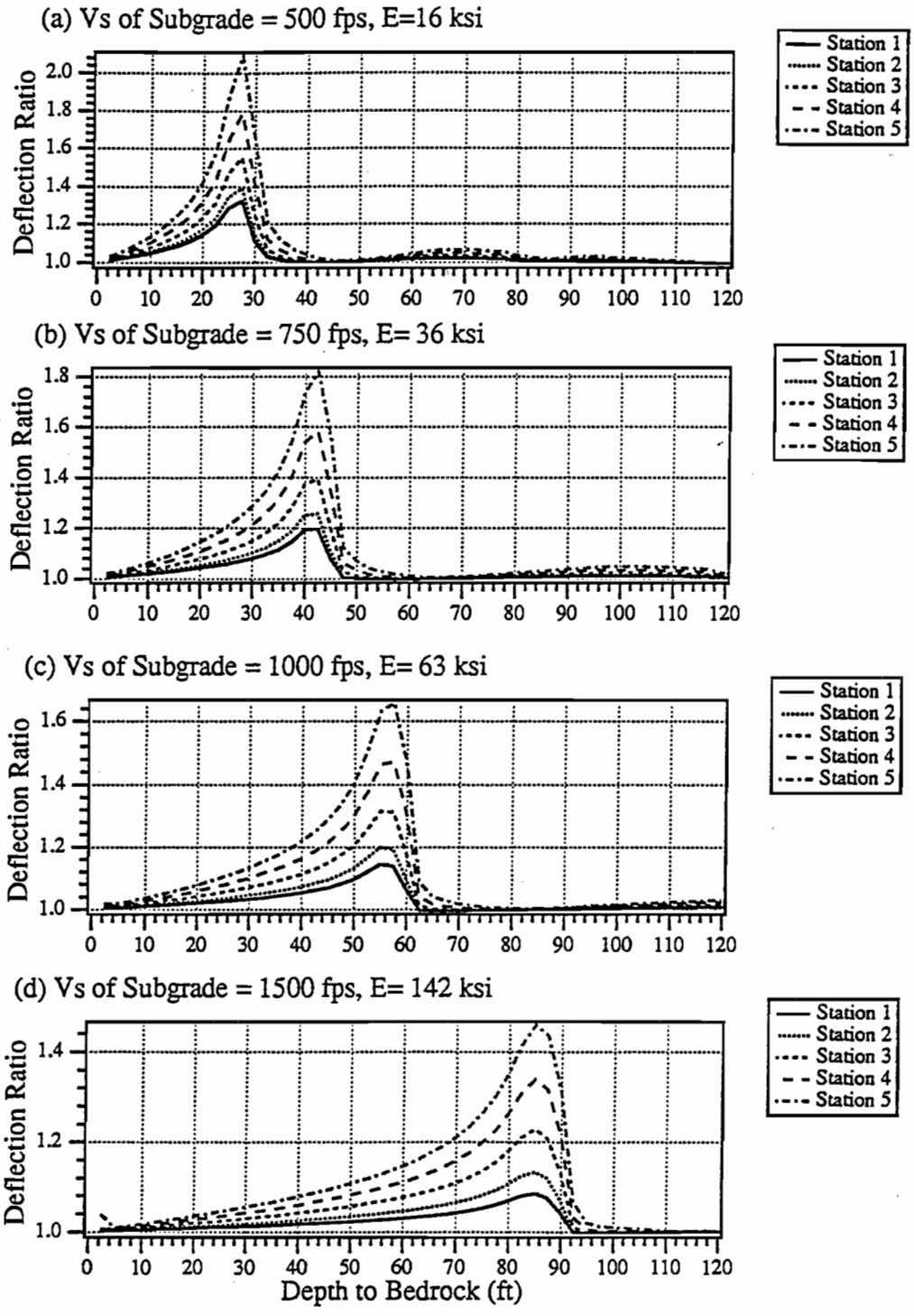

Figure A.2 Deflection ratio versus depth to bedrock for Dynaflect testing at Profile 1 (V_s of AC = 2000 fps (E = 312 ksi) and V_s of base = 1500 fps (E = 152 ksi))

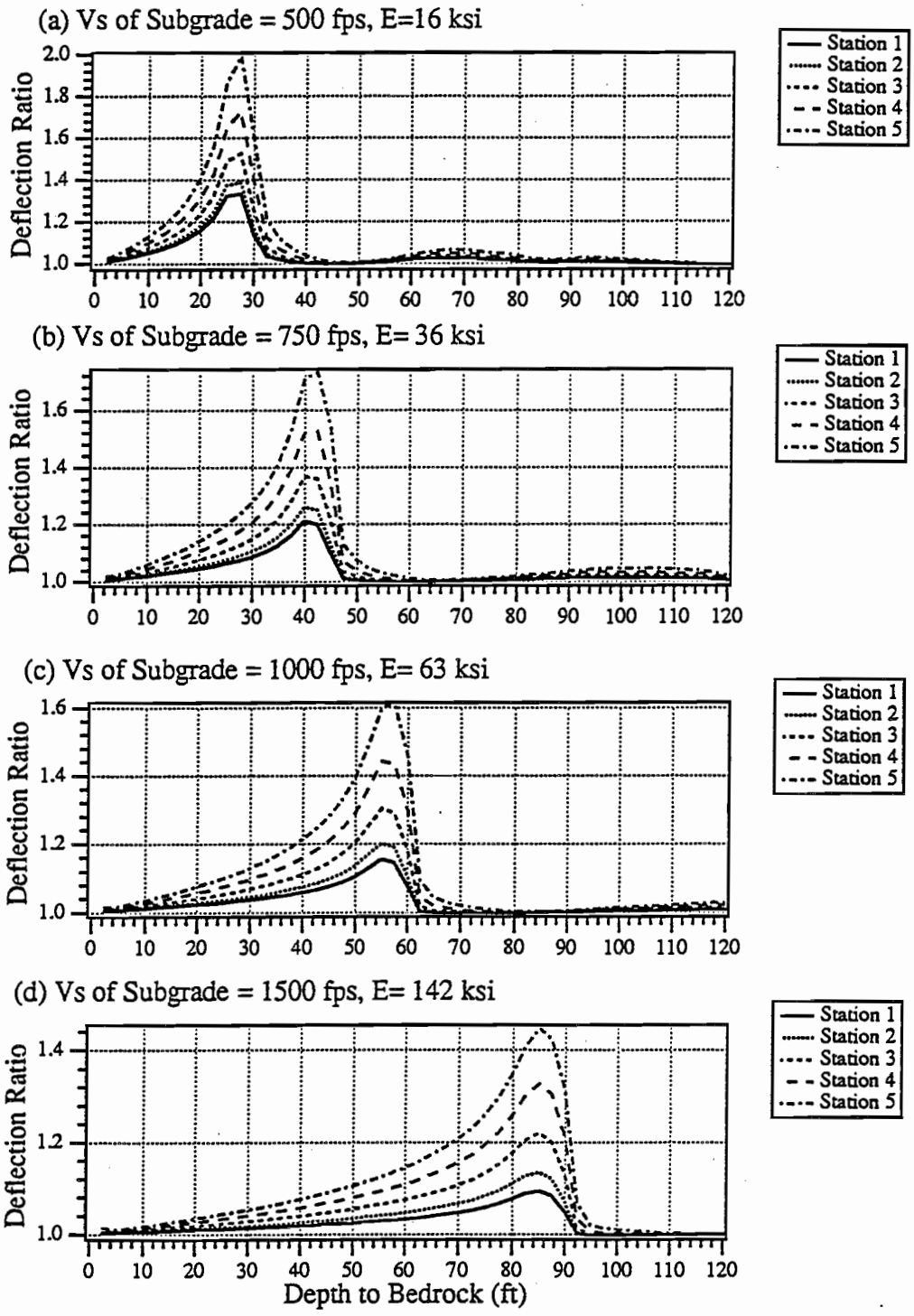

Figure A.3 Deflection ratio versus depth to bedrock for Dynaflect testing at Profile 1 (V_s of AC = 2000 fps (E = 312 ksi) and V_s of base = 2000 fps (E = 270 ksi))

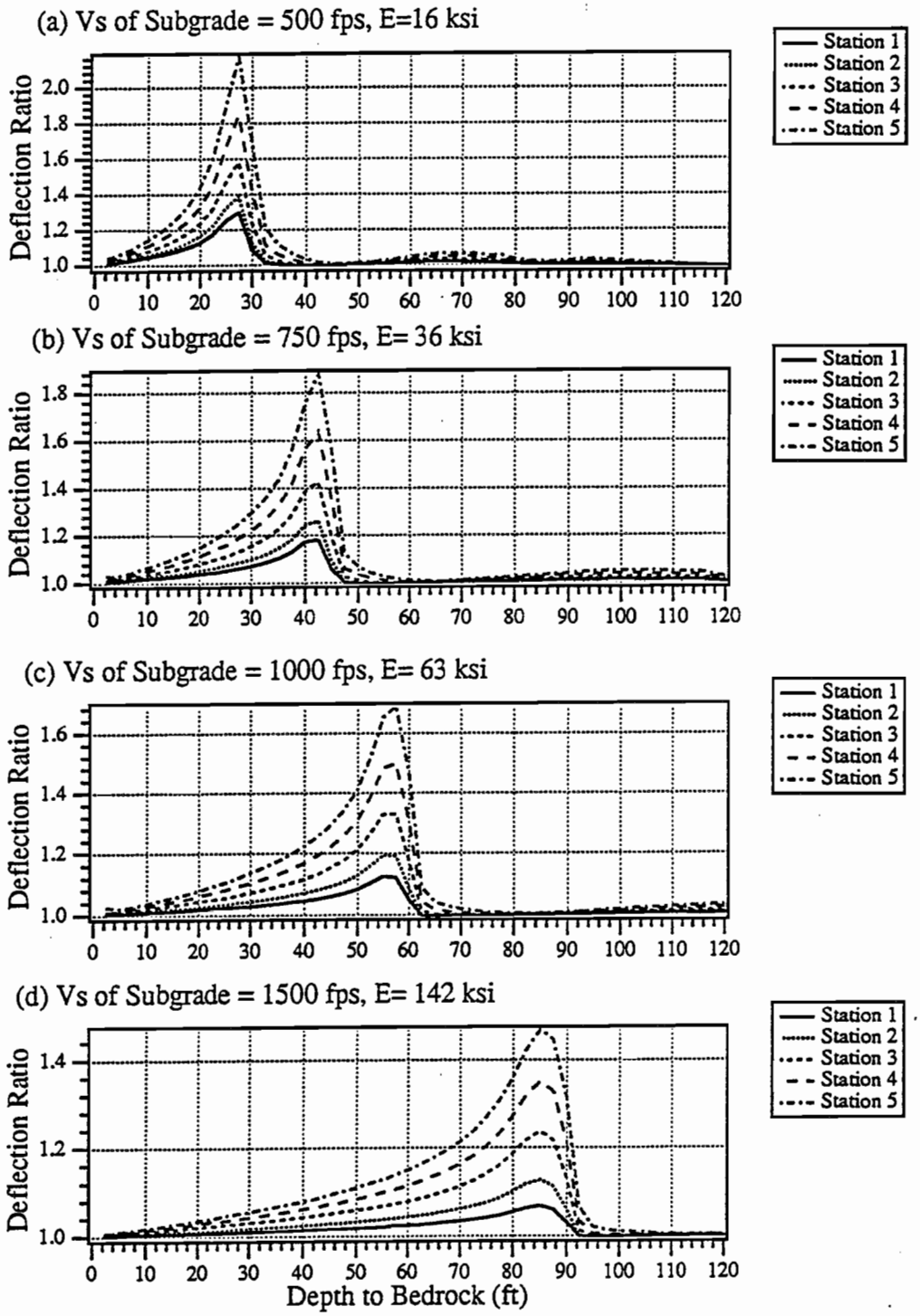

Figure A.4 Deflection ratio versus depth to bedrock for Dynaflect testing at Profile 1 (V_s of AC = 3000 fps (E = 690 ksi) and V_s of base = 1000 fps (E = 67 ksi))

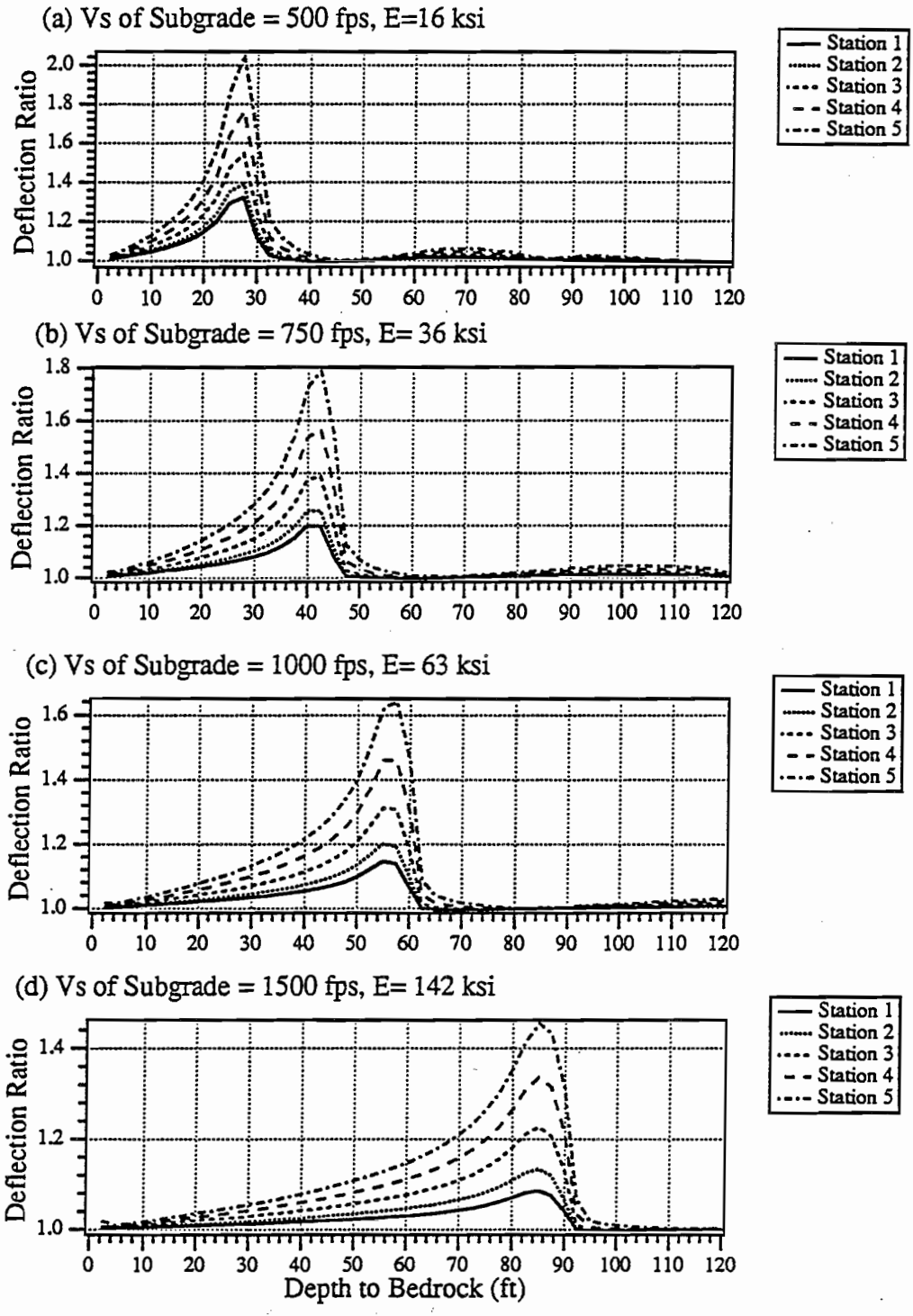

Figure A.5 *Deflection ratio versus depth to bedrock for Dynaflect testing at Profile 1 (V_s of AC = 3000 fps (E = 690 ksi) and V_s of base = 1500 fps (E = 152 ksi))*

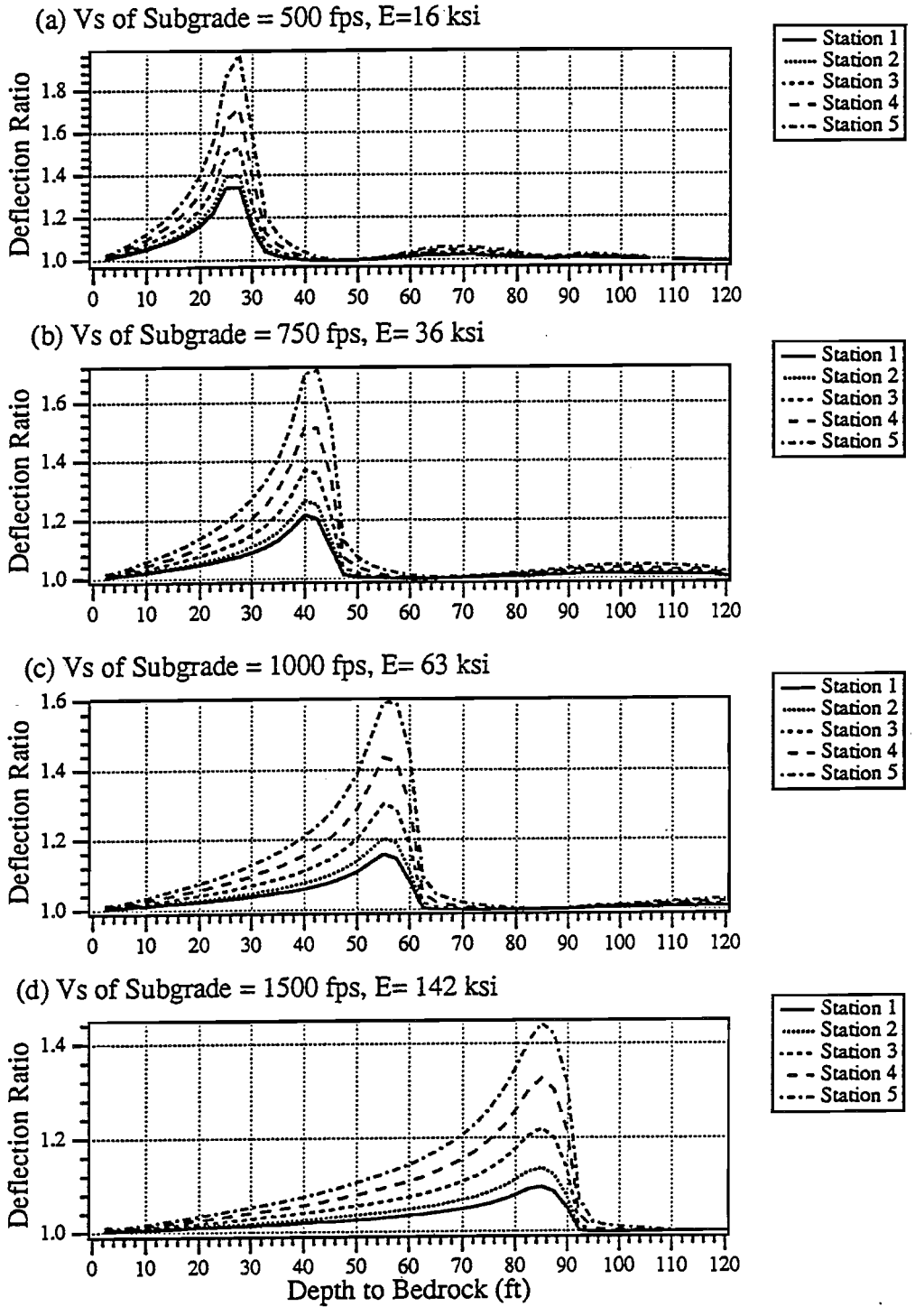

Figure A.6 Deflection ratio versus depth to bedrock for Dynaflect testing at Profile 1 (V_s of AC = 3000 fps (E = 690 ksi) and V_s of base = 2000 fps (E = 270 ksi))

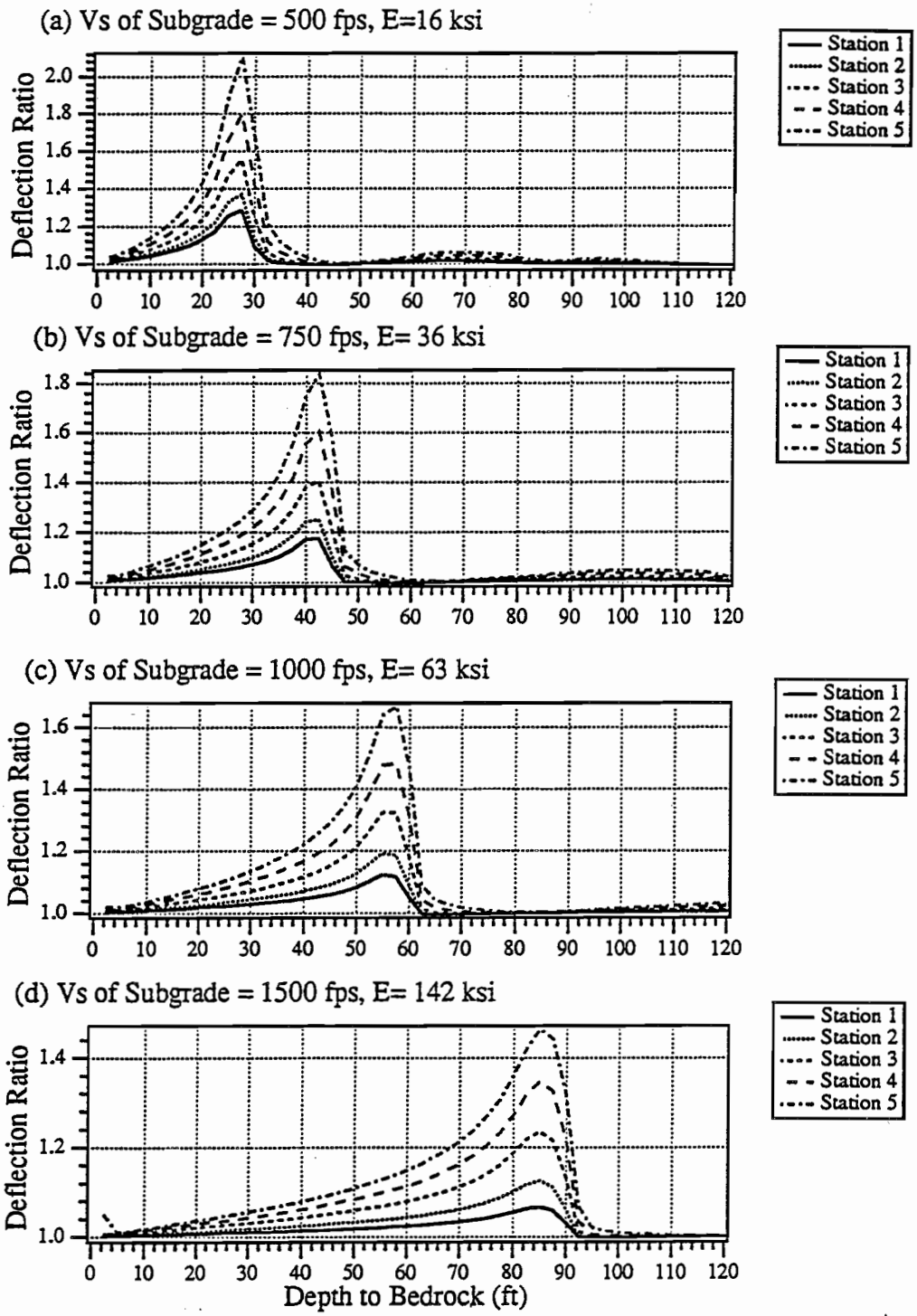

Figure A.7 *Deflection ratio versus depth to bedrock for Dynaflect testing at Profile 1 (V_s of AC = 4000 fps (E = 1225 ksi) and V_s of base = 1000 fps (E = 67 ksi))*

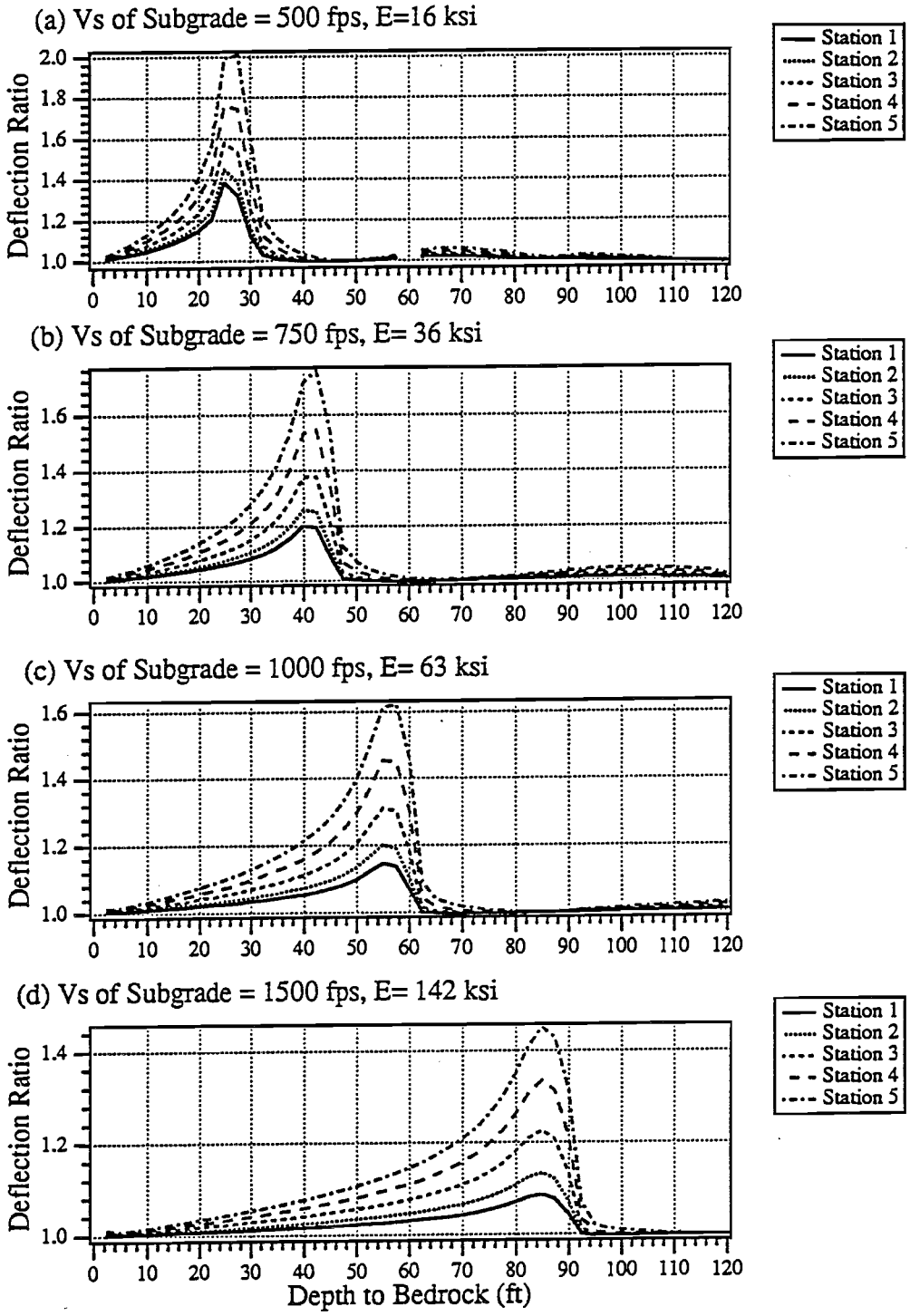

Figure A.8 *Deflection ratio versus depth to bedrock for Dynaflect testing at Profile 1 (V_s of AC = 4000 fps (E = 1225 ksi) and V_s of base = 1500 fps (E = 152 ksi))*

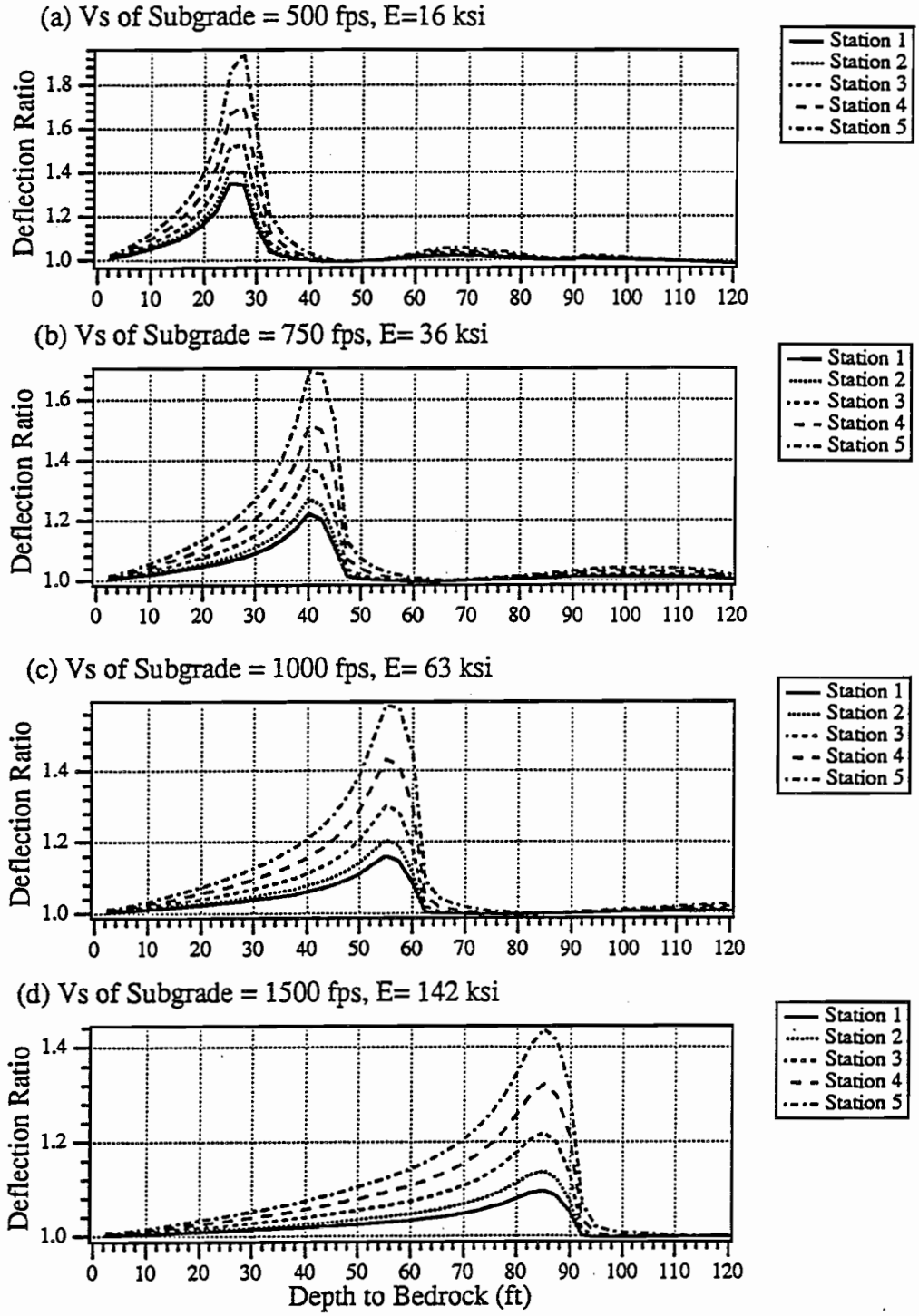

Figure A.9 Deflection ratio versus depth to bedrock for Dynaflect testing at Profile 1 (V_s of AC = 4000 fps (E = 1225 ksi) and V_s of base = 2000 fps (E = 270 ksi))

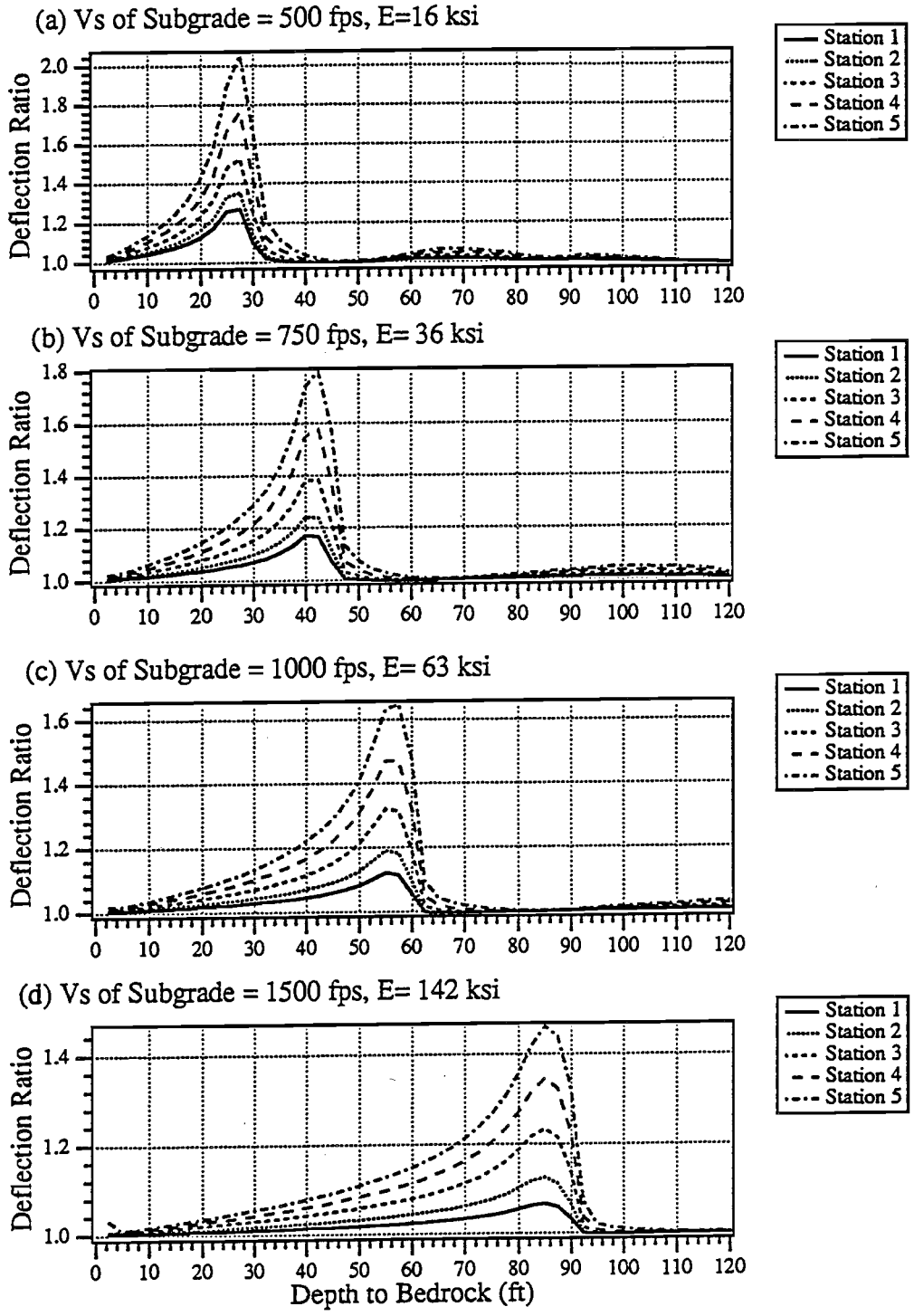

Figure A.10 Deflection ratio versus depth to bedrock for Dynaflect testing at Profile 1 (V_s of AC = 5000 fps (E = 1920 ksi) and V_s of base = 1000 fps (E = 67 ksi))

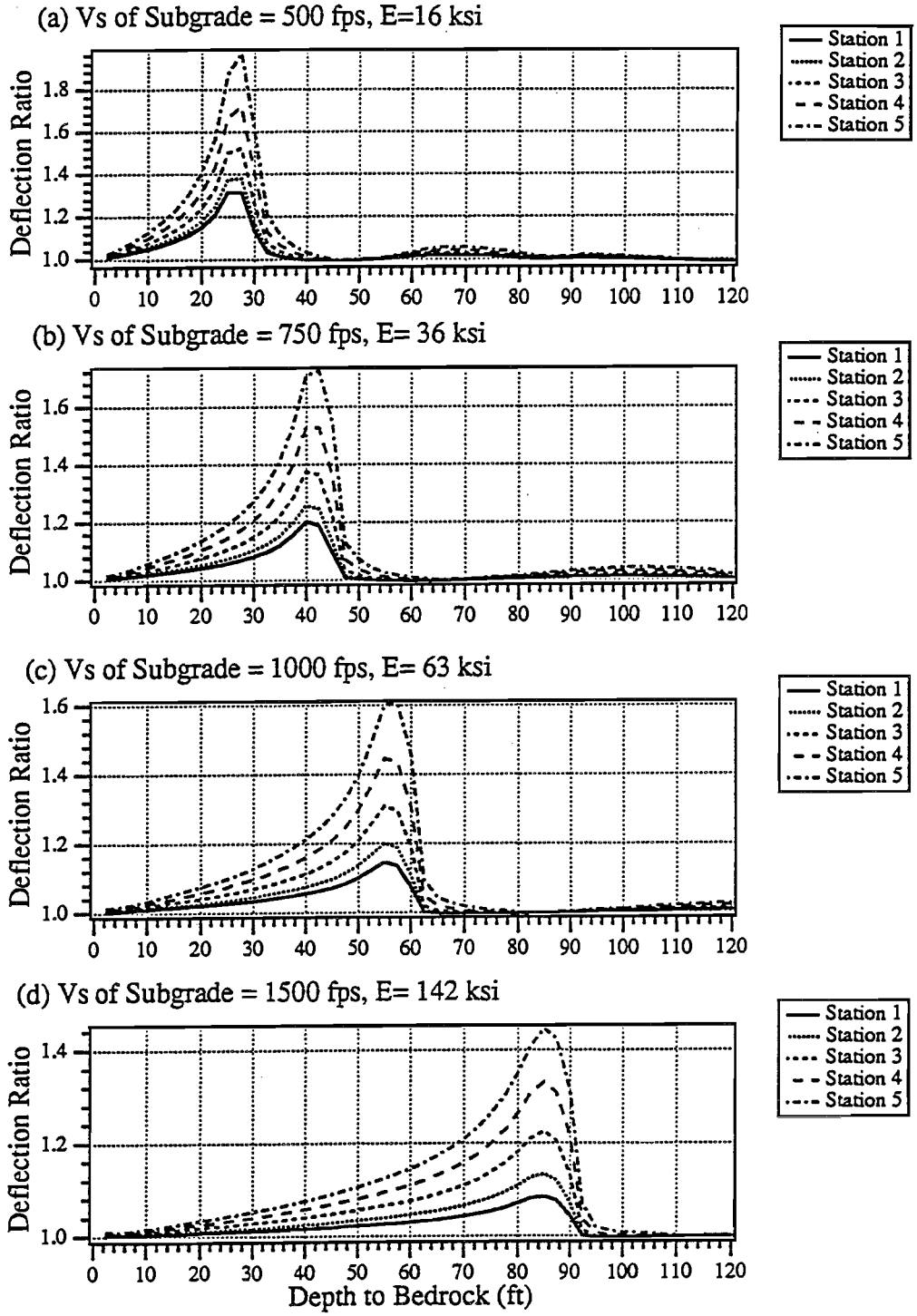

Figure A.11 Deflection ratio versus depth to bedrock for Dynaflect testing at Profile 1 (V_s of AC = 5000 fps (E = 1920 ksi) and V_s of base = 1500 fps (E = 152 ksi))

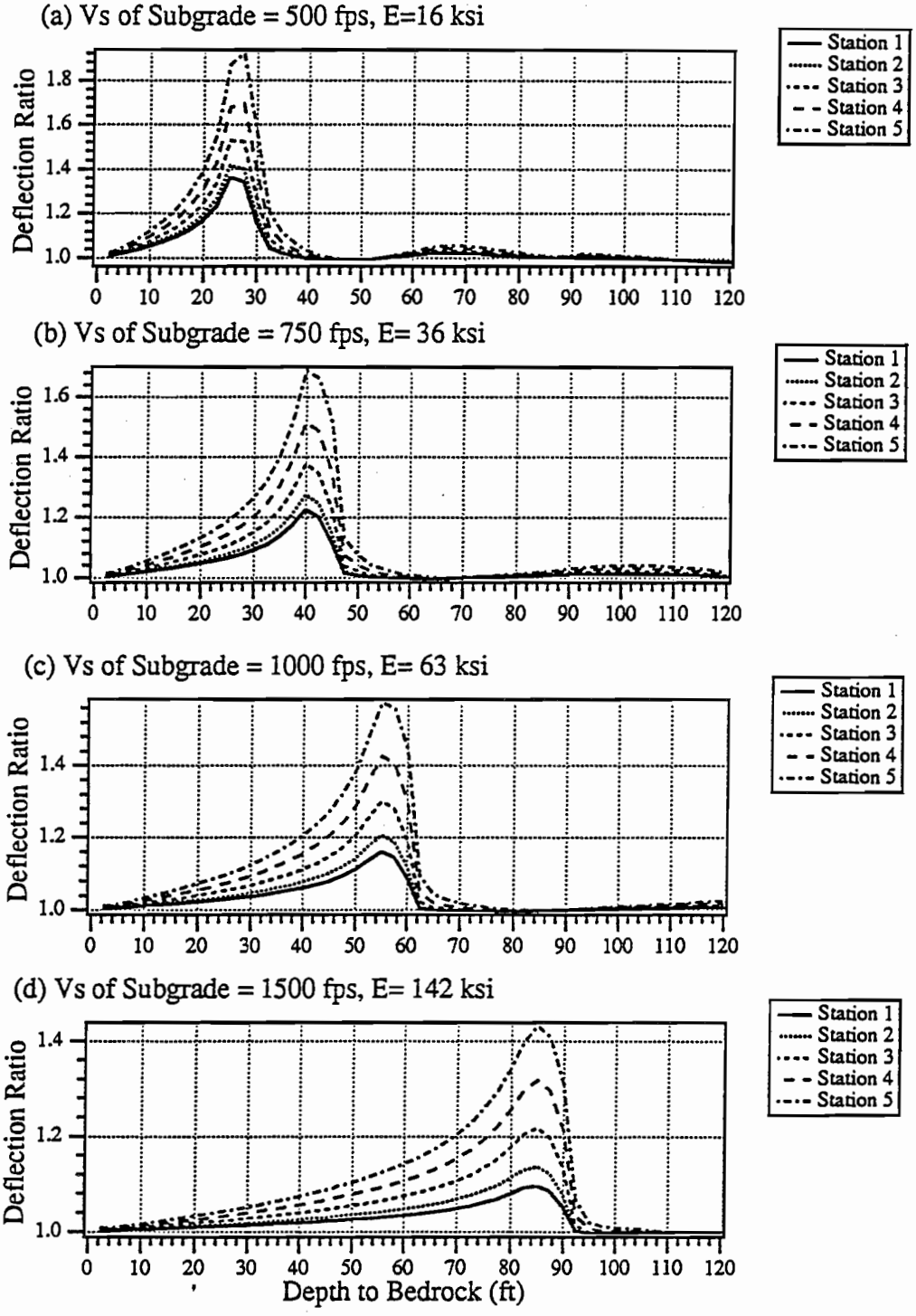

Figure A.12 Deflection ratio versus depth to bedrock for Dynaflect testing at Profile 1 (V_s of AC = 5000 fps (E = 1920 ksi) and V_s of base = 2000 fps (E = 270 ksi))

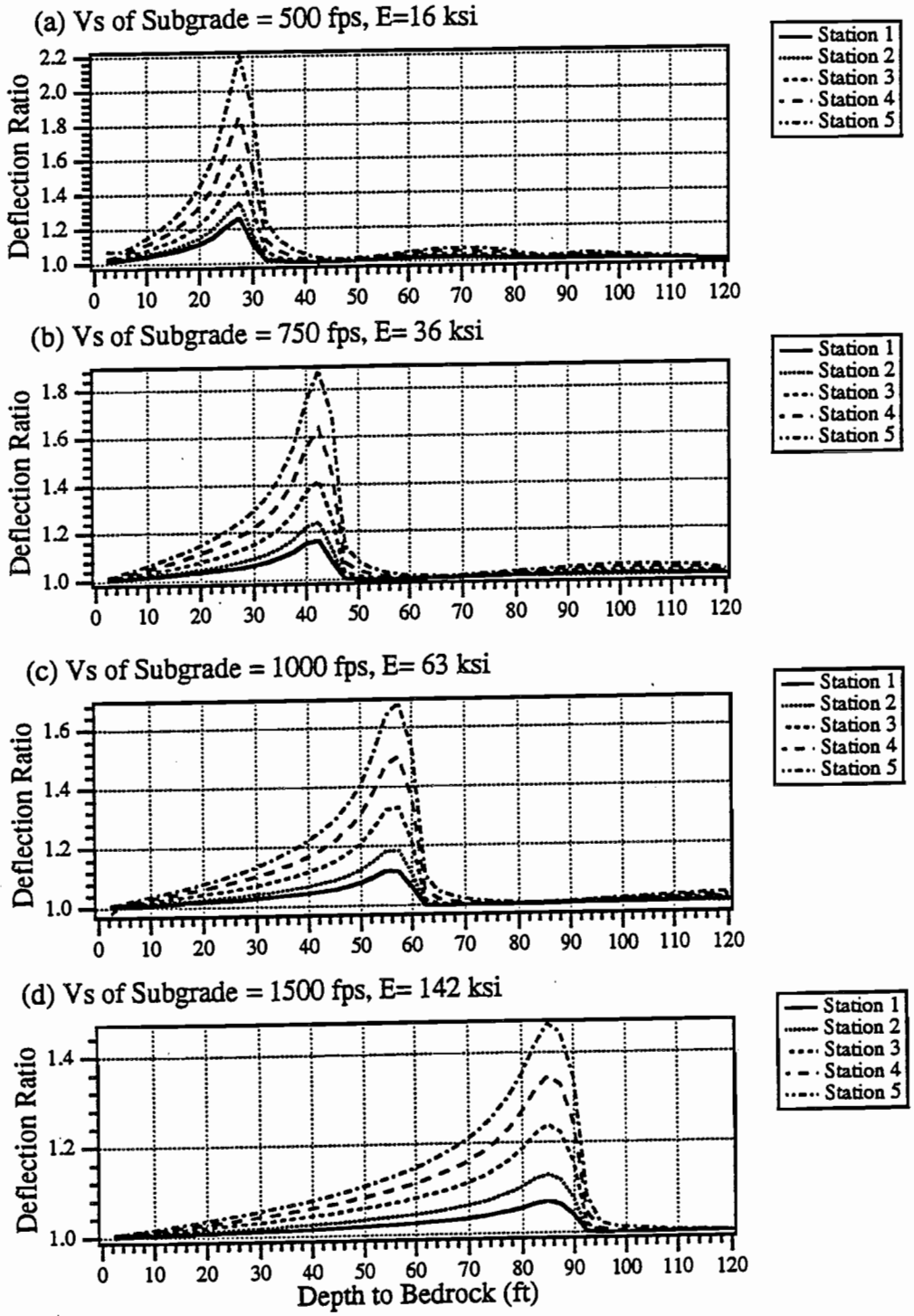

Figure A.13 Deflection ratio versus depth to bedrock for Dynaflect testing at Profile 2 (V_s of AC = 2000 fps (E = 312 ksi) and V_s of base = 1000 fps (E = 67 ksi))

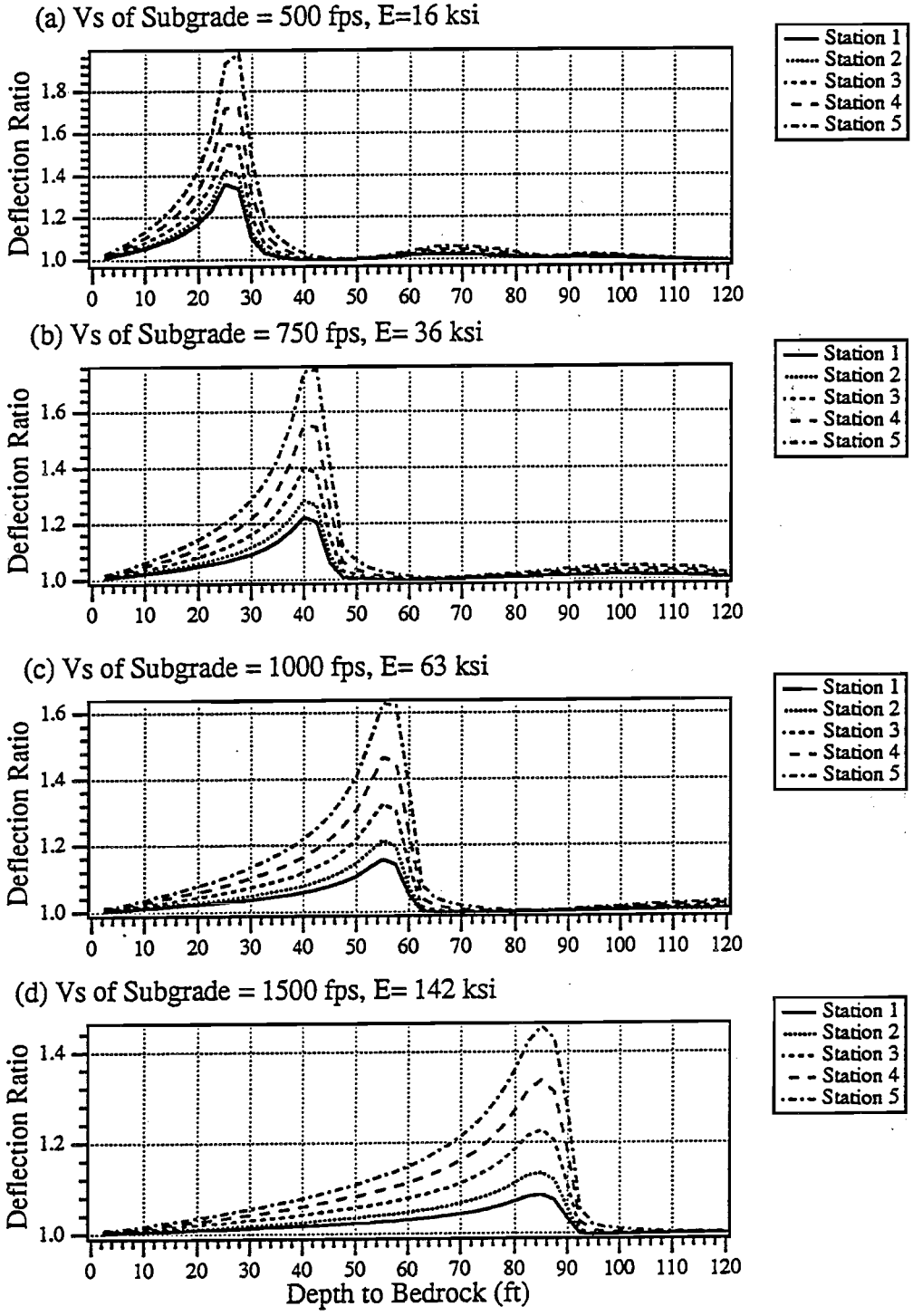

Figure A.14 Deflection ratio versus depth to bedrock for Dynaflect testing at Profile 2 (V_s of AC = 2000 fps (E = 312 ksi) and V_s of base = 1500 fps (E = 152 ksi))

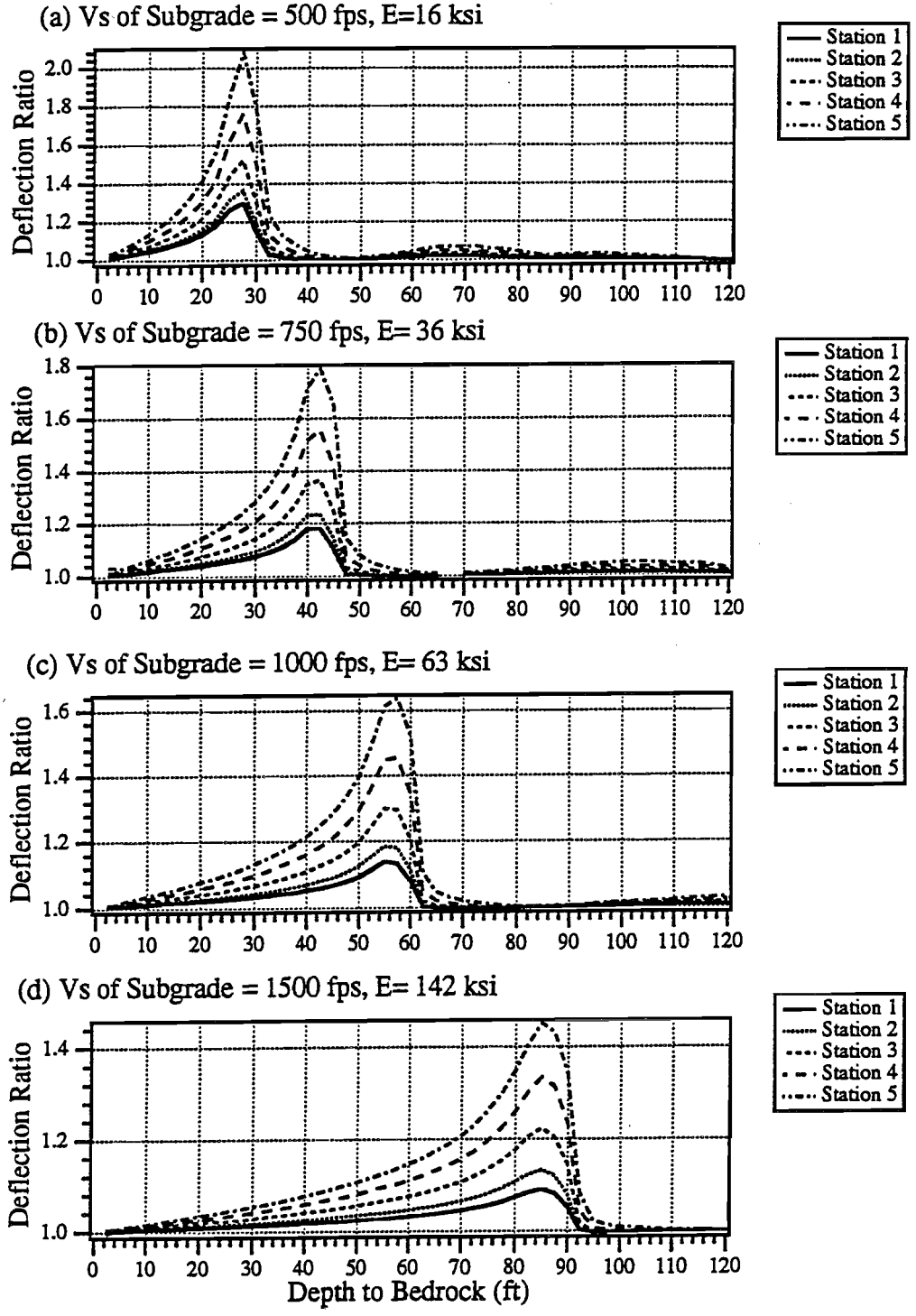

Figure A.15 Deflection ratio versus depth to bedrock for Dynaflect testing at Profile 2 (V_s of AC = 2000 fps (E = 312 ksi) and V_s of base = 2000 fps (E = 270 ksi))

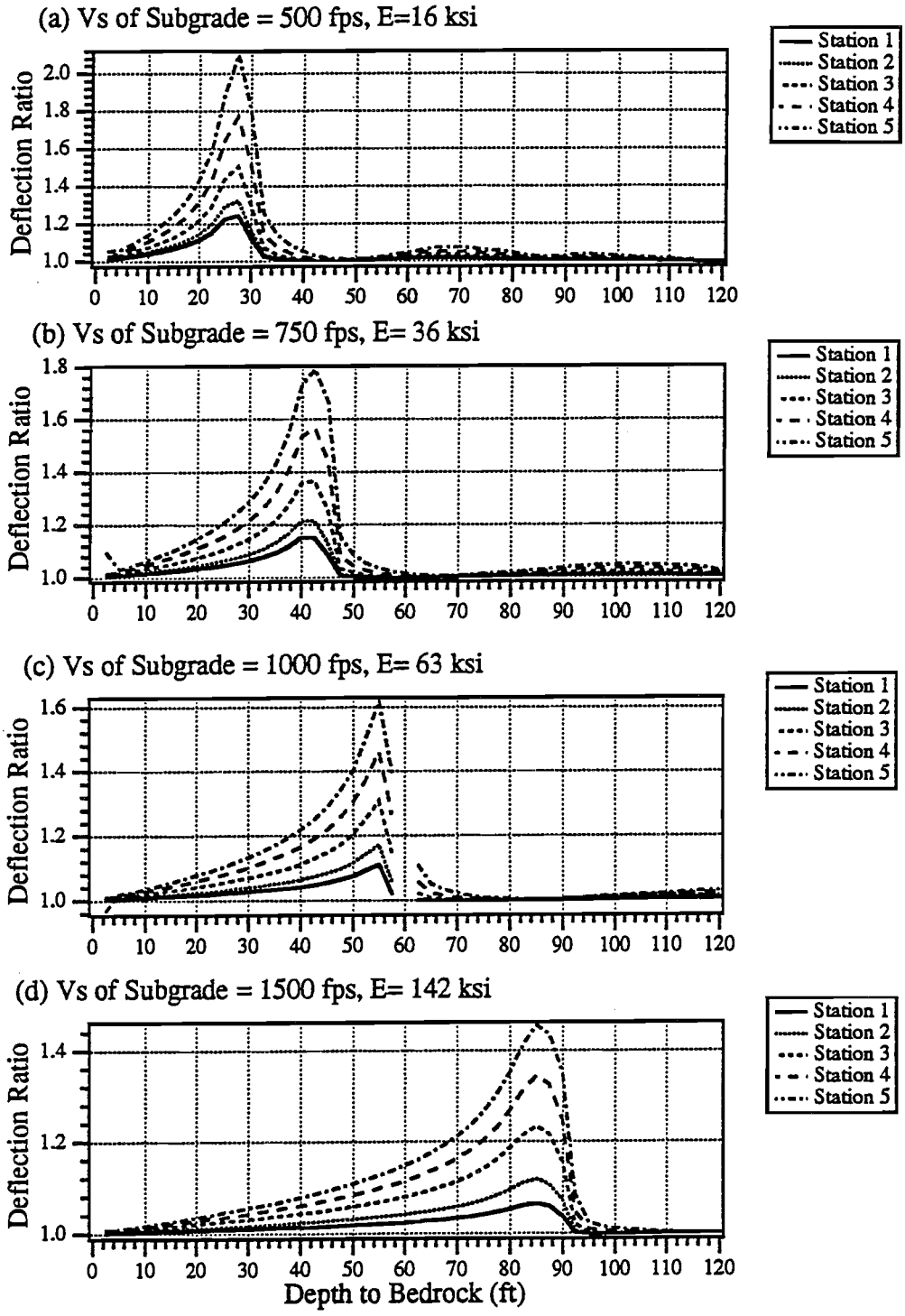

Figure A.16 Deflection ratio versus depth to bedrock for Dynaflect testing at Profile 2 (V_s of AC = 3000 fps (E = 690 ksi) and V_s of base = 1000 fps (E = 67 ksi))

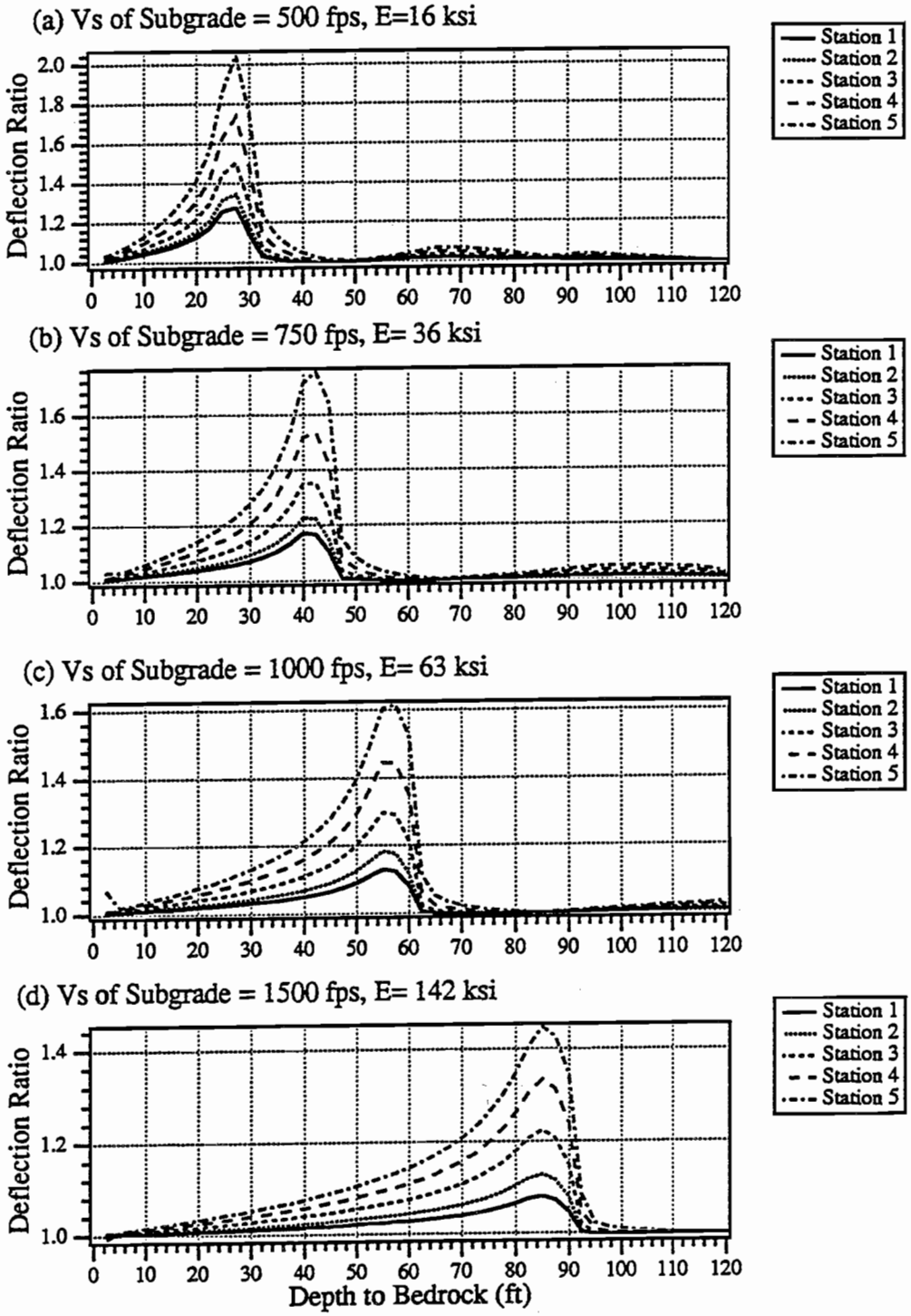

Figure A.17 Deflection ratio versus depth to bedrock for Dynaflect testing at Profile 2 (V_s of AC = 3000 fps (E = 690 ksi) and V_s of base = 1500 fps (E = 152 ksi))

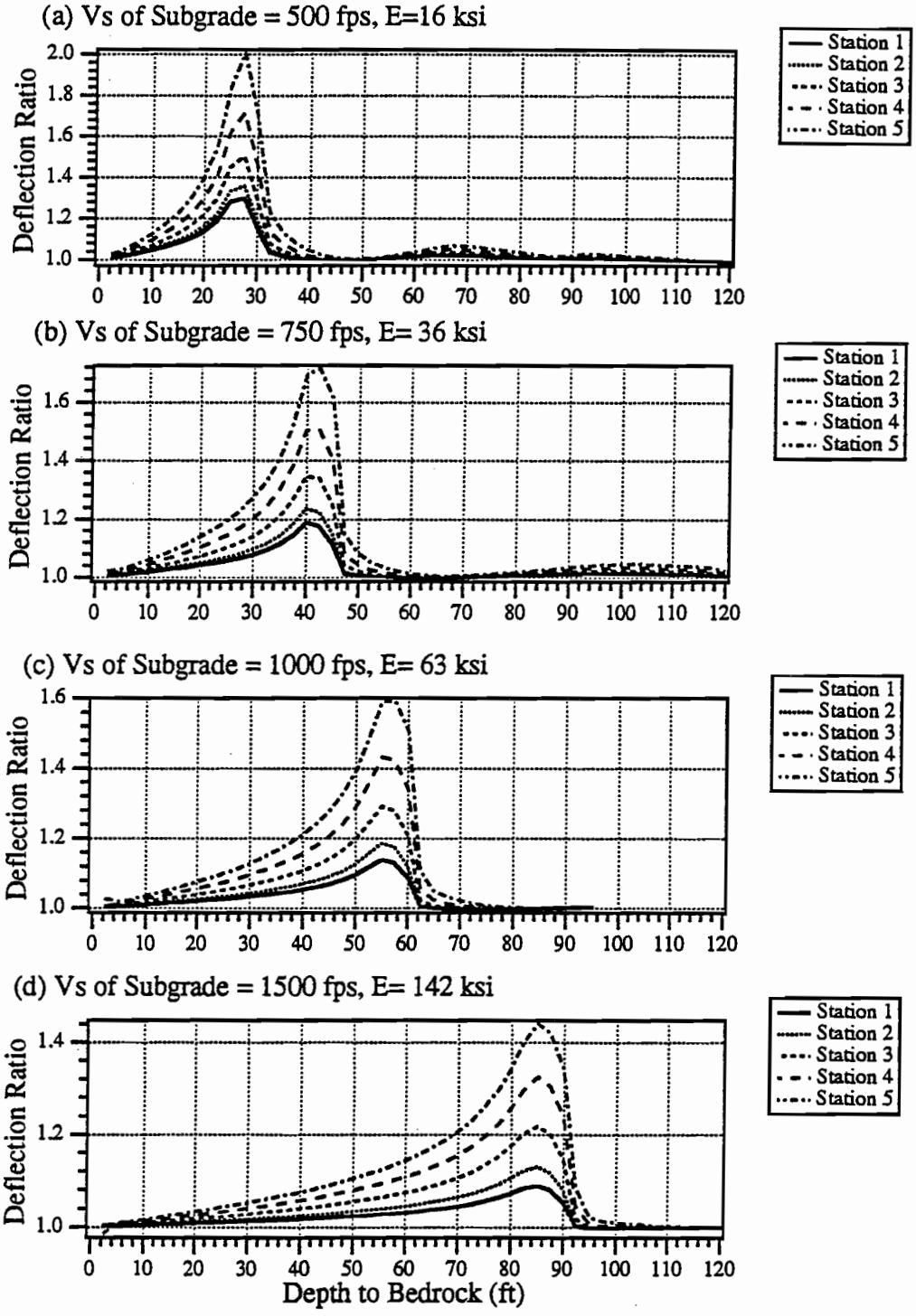

Figure A.18 Deflection ratio versus depth to bedrock for Dynaflect testing at Profile 2 (V_s of AC = 3000 fps (E = 690 ksi) and V_s of base = 2000 fps (E = 270 ksi))

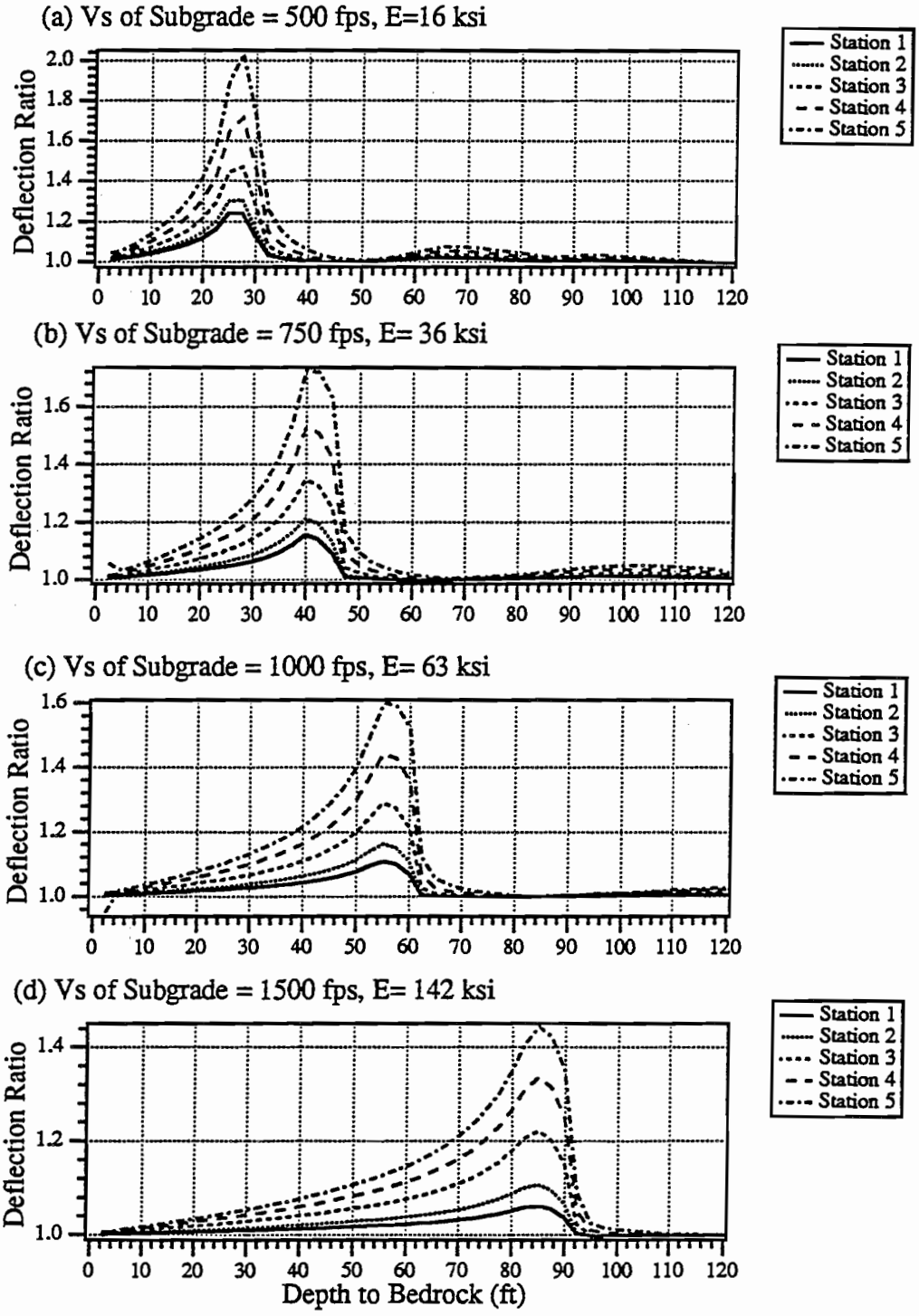

Figure A.19 Deflection ratio versus depth to bedrock for Dynaflect testing at Profile 2 (V_s of AC = 4000 fps (E = 1225 ksi) and V_s of base = 1000 fps (E = 67 ksi))

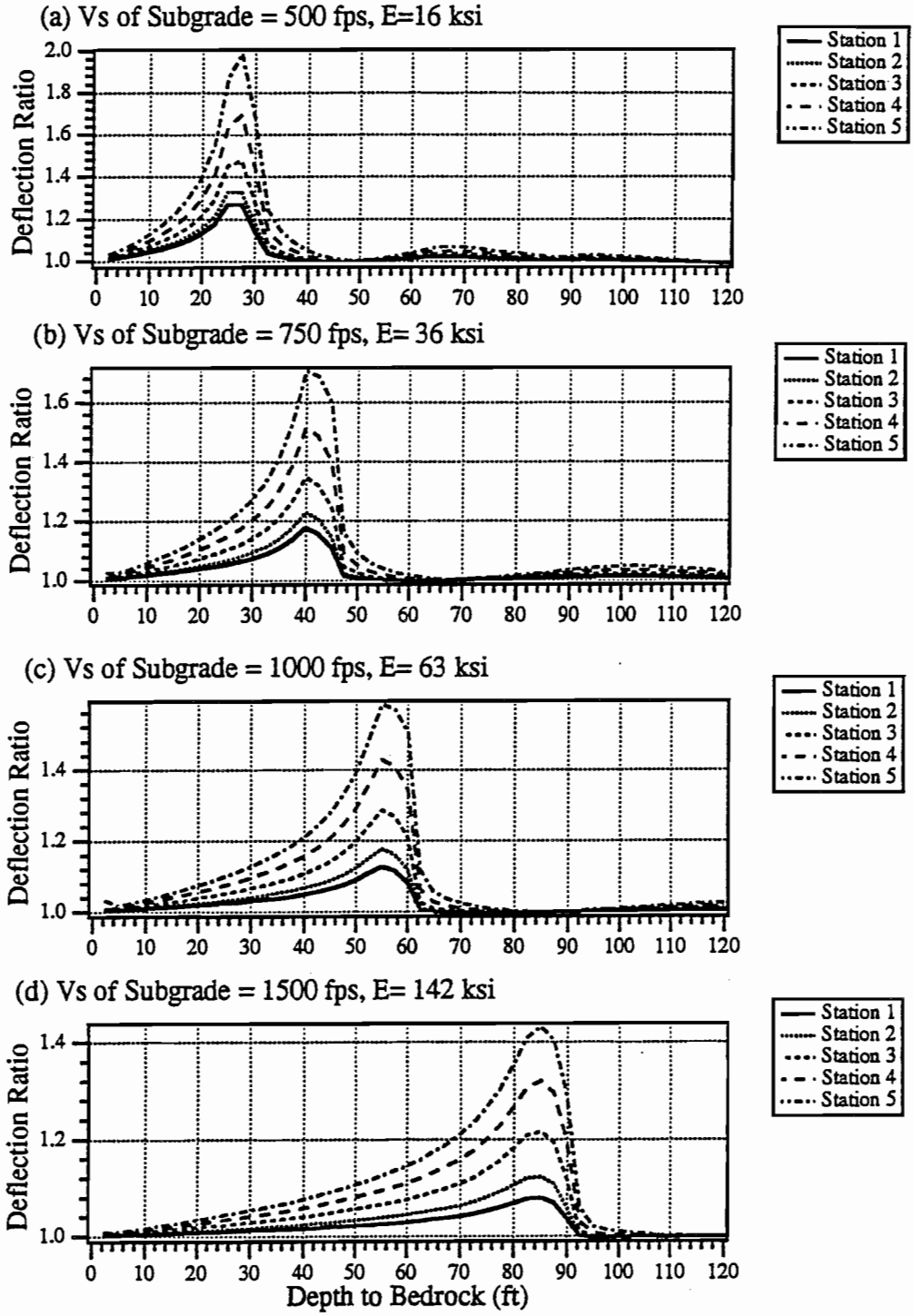

Figure A.20 Deflection ratio versus depth to bedrock for Dynaflect testing at Profile 2 (V_s of AC = 4000 fps (E = 1225 ksi) and V_s of base = 1500 fps (E = 152 ksi))

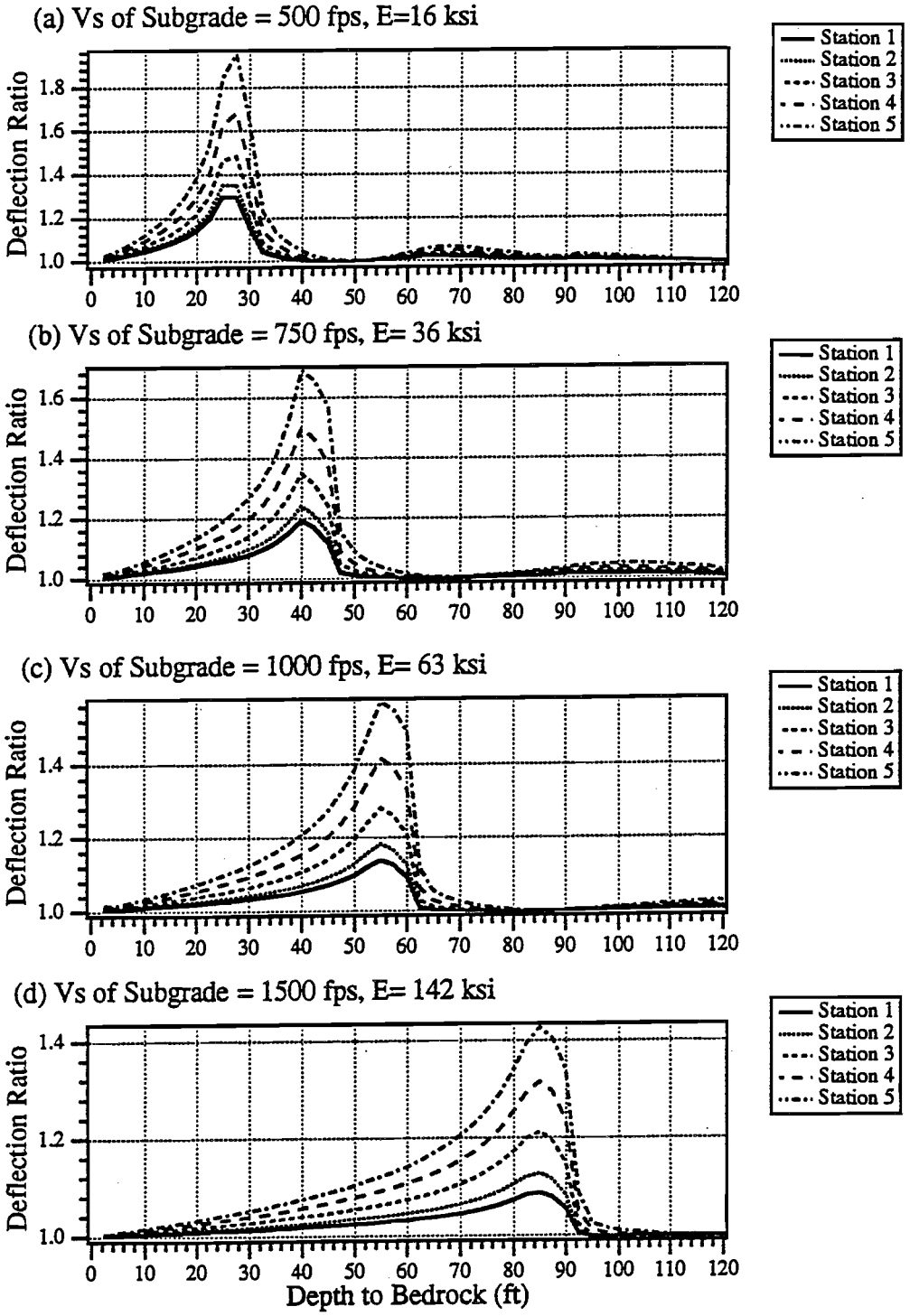

Figure A.21 Deflection ratio versus depth to bedrock for Dynaflect testing at Profile 2 (V_s of AC = 4000 fps (E = 1225 ksi) and V_s of base = 2000 fps (E = 270 ksi))

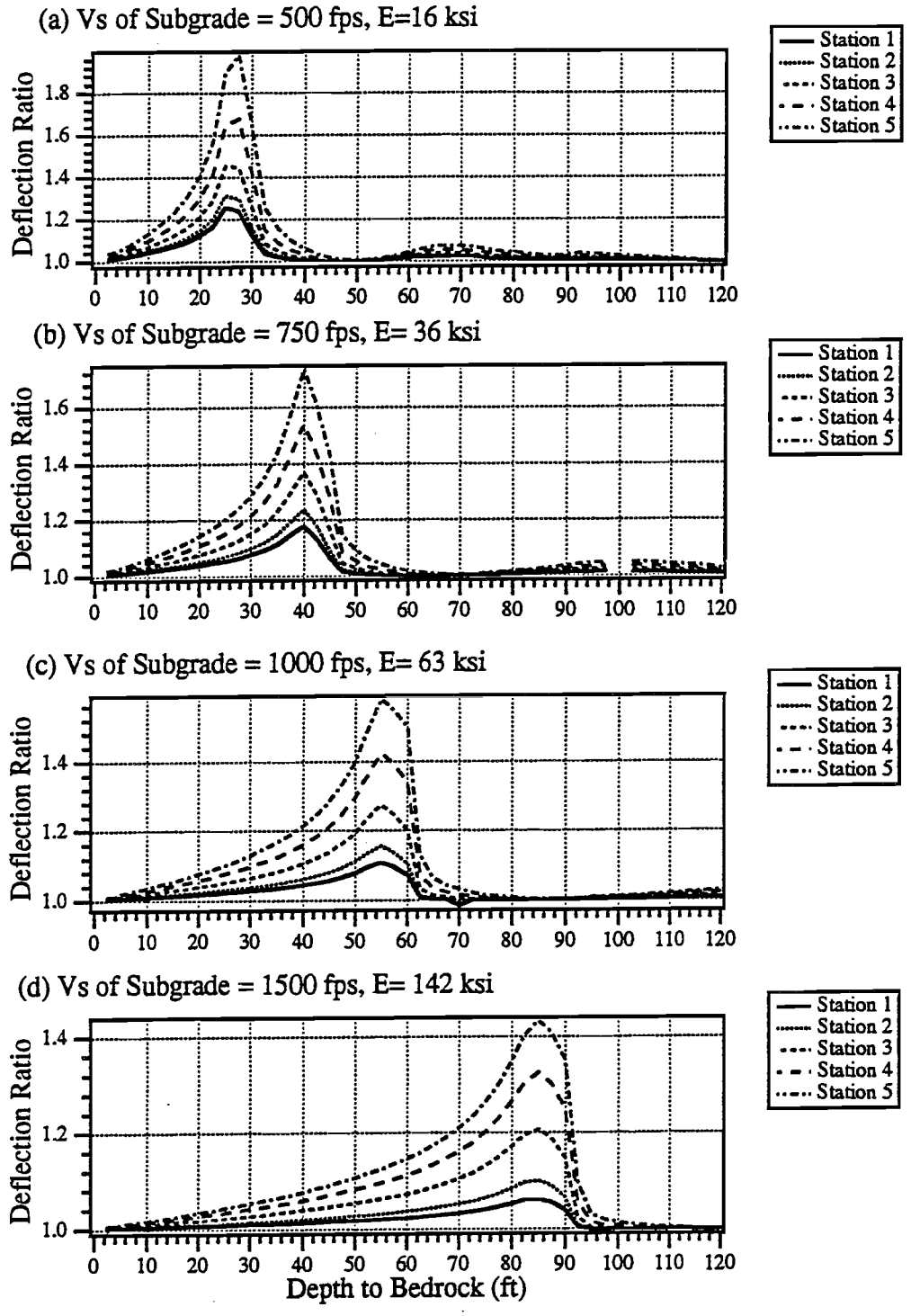

Figure A.22 Deflection ratio versus depth to bedrock for Dynaflect testing at Profile 2 (V_s of AC = 5000 fps (E = 1920 ksi) and V_s of base = 1000 fps (E = 67 ksi))

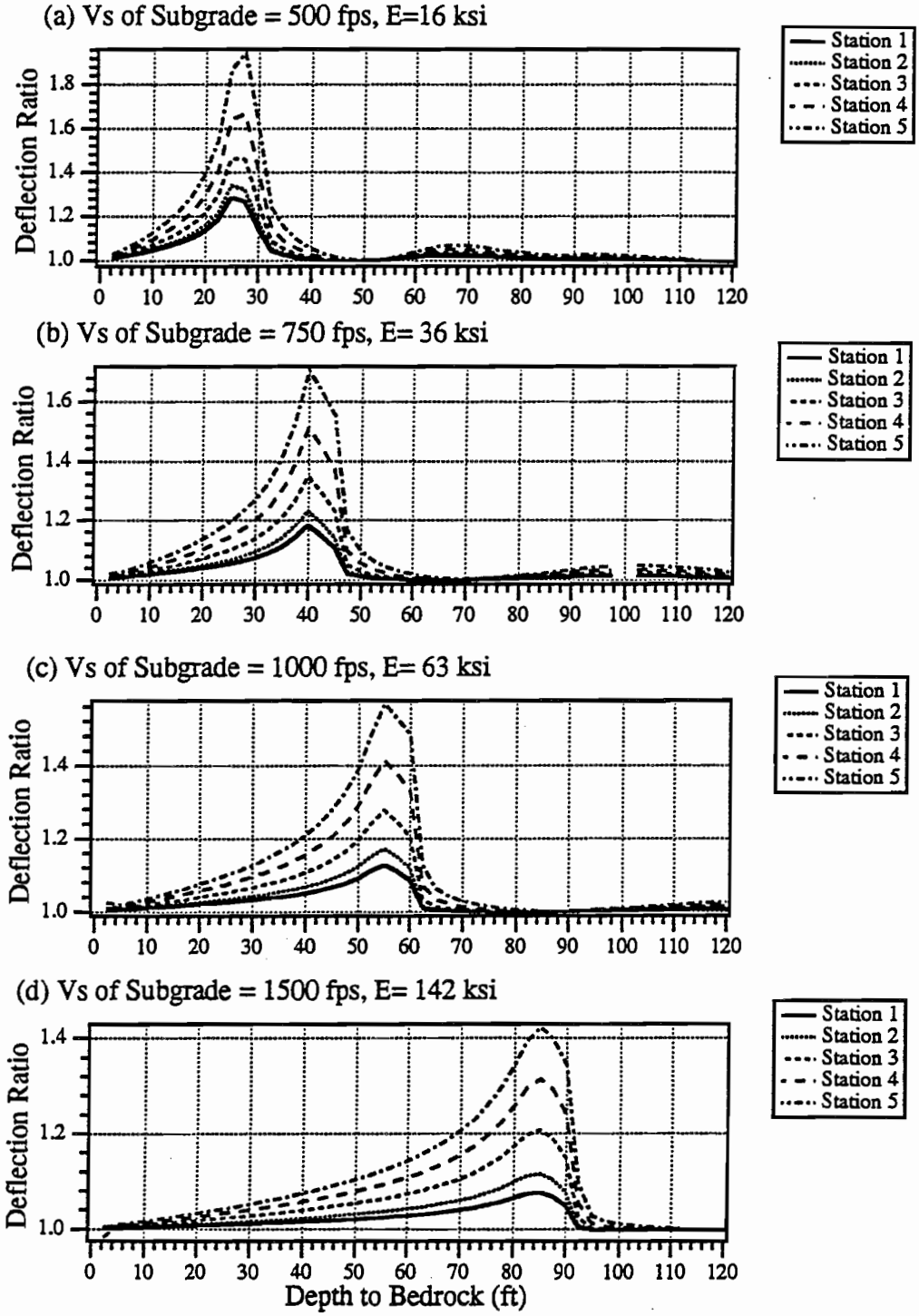

Figure A.23 Deflection ratio versus depth to bedrock for Dynaflect testing at Profile 2 (V_s of AC = 5000 fps (e = 1920 ksi) and V_s of base = 1500 fps (E = 152 ksi))

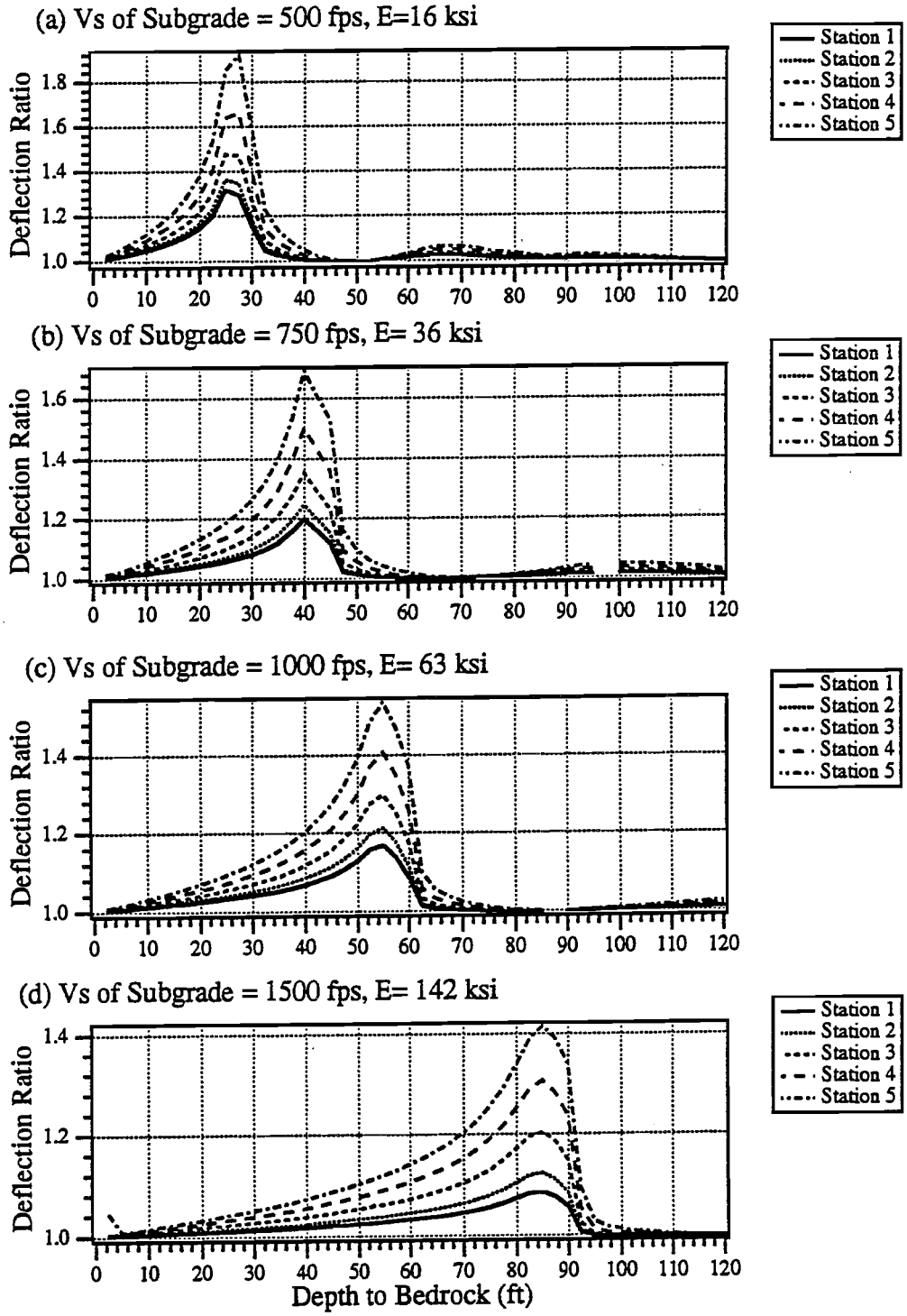

Figure A.24 Deflection ratio versus depth to bedrock for Dynaflect testing at Profile 2 (V_s of AC = 5000 fps (E = 1920 ksi) and V_s of base = 2000 fps (E = 270 ksi))

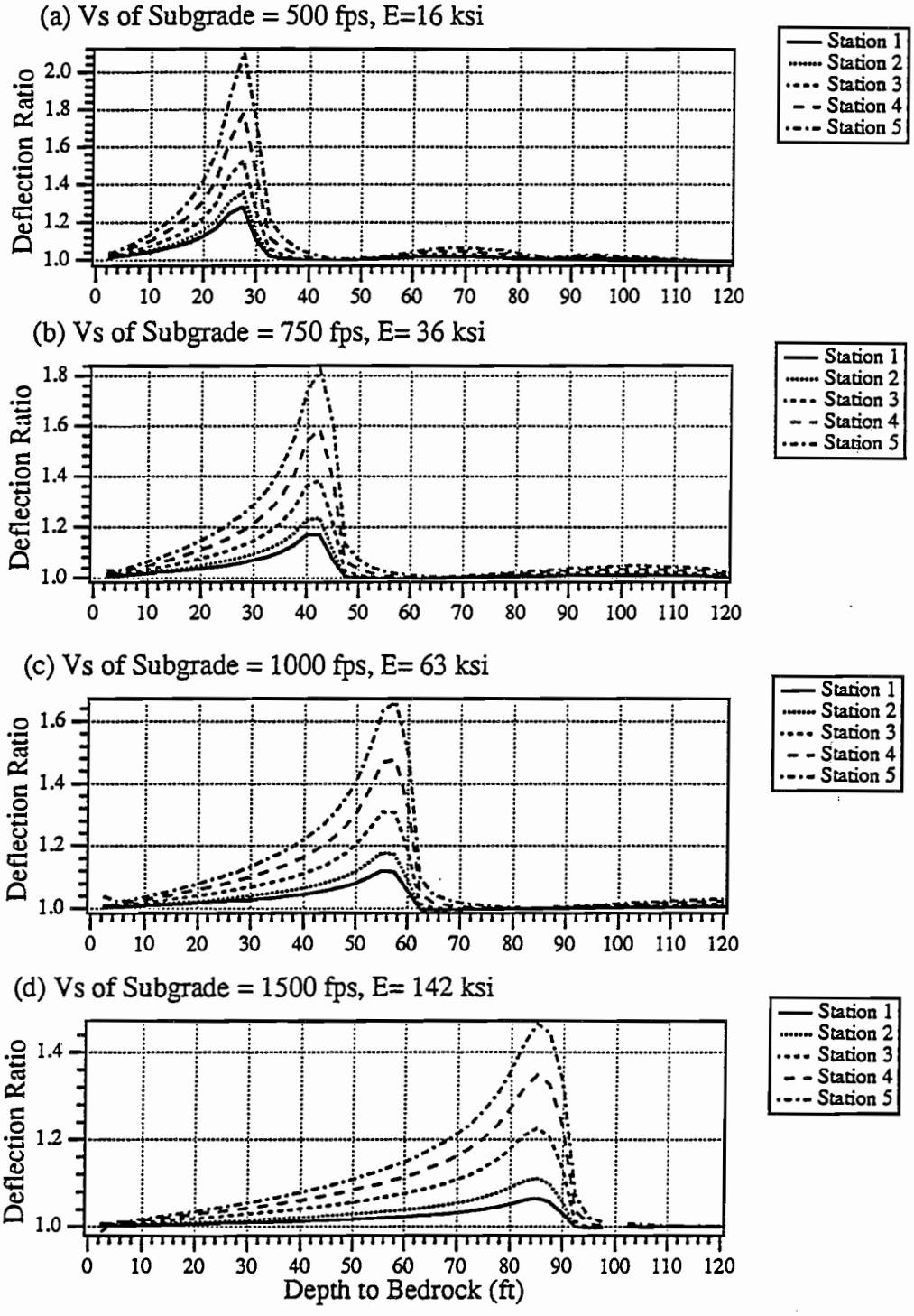

Figure A.25 Deflection ratio versus depth to bedrock for Dynaflect testing at Profile 3 (V_s of AC = 2000 fps (E = 312 ksi) and V_s of base = 1000 fps (E = 67 ksi))

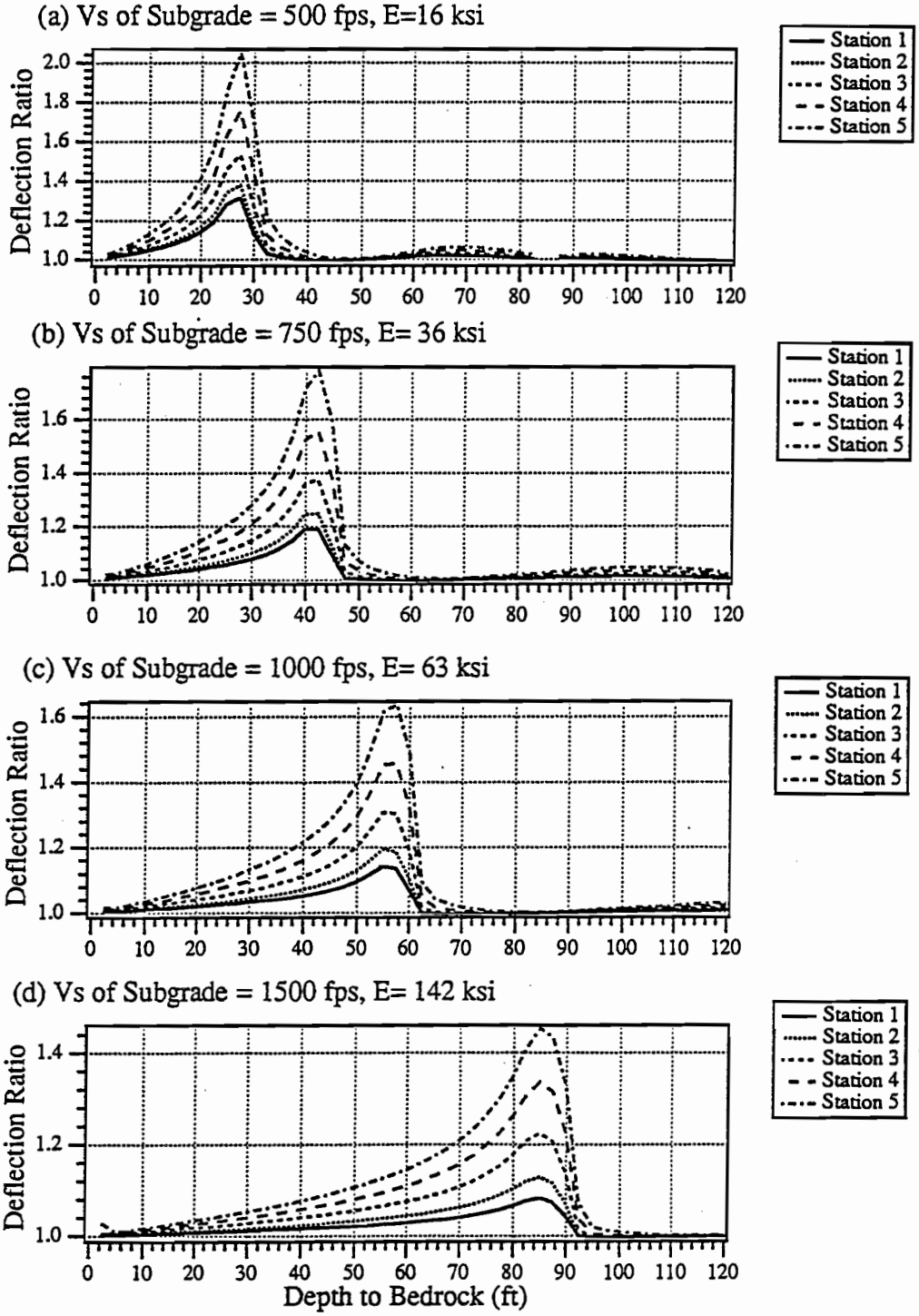

Figure A.26 Deflection ratio versus depth to bedrock for Dynaflect testing at Profile 3 (V_s of AC = 2000 fps (E = 312 ksi) and V_s of base = 1500 fps (E = 152 ksi))

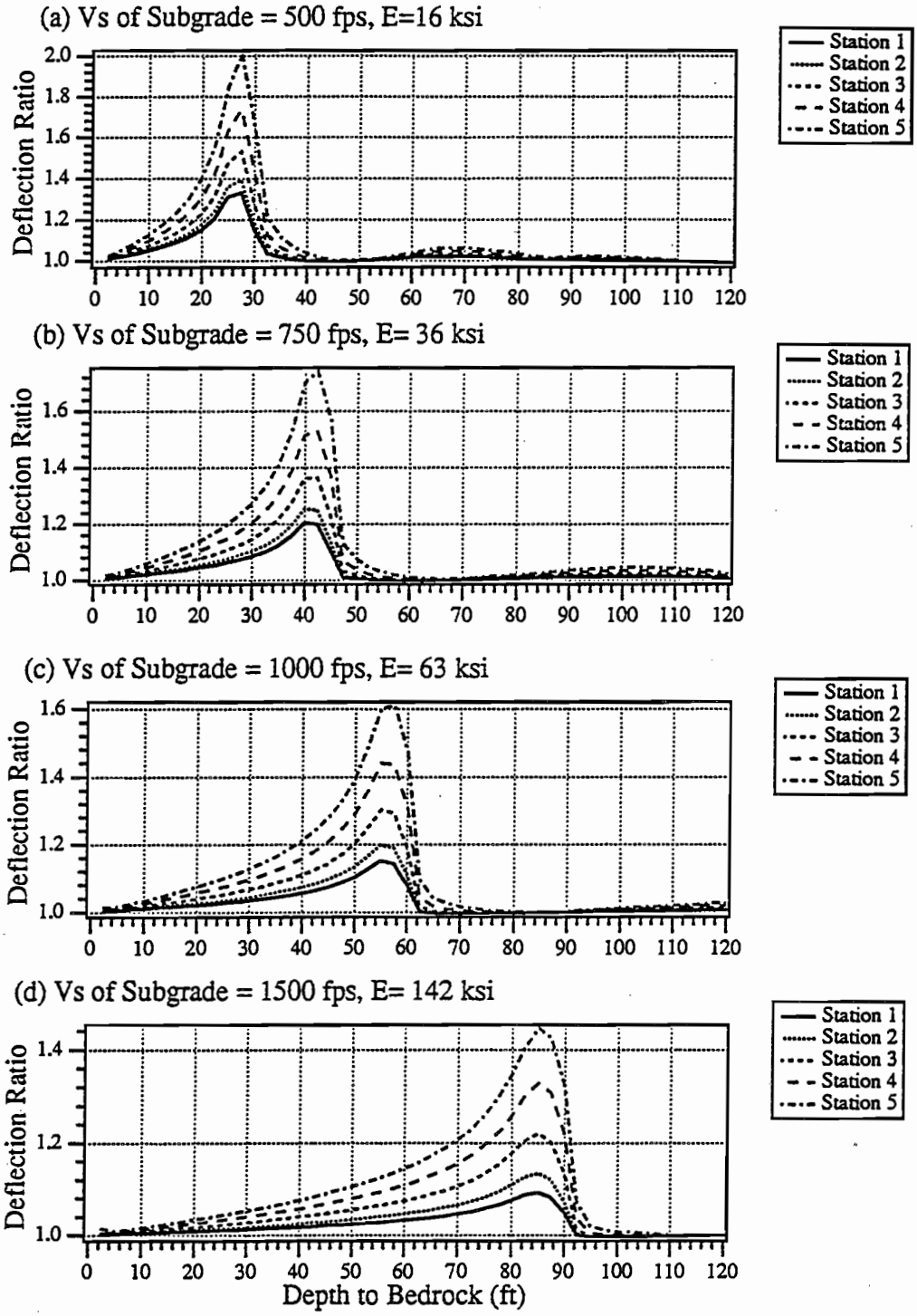

Figure A.27 Deflection ratio versus depth to bedrock for Dynaflect testing at Profile 3 (V_s of AC = 2000 fps (E = 312 ksi) and V_s of base = 2000 fps (E = 270 ksi))

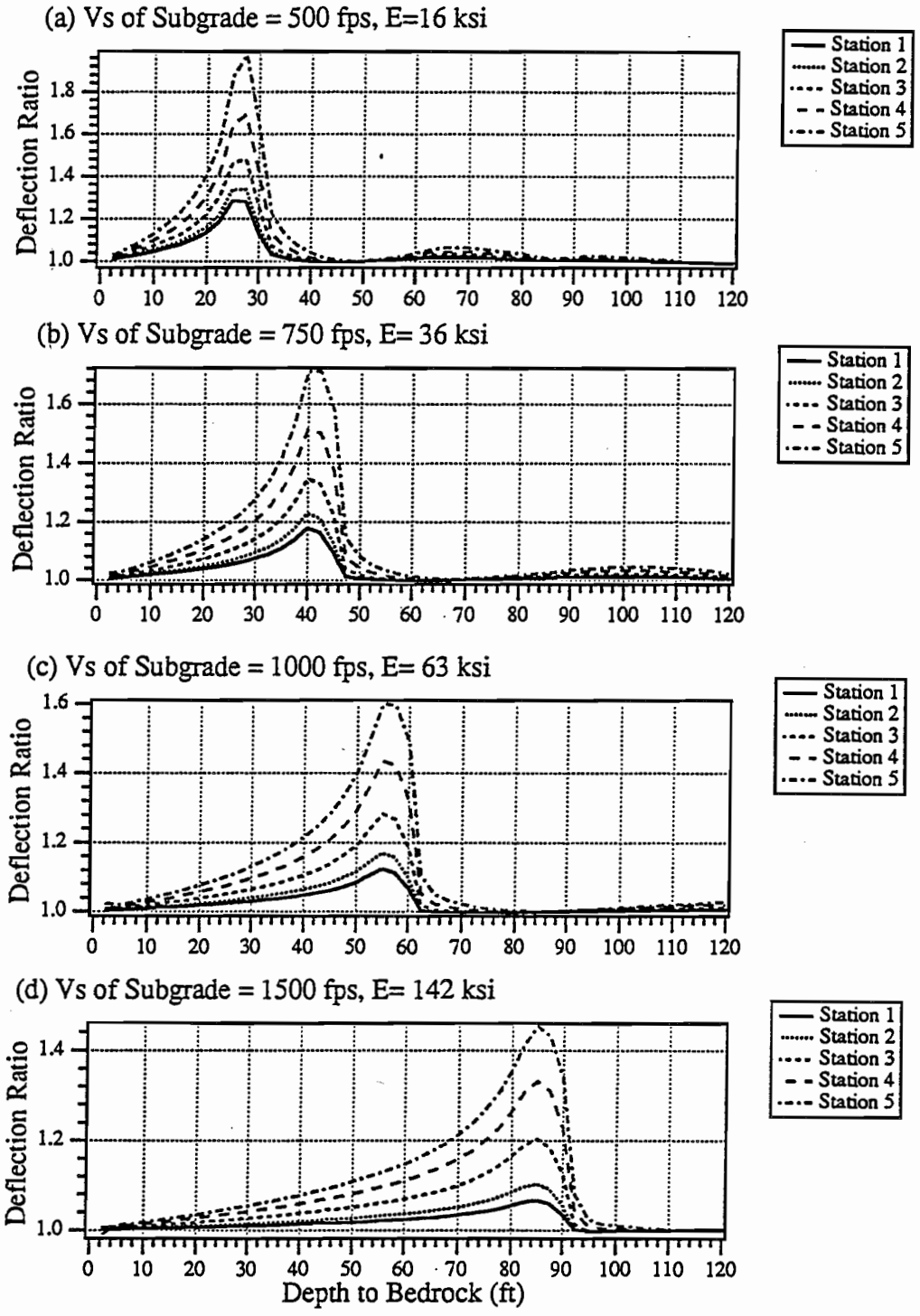

Figure A.28 Deflection ratio versus depth to bedrock for Dynaflect testing at Profile 3 (V_s of AC = 3000 fps (E = 690 ksi) and V_s of base = 1000 fps (E = 67 ksi))

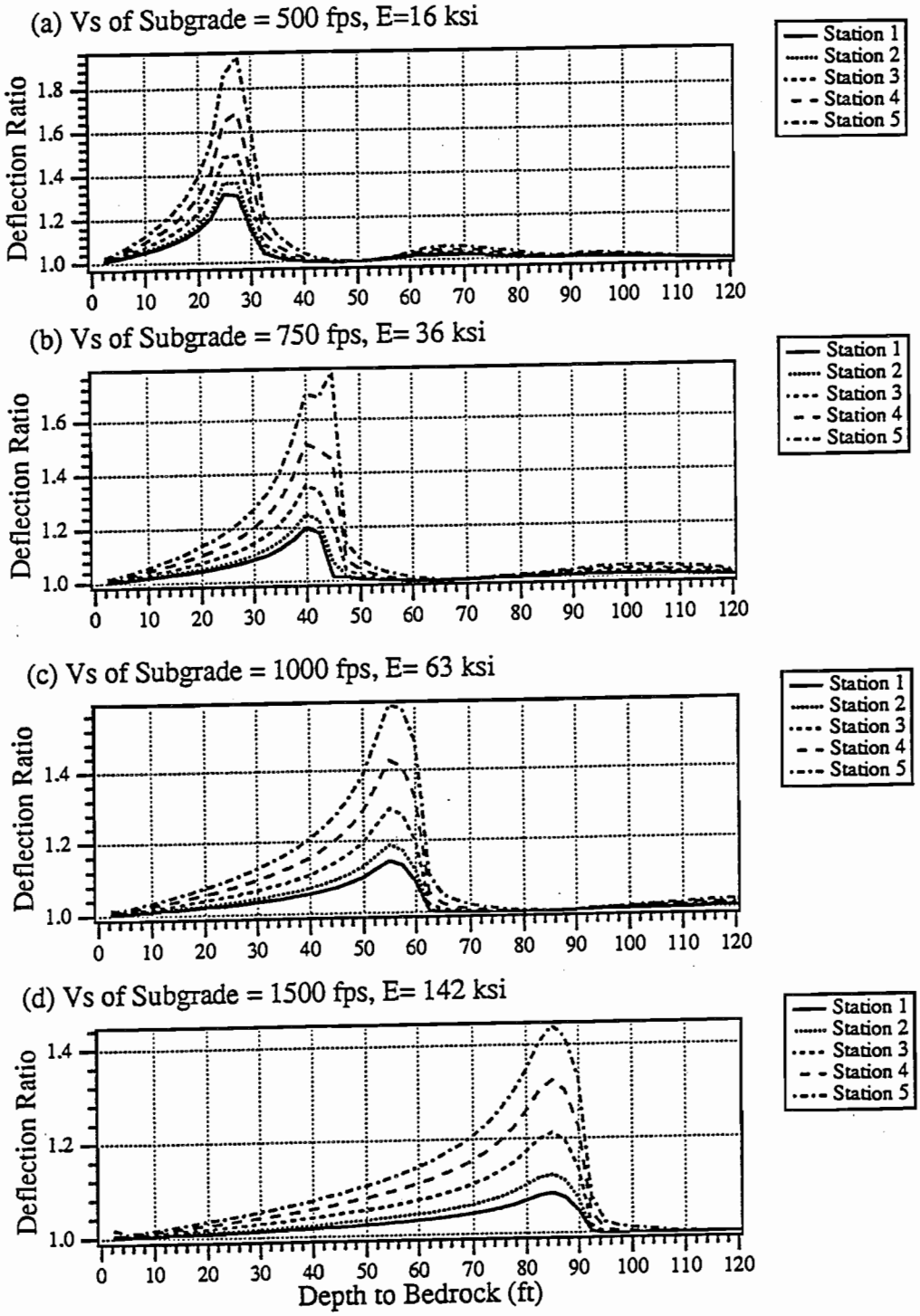

Figure A.29 Deflection ratio versus depth to bedrock for Dynaflect testing at Profile 3 (V_s of AC = 3000 fps (E = 690 ksi) and V_s of base = 1500 fps (E = 152 ksi))

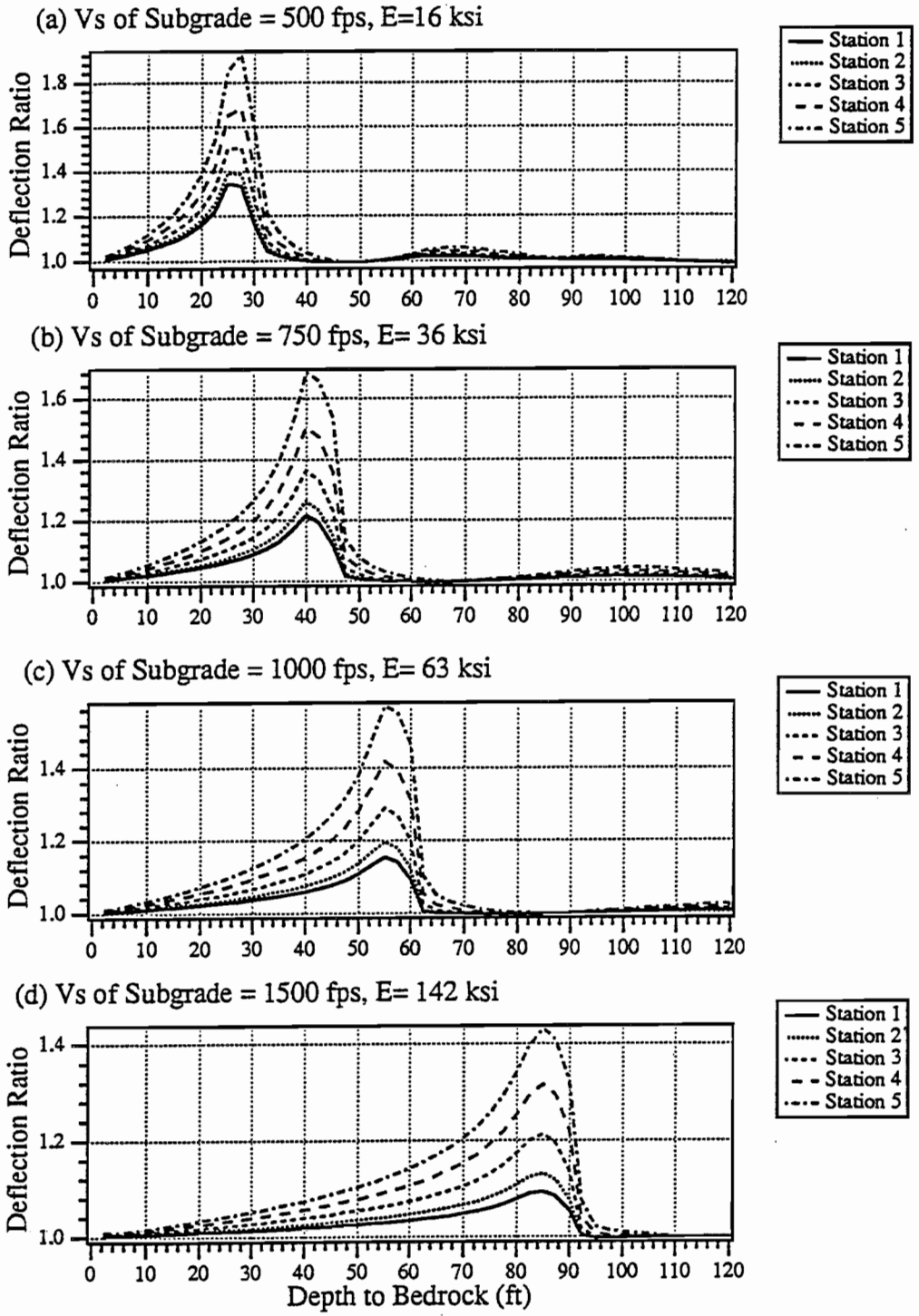

Figure A.30 Deflection ratio versus depth to bedrock for Dynaflect testing at Profile 3 (V_s of AC = 3000 fps (E = 690 ksi) and V_s of base = 2000 fps (E = 270 ksi))

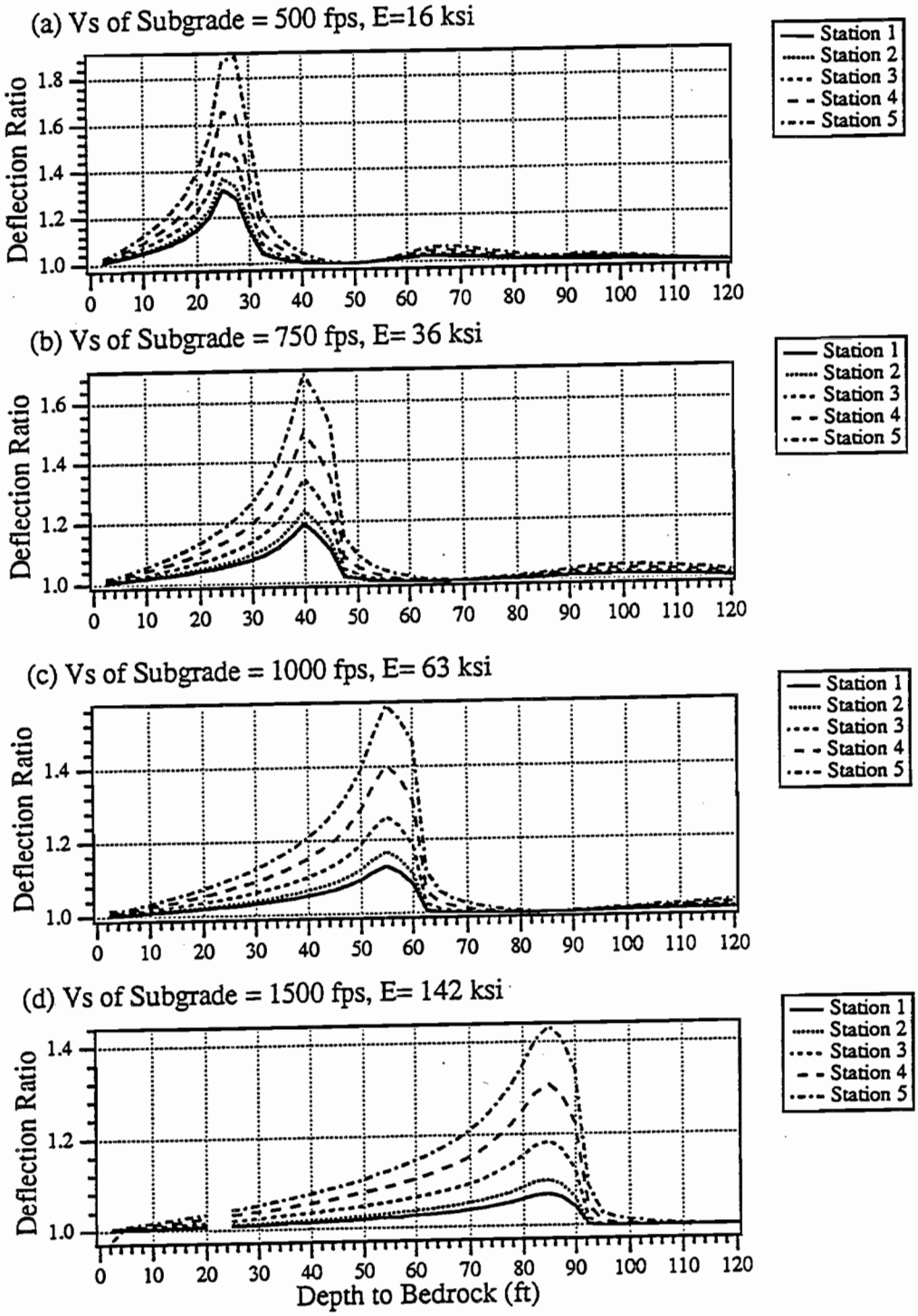

Figure A.31 Deflection ratio versus depth to bedrock for Dynaflect testing at Profile 3 (V_s of AC = 4000 fps (E = 1225 ksi) and V_s of base = 1000 fps (E = 67 ksi))

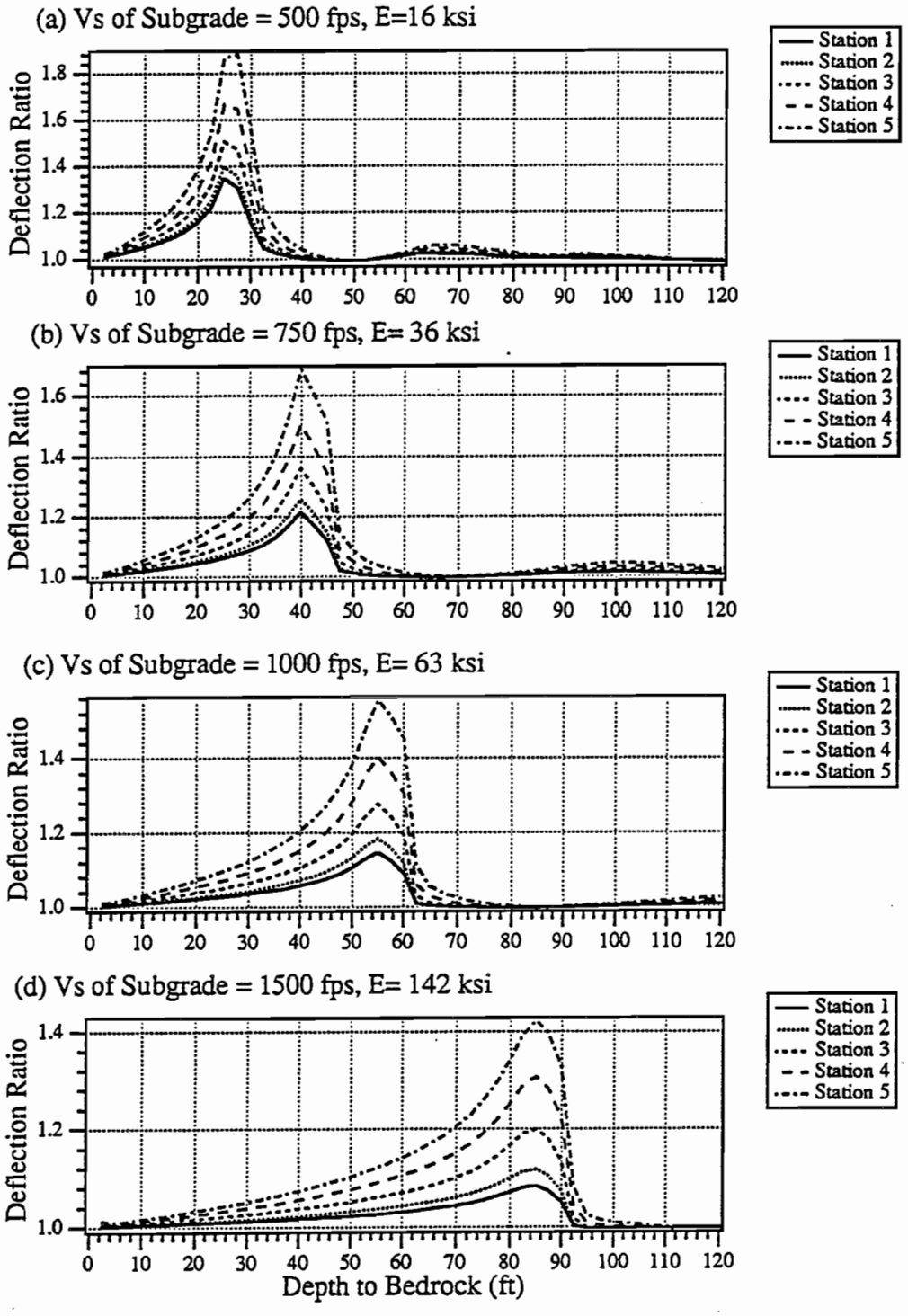

Figure A.32 Deflection ratio versus depth to bedrock for Dynaflect testing at Profile 3 (V_s of AC = 4000 fps (E = 1225 ksi) and V_s of base = 1500 fps (E = 152 ksi))

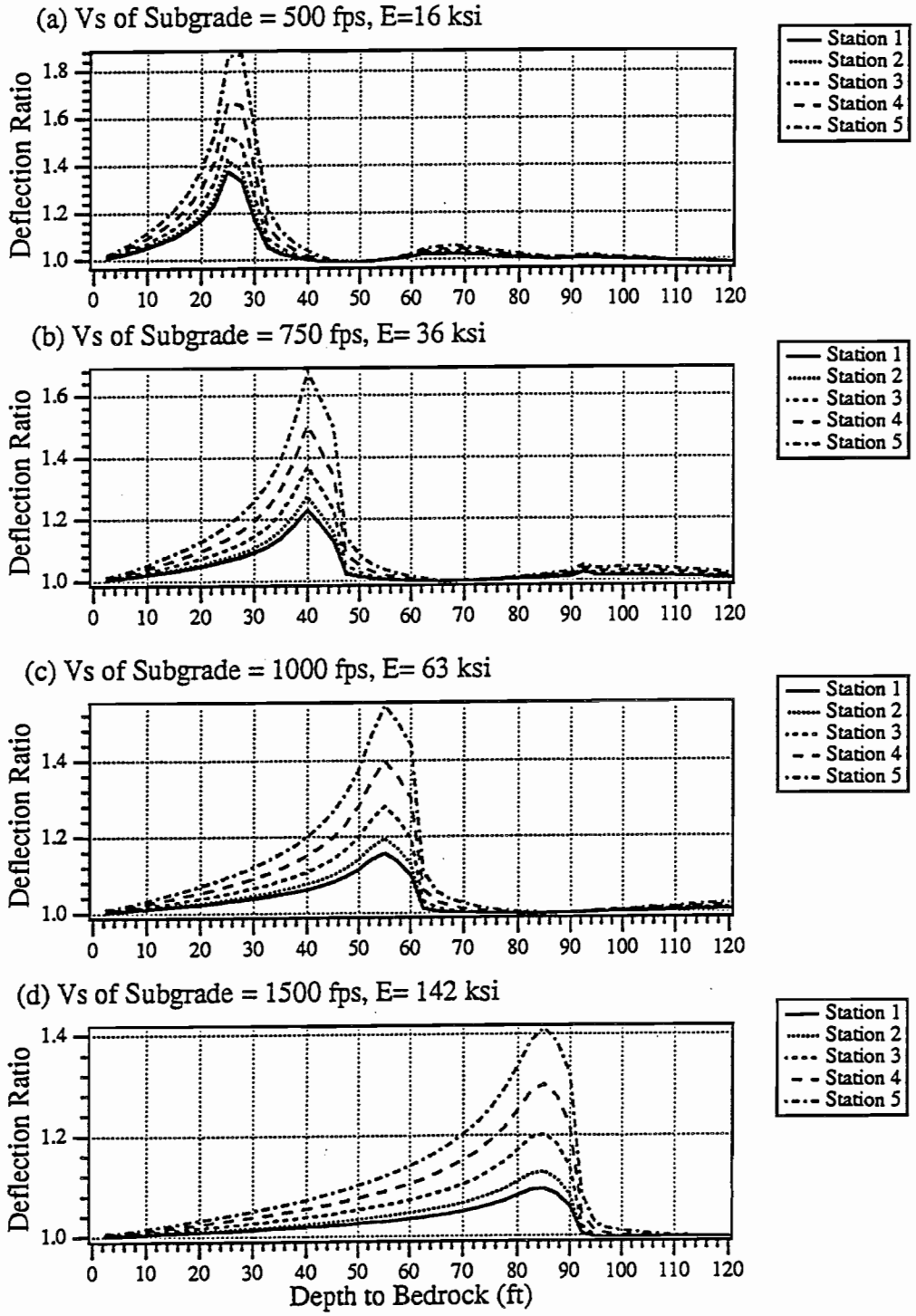

Figure A.33 Deflection ratio versus depth to bedrock for Dynaflect testing at Profile 3 (V_s of AC = 4000 fps (E = 1225 ksi) and V_s of base = 2000 fps (E = 270 ksi))

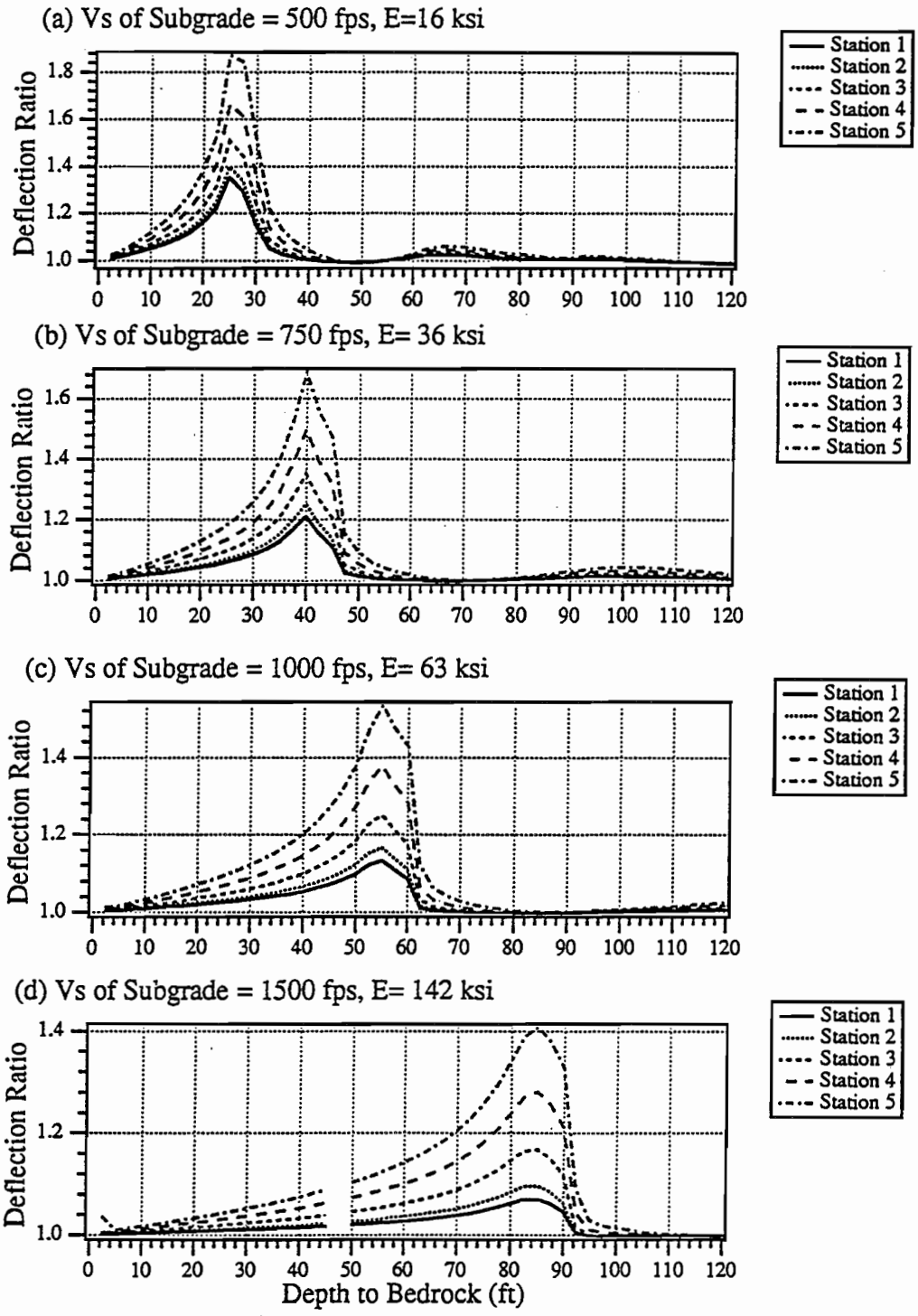

Figure A.34 Deflection ratio versus depth to bedrock for Dynaflect testing at Profile 3 (V_s of AC = 5000 fps (E = 1920 ksi) and V_s of base = 1000 fps (E = 67 ksi))

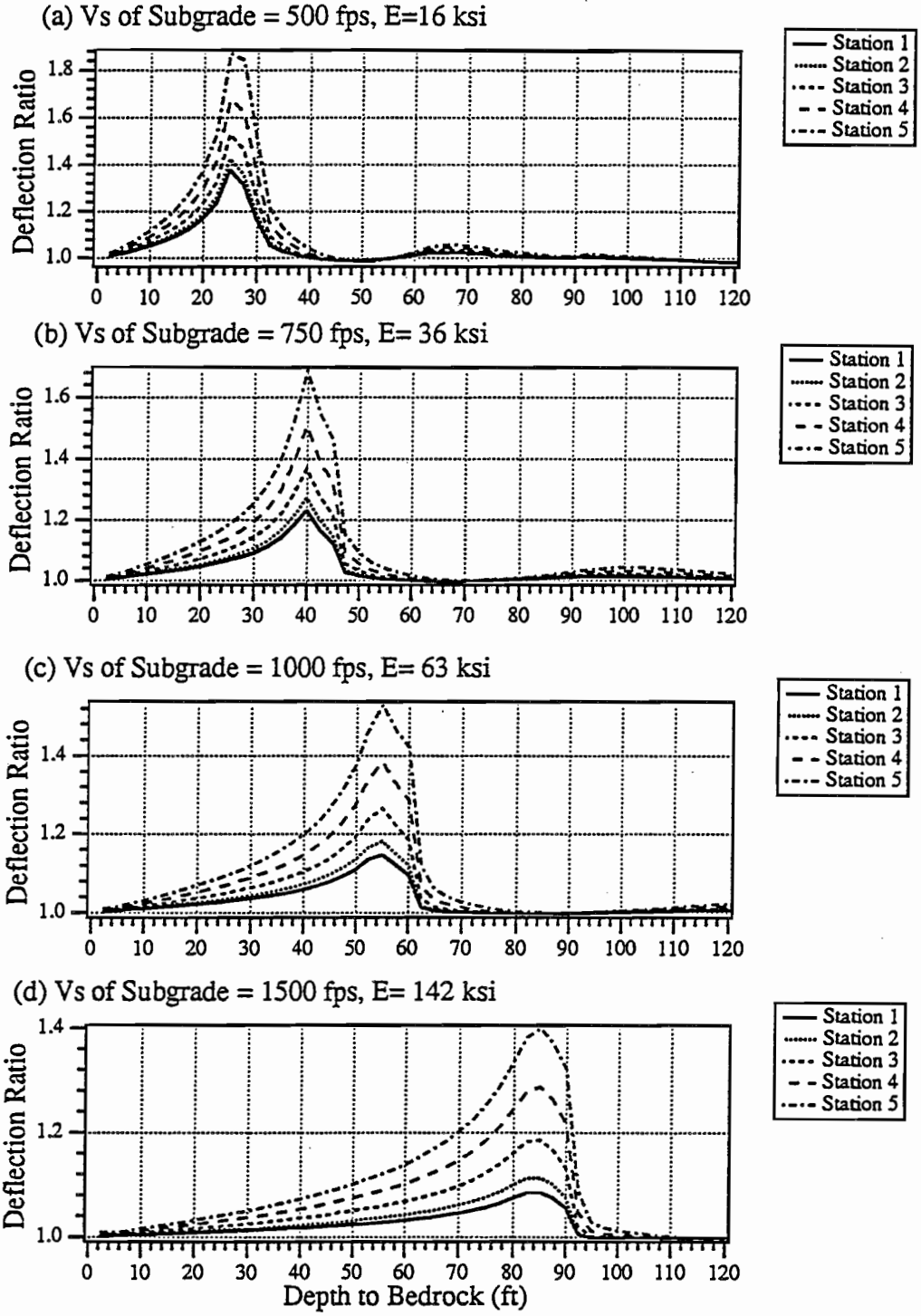

Figure A.35 Deflection ratio versus depth to bedrock for Dynaflect testing at Profile 3 (V_s of AC = 5000 fps (E = 1920 ksi) and V_s of base = 1500 fps (E = 152 ksi))

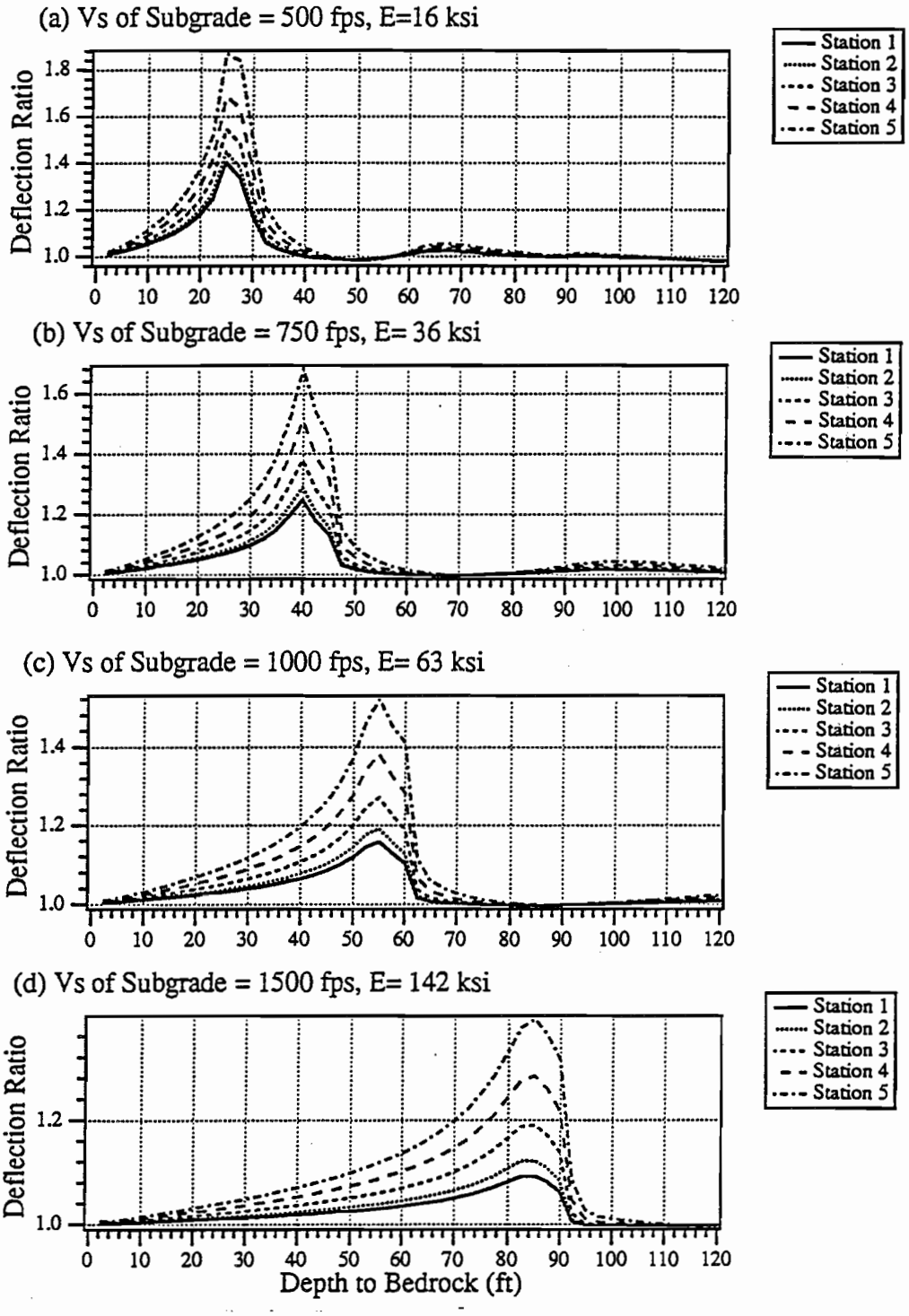

Figure A.36 Deflection ratio versus depth to bedrock for Dynaflect testing at Profile 3 (V_s of AC = 5000 fps (E = 1920 ksi) and V_s of base = 2000 fps (E = 270 ksi))

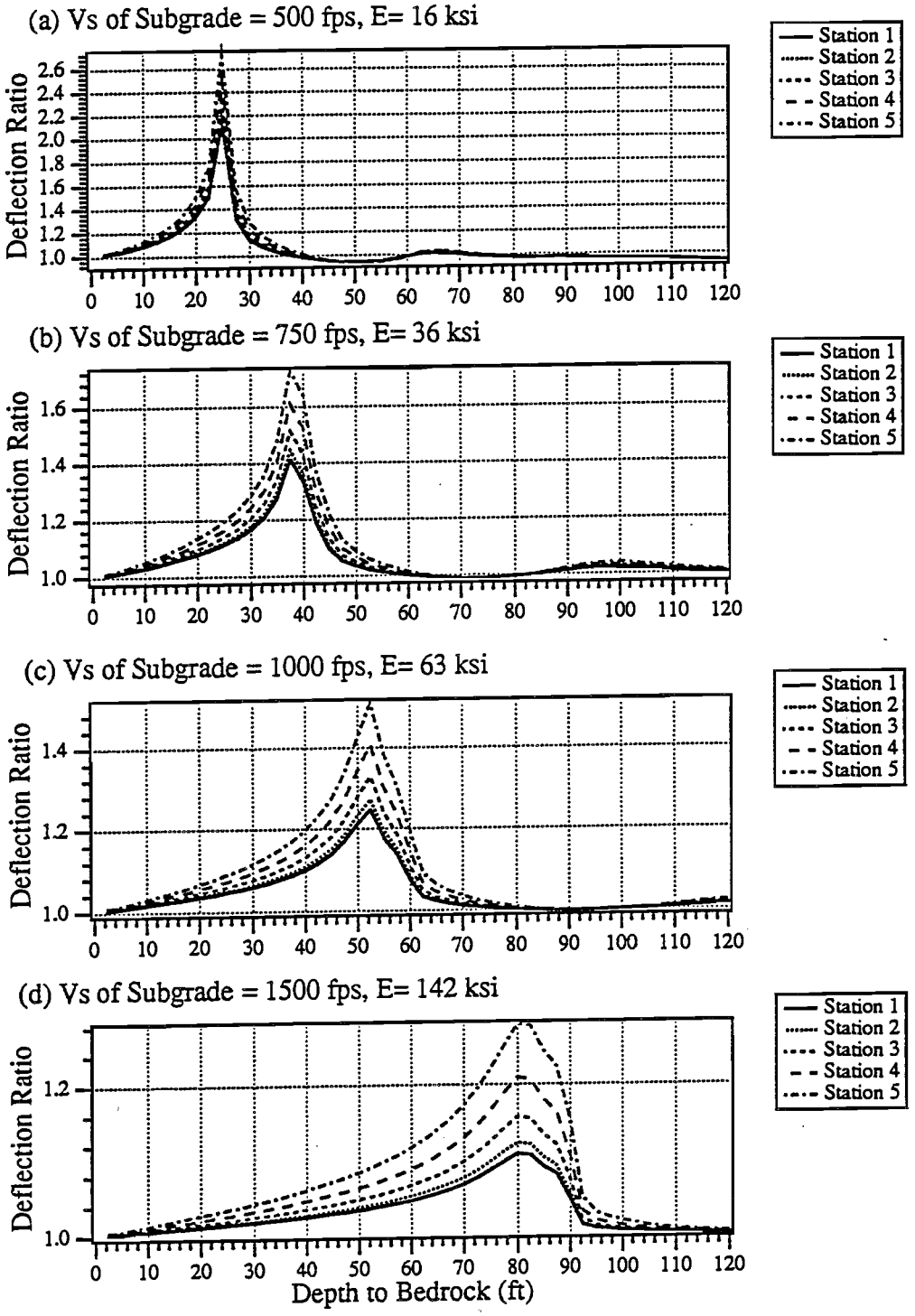

Figure A.37 Deflection ratio versus depth to bedrock for Dynaflect testing at Profile 4 (V_s of AC = 2000 fps (E = 312 ksi) and V_s of base = 1000 fps (E = 67 ksi))

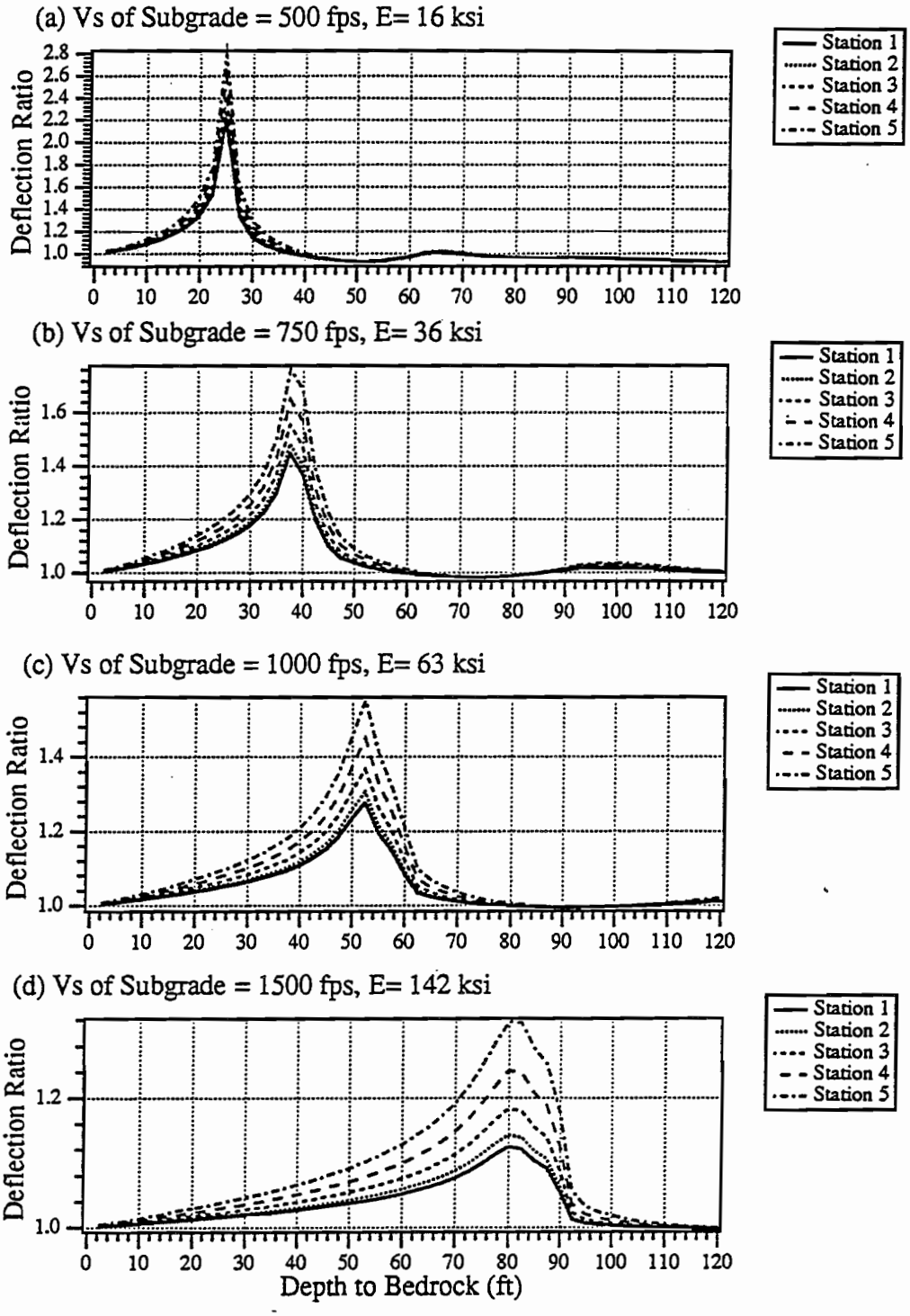

Figure A.38 Deflection ratio versus depth to bedrock for Dynaflect testing at Profile 4 (V_s of AC = 2000 fps (E = 312 ksi) and V_s of base = 1500 fps (E = 152 ksi))

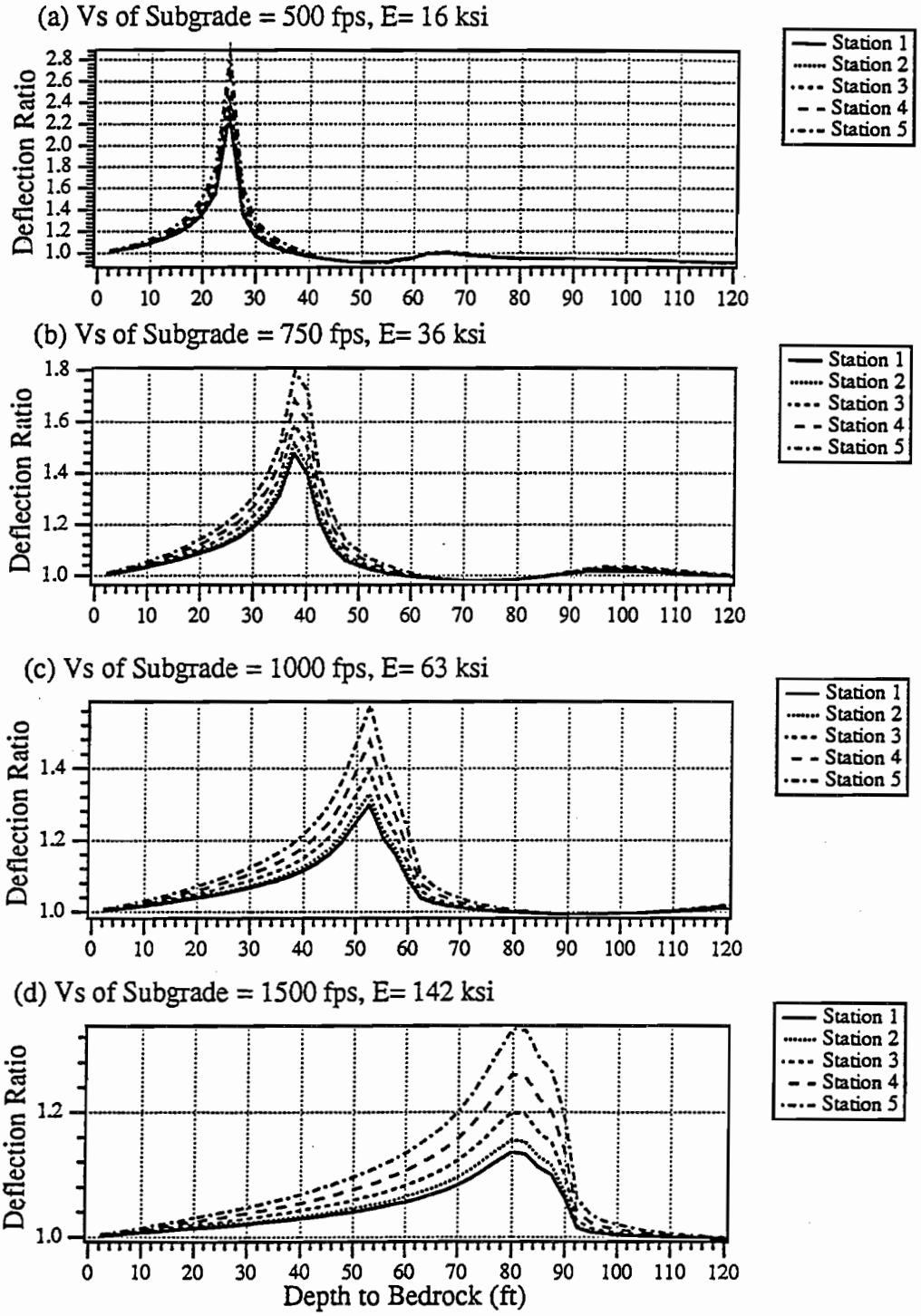

Figure A.39 Deflection ratio versus depth to bedrock for Dynaflect testing at Profile 4 (V_s of AC = 2000 fps (E = 312 ksi) and V_s of base = 2000 fps (E = 270 ksi))

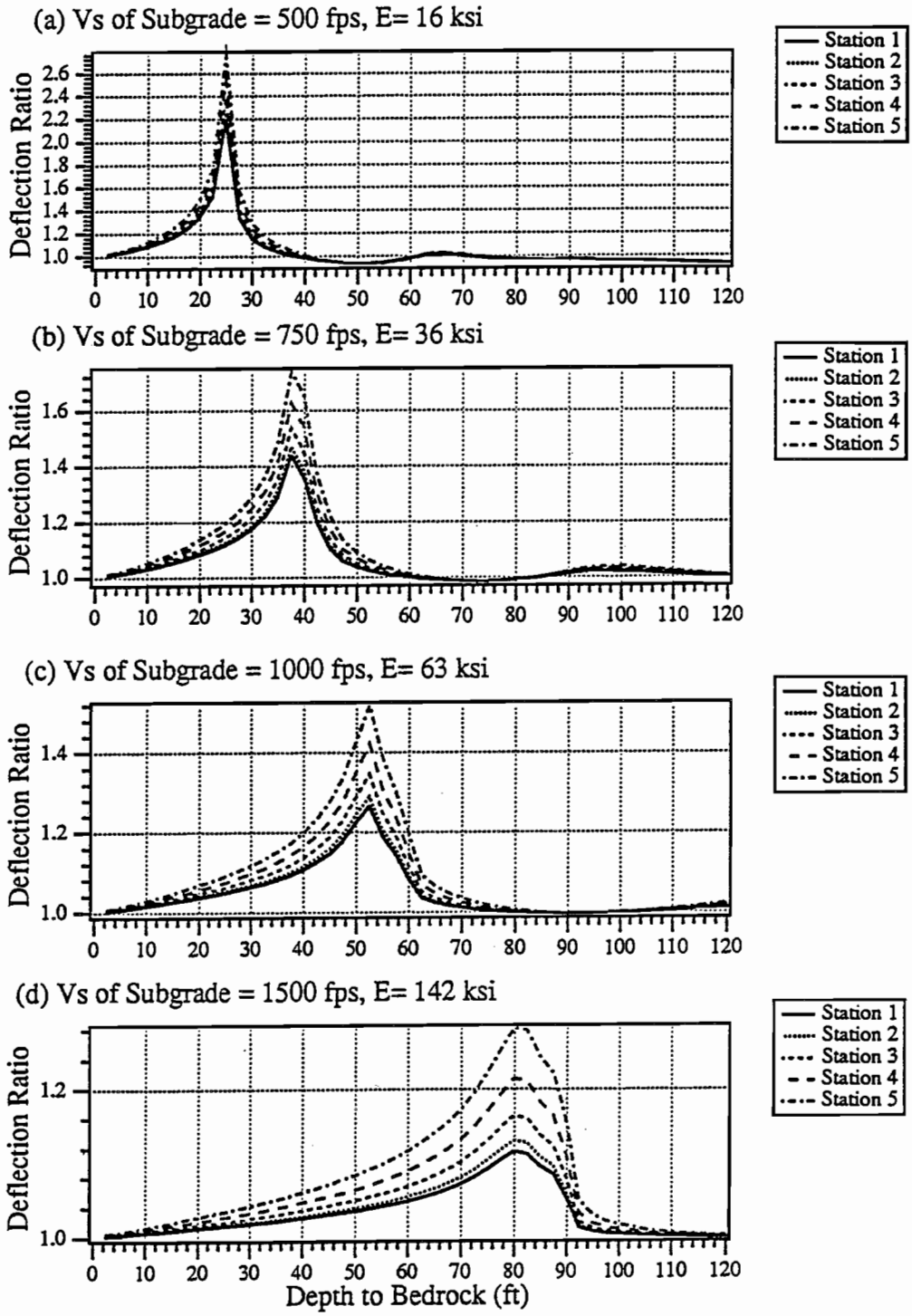

Figure A.40 Deflection ratio versus depth to bedrock for Dynaflect testing at Profile 4 (V_s of AC = 3000 fps (E = 6 and V_s of base = 1000 fps (E = 67 ksi))

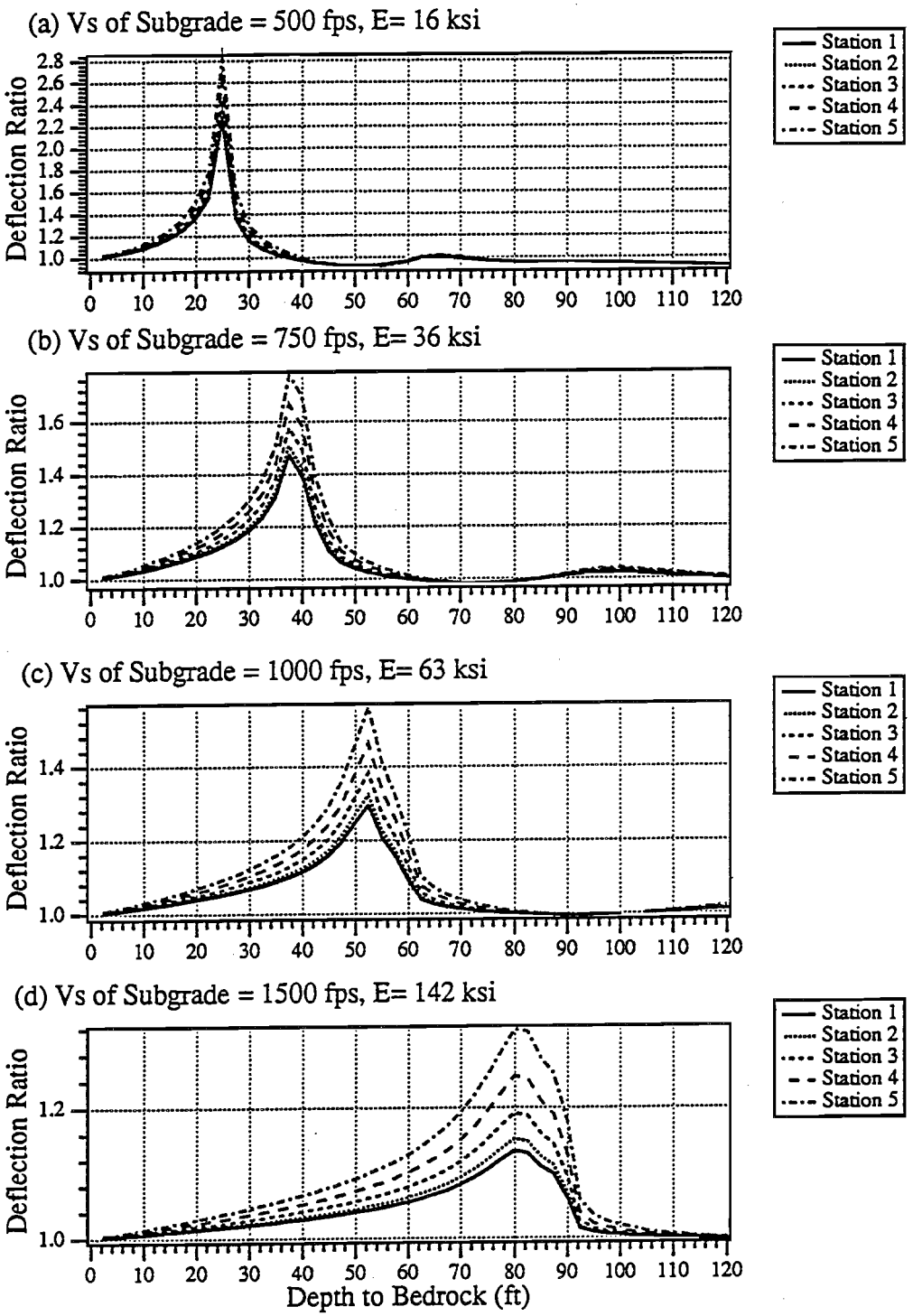

Figure A.41 Deflection ratio versus depth to bedrock for Dynaflect testing at Profile 4 (V_s of AC = 3000 fps (E = 690 ksi) and V_s of base = 1500 fps (E = 152 ksi))

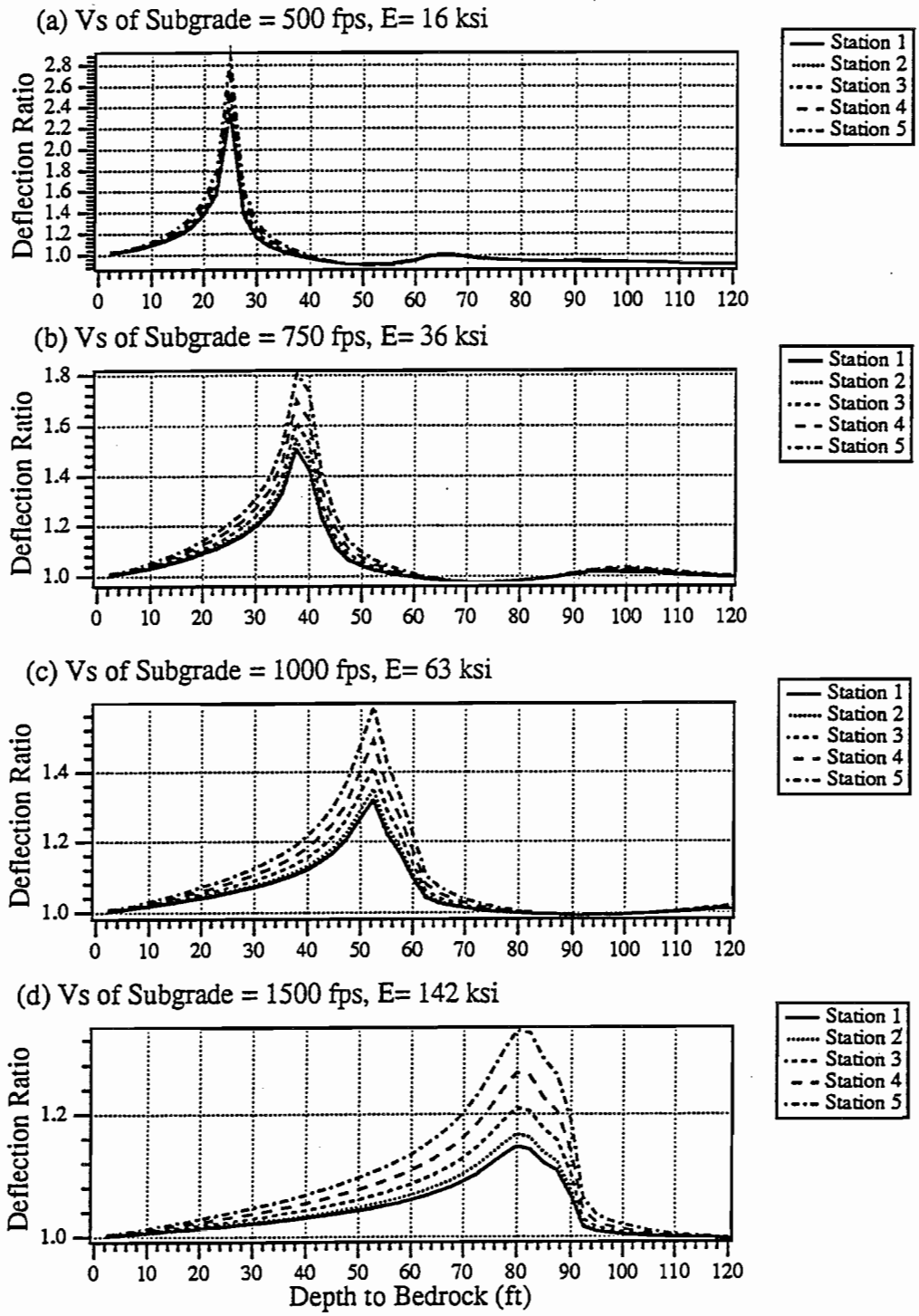

Figure A.42 Deflection ratio versus depth to bedrock for Dynaflect testing at Profile 4 (V_s of AC = 3000 fps (E = 690 ksi) and V_s of base = 2000 fps (E = 270 ksi))

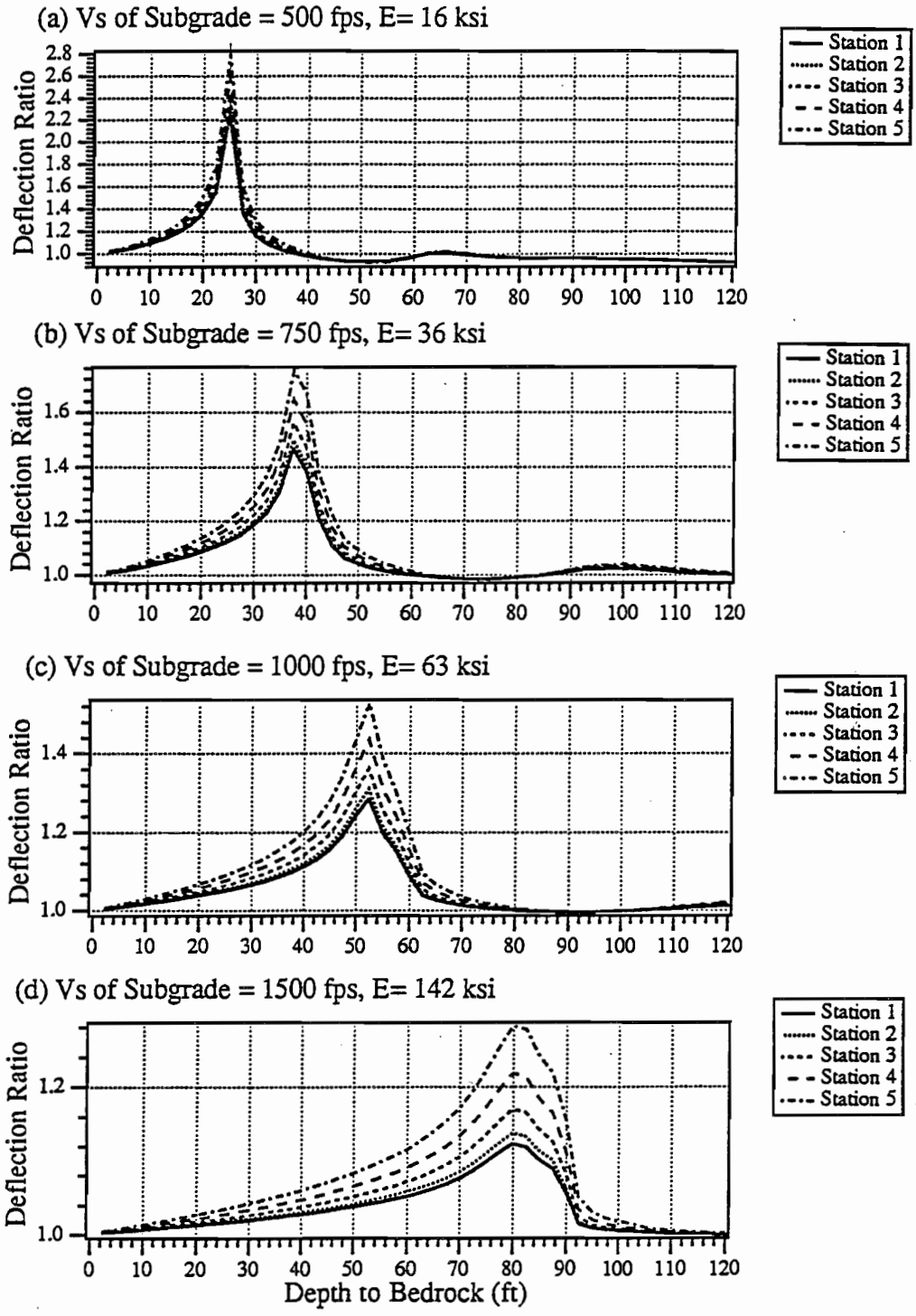

Figure A.43 Deflection ratio versus depth to bedrock for Dynaflect testing at Profile 4 (V_s of AC = 4000 fps (E = 1225 ksi) and V_s of base = 1000 fps (E = 67 ksi))

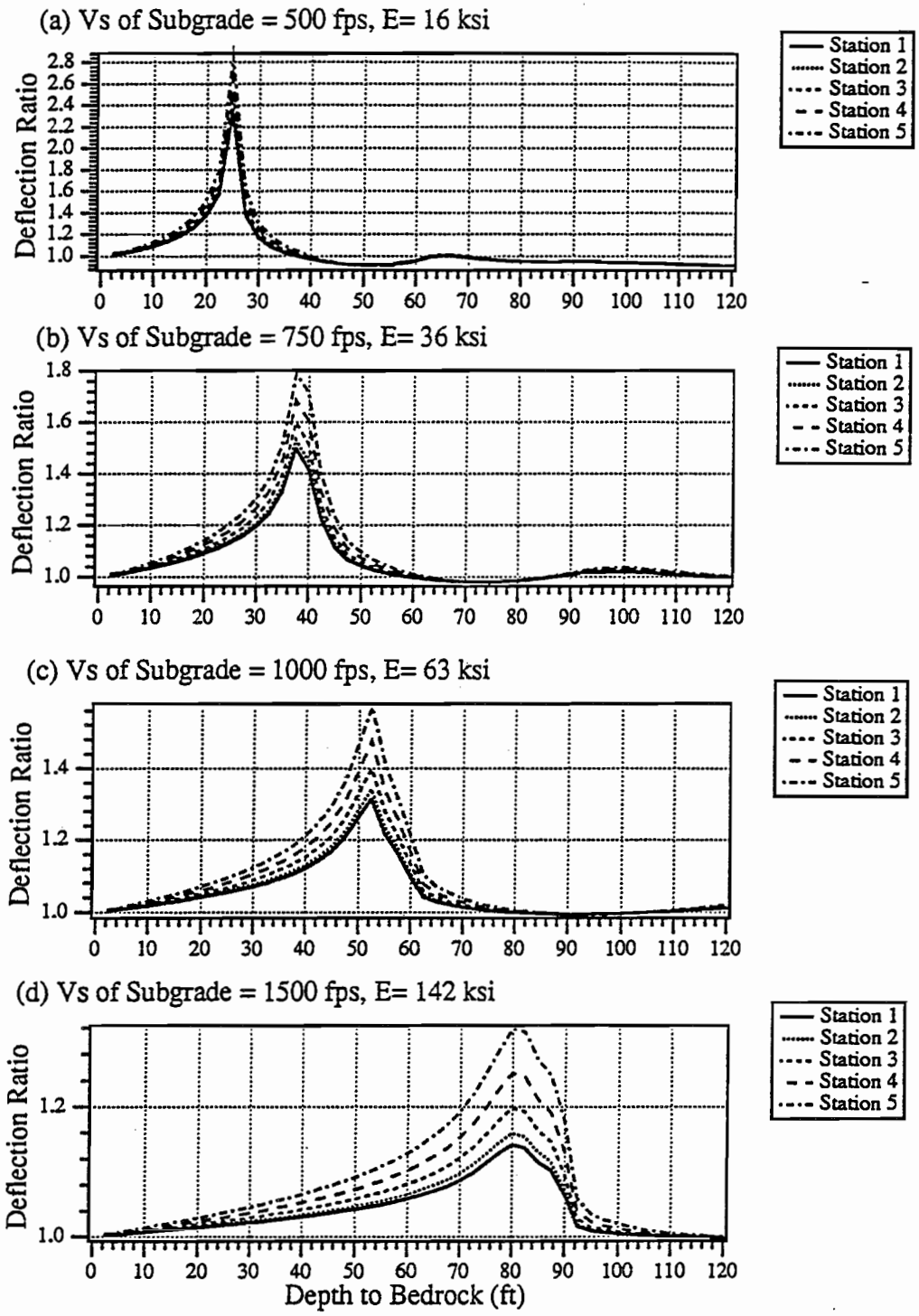

Figure A.44 Deflection ratio versus depth to bedrock for Dynaflect testing at Profile 4 (V_s of AC = 4000 fps (E = 1225 ksi) and V_s of base = 1500 fps (E = 152 ksi))

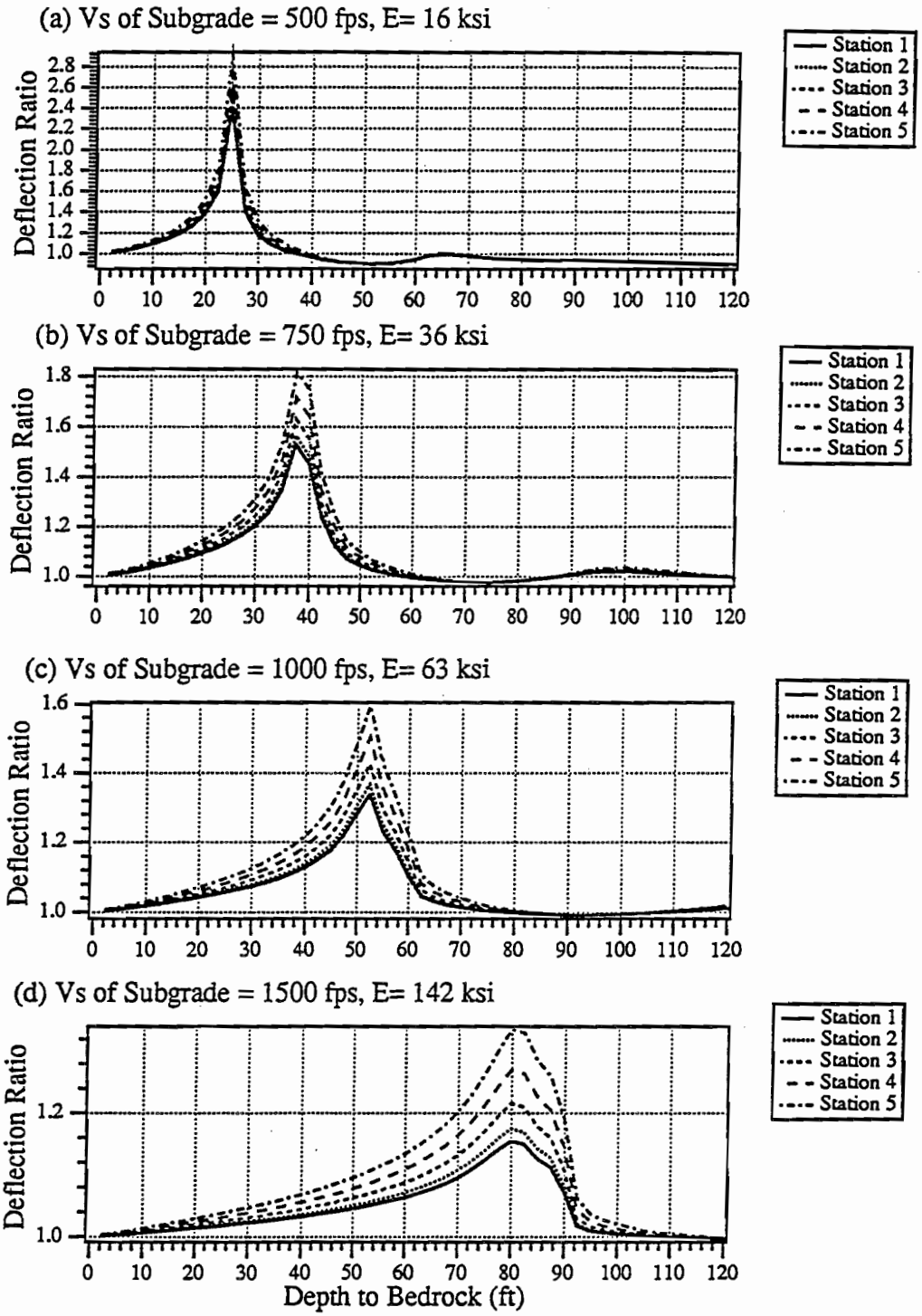

Figure A.45 Deflection ratio versus depth to bedrock for Dynaflect testing at Profile 4 (V_s of AC = 4000 fps (E = 1225 ksi) and V_s of base = 2000 fps (E = 270 ksi))

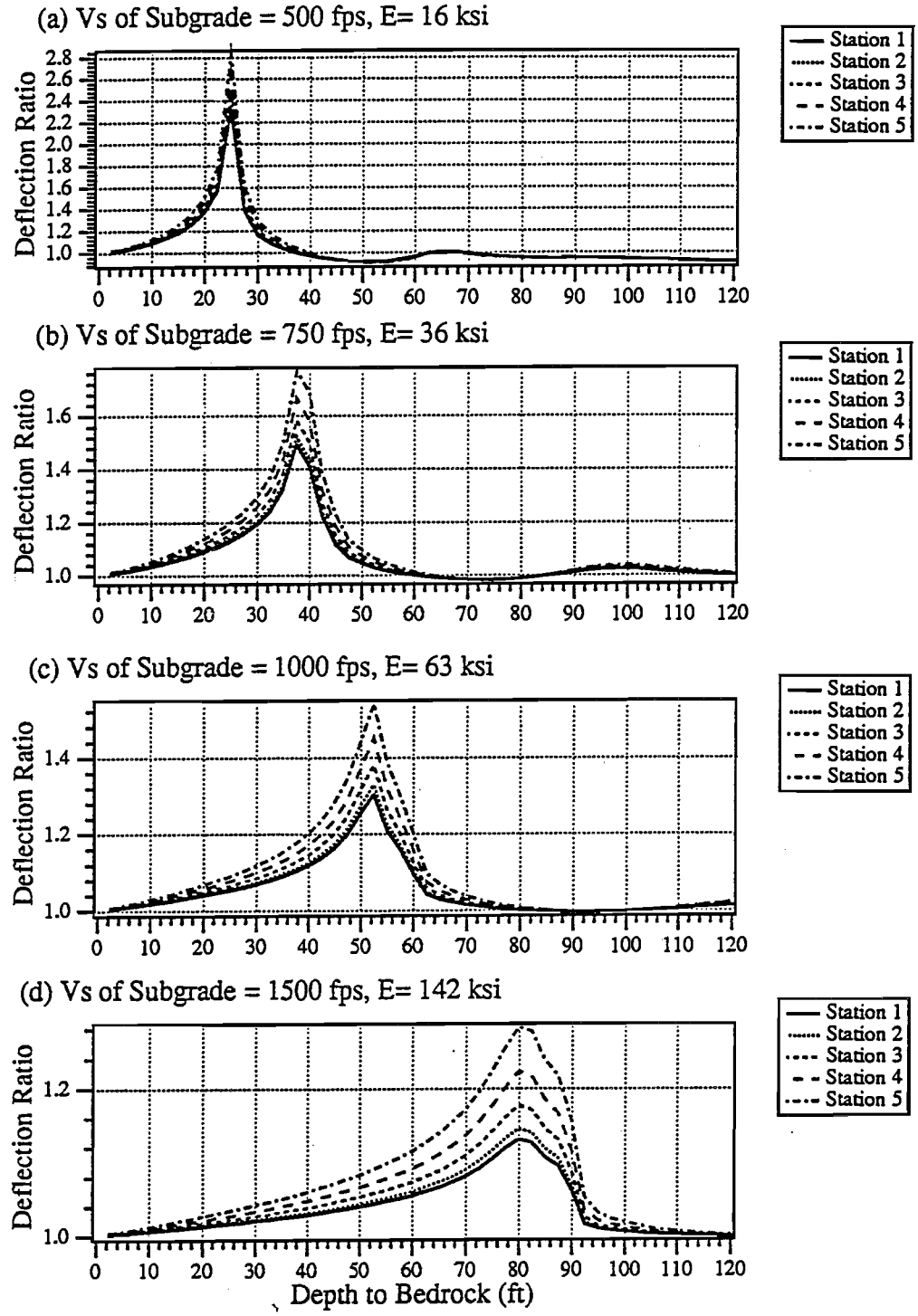

Figure A.46 Deflection ratio versus depth to bedrock for Dynaflect testing at Profile 4 (V_s of AC = 5000 fps (E = 1920 ksi) and V_s of base = 1000 fps (E = 67 ksi))

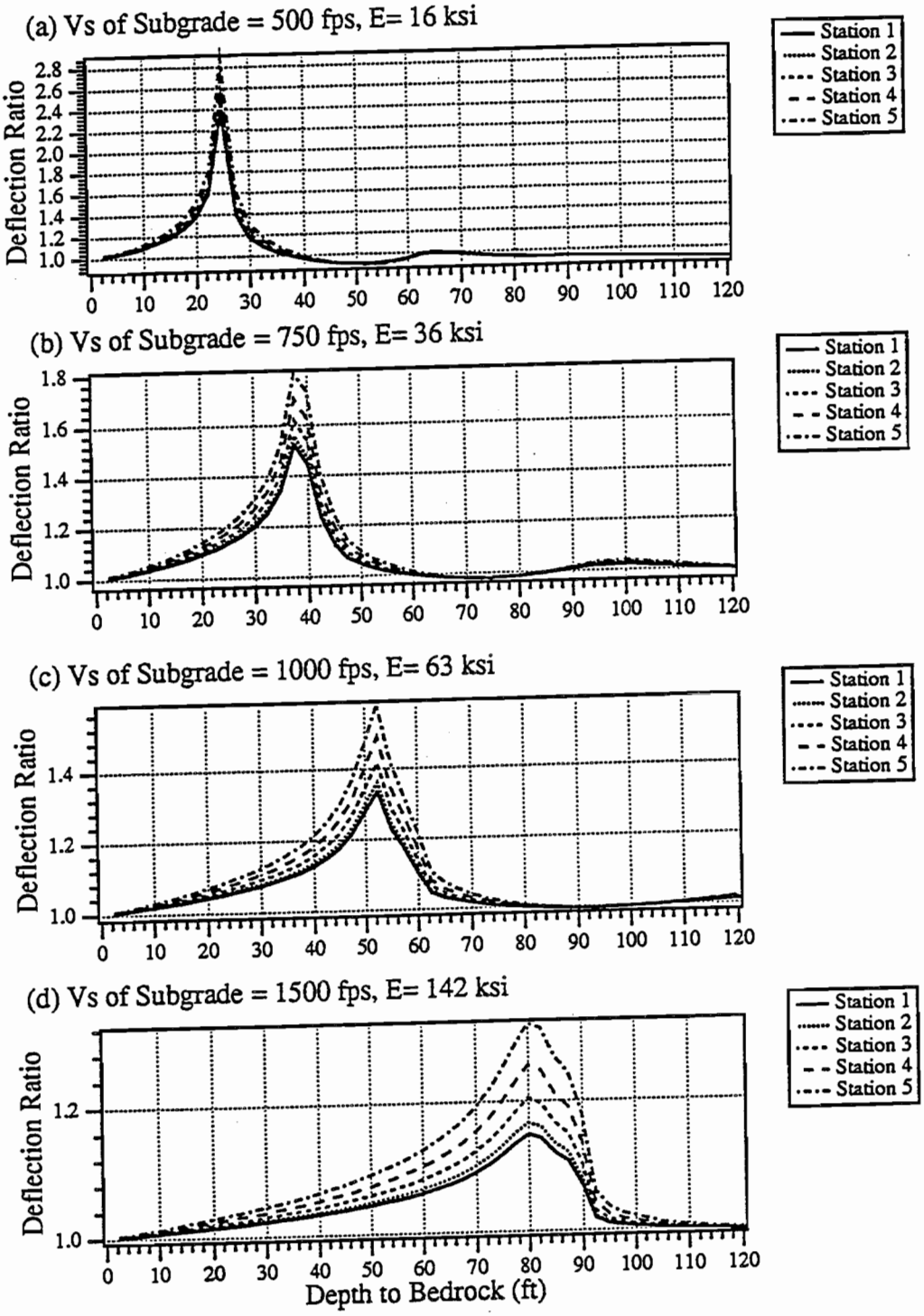

Figure A.47 Deflection ratio versus depth to bedrock for Dynaflect testing at Profile 4 (V_s of AC = 5000 fps (E = 1920 ksi) and V_s of base = 1500 fps (E = 152 ksi))

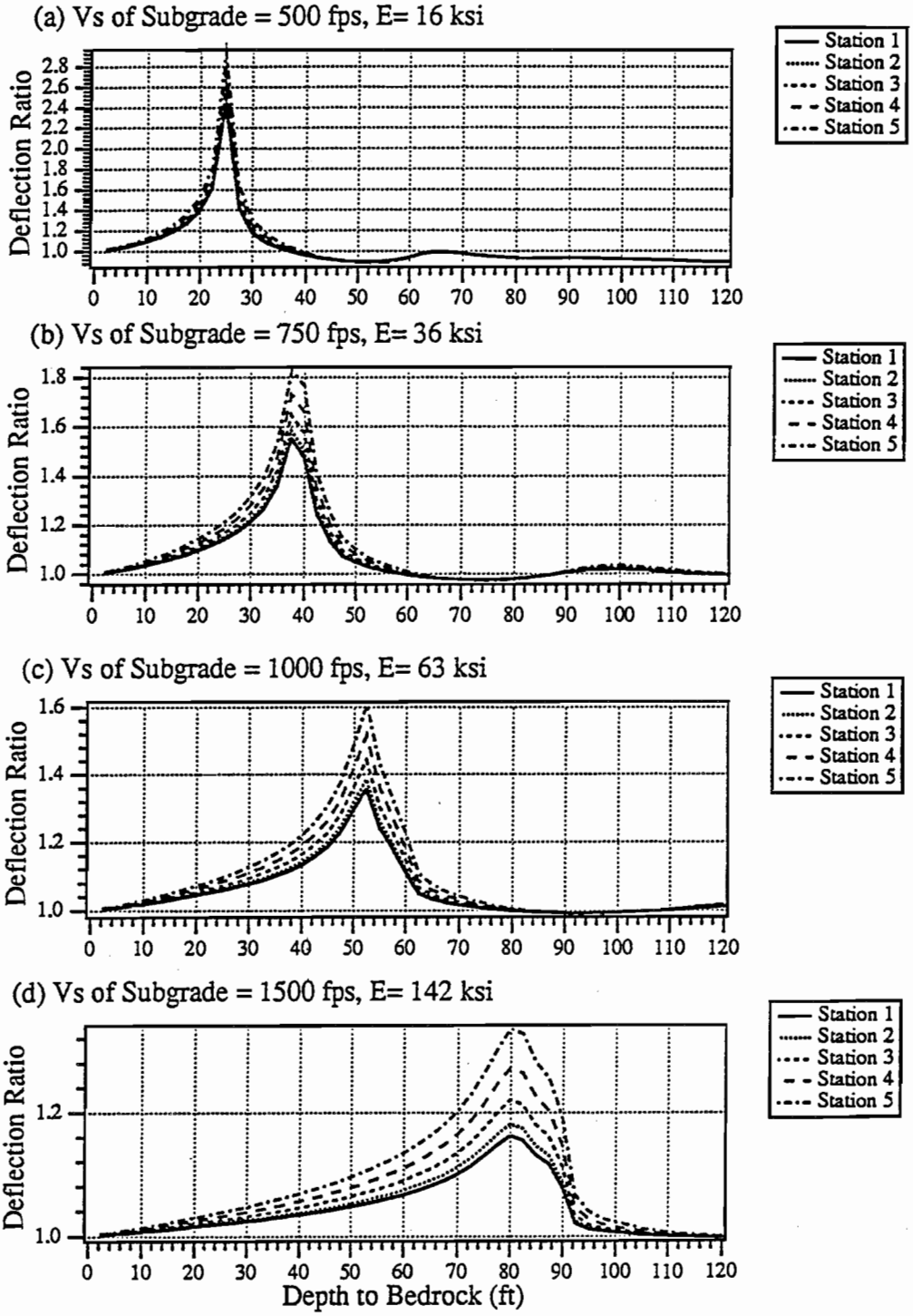

Figure A.48 Deflection ratio versus depth to bedrock for Dynaflect testing at Profile 4 (V_s of AC = 5000 fps (E = 1920 ksi) and V_s of base = 2000 fps (E = 270 ksi))

APPENDIX B. RESULTS OF ANALYTICAL SIMULATION OF THE FWD TEST

The analytical simulations of the FWD test were obtained using computer program UTFWD (Chang, 1991). The motions are expressed in terms of deflection ratios as a function of depth to bedrock, a format similar to that used for the Dynaflect test in Appendix A.

There are some numerical problems with the deflection ratios obtained from shallow bedrock depths (less than 10 feet (3.1 m)). These problems caused the first pulses in the deflection-time records to be distorted, so that the maximum deflections were incorrect as discussed in Section 4.7.

However, for unsaturated subgrade conditions, numerical problems did not have any effect on the values of the maximum deflection ratios and the resonant depths to bedrock. They had no effect because numerical problems always occurred at shallower bedrock depths than the resonant depths obtained with unsaturated subgrade conditions, as shown in Figure B.1. The maximum deflection ratios and the resonant depths to bedrock can be determined without difficulties, as shown in Figures B.2 to B.5 (the data generated by numerical problems were removed from these figures).

For saturated subgrade conditions, the numerical problems tend to occur at greater depths than those for the unsaturated subgrade conditions, as shown in Figure B.6. Generally, the measurement stations away from the source (stations 5, 6, and 7) exhibit the poorest results. Therefore, the resonant depths to bedrock were determined from the bedrock depths corresponding to the maximum deflection ratios of the first three measurement stations (stations 1, 2, and 3). The values of the maximum deflection ratios of the farthest station (station 7) were estimated based on the trends of the deflection ratios of the stations which were not affected by the numerical problems.

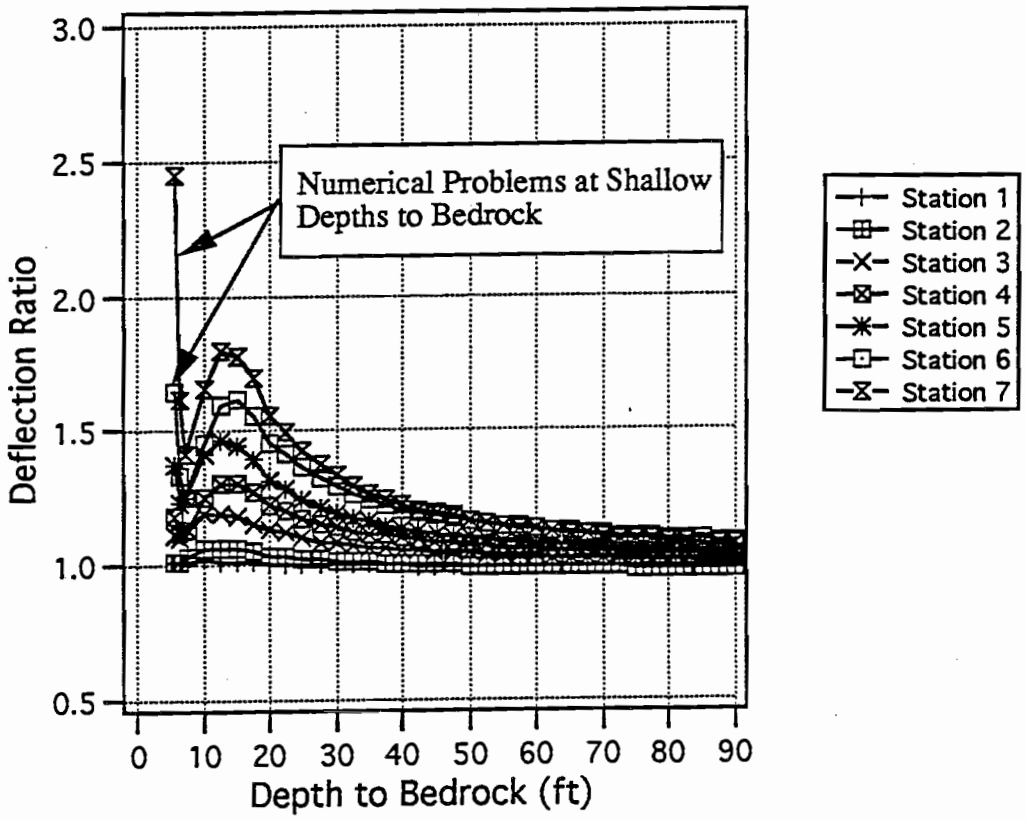

Figure B.1 *Numerical problems with UTFWD program at shallow depths to bedrock for unsaturated subgrade conditions (Profile 1 with V_s of subgrade = 1000 fps (E = 63 ksi))*

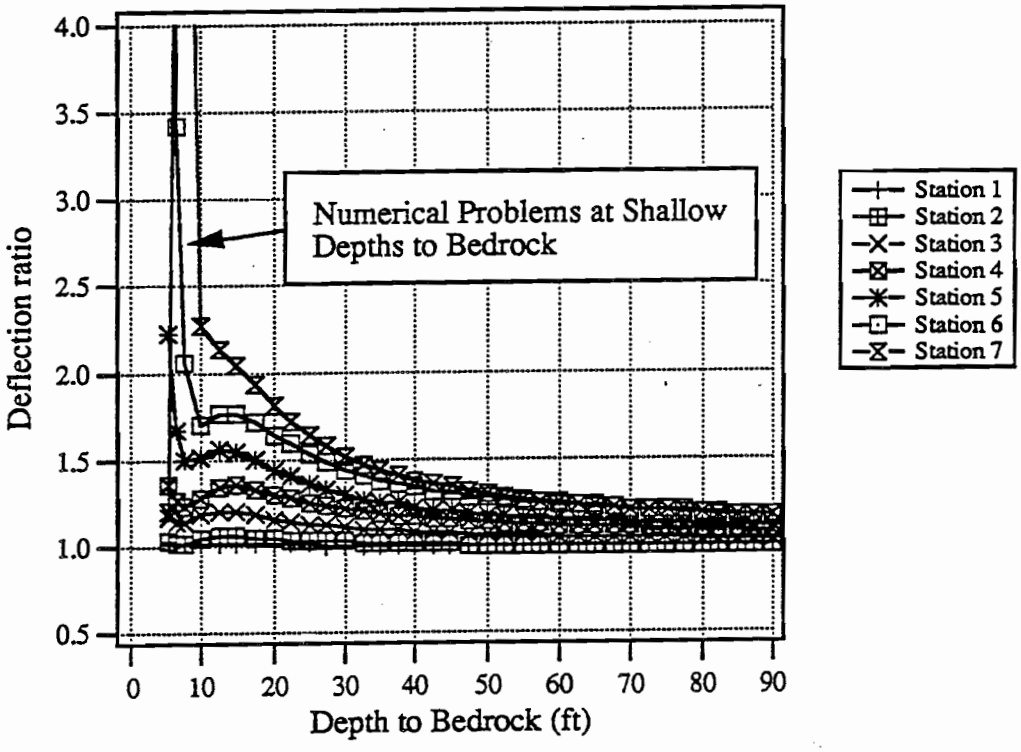

Figure B.2 *Numerical problems with UTFWD program at shallow depths to bedrock for saturated subgrade conditions (Profile 1 with V_s of subgrade = 1000 fps (E = 63 ksi))*

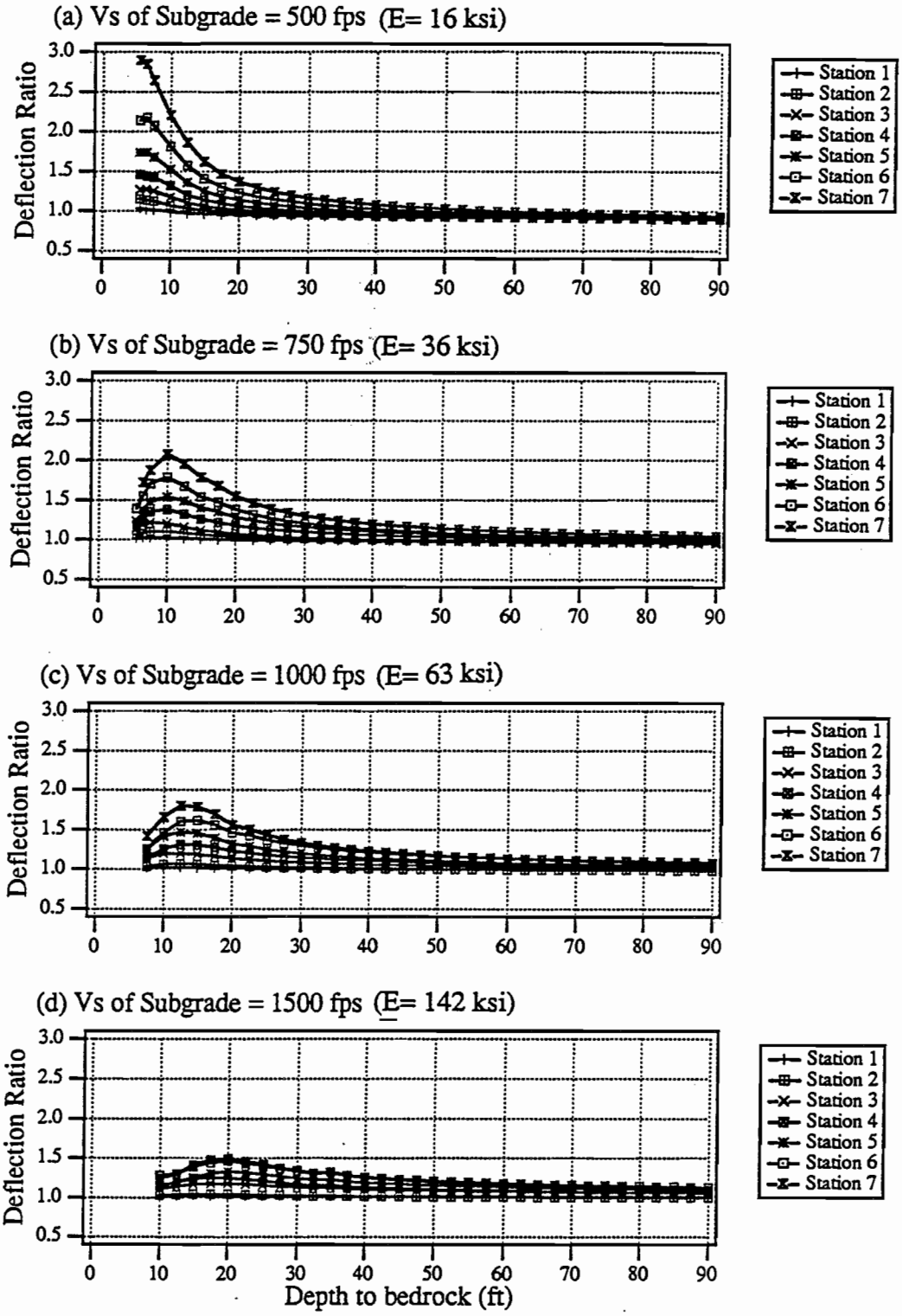

Figure B.3 Deflection ratio versus depth to bedrock for FWD tests at Profile 1 with unsaturated subgrade conditions

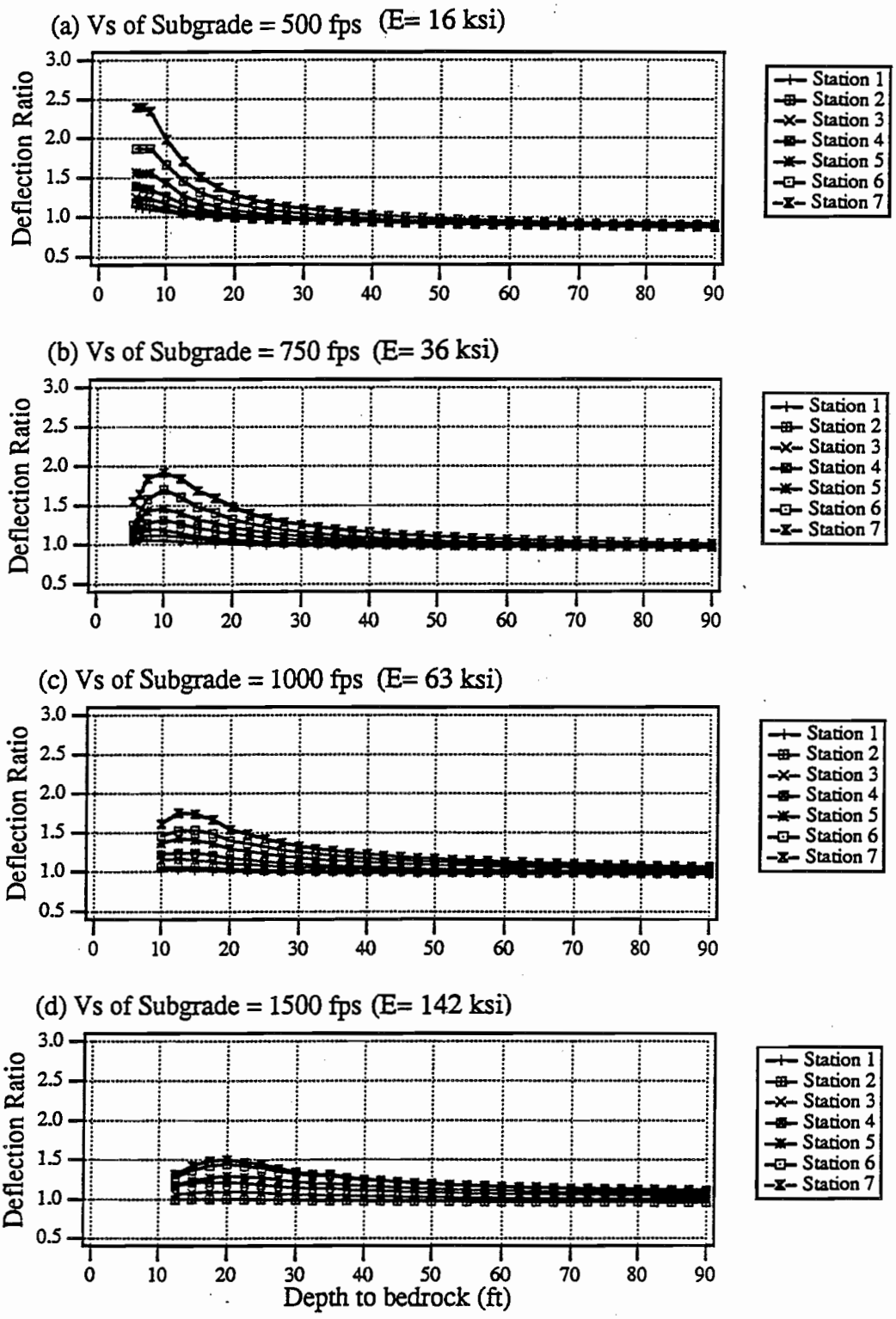

Figure B.4 Deflection ratio versus depth to bedrock for FWD tests at Profile 2 with unsaturated subgrade conditions

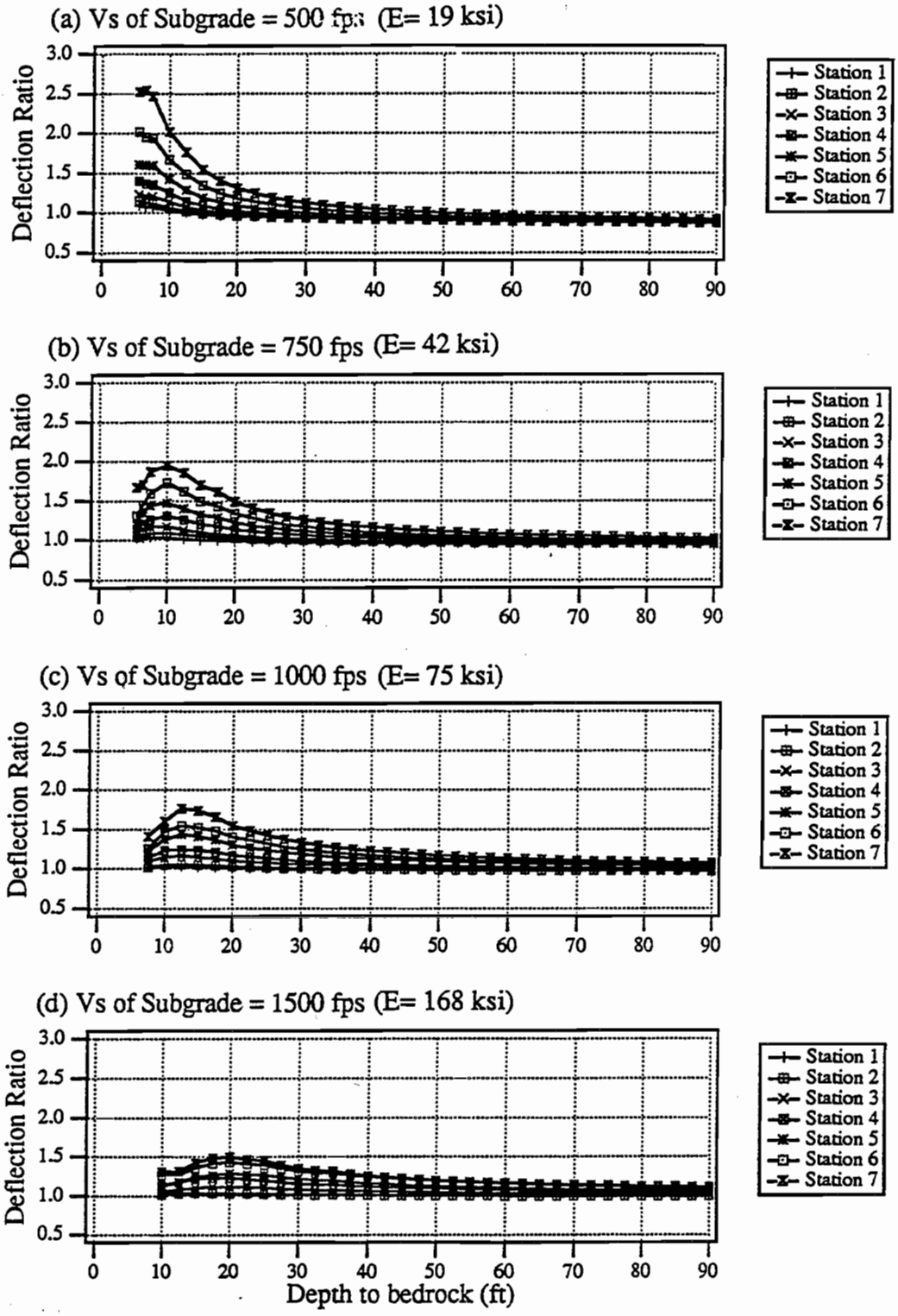

Figure B.5 ***Deflection ratio versus depth to bedrock for FWD tests at Profile 3 with unsaturated subgrade conditions***

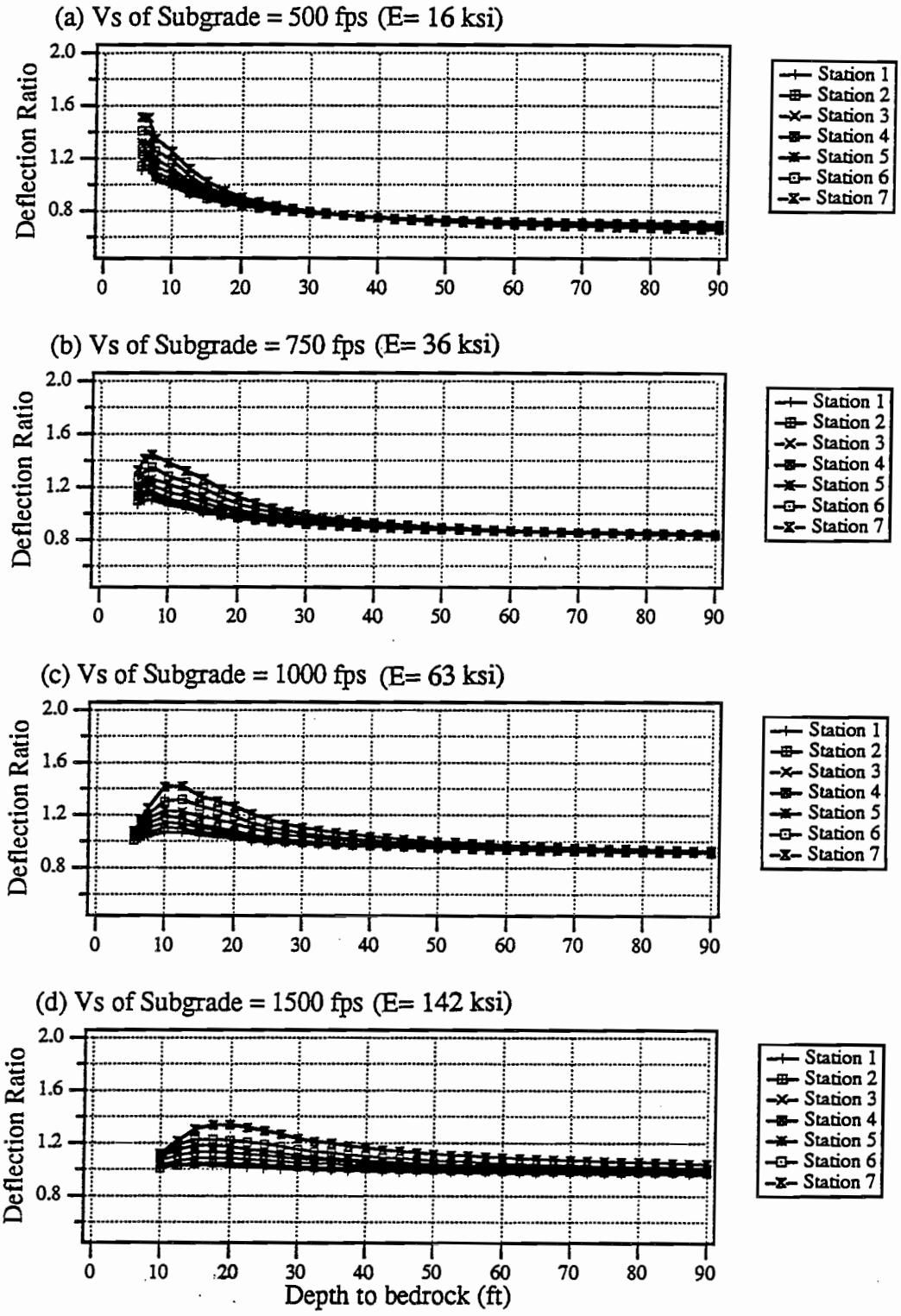

Figure B.6 *Deflection ratio versus depth to bedrock for FWD tests at Profile 4 with unsaturated subgrade conditions*

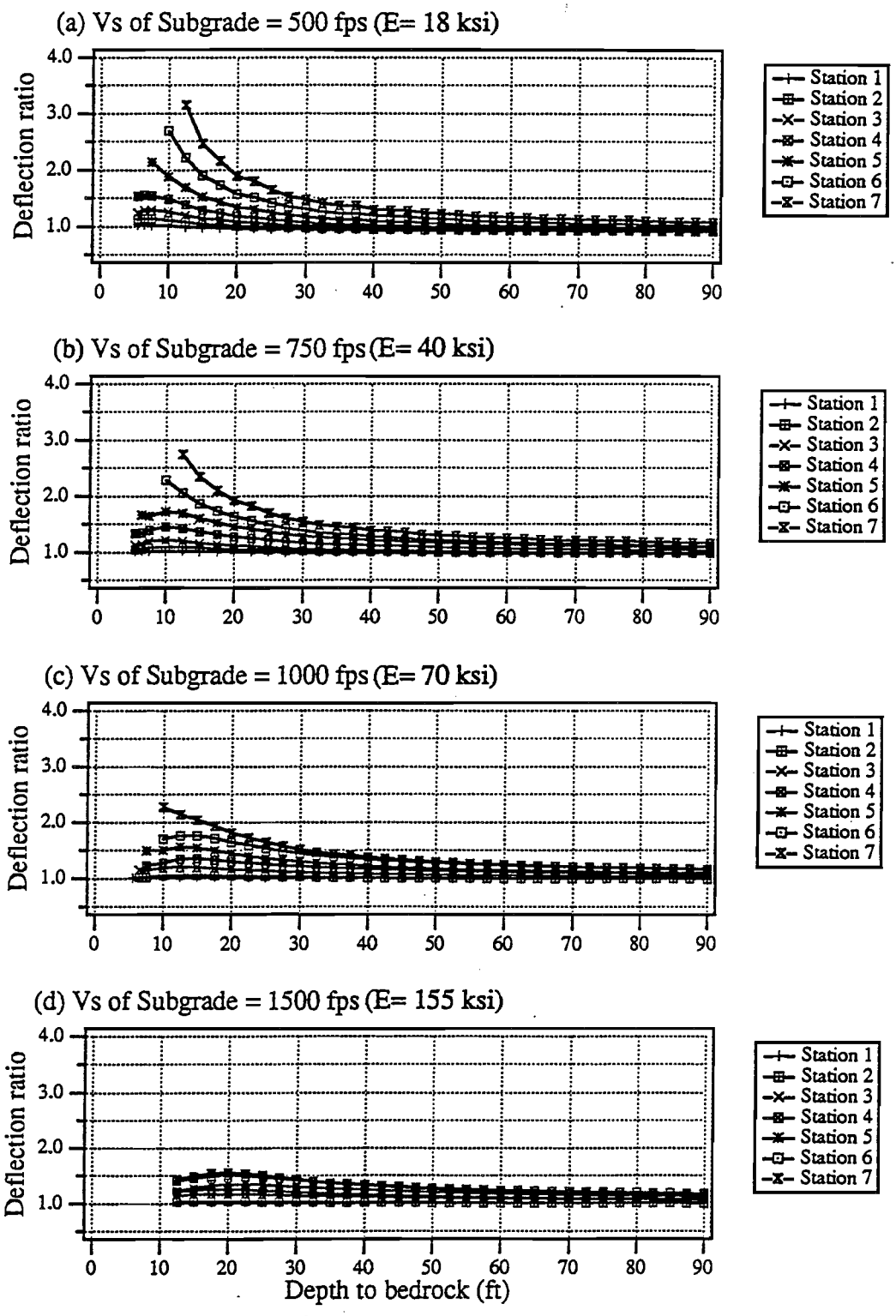

Figure B.7 ***Deflection ratio versus depth to bedrock for FWD tests at Profile 1 with saturated subgrade conditions***

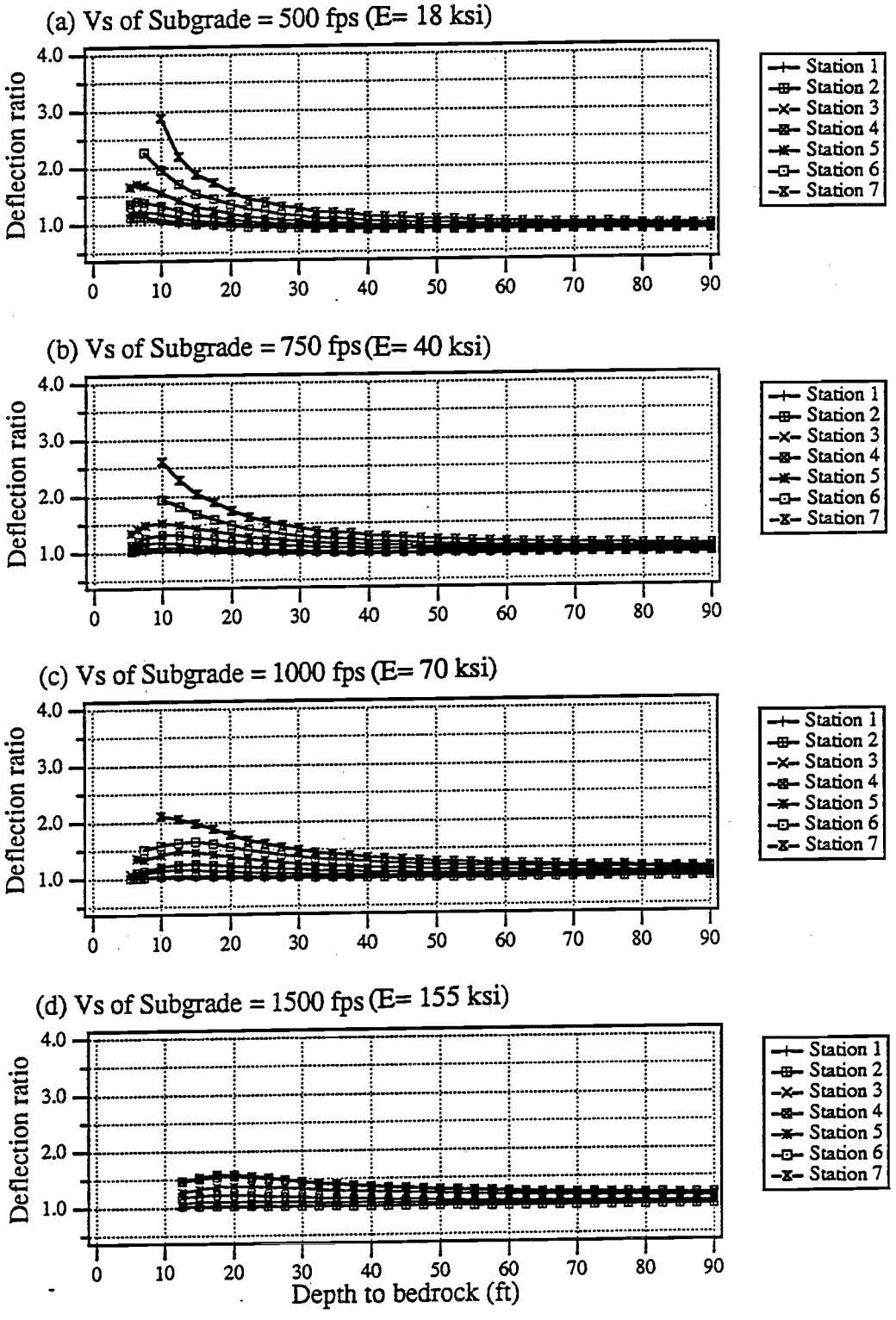

Figure B.8 *Deflection ratio versus depth to bedrock for FWD tests at Profile 2 with saturated subgrade conditions*

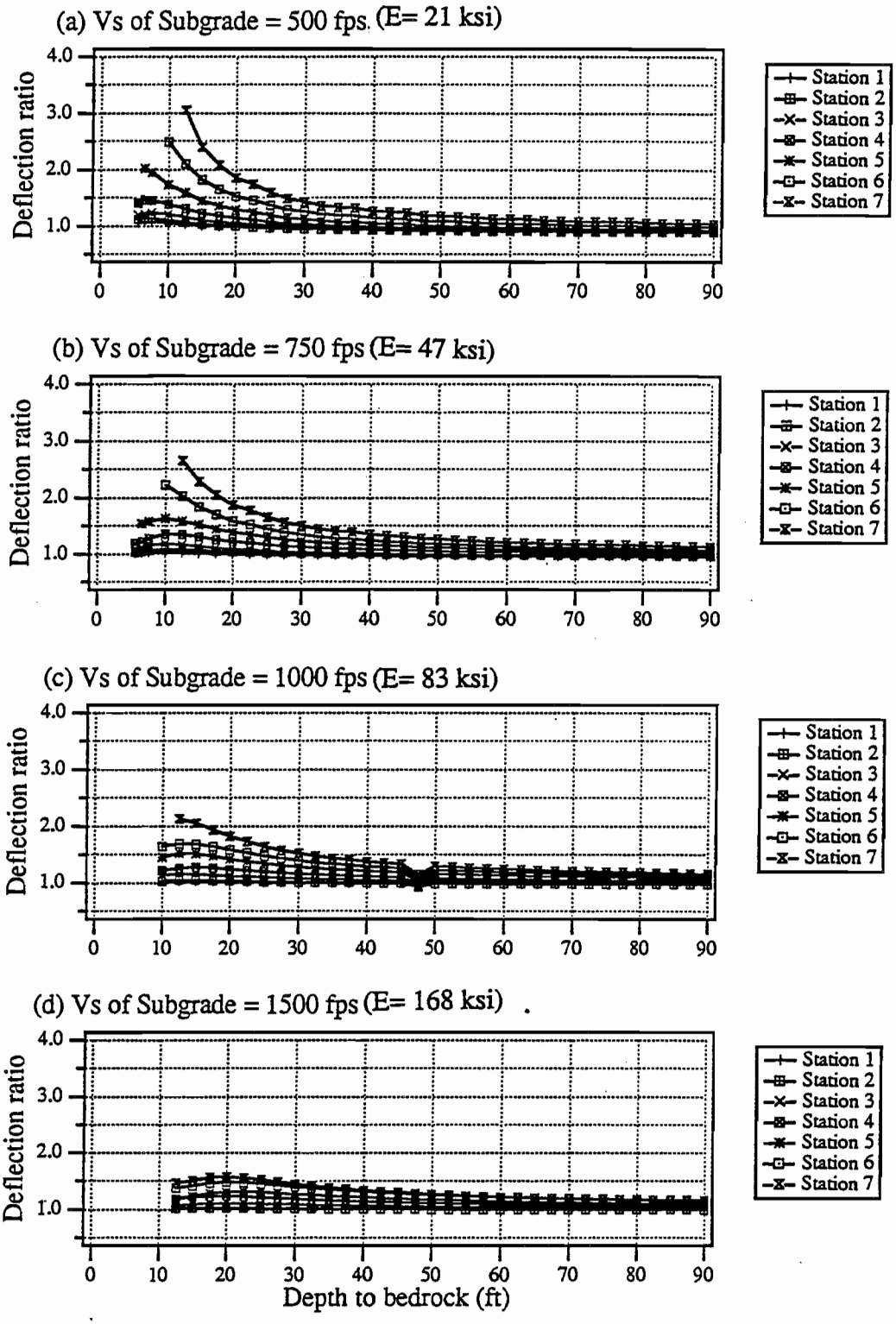

Figure B.9 *Deflection ratio versus depth to bedrock for FWD tests at Profile 3 with saturated subgrade conditions*

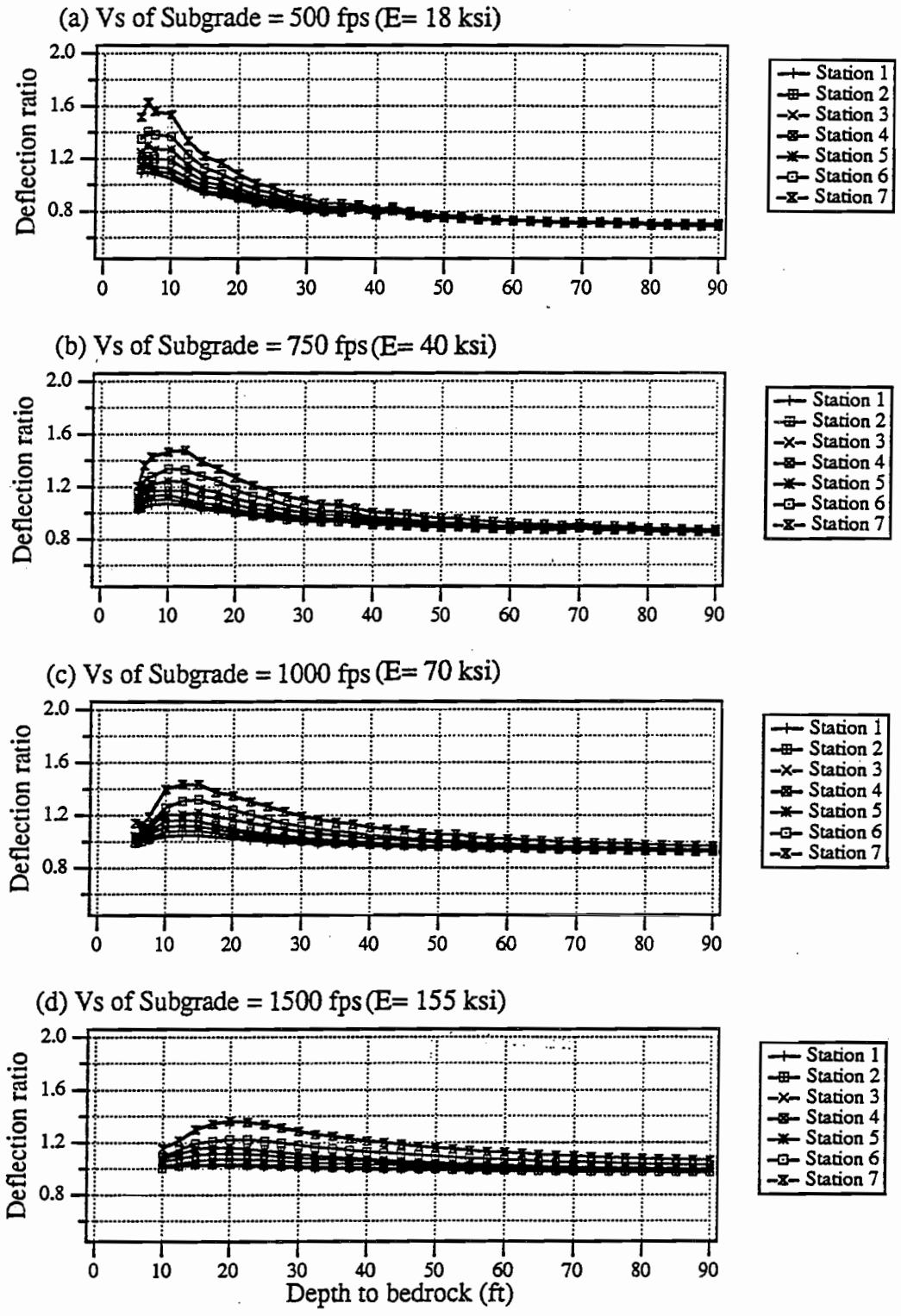

Figure B.10 Deflection ratio versus depth to bedrock for FWD tests at Profile 4 with saturated subgrade conditions

APPENDIX C. DEFLECTION-TIME RECORDS IN THE FWD TEST

Shear Wave Velocity of Subgrade (fps)	Approx. Young's Modulus (ksi)	Depth to Bedrock (ft)	Dampted Naturated Period (sec) Profile 1 (FM 137)	Profile 2 (FM195)	Profile 3 (Route 1)	Profile 4 (IH10)
500	14	5	0.0300	0.0300	0.0300	0.0365
500	14	7.5	0.0435	0.0425	0.0425	0.0490
500	14	10	0.0560	0.0550	0.0550	0.0615
500	14	20	0.1170	0.1080	0.1090	0.1200
750	32	5	0.0190	0.0200	0.0190	0.0240
750	32	7.5	0.0290	0.0290	0.0280	0.0320
750	32	10	0.0370	0.0038	0.0380	0.0410
750	32	20	0.0700	0.0710	0.0690	0.0715
1000	57	5	0.0165	0.0150	0.0150	0.0170
1000	57	7.5	0.0215	0.0200	0.0215	0.0240
1000	57	10	0.0270	0.0280	0.0270	0.0310
1000	57	20	0.0525	0.0525	0.0530	0.0535
1500	128	5	0.0100	0.0110	0.0085	0.0120
1500	128	7.5	0.0145	0.0145	0.0150	0.0160
1500	128	10	0.0180	0.0175	0.0185	0.0190
1500	128	20	0.0350	0.0350	0.0350	0.0385

Table C.1 Damped natural period in the deflection-time histories for FWD testing at the four pavement profiles, with Poisson's ratio of unsaturated subgrade equal to 0.20

Shear Wave Velocity of Subgrade (fps)	Approx. Young's Modulus (ksi)	Depth to Bedrock (ft)	Dampted Naturated Period (sec) Profile 1 (FM 137)	Profile 2 (FM195)	Profile 3 (Route 1)	Profile 4 (IH10)
500	16	5	0.0275	0.0280	0.0260	0.0310
500	16	7.5	0.0360	0.0380	0.0375	0.0425
500	16	10	0.0480	0.0500	0.0490	0.0540
500	16	20	0.0940	0.0910	0.0980	0.1050
750	36	5	0.0175	0.0175	0.0160	0.0210
750	36	7.5	0.0250	0.0350	0.0250	0.0290
750	36	10	0.0325	0.0340	0.0320	0.0360
750	36	20	0.0620	0.0620	0.0620	0.0700
1000	63	5	0.0140	0.0135	0.0135	0.0130
1000	63	7.5	0.0175	0.0190	0.0190	0.0220
1000	63	10	0.0235	0.0240	0.0245	0.0260
1000	63	20	0.0450	0.0480	0.0475	0.0500
1500	142	5	0.0090	0.0095	0.0090	0.0100
1500	142	7.5	0.0120	0.0125	0.0120	0.0160
1500	142	10	0.0160	0.0170	0.0160	0.0180
1500	142	20	0.0290	0.0300	0.0305	0.0320

Table C.2 ***Damped natural period in the deflection-time histories for FWD testing at the four pavement profiles, with Poisson's ratio of unsaturated subgrade equal to 0.33***

Shear Wave Velocity of Subgrade (fps)	Approx. Young's Modulus (ksi)	Depth to Bedrock (ft)	Dampted Naturated Period (sec) Profile 1 (FM 137)	Profile 2 (FM195)	Profile 3 (Route 1)	Profile 4 (IH10)
500	17	5	0.0265	0.0265	0.0250	0.0290
500	17	7.5	0.0385	0.0380	0.0380	0.0405
500	17	10	0.0480	0.0490	0.0510	0.0500
500	17	20	0.0880	0.0850	0.0970	0.0975
750	37	5	0.0165	0.0160	0.0160	0.0190
750	37	7.5	0.0235	0.0260	0.0240	0.0270
750	37	10	0.0310	0.0320	0.0310	0.0355
750	37	20	0.0540	0.0640	0.0610	0.0670
1000	66	5	0.0120	0.0125	0.0130	0.0155
1000	66	7.5	0.0175	0.0175	0.0175	0.0205
1000	66	10	0.0225	0.0225	0.0240	0.0260
1000	66	20	0.0420	0.0435	0.0415	0.0520
1500	150	5	0.0085	0.0090	0.0080	0.0105
1500	150	7.5	0.0110	0.0110	0.0110	0.0120
1500	150	10	0.0130	0.0130	0.0140	0.0165
1500	150	20	0.0280	0.0285	0.0280	0.0330

Table C.3 ***Damped natural period in the deflection-time histories for FWD testing at the four pavement profiles, with Poisson's ratio of unsaturated subgrade equal to 0.40***

Shear Wave Velocity of Subgrade (fps)	Approx. Young's Modulus (ksi)	Depth to Bedrock (ft)	Dampted Naturated Period (sec) Profile 1 (FM 137)	Profile 2 (FM195)	Profile 3 (Route 1)	Profile 4 (IH10)
500	18	5	0.0225	0.0240	0.0225	0.0250
500	18	7.5	0.0350	0.0350	0.0350	0.0350
500	18	10	0.0425	0.0445	0.0450	0.0450
500	18	20	0.0875	0.0880	0.0875	0.0875
750	40	5	0.0150	0.0175	0.0150	0.0175
750	40	7.5	0.0225	0.0215	0.0250	0.0250
750	40	10	0.0325	0.0295	0.0300	0.0300
750	40	20	0.0550	0.0585	0.0575	0.0575
1000	70	5	0.0125	0.0120	0.0125	0.0150
1000	70	7.5	0.0175	0.0175	0.0175	0.0175
1000	70	10	0.0225	0.0220	0.0225	0.0250
1000	70	20	0.0425	0.0440	0.0425	0.0450
1500	155	5	0.0075	0.0100	0.0075	0.0075
1500	155	7.5	0.0125	0.0125	0.0125	0.0125
1500	155	10	0.0150	0.0150	0.0150	0.0150
1500	155	20	0.0300	0.0300	0.0275	0.0325

Table C.4 ***Damped natural period in the deflection-time histories for FWD testing at the four pavement profiles with saturated subgrade conditions***